EVALUATION OF THE ROLE OF IRON ON PHYSIOLOGICAL PERFORMANCE AND FUNCTIONAL CHARACTERIZATION OF MAJOR IRON TRANSPORTER IN ZEBRAFISH (*DANIO RERIO*)

THEANUGA CHANDRAPALAN

A DISSERTATION SUBMITTED TO

THE FACULTY OF GRADUATE STUDIES

IN PARTIAL FULFILLMENT OF THE REQUIREMENTS

FOR THE DEGREE OF

DOCTOR OF PHILOSOPHY

GRADUATE PROGRAM IN BIOLOGY

YORK UNIVERSITY

TORONTO, ONTARIO

DECEMBER 2025

Abstract

Iron is essential for a multitude of biological processes, and its acquisition and regulation are critical for survival. In fishes, iron is obtained from the water via the gills and the diet through the gastrointestinal tract. While the diet is the predominant source of iron absorption, the physiological consequences of dietary iron availability and its underlying mechanisms of uptake and metabolism remain poorly understood compared to waterborne studies. In this thesis, I investigated the effects of dietary iron levels (~11, 420, and 2300 mg Fe/kg) and exposure duration (20 and 40 days) in zebrafish (*Danio rerio*). Short-term iron supplementation enhanced aerobic scope, maximum metabolic rate, and critical swimming speed, as well as reproductive output and offspring survival. In contrast, prolonged high-iron exposure led to iron loading in the brain and intestine, highlighting a narrow window between nutritional benefits and overload. Offspring of high-iron-fed parents exhibited greater swimming and metabolic performance than those of the low-iron group, revealing potential intergenerational consequences of parental iron status. To help elucidate the molecular mechanisms underlying iron homeostasis, a CRISPR-Cas9 knockout of the iron transporter, divalent metal transporter 1 (DMT1; slc11a2), was generated. The systemic consequences of DMT1 loss in developing and adult zebrafish were characterized using trace metal analysis, gene expression, and RNA sequencing. During early development, DMT1 loss caused anemia and disrupted iron, zinc, cobalt, and manganese homeostasis. Despite these disruptions, mutants displayed remarkable physiological plasticity and partial recovery through compensatory regulation of alternate transporters, including heme carrier protein 1 (*hcp1*). Broad transcriptional reprogramming was also evident in the gill and intestine of adult *dmt1*$^{-/-}$ fish, which included induction of iron transport, storage, and erythropoietic genes, alongside suppression of hepcidin/BMP-Smad signalling. Tissue-specific responses identified two candidates for DMT1-

compensation, including zrt- and irt-like protein 4 (*zip4*) in the intestine and epithelial calcium channel (*ecac*) in the gills. Broad reprogramming of ion regulation, immunity, and redox pathways was also present. Collectively, this thesis advances our understanding of iron metabolism from cellular transport to whole-animal physiology, providing a framework with implications for environmental toxicology, aquaculture nutrition, and a vertebrate model for studying iron-related disorders.

Dedication

I dedicate my work to my parents, **Dr. Chandrapalan Seenithamby** and **Indrani Chandrapalan**. I would not have had the privilege and luxury of this education if it had not been for every one of your sacrifices.

Acknowledgements

First and foremost, I would like to thank my supervisor, **Dr. Raymond Kwong**, for all your years of guidance and wisdom, which have been an invaluable foundation in my studies. You have not only been a pillar of support during my entire graduate studies, but also an inspiration and someone that I will always look up to.

I have also had the privilege to learn from many more outstanding members of the Faculty of Biology at York University:

To my advisors, **Dr. Scott P. Kelly** and **Dr. Andrew Donini**, I am beyond grateful to have had you both on my supervisory committee; your expertise and guidance not only encompass my doctoral studies but also extend well beyond to when I was just an undergraduate/MSc student attending your lectures and an MSc candidate defending my thesis.

I would also like to extend my gratitude to **Dr. Carol Bucking**, who has always been a source of support during my graduate studies. I am thankful to **Dr. Christopher Jang**, **Dr. Yi Sheng**, and **Dr. Michael Gadsden** for the opportunity to coordinate for your courses and inspiring my perspective on pedagogy. To **Dr. Nicole Nivillac**, **Dr. Jean-Paul Paluzzi**, and again **Dr. Raymond Kwong**, your Introduction to Biology, Membrane Transport, and Fish Biology lectures, among your many other courses, added to my interest in the biological sciences.

I thank **Ms. Janet Fleites** and **Ms. Veronica Scavo** for their technical support in zebrafish husbandry. Over countless early mornings, Janet has taught me everything I know about working with zebrafish, alongside many other life lessons.

Dr. Yu Yue, I am so grateful for all of the time and effort you put into the massive RNA-Seq datasets. **Dr. Chun Chih Chen**, I am so lucky to have such a remarkable and inspiring friend like you. Thank you for always motivating me and for being a constant source of support.

Present and past members of the **Kwong Lab** and **Bucking Lab**, our shared experiences as graduate students and our time together at Rice Lake, the Canadian Society of Zoologists (CSZ), and the Society of Environmental Toxicology and Chemistry (SETAC) conferences have been core memories that I will always cherish. I still laugh when I think back on our nutritional priorities during conferences.

Students that I have had the privilege to mentor, including **Suhani Walia** (Dental student), **Preeti Dave** (Veterinary candidate), **Thi My Nhi Ngugen** (PhD Candidate), **Sajid Alvi** (PhD Candidate), **Morteza Ghafar-Zadeh** (PhD candidate), and **Umaimah Chudawala (**Medical student**)**, it was a great experience learning and growing together.

I am also thankful to the members of the Association of Graduate Studies in the Biological Sciences (AGSBS) who have supported me during my time as the Chair of AGSBS, including **Rebecca Whiley**, **Jennifer Seung Hee Im**, **Gabriella Gerzon**, and **Farnaz Mansouri-Noori**. It was such an honor to represent the graduate students in Biology alongside you.

To my parents, sister (**Mathura**), and my two beloved cats: I could not have completed my studies without your constant support and love.

Table of contents

List of tables

Chapter 4 Tables

List of figures

Chapter 1 Figures

Chapter 2 Figures

Chapter 3 Figures

Chapter 4 Figures

List of Abbreviations

ANOVA	Analysis of variance
AS	Aerobic scope
ASIC	Acid-sensing ion channel
ATOX1	Antioxidant 1 copper chaperone
CCS	Copper chaperone for superoxide dismutase
COT	Cost of transport
COX17	Cytochrome C oxidase copper chaperone
CPM	Counts per million
CRISPR	Clustered regularly interspaced short palindromic repeats
CTR1	Copper transporter 1
Cybrd1	Cytochrome b reductase 1
Dcytb	Duodenal cytochrome b
ddPCR	Droplet digital polymerase chain reaction
DE	Differentially expressed
DEG	Differentially expressed genes
DHA	Docosahexaenoic acid
DMT1	Divalent metal transporter-1
Dpf	Days post fertilization
ECaC	Epithelial calcium channel
ENaC	Epithelial sodium channel
EPA	Eicosapentaenoic acid
FDR	False discovery rate

Fth1	Ferritin heavy chain 1
GIT	Gastrointestinal tract
GSI	Gonadosomatic index
HCP1	Heme carrier protein 1
HIF	hypoxia-inducible factor
Hpf	Hours post fertilization
HSI	Hepatosomatic index
ICP-MS	Inductively coupled plasma mass spectrometry
IRE	Iron response element
IREG1	Iron regulated transporter 1
IRP	Iron response protein
ISI	Intestinal somatic index
K	Condition factor
KO	Knockout
LEAP-1	Liver-expressed antimicrobial peptide
MT	Metallothionein
MDS	Multidimensional scaling
MMR	Maximum metabolic rate
MO_2	Oxygen consumption rate
MTF1	Metal-responsive transcription factor 1
ORA	Overrepresentation analysis
RBC	Red blood cell
ROS	Reactive oxygen species

SL	Standard length
SLC	Solute carrier
SMR	Standard metabolic rate
SOD	Superoxide dismutase
T_3	Triiodothyronine
TfR1	Transferrin receptor 1
U_{crit}	Critical swimming speed
V_{O2} max	Maximum rate of oxygen consumption
WT	wildtype
ZIP	Zrt- and Irt-like protein
ZnT	Zinc transporter

Statement of Contribution

Chapter One: Overview

Contributors: Theanuga Chandrapalan, Raymond W. M. Kwong
Contributions: Conceptualization – T.C., R.W.M.K.; Figure Illustration – T.C.; Writing (original draft) – T.C.; Writing (review and editing) – T.C., R.W.M.K.

Chapter Two: Intergenerational Effects of Dietary Iron on Swimming and Metabolic Performance in Zebrafish

Contributors: Theanuga Chandrapalan, Suhani Walia, Raymond W. M. Kwong
Contributions: Conceptualization – T.C., R.W.M.K.; Methodology – T.C.; Validation – T.C.; Formal analysis – T.C.; Investigation – T.C., S.W.; Data curation: T.C.; Writing - original draft – T.C.; Writing – review & editing: T.C., R.W.M.K.; Supervision - R.W.M.K.; Funding acquisition: R.W.M.K.

Chapter Three: CRISPR-Cas9 Mediated Knock Out of Major Iron Transporter Affects Homeostasis of Multiple Essential Metals

Contributors: Theanuga Chandrapalan, Raymond W. M. Kwong
Contributions: Conceptualization – T.C., R.W.M.K.; Methodology – T.C.; Validation – T.C.; Formal analysis – T.C.; Investigation – T.C.; Data curation: T.C.; Writing - original draft – T.C.; Writing – review & editing: T.C., R.W.M.K.; Supervision - R.W.M.K.; Funding acquisition: T.C., R.W.M.K.

Chapter Four: Transcriptomic Analysis of DMT1 Mutant Zebrafish: Comparative Insights from the Gill and Gut

Contributors: Theanuga Chandrapalan, Yue Yu, Raymond W. M. Kwong
Contributions: Conceptualization – T.C., R.W.M.K.; Methodology – T.C., Y.Y.; Validation – T.C.; Formal analysis – T.C., Y.Y.; Investigation – T.C.; Data curation: T.C., Y.Y.; Writing - original draft – T.C; Writing – review & editing: T.C., R.W.M.K.; Supervision - R.W.M.K.; Funding acquisition: R.W.M.K.

Chapter Five: General Discussion and Integration

Contributors: Theanuga Chandrapalan
Contributions: Conceptualization – T.C.; Writing (original draft) – T.C.; Writing (review and editing) – T.C.

Contributors Affiliation:

T.C., S.W., R.W.M.K: Department of Biology, York University, Toronto, ON, Canada
Y.Y: Contigs, Toronto, ON, Canada

Chapter 1. Overview

Part of this chapter has been published and reproduced with permission.

Chandrapalan, T., Kwong, R.W.M., 2021. Functional significance and physiological regulation of essential trace metals in fish. J. Exp. Biol. 224, jeb243834. https://doi.org/10.1242/JEB.238790

1.1 **Introduction**

Essential trace metals such as iron, copper, zinc and manganese are vital components for a multitude of biochemical reactions and act as cofactors for various enzymes. They can be found in proteins such as the oxygen-transporting hemoproteins (iron as a cofactor), iron–sulfur clusters involved in DNA synthesis, cytochrome c oxidase of the electron transport chain (copper) and superoxide dismutase (SOD; copper, zinc, manganese) of the antioxidant defense system (Dalziel et al., 2006; de Souza and Bonilla-Rodriguez, 2007; Harris, 1992; Puig et al., 2017). In fish, trace metal deficiency results in impairment to health and physiological performance (Clearwater et al., 2002; Makwinja and Geremew, 2020; Song et al., 2017). On the contrary, these essential metals can become detrimental when in excess, often as a result of increased oxidative stress and induced pathophysiological conditions (Wood et al., 2011). Hence, it is important to tightly regulate and maintain trace metal levels within physiologically safe concentrations.

In adult fish, the acquisition of trace metals occurs via the gill and the gastrointestinal tract (Bury et al., 2003). The precise molecular mechanisms regulating the epithelial transport and metabolism of essential metals in fish have remained an active research question, as most of our current understanding is primarily based on mammalian studies. Despite this knowledge gap, recent research has provided new information on the biological significance, physiological regulation and functional involvement of various metal regulatory proteins in fish. These research efforts have demonstrated the complex nature of the regulatory and compensatory mechanisms involved in the maintenance of trace metal balance in fish. Additionally, several essential trace metals have been shown to interact at multiple biological levels (e.g. metal transporters, metal-binding proteins, metal-regulatory signalling pathways). Therefore, an alteration in the homeostasis of one trace metal may have the potential to affect the regulation of several other

metals. Moreover, a variety of factors have been shown to influence the way fish regulate metal metabolism and respond to changes in metal availability. These factors include, for example, developmental stage, dietary composition and environmental perturbations (Bury et al., 2003; Chandrapalan and Kwong, 2020; Glover et al., 2016; Long et al., 2015).

The uptake and metabolism of essential trace metals in fish have been previously reviewed in several articles and book chapters (Bury et al., 2003; Wood et al., 2011; Zhao et al., 2014). In the present Review, we provide an overview of the current state of knowledge on the physiological function of essential trace metals in fish, with a focus on iron, copper, zinc and manganese. We also discuss the interactions between metals (e.g. epithelial transport, transporter expression, cellular and systemic handling), the mechanisms underlying their regulation and recent progress in these topics. Finally, we identify knowledge gaps and discuss potential future research directions.

1.2 **Physiological significance of essential trace metals in fish**

1.2.1 *Essentiality in development*

Iron, copper, zinc and manganese are found in an array of metalloproteins and are cofactors for enzymes essential in various physiological functions, including oxygen transport, antioxidant activity, metal storage, and metabolism and redox balance (Table 1-1). Before the onset of exogenous feeding, fish embryos obtain nutrients, including essential metals, primarily from the maternally derived yolk stores via the yolk syncytial layer (Carvalho and Heisenberg, 2010; Fraenkel et al., 2005; Riggio et al., 2003; Thomason et al., 2017). Parental deficiency in essential metals such as zinc can have adverse effects on the offspring, including elevated mortality, decreased activity and possible alterations in epigenetic regulators (DNA methyltransferases)

(Beaver et al., 2017). In vertebrates, iron is known to be essential for the development of the brain, including neurocognitive development and neurotransmitter metabolism (McCann et al., 2020; Wang et al., 2019). In zebrafish (*Danio rerio*) embryos, both high levels of iron and copper are deposited in the yolk syncytial layer (Bourassa et al., 2014). High levels of iron are also present in the brain and tail of developing zebrafish (Bourassa et al., 2014). The head also appeared to be the major region of iron deposition in larval zebrafish exposed to iron, leading to a disruption in neurobehavioral performance (Hassan and Kwong, 2020). Similarly, dysregulation of manganese balance in the brain is found to adversely affect neurosensory function in larval zebrafish (Bakthavatsalam et al., 2014; Xia et al., 2017). These results suggest that the maintenance of trace metal balance in the brain is of critical importance during periods of neurodevelopment. Likewise, a few previous studies have shown that zinc is involved in embryogenesis in fish. For example, morpholino-mediated gene knockdown of the zinc transporter ZIP7 resulted in morphological defects and reduced zinc concentrations in the brain, eyes and gills of larval zebrafish (Yan et al., 2012). Additionally, zinc was found to be highly deposited in the hatching gland cells of larval zebrafish, and knockdown of ZIP10 resulted in an impairment in the development of the hatching gland, leading to failure in hatching (Muraina et al., 2020). These results indicate the essential role of zinc and specific zinc transporters in the early development of fish.

Recent studies have shown that iron is involved in bone formation signalling pathways and that feeding with an iron-enriched diet can increase the standard body length of developing zebrafish (Bo et al., 2016; Chandrapalan and Kwong, 2020). Similarly, copper is found to be essential for notochord development in zebrafish, primarily owing to its role in the enzyme lysyl oxidase, which promotes elastin–collagen crosslinking in the notochord (Gansner et al., 2007; Mendelsohn et al., 2006a). Copper is also important in the formation of pigmentation in zebrafish

through its involvement in the copper-dependent melanogenic enzyme tyrosinase (Ishizaki et al., 2010). Additionally, supplementation of diets with manganese and zinc has been shown to improve survival, bone mineralization and skeletal formation in the post-larvae of Senegalese sole (*Solea senegalensis*) (Viegas et al., 2021). In another study with post-smolt Atlantic salmon (*Salmo salar*), however, a change in dietary manganese level (5–65 mg kg^{-1}) was found to have no effect on specific growth rate over an 8-week experimental period (Antony Jesu Prabhu et al., 2019). In addition to possible species-specific differences in dietary metal requirements, differences in the developmental stages and dietary composition used across studies may also account for some of these mixed results.

Current understanding of the nutritional requirement for most essential metals is limited to a few fishes, particularly commercially important taxa such as carps, yellow catfish, groupers and salmonids (Chanda et al., 2015; Davis and Gatlin, 1996; Watanabe et al., 1997). For example, a range of 30–170 mg iron, 15–40 mg zinc, 2–20 mg manganese and 1–5 mg copper (per kg of diet) is proposed to be the minimal requirement for the maintenance of fish health in aquaculture practice (Watanabe et al., 1997). However, it should be noted that most of these studies were conducted with metal salts added in formulated diets, whereas biologically incorporated metals such as those found in prey and natural fish feeds are generally more bioavailable (Deforest and Meyer, 2015; Mebane et al., 2020). Therefore, the actual nutritional requirements for dietary metals in feral fish are likely to be lower than those estimated using formulated diets. Assessing the dietary requirements of metals with natural live diets would be invaluable to better understand how fish regulate metal absorption and balance during periods of metal deficiency or overload.

1.2.2 *Energy metabolism*

In vertebrates, iron is essential in the synthesis of oxygen transport proteins (e.g. hemoglobin and myoglobin) and enzymes involved in electron transfer and oxidation–reduction (Ganz, 2013). Manganese and copper are also known to be involved in glucose metabolism and mitochondrial functioning (Baker et al., 2017; Li and Yang, 2018). Therefore, these metals play an essential role in energy metabolism. A few studies have demonstrated that iron and copper status are also linked to the energetic parameters of fish. For example, lower critical swim speeds (U_{crit}) and reduced maximal oxygen uptake ($\dot{V}_{O2,max}$) values were observed in rainbow trout (*Oncorhynchus mykiss*) experiencing anemia (i.e. through blood removal) (Gallaugher et al., 1995). In yellow catfish (*Pelteobagrus fulvidraco*), changes in dietary copper levels were found to alter lipogenic enzyme activities and lipid metabolism (Chen et al., 2015). Additionally, dietary supplementation of iron or copper was found to improve hematological parameters in Siberian sturgeon (*Acipenser baerii*) and stinging catfish (*Heteropneustes fossilis*), including increases in hemoglobin content, erythrocyte count and hematocrit value (Moazenzadeh et al., 2020; Zafar and Khan, 2020). These enhancements are thought to increase oxygen transport capabilities in fish.

1.2.3 *Immune function*

Hepcidin (previously termed as liver-expressed antimicrobial peptide; LEAP-1) is a peptide hormone that regulates intestinal iron uptake and is associated with innate immune signalling (Drakesmith and Prentice, 2012). The first study that demonstrated the potential role of hepcidin in the immune response of fish was conducted in white bass (*Morone chrysops*), which showed that an infection with a pathogen in this fish species resulted in a 4500-fold induction of hepcidin mRNA expression (Shike et al., 2002). Since this pioneering study, increasing evidence

has indicated a close association between hepcidin and iron status in immune function across many fish species (Cuesta et al., 2008; Shi and Camus, 2006; Tarifeño-Saldivia et al., 2018). Nevertheless, how hepcidin orchestrates its dual functional roles in iron regulation and immune response in fish has remained unclear. In zebrafish, it was found that intraperitoneal injection of bacterial DNA can stimulate hepatic hepcidin expression and reduce serum iron levels (Jiang et al., 2017). The shift from circulating iron to intracellular storage was suggested to reduce the availability of iron to invading microorganisms, thereby enhancing antibacterial immunity (Drakesmith and Prentice, 2012). Several studies have also shown that the immune response of fish can be influenced by dietary metals. For example, iron deficiency has been shown to impair the immune function of grass carp (*Ctenopharyngodon idella*) by reducing the content of immunoglobulin and the transcript abundance of various anti-inflammatory cytokines (Guo et al., 2018a). Juvenile Siberian sturgeon fed on a copper-enriched diet also exhibit an increase and a decrease in the levels of neutrophil and lymphocyte, respectively (Moazenzadeh et al., 2020). In mammals, zinc is involved in various aspects of the immune function, including activation of immune cell signalling and stimulation of the development of immune cells (Prasad, 2008; Wessels et al., 2017). A few previous studies have also shown that zinc promotes immune functioning in fish. For example, feeding of iridescent shark (*Pangasianodon hypophthalmus*) with a zinc-enriched diet has been found to enhance the immune-hematological status and improve their survival rate after pathogen infection (Kumar et al., 2017). Likewise, grass carp (*Ctenopharyngodon idella*) fed on a zinc-deficient diet have been shown to exhibit an impairment in enteritis resistance (Song et al., 2017). The role of manganese in immune response in fish is less understood, but exposure to high levels of waterborne manganese has been shown to alter the

number of immune cells and the level of antimicrobial enzymes (Aliko et al., 2018; Do et al., 2019; Zafar and Khan, 2019).

Increasing evidence has also suggested that the iron-binding proteins ferritin and transferrin are responsive to bacterial infection in fish. For example, in rock cod (*Eleginops maclovinus*), bacterial infection increases the mRNA abundance of the ferritin-H subunit (Martínez et al., 2017). In Japanese flounder (*Paralichthys olivaceus*) and rock bream (*Oplegnathus fasciatus*), bacterial infection increases the mRNA expression of the ferritin-M subunit (Elvitigala et al., 2013; Wang and Sun, 2015). Additionally, both ferritin and transferrin expression are modulated in sea bass (*Dicentrarchus labrax*) during bacterial infection, with the levels of ferritin increased in both the liver and the brain (Neves et al., 2009). An increase in transferrin expression was also observed in common carp (*Cyprinus carpio*) during blood parasite infection (Kamińska-Gibas et al., 2020). The induction of iron-binding proteins during infection is proposed to be an acute inflammatory response to sequester iron and thereby reduce its availability for microbial or pathogen proliferation in the host (Ong et al., 2006). Alternatively, when excess iron is accumulated in macrophages, it can result in the production of free radicals via the Fenton reaction and subsequently aid in the elimination of the intruding pathogen (Tarifeño-Saldivia et al., 2018).

Table 1-1. An overview of the function of metalloproteins and their associated metal co-factors.

Protein/enzyme	Function	Metal/co-factor
Oxygen transport		
Hemoglobin	Oxygen binding protein found in red blood cells	Fe
Myoglobin	Oxygen binding protein found primarily in muscles	Fe
Antioxidant activity		
Catalases	Catalyzes decomposition of hydrogen peroxide	Fe, Cu, Mn, Zn
Peroxidases	Catalyzes the decomposition of peroxides	Fe
Superoxide dismutase	Catalyzes dismutation of superoxide radicals	Cu, Mn, Zn
Metal storage and metabolism		
Ferritin	Intracellular iron storage	Fe
Transferrin	Iron transport in the blood	Fe
Metallothionein	Zinc transport, storage and detoxification	Cu, Zn
Ceruloplasmin	Copper transport to tissues	Cu
Hephaestin	Ferroxidase for the conversion of Fe^{2+} to Fe^{3+}	Cu
Ferric reductase	Oxidizes Fe^{3+} to Fe^{2+}	Cu
Other metabolic and redox activities		
Cytochromes and NADH dehydrogenase	Involved in the electron transport chain and cellular respiration	Fe, Cu
Glutamine synthetase	Catalyzes glutamine synthesis from glutamate	Mn
Pyruvate carboxylase	Catalyzes carboxylation of pyruvate	Mn
Lipase	Enzyme that breaks down fats	Mn
Tyrosinase	Catalyzes the production of pigments	Cu

NADH, nicotinamide adenine dinucleotide.

1.3 **Homeostatic regulation of essential trace metals**

1.3.1 *Regulation of transepithelial metal uptake*

During early developmental stages, before the gills and the gastrointestinal tract (GIT) are fully developed, the uptake of essential trace metals from the environment can occur through the skin. Several studies have shown that larval fish can acquire and accumulate essential metals from the water (Guo et al., 2016; Hassan and Kwong, 2020; Puar et al., 2020). However, the precise pathways for their uptake remain unclear. A few previous studies with the zebrafish model have shown that several specific metal transporters, including those mediating the uptake of iron or zinc, do not appear to be expressed in the skin during early development (Donovan et al., 2002; Haller et al., 2018; Puar et al., 2020). Nevertheless, the epithelial calcium (Ca^{2+}) channel (ECaC), which is expressed in the skin of larval fish (Kwong et al., 2014; Lin and Hwang, 2016; Pan et al., 2005), can transport not only calcium but also iron and zinc (Qiu and Hogstrand, 2004). In contrast, the uptake of copper has been found to be sodium sensitive and is proposed to occur via sodium transporting channels (Grosell and Wood, 2002; Handy et al., 2002). Although the epithelial sodium channels (ENaCs) were considered a potential candidate in previous studies, current genomic data suggest that ENaCs are lost in the actinopterygian lineage and thus absent in teleost fish (Wichmann and Althaus, 2020). Instead, it has been proposed that acid-sensing ion channels (ASICs), which have been documented in other vertebrates for copper transport, are responsible for the sodium-dependent copper transport in fish. Indeed, ASICs are expressed in several fish species including rainbow trout and zebrafish (Dymowska et al., 2015; Zimmer et al., 2018); however, whether ASICs can in fact transport copper awaits investigation. Overall, it seems possible that the waterborne uptake of trace metals during the early developmental stages is mediated by ion transporters (i.e. via ionocytes) expressed in the skin. Interestingly, the skin is also

suggested to be an important site for the absorption of iron in adult Pacific hagfish (*Eptatretus stoutii*) (Glover et al., 2016), although the molecular pathways that mediate iron uptake in this species are yet to be determined.

In juvenile and adult fish, the acquisition of essential trace metals occurs via the gill and the GIT. Despite the capability of the gill to absorb trace metals from water, the diet is thought to be the major source of essential metals in fish (Bury and Glover, 2003; Watanabe et al., 1997). This is because in clean environments, the concentration of essential metals is generally quite low and at circumneutral pH, some of these metals such as iron may precipitate and form insoluble metal oxides and hydroxides. A previous study with the marine teleost *Psetta maxima* and elasmobranch *Scyliorhinus canicular* has shown that over 60% of the uptake of essential metals, including manganese, cobalt and zinc, occurs via the dietary route (Mathews and Fisher, 2009). In the GIT, the predominant region for the absorption of essential metals varies for different metals and among species. For example, iron absorption occurs primarily in the posterior region of the GIT in marine flounder (*Platichthys flesus*) (Bury et al., 2001) as opposed to the anterior region in freshwater rainbow trout (Kwong and Niyogi, 2009). Interestingly, the stomach is the major region for the absorption of copper in rainbow trout (Nadella et al., 2011). The mechanisms for the absorption of copper also appear to be different between the stomach and intestine, with the latter partially mediated by sodium- or iron-sensitive pathways (Nadella et al., 2007, 2011). In African walking catfish (*Clarias gariepinus*), copper uptake occurs predominantly in the distal intestine and is dependent on a chloride gradient (Handy et al., 2000). Furthermore, the levels of dietary trace metals and major ions (e.g. sodium, calcium, magnesium and potassium) have been shown to influence the acquisition of metals from water. For example, waterborne iron uptake was found to increase in zebrafish fed on an iron-deficient diet (Cooper et al., 2006a). Marine medaka

(*Oryzias melastigma*) fed on a low-iron diet also exhibited an increase in waterborne iron uptake (Wang and Wang, 2016). Interestingly, in rainbow trout, it has been shown that increasing the levels of dietary sodium reduced copper acquisition via the gills (Pyle et al., 2003). Similarly, elevated dietary calcium levels have been found to reduce the branchial absorption of zinc in rainbow trout (Niyogi and Wood, 2006). These findings suggest that the levels of trace metals and major ions in the diet can modulate trace metal uptake at the gill. How fish coordinate metal uptake between the gill and the GIT requires further investigation.

1.3.2 *Molecular machinery and metal-metal interactions*

Iron in the diet primarily exists in the ferric form (Fe^{3+}) and is first converted to the ferrous form (Fe^{2+}) by ferric reductase (also called duodenal cytochrome b; Dcytb) before its absorption from the intestine via the divalent metal transporter-1 (DMT1). According to the NCBI database, the gene encoding for ferric reductase has been identified in various fish species, such as rainbow trout, medaka, Indian glassy fish (*Parambassis ranga*) and zebrafish. Additionally, the activity of ferric reductase has been detected in rainbow trout and the air-breathing fish *Anabas testudineus* (Carriquiriborde et al., 2003; Rejitha and Peter, 2013). In mammals, ferric reductase is also proposed to mediate the reduction of cupric ion (Cu^{2+}) to cuprous ion (Cu^{+}) before its absorption by the copper transporter CTR1 (Wyman et al., 2008). In fish, DMT1 is thought to be the major transporter for the acquisition of iron from the diet and water (Bury, 2003). Notably, zebrafish mutants that produced truncated *dmt1* mRNA developed hypochromic and microcytic anemia (Donovan et al., 2002), suggesting its essential role in maintaining iron homeostasis. The gene encoding for DMT1 has been detected in early life stages and various tissues in adults (Chandrapalan and Kwong, 2020; Craig et al., 2008; Donovan et al., 2002; Hassan and Kwong, 2020; Wang and Wang, 2016). Interestingly, both an increase and a decrease in dmt1 expression

levels following iron exposure have been reported (Chandrapalan and Kwong, 2020; Cooper et al., 2006a; Craig et al., 2008; Hassan and Kwong, 2020; Kwong et al., 2013; Wang and Wang, 2016). The changes in *dmt1* expression could be indirect effects induced by iron because the iron transport pathways are also involved in the absorption and homeostatic regulation of several other essential metals (e.g. compensation for other metals; discussed below).

In mammals, DMT1 is capable of transporting not only iron but also other divalent metals such as manganese and copper (Arredondo et al., 2003; Garrick et al., 2003). However, a few recent studies have argued that DMT1 is not physiologically important in the intestinal absorption of copper or manganese (Illing et al., 2012; Shawki et al., 2015). In fish, direct evidence that shows the substrate selectivity of piscine DMT1 is limited to iron and the nonessential metal cadmium (Cooper et al., 2007). Nevertheless, many studies have demonstrated the interactions between iron and other essential metals, such as copper, manganese and zinc (Chandrapalan and Kwong, 2020; Craig et al., 2008; Hassan and Kwong, 2020; Kwong and Niyogi, 2009; Nadella et al., 2007). These interactions were observed either at the uptake surfaces or in regulating internal metal balance. In mammals, copper and zinc were also found to affect DMT1 expression (Iyengar et al., 2009; Tennant et al., 2002; Yamaji et al., 2001), whereas calcium appeared to be a non-competitive inhibitor for iron absorption in the enterocytes (Shawki and Mackenzie, 2010; Thompson et al., 2010). In addition to DMT1, the apical uptake of manganese and copper can also be mediated by other transporters, such as the zinc transporters ZIP14 and CTR1 (Mackenzie et al., 2004; Tuschl et al., 2016; Zhao et al., 2014). In the stomach of rainbow trout, CTR1 is proposed to be the major transporter responsible for the absorption of copper (Nadella et al., 2011).

The basolateral extrusion of iron and copper from absorptive cells is known to be mediated by ferroportin and copper transporting ATPases (e.g. ATP7a), respectively (Donovan et al., 2000;

Mendelsohn et al., 2006). Ferroportin is also thought to mediate the extrusion of manganese (Madejczyk and Ballatori, 2017; Seo and Wessling-Resnick, 2015). In a human colorectal adenocarcinoma cell line, Caco-2, copper has been shown to induce the expression of ferroportin (Tennant et al., 2002). These findings indicate that in addition to the apical surfaces (e.g. via DMT1), metal–metal interactions may also occur at the basolateral membrane, via either competition for export or modulation in the expression of metal export proteins. Advances in gene editing also provide a useful tool to reveal the functional significance of metal transporters and related proteins (Table 1-2). A recent study with zebrafish larvae has demonstrated that CRISPR/Cas9-mediated knockout of the zinc transporter ZnT10, a putative manganese exporter, results in manganese overload and hypermanganesaemia-related phenotypes, which can be partially rescued by iron treatment (Xia et al., 2017). This finding suggests that the interaction between iron and manganese is likely to be competitive in nature. Moreover, feeding with different levels of dietary iron can modulate the whole-body content of zinc and mRNA expression levels of the zinc transporters ZIP8 and ZIP14 in developing zebrafish (Chandrapalan and Kwong, 2020). Interestingly, zebrafish experiencing a knockout of ZIP14, which is a major transporter for zinc, but also capable of transporting manganese and iron, were found to increase manganese accumulation without affecting zinc and iron balance in their body (Tuschl et al., 2016). This result suggests that ZIP14 is important in manganese clearance in the kidney and that there are additional transport pathways to regulate and maintain the homeostasis of zinc and iron. To conclude, trace metal interactions may occur during the uptake process, potentially via direct metal–metal competition for absorption and/or modulation in the expression of metal transport proteins (Figure 1-1).

Table 1-2. Application of forward and reverse genetics with the zebrafish (*Danio rerio*) model in understanding the functional involvement of metal transport-/metal metabolism-related proteins in development and in the regulation of iron, copper or manganese.

Protein	Major substrate*	Findings	Reference
DMT1	Iron	DMT1-deficient fish experience microcytic anemia and hypochromic anemia, and have a decreased number of erythroid cells	(Donovan et al., 2002; Grillo et al., 2017)
FPN1	Iron	Required for Fe absorption and mutants develop hypochromic anemia	(Donovan et al., 2005, 2000)
Frrs1b	Iron	Important for normal cellular and mitochondrial Fe metabolism	(Xue et al., 2015)
Tfa	Iron	Tfa is required for Fe transport from the yolk to the embryo and morphants displayed anemia	(Fraenkel et al., 2009)
TfR1		Knockdown of TfR1a produces anemia in embryos whereas knockdown of TfR1b does not	
TfR2		TfR2-deficient fish have reduced hepcidin expression but do not exhibit anemia nor morphological defects	
Mfrn	Iron	Import Fe into the mitochondria of developing erythroid cells	(Shaw et al., 2006)
CTR1	Copper	Mutant larvae exhibit pigmentation defects and mitochondrial Cu deficiency	(Soma et al., 2018)
		Embryonic lethality in morphants. Neural tissue is most sensitive to *ctr1* loss	(Mackenzie et al., 2004)
ATP7a	Copper	Involved in notochord development and pigmentation in zebrafish	(Mendelsohn et al., 2006b)
ATP7b	Copper	Mutants exhibit increased Cu accumulation, histopathology in the liver, behavioral impairment and defects in central nervous system myelination	(Mi et al., 2020); (Zhang et al., 2020)
ZnT10	Zinc	Mutant larvae exhibit impaired Mn efflux and increased Mn accumulation in the brain and liver. Mutants develop neurological deficits in adulthood.	(Xia et al., 2017)

Protein	Major substrate*	Findings	Reference
ZIP8	Zinc	Mutants develop idiopathic scoliosis-like phenotypes and display abnormal vertebral development, delayed growth and decreased motor activity	(Haller et al., 2018)
ZIP14	Zinc	Mutants develop Mn overload and impaired locomotor activity.	(Tuschl et al., 2016)

* Note the some of the metal transporters are known to transport multiple metals (please see main text for details). DMT1, divalent metal transporter 1; FPN1, ferroportin 1; Frrs, ferric reductase; Tf, transferrin; TfR, transferrin receptor; Mfrn, mitoferrin; CTR1, copper transporter 1; ATP7, copper transporting ATPase; ZnT, zinc transporter; ZIP, Zrt- and Irt-like protein.

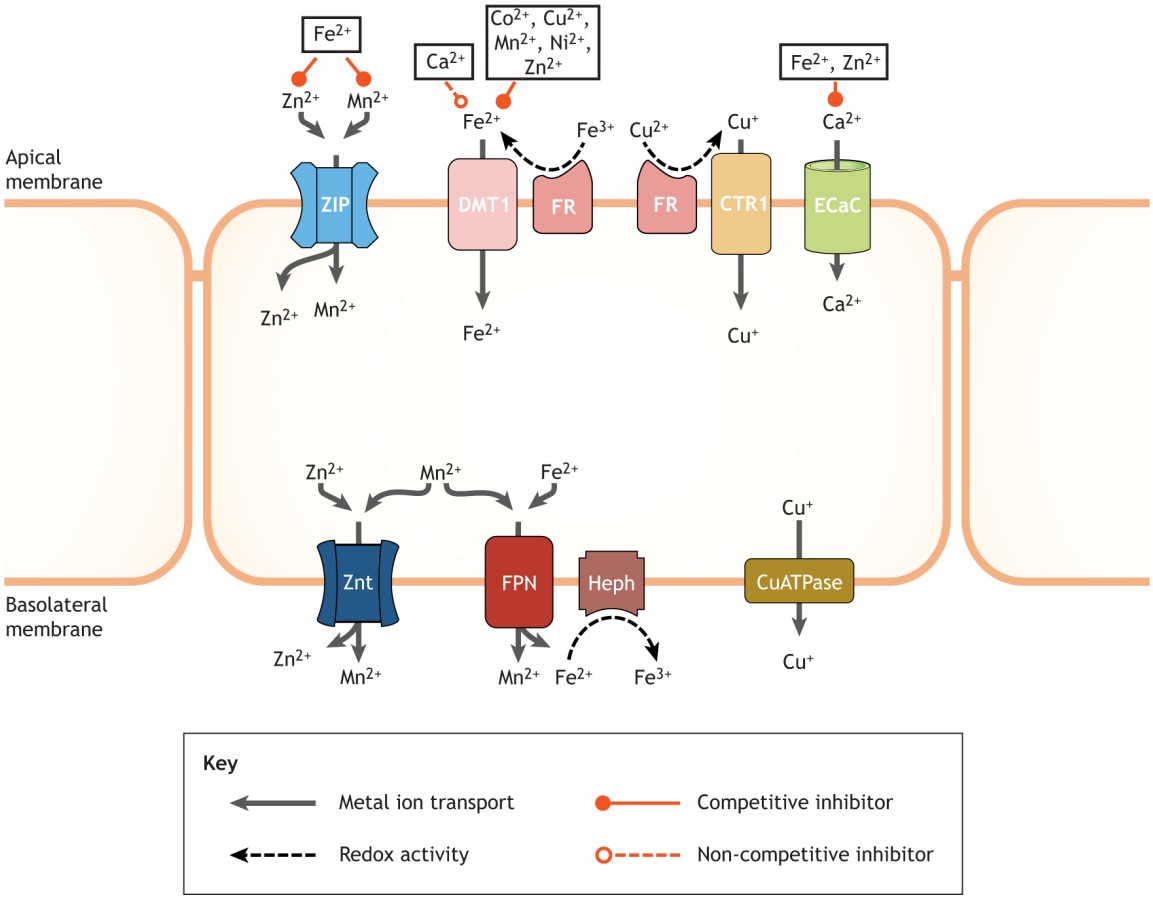

Figure 1-1. Proposed model for the transport and interactions among essential trace metals in the transport epithelia of fish. There are complex interactions among trace metals in the process of transepithelial transport. The interactions can be competitive (solid orange lines) or non-competitive (dashed orange line). ZIP, Zrt- and Irt-like proteins (i.e. ZIP8 and ZIP14); DMT1, divalent metal transporter-1; FR, ferric reductase; CTR1, copper transporter-1; ECaC, epithelial calcium channel; ZnT, zinc transporter; FPN, ferroportin; Heph, hephaestin; CuATPase, copper transporting ATPase. Illustrated by Dr. Chun Chih Chen.

1.3.3 *Cellular and systemic handling of essential trace metals*

In vertebrates, including fish, ferritin and transferrin regulate intracellular iron storage and iron delivery to various tissues, respectively (Bury et al., 2011). Their levels and binding capacities are known to be induced by iron exposure in fish (Carriquiriborde et al., 2003; Kwong et al., 2013). Recent advances with size or subcellular fractionation have provided some new information on the distribution of trace metals among cytosolic proteins within a cell. For example, in the liver of European chub (*Squalius cephalus*), it was suggested that copper was predominantly associated with metallothionein and, to a lesser extent, carbonic anhydrase and SOD (Krasnići et al., 2013). Iron appeared to be primarily bound to ferritin, whereas manganese was associated with albumin and transferrin (Krasnići et al., 2013). These results suggest that in addition to their interactions during absorption (see above), trace metals may also compete for binding sites within a cell or in circulation.

The delivery of copper in the blood is primarily mediated by ceruloplasmin (Das and Sahoo, 2018). In mammals, ceruloplasmin is also known to play an important role in systemic iron handling by oxidizing ferrous iron into ferric iron to facilitate its binding to transferrin (Hellman and Gitlin, 2002). Ceruloplasmin has been identified in various fish species, including icefish (*Chionodraco rastrospinosus*), Indian carp (*Aeromonas hydrophila*) and channel catfish (*Ictalurus punctatus*) (Liu et al., 2011; Sahoo et al., 2013; Scudiero et al., 2007). The mRNA expression level of ceruloplasmin has also been found to increase in channel catfish experiencing bacterial infection and iron overload (Liu et al., 2011). Copper is transported into cells by copper transporters (e.g. CTR1 and DMT1), and within the cell, virtually all free copper is sequestered by metal binding proteins including the copper chaperones (Kaplan and Maryon, 2016; Rae et al., 1999). The copper chaperones perform the dual functions of intracellular copper storage and trafficking. These

proteins include the antioxidant 1 copper chaperone (ATOX1) for transporting copper to copper-ATPase in the Golgi network, the cytoplasmic copper chaperone (also called copper chaperone for superoxide dismutase; CCS) for delivering copper to SOD, and cytochrome c oxidase copper chaperone (i.e. COX17) for delivering copper to cytochrome c oxidase in the mitochrondria (Cheng et al., 2017; Kwok and Chan, 2019; Leung et al., 2014).

Our current understanding of the signalling pathways (e.g. initiation of transcription, post-translational modifications) involved in trace metal regulation is primarily derived from studies from mammalian counterparts. Several iron transport- and metabolism-related proteins, including DMT1, ferroportin, ferritin and transferrin receptors, can be regulated post-transcriptionally. These proteins have an iron-responsive element (IRE) located either on the 3′- or 5′-untranslated region of the mRNA (Eisenstein, 2000). This region allows for the binding of iron regulatory proteins (IRPs) to the IRE, which can alter mRNA stability and translation of these proteins. IRPs can act as either a translational activator (e.g. binding to the 3′-end of an mRNA to protect against endonuclease cleavage) or a translational inhibitor (e.g. binding to the 5′-end of an mRNA to block the translation process) (Pantopoulos, 2004) (Figure 1-2). Another mechanism to regulate the expression of metal storage proteins is the activation of the metal-responsive element (i.e. DNA-binding motif) by the zinc finger metal-responsive transcription factor (i.e. MTF1). Such induction enhances the transcription of the metal-binding protein metallothionein (MT) to store excess zinc and copper (Chen et al., 2020; Tapia et al., 2004). The induction of MT by excess zinc and copper and its role in sequestering free metals are well documented in fish (Bervoets et al., 2013; De Boeck et al., 2003b; Hashemi et al., 2008; McDonald et al., 2021; Wang et al., 2014). However, the mechanism underpinning MTF1–MT activiation by metals is not completely understood. Mulitple models for MTF1–MT activiation have been proposed, including: (i) direct activation of

MTF1 by excess zinc in the cytosol, (ii) displacement of zinc from MT by other metals, (iii) stimulation of MTF1 phosphorylation and thereby its transactivation activity, and (iv) promotion of MTF1 translocation to the nucleus through conformational changes and uncovering of the nuclear localization motif (LaRochelle et al., 2001; Smirnova et al., 2000; Wang et al., 2014).

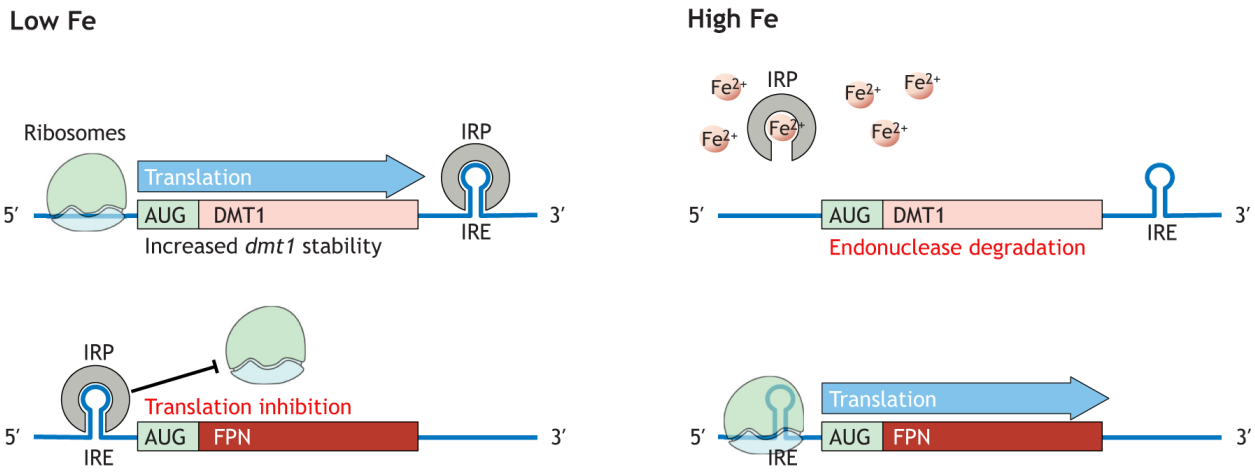

Figure 1-2. Cellular sensing and signalling mechanisms in the regulation of the expression of metal transport- and metabolism-related proteins. Several iron transport- and metabolism-related proteins can be regulated post-transcriptionally through the actions between the iron-regulatory protein (IRP) and iron-responsive element (IRE). The IRE is located either in the 3′- or 5′-untranslated regions of the mRNA. This region allows for the binding of IRP to the IRE, which can alter mRNA stability and translation for these proteins. IRP can act as either a translational activator (e.g. binding to the 3′-end of an mRNA to protect against endonuclease cleavage) or a translational inhibitor (e.g. binding to the 5′-end of an mRNA to block the translation process). Alternatively, excess iron may bind to IRP, which prevents IRP from acting on the IRE. Divalent metal transport-1 (DMT1) and ferroportin (FPN) are used as examples in this illustration. AUG denotes the start codon. Illustrated by Dr. Chun Chih Chen.

Certain metals can also be regulated by hormones. For example, hepcidin is a peptide hormone that acts as a central regulator of iron homeostasis. It functions by promoting the internalization and degradation of ferroportin at the basolateral membrane during iron overload (Nemeth et al., 2004). In both mammals and fish, hepcidin is primarily synthesized in the liver (Chandrapalan and Kwong, 2020; Nemeth et al., 2004). Several studies have suggested that the mRNA expression of hepcidin is positively regulated by iron in fish (e.g. Neves et al., 2017; Wang and Wang, 2016). Likewise, microinjection of hepcidin cRNA decreases whole-body iron content in zebrafish experiencing iron overload (Jiang et al., 2019). Moreover, intraperitoneal injection of adrenaline or triiodothyronine (T_3) has been found to reduce the activity of ferric reductase in various organs of climbing perch (*Anabas testudineus*), and the effects appeared to be dependent on the feeding status of fish (Rejitha and Peter, 2013). Several previous studies have also shown that trace metal exposure can affect the production of the stress hormone cortisol in fish (Gagnon et al., 2006; Tellis et al., 2012); however, whether cortisol can directly influence metal transport has not been fully characterized. Interestingly, cortisol is reported to reduce copper absorption by common carp (De Boeck et al., 2003a), whereas it stimulates zinc uptake in rainbow trout (Bury et al., 2008). These results suggest that cortisol may have different effects on the uptake of different metals. Alternatively, cortisol is known to promote major ion uptake by increasing the expression of ion transporters and the density of ion-transporting cells, including those that facilitate the uptake of calcium and sodium (Guh et al., 2015; Kwong et al., 2016a). These pathways may also mediate the uptake of essential trace metals (see above). Additionally, there is emerging evidence from mammalian studies that the status of essential metals in the body may affect various endocrine systems, such as iron in gastrin activity and copper in oxytocin signalling (Stevenson et

al., 2019). The mechanism underlying the interplay between essential trace metals and hormonal status in fish is a relatively poorly studied area and requires further characterization.

1.4 **Abiotic factors influencing metal regulation and homeostasis**

The regulation of essential trace metals can be influenced by many environmental/abiotic factors. The effects of water chemistry (e.g. water pH, hardness, dissolved organic matter) on the branchial uptake of trace metals are primarily due to its influence on metal bioavailability and are often discussed in the context of toxicology. In this section, we provide an overview of our understanding of the influence of temperature, dissolved oxygen content and GIT chemistry/diet composition on the transport and metabolism of essential metals in fish.

The temperature in aquatic environments fluctuates throughout the day according to the day/night cycle and seasonally, and could also be affected by climate change. Many studies have demonstrated that trace metal absorption is positively related to water temperature in fish. For example, zebrafish conditioned to elevated water temperature exhibited an increase in copper accumulation (Pilehvar et al., 2019). Similarly, zinc uptake was found to increase in rainbow trout acclimated to increased water temperature (Glover et al., 2003). In common carp and turbot (*Scophthalmus maximus*), the assimilation efficiency of dietary zinc was shown to increase with increasing water temperature (Pouil et al., 2018; Van Campenhout et al., 2007). One possible reason for the increased metal absorption at higher temperatures could be associated with the general increase in metabolic activities and ventilation rates. For instance, when metabolic parameters were compared in common carp at 10°C and 20°C, standard metabolic rate, maximum metabolic rate and aerobic scope were elevated at the higher temperature (Pillet et al., 2021). In female zebrafish, increases in water temperature induce the hepatic expression of metallothioneins, but not *ctr1* nor *zip8* (Guo et al., 2018b). In contrast, a transient increase in the branchial expression

of *ctr1* was observed in common carp during acclimation to increased water temperature (Castaldo et al., 2021). In another study with common carp, however, changes in water temperature were found to have no effect on copper and zinc accumulation in the gill (Pillet et al., 2021). Therefore, it seems likely that changes in water temperature may affect the expression of metal transporters in a tissue-specific manner and that different species may have different capacities to regulate and maintain trace metal balance during acclimation to elevated water temperature. Additionally, the different responses to temperature stress can also be attributed to differences in acclimation duration and the magnitude of temperature changes. Interestingly, cold stress was also found to increase the mRNA abundance of ceruloplasmin, transferrin and metalloreductase (i.e. steap3; reduces both Fe^{3+} and Cu^{2+} ions) in zebrafish larvae (Long et al., 2015). These proteins facilitate metal transport in the circulatory system and endosomal entry of metals into cells; however, the physiological significance of these increases by cold stress requires further study. Finally, the temperature can have indirect effects on the absorption of trace metals from the GIT. For example, an increase in temperature is known to affect GIT physiology by altering phospholipid membrane compositions and intestinal barrier function in fish (Fadhlaoui and Couture, 2016; Sundh et al., 2010).

In mammals, exposure to hypoxia can induce the expression of a variety of iron transport-related proteins through the activation of the hypoxia-inducible factors (HIF) (Renassia and Peyssonnaux, 2019). The increases in iron transport-related proteins (e.g. DMT1, transferrin receptor) by hypoxia are probably due to the increases in iron demand for enhancing oxygen transport capacity (Renassia and Peyssonnaux, 2019). Direct evidence that links the HIF-signalling pathway to micronutrient balance in fish is currently limited to ionic regulation (e.g. calcium) (Kwong et al., 2016b); nevertheless, because HIF signalling is highly conserved among

vertebrates, this signalling pathway is also thought to control the expression of iron transport proteins in fish (Pelster and Egg, 2018). In agreement with this hypothesis, a study with larval zebrafish has shown that hypoxia exposure increases mRNA expression of transferrin, metalloreductase and ceruloplasmin (Long et al., 2015). Genes that are involved in oxygen transport and the heme biosynthesis process are also induced by hypoxic treatment (Long et al., 2015). Interestingly, reduction in dissolved oxygen does not affect iron uptake across the skin and GIT of Pacific hagfish, likely because of their tolerance to hypoxic conditions (Glover et al., 2016).

The transport and metabolism of metals are influenced by the chemistry in the GIT. For example, in rainbow trout, the intestinal absorption of copper was found to decrease when luminal pH was increased from 7.4 to 8.0 (Nadella et al., 2007). Similarly, a reduction in intestinal iron absorption was observed when luminal pH was raised to a more alkaline condition (Kwong et al., 2010). In contrast, the presence of the reducing agent ascorbic acid, which promotes the conversion from ferric iron to ferrous iron, was shown to enhance the intestinal uptake of iron in various fish species including rainbow trout, European flounder and gulf toadfish (*Opsanus beta*) (Bury et al., 2001; Cooper et al., 2006b; Kwong and Niyogi, 2008). These observations are likely a result of the transport properties of DMT1 (a Fe^{2+}/H^{+} symporter), which preferentially transports divalent metals and is driven by a proton gradient (Gunshin et al., 1997). In Atlantic salmon, dietary supplementation with long-chain polyunsaturated fatty acids of the n-3 family [eicosapentaenoic acid/docosahexaenoic acid (EPA/DHA)] has been found to reduce hepatic iron content, which appears to be associated with a decrease in the mRNA abundance of transferrin and ferritin in the liver (Rørvik et al., 2003). In rainbow trout, it has also been suggested that copper–histidine and zinc–histidine complexes can be directly absorbed through specific amino acid transporters

(Glover and Wood, 2008; Glover et al., 2003). These results indicated that diet composition has a significant impact on trace metal uptake and metabolism in fish.

1.5 **Conclusions and perspectives**

Iron, copper, zinc and manganese are constituents of an array of metalloproteins and act as cofactors to facilitate various enzymatic reactions. They are also involved in a variety of biological processes, including development, oxygen transport and the immune response. In fish, their uptake may occur through specific metal transporters and via major ion transporters. These trace metals can interact at multiple biological levels from transepithelial transport to intracellular and systemic handling. Their interactions may also influence the function and expression of various metal transport- and metabolism-related proteins. All of this crosstalk may subsequently influence the whole-body homeostasis of trace metals in fish. Recent research efforts have revealed the complex processes involved in the regulation of trace metal homeostasis in fish. However, it is still unclear how the various metal transport pathways in the gill and GIT coordinate to maintain trace metal balance in fish. To date, the molecular machinery in the transport and metabolism of essential trace metals in fish is not completely understood. For example, the functional involvement of specific metal transporters and their cellular/subcellular localization in various organs have not been fully characterized. Additionally, most of our understanding of metal–metal interactions in fish relies primarily on measuring changes in mRNA expression levels following exposure or kinetic analysis through competition study. Direct *in vivo* evidence showing the functional significance of specific metal transporters in metal metabolism and interactions in fish has remained limited. Among the metals discussed, the regulation of manganese homeostasis is much less understood (e.g. uptake mechanism and cellular/systemic handling) and should be addressed in future studies. Recent advances in functional genetics may prove beneficial to enhancing our knowledge of the molecular

pathways involved in trace metal homeostasis (Zimmer et al., 2019). This strategy may also have the potential for the discovery of novel compensatory mechanisms in response to trace metal dysregulation. Additionally, most previous studies on examining the influence of abiotic factors on trace metal homeostasis were primarily focused on the toxicology context, thus key knowledge gaps exist in how environmental stressors such as hypoxia and temperature affect the physiological regulation of metals. Moreover, our understanding of essential trace metal homeostasis is mostly limited to a few fish species, including some commercially important species and traditional model organisms such as zebrafish and rainbow trout. Fish in different habitats likely employ different physiological strategies to maintain trace metal balance, and therefore future research should address how the regulation of metal transport function may differ across species.

1.6 **Research aims and objectives**

1.6.1 Rationale

This thesis focuses on iron as the central trace element of interest, with an emphasis on its transport pathways and their interaction with the homeostasis of other trace elements in zebrafish. Iron is biologically indispensable, yet like most trace metals, it has both essential and toxic properties. At low concentrations, iron deficiency can result in anemia, while excessive levels can lead to systemic overload and reactive oxygen species (ROS) mediated toxicity. Consequently, fish must efficiently coordinate environmental iron availability with whole-body iron regulation to sustain health and survival.

Iron concentrations in freshwater environments fluctuate widely from severely limited to heavily contaminated and fish are often simultaneously challenged by additional stressors such as hypoxia, elevated temperature, and metal pollution. Although the diet is the primary source of iron absorption in most fish, the consequences of dietary iron exposure at environmentally relevant concentrations remain poorly understood. Furthermore, the mechanisms of dietary iron uptake and its interaction with other trace elements including zinc, copper, nickel, manganese, cobalt, and selenium are not fully characterized.

In addition to its role in cellular metabolism, iron status can affect physiology and performance traits that are directly linked to ecological fitness and survival. For example, swimming performance is an integrative measure of aerobic capacity and metabolic efficiency, both of which depend on an adequate supply of iron for hemoglobin synthesis, mitochondrial function, and energy metabolism. However, few studies have directly examined how dietary iron may affect swimming performance in fish. Similarly, reproductive success represents another

ecologically relevant measure that is also dependent on iron status (i.e., gametogenesis and embryonic development); however, little is known about how parental dietary iron exposures may affect fecundity, offspring survival, or if they can elicit intergenerational consequences.

To elucidate the mechanisms underlying iron homeostasis and physiological performance, it is important to understand the molecular mechanisms of iron uptake. Notably, DMT1, which is recognized as the principal iron transporter, exhibits broad substrate specificity *in vitro*. However, its *in vivo* role in maintaining trace metal balance in fish remains unexplored. Together, elucidating the effects of environmentally relevant dietary iron exposure has ecological importance (fish survival and fitness under variable environmental iron), and the establishment of a *dmt1* knockout (*dmt1*$^{-/-}$) zebrafish model offers a valuable tool to discern the molecular mechanisms of iron uptake, coordinated multi-metal homeostasis, and potential compensatory responses.

1.6.2 Hypotheses

This thesis tests the following hypotheses:

1. Dietary iron concentrations affect key determinants of zebrafish survival and fitness, including swimming capacity, metabolic rate, and reproductive performance.
2. In zebrafish, dietary iron exposure and accumulation exert broad effects on multi-metal balance and extend across generations.
3. Zebrafish DMT1 is critical for iron metabolism but also contributes to the regulation of other trace metals.
4. In zebrafish, the loss of DMT1 function will elicit compensatory responses through altered expression of alternate trace metal transporters and iron regulatory pathways.

1.6.3 Experimental model

Danio rerio (zebrafish) represents a well-established model for studying vertebrate physiology, development, and environmental biology. As a freshwater teleost, they are an ecologically relevant model to investigate the impact of fluctuating iron levels in freshwater ecosystems. Zebrafish share highly conserved metal transport and regulatory pathways with other vertebrates, which enhances the translational significance of research findings. Their optical transparency during early development enables direct visualization of developmental processes such as hematopoiesis and their rapid life cycle and high fecundity are useful for multi-generational studies. Zebrafish are also highly amenable to genetic manipulation like CRISPR-Cas9, allowing targeted knockouts to explore protein function *in vivo*. Furthermore, zebrafish are internationally recognized by the OECD as a standard organism for ecotoxicological testing, making them a valuable model to investigate dietary iron exposure and multi-metal homeostasis. Together, these attributes make zebrafish a powerful model organism to integrate ecological, physiological, and molecular endpoints in this study.

1.6.4 Objectives

The overarching goal of this thesis is to determine the effects of dietary iron exposure in fish from both ecological and physiological perspectives, and to uncover the molecular mechanisms of iron uptake, multi-metal homeostasis, and compensatory gene regulation. The specific research objectives are outlined below:

Objective #1: Assess the effects of dietary iron on swimming performance, metabolism, and intergenerational metal accumulation (Chapter 2)

Adult zebrafish were exposed to diets containing low, control, or high levels of iron for 20 days (short-term) or 40 days (long-term). To identify the broad effects of dietary iron exposure on key determinants of survival and fitness, physiological indices, metal accumulation, swimming performance, and reproductive output were evaluated. To assess intergenerational consequences, offspring of iron-exposed parents were subsequently subjected to the same dietary treatment, and their swimming and metabolic parameters were compared to parents.

Objective #2: Characterize the physiological significance of the iron transporter DMT1 in zebrafish (Chapter 3)

A CRISPR-Cas9 knockout of *dmt1* was generated to establish a novel *in vivo* model in fish. Morphological traits, physiological performance, and trace metal homeostasis were characterized in *dmt1*$^{-/-}$ mutants during early development and in adulthood. Potential compensatory mechanisms employed by *dmt1*$^{-/-}$ fish were assessed through expression profiling of alternate iron uptake pathways.

Objective #3: Conduct transcriptomic analysis of major iron uptake tissues in wildtype and dmt1$^{-/-}$ *zebrafish (Chapter 4)*

RNA-sequencing was performed on the gill and intestine as the two primary sites of iron absorption to examine the genome-wide transcriptional responses to *dmt1* knockout. These analyses aimed to uncover the molecular mechanisms underlying iron and trace metal regulation, and to provide insight into the survival and functional resilience of *dmt1*$^{-/-}$ fish.

1.6.5 Significance of research

This thesis addresses critical gaps in our understanding of dietary iron regulation and its interaction with other trace metals in fishes. By integrating physiological, ecological, and molecular approaches, it establishes the first *in vivo* model to investigate the functional role of DMT1 in trace metal homeostasis. The result of this thesis has broad significance: it will advance fundamental knowledge of vertebrate iron metabolism, provide mechanistic insight into how fishes adjust to fluctuating metal environments, and inform environmental monitoring and aquaculture practices. More broadly, this research contributes to comparative physiology by identifying conserved and compensatory pathways that may be relevant across taxa.

1.7 **References**

Aliko, V., Qirjo, M., Sula, E., Morina, V. and Faggio, C. (2018). Antioxidant defense system, immune response and erythron profile modulation in gold fish, *Carassius auratus*, after acute manganese treatment. Fish Shellfish Immunol. 76, 101-109. https://doi.org/10.1016/j.fsi.2018.02.042

Antony Jesu Prabhu, P., Silva, M. S., Kröeckel, S., Holme, M. H., Ørnsrud, R., Amlund, H., Lock, E. J. and Waagbø, R. (2019). Effect of levels and sources of dietary manganese on growth and mineral composition of post-smolt Atlantic salmon fed low fish meal, plant-based ingredient diets. Aquaculture 512, 734287. https://doi.org/10.1016/j.aquaculture.2019.734287

Arredondo, M., Muñoz, P., Mura, C. V. and Núñez, M. T. (2003). DMT1, a physiologically relevant apical $Cu1^{+}$ transporter of intestinal cells. Am. J. Physiol. Cell Physiol. 284, C1525-C1530. https://doi.org/10.1152/ajpcell.00480.2002

Baker, Z. N., Cobine, P. A. and Leary, S. C. (2017). The mitochondrion: a central architect of copper homeostasis. Metallomics 9, 1501-1512. https://doi.org/10.1039/c7mt00221a

Bakthavatsalam, S., Sharma, S. D., Sonawane, M., Thirumalai, V. and Datta, A. (2014). A zebrafish model of manganism reveals reversible and treatable symptoms that are independent of neurotoxicity. Dis. Model. Mech. 7, 1239-1251. https://doi.org/10.1242/dmm.016683

Beaver, L. M., Nkrumah-Elie, Y. M., Truong, L., Barton, C. L., Knecht, A. L., Gonnerman, G. D., Wong, C. P., Tanguay, R. L. and Ho, E. (2017). Adverse effects of parental zinc

deficiency on metal homeostasis and embryonic development in a zebrafish model. J. Nutr. Biochem. 43, 78-87. https://doi.org/10.1016/j.jnutbio.2017.02.006

Bervoets, L., Knapen, D., De Jonge, M., Van Campenhout, K. and Blust, R. (2013). Differential hepatic metal and metallothionein levels in three feral fish species along a metal pollution gradient. PLoS ONE 8, 60805. https://doi.org/10.1371/journal.pone.0060805

Bo, L., Liu, Z., Zhong, Y., Huang, J., Chen, B., Wang, H. and Xu, Y. (2016). Iron deficiency anemia's effect on bone formation in zebrafish mutant. Biochem. Biophys. Res. Commun. 475, 271-276. https://doi.org/10.1016/j.bbrc.2016.05.069

Bourassa, D., Gleber, S.-C., Vogt, S., Yi, H., Will, F., Richter, H., Shin, C. H. and Fahrni, C. J. (2014). 3D imaging of transition metals in the zebrafish embryo by X-ray fluorescence microtomography. Metallomics 6, 1648-1655. https://doi.org/10.1039/c4mt00121d

Bury, N. (2003). Iron acquisition by teleost fish. Comp. Biochem. Physiol. C 135, 97-105. https://doi.org/10.1016/S1532-0456(03)00021-8

Bury, N. R. and Glover, C. N. (2003). Nutritive metal uptake in teleost fish. J. Exp. Biol. 206, 11-23. https://doi.org/10.1242/jeb.00068

Bury, N. R., Grosell, M., Wood, C. M., Hogstrand, C., Wilson, R. W., Rankin, J. C., Busk, M., Lecklin, T. and Jensen, F. B. (2001). Intestinal iron uptake in the European flounder (*Platichthys flesus*). J. Exp. Biol. 204, 3779-3787. https://doi.org/10.1242/jeb.204.21.3779

Bury, N. R., Chung, M. J., Sturm, A., Walker, P. A. and Hogstrand, C. (2008). Cortisol stimulates the zinc signaling pathway and expression of metallothioneins and ZnT1 in rainbow trout

gill epithelial cells. Am. J. Physiol. Regul. Integr. Comp. Physiol. 294, 623-629. https://doi.org/10.1152/ajpregu.00646.2007

Bury, N. R., Boyle, D. and Cooper, C. A. (2011). Iron. In Fish Physiology (ed. C. M. Wood, A. P. Farrell and C. J. Brauner), pp. 201-251. Academic Press.

Carriquiriborde, P., Handy, R. D. and Davies, S. (2003). Physiological modulation of iron metabolism in rainbow trout (*Oncorhynchus mykiss*) fed low and high iron diets. J. Exp. Biol. 207, 75-86. https://doi.org/10.1242/jeb.00712

Carvalho, L. and Heisenberg, C. P. (2010). The yolk syncytial layer in early zebrafish development. Trends Cell Biol. 20, 586-592. https://doi.org/10.1016/j.tcb.2010.06.009

Castaldo, G., Pillet, M., Ameryckx, L., Bervoets, L., Town, R. M., Blust, R. and De Boeck, G. (2021). Temperature effects during a sublethal chronic metal mixture exposure on common carp (*Cyprinus carpio*). Front. Physiol. 12, 1-16. https://doi.org/10.3389/fphys.2021.651584

Chanda, S., Paul, B. N., Ghosh, K. and Giri, S. S. (2015). Dietary essentiality of trace minerals in aquaculture-A Review. Agric. Rev. 36, 100-112. https://doi.org/10.5958/0976-0741.2015.00012.4

Chandrapalan, T. and Kwong, R. W. M. (2020). Influence of dietary iron exposure on trace metal homeostasis and expression of metal transporters during development in zebrafish. Environ. Pollut. 261, 114159. https://doi.org/10.1016/j.envpol.2020.114159

Chen, Q. L., Luo, Z., Wu, K., Huang, C., Zhuo, M. Q., Song, Y. F. and Hu, W. (2015). Differential effects of dietary copper deficiency and excess on lipid metabolism in yellow

catfish Pelteobagrus fulvidraco. Comp. Biochem. Physiol. B Biochem. Mol. Biol. 184, 19-28. https://doi.org/10.1016/j.cbpb.2015.02.004

Chen, J., Jiang, Y., Shi, H., Peng, Y., Fan, X. and Li, C. (2020). The molecular mechanisms of copper metabolism and its roles in human diseases. Pflugers Arch. Eur. J. Physiol. 472, 1415-1429. https://doi.org/10.1007/s00424-020-02412-2

Cheng, J., Luo, Z., Chen, G. H., Wei, C. C. and Zhuo, M. Q. (2017). Identification of eight copper (Cu) uptake related genes from yellow catfish *Pelteobagrus fulvidraco*, and their tissue expression and transcriptional responses to dietborne Cu exposure. J. Trace Elem. Med. Biol. 44, 256-265. https://doi.org/10.1016/j.jtemb.2017.09.004

Clearwater, S. J., Farag, A. M. and Meyer, J. S. (2002). Bioavailability and toxicity of dietborne copper and zinc to fish. Comp. Biochem. Physiol. C Toxicol. Pharmacol. 132, 269-313. https://doi.org/10.1016/S1532-0456(02)00078-9

Cooper, C. A., Handy, R. D. and Bury, N. R. (2006a). The effects of dietary iron concentration on gastrointestinal and branchial assimilation of both iron and cadmium in zebrafish (*Danio rerio*). Aquat. Toxicol. 79, 167-175. https://doi.org/10.1016/j.aquatox.2006.06.008

Cooper, C. A., Bury, N. R. and Grosell, M. (2006b). The effects of pH and the iron redox state on iron uptake in the intestine of a marine teleost fish, gulf toadfish (*Opsanus beta*). Comp. Biochem. Physiol. A Mol. Integr. Physiol. 143, 292-298. https://doi.org/10.1016/j.cbpa.2005.11.024

Cooper, C. A., Shayeghi, M., Techau, M. E., Capdevila, D. M., MacKenzie, S., Durrant, C. and Bury, N. R. (2007). Analysis of the rainbow trout solute carrier 11 family reveals iron

import ⩽ pH 7.4 and a functional isoform lacking transmembrane domains 11 and 12. FEBS Lett. 581, 2599-2604. https://doi.org/10.1016/j.febslet.2007.04.081

Craig, P. M., Galus, M., Wood, C. M. and McClelland, G. B. (2008). Dietary iron alters waterborne copper-induced gene expression in soft water acclimated zebrafish (*Danio rerio*). AJP Regul. Integr. Comp. Physiol. 296, R362-R373. https://doi.org/10.1152/ajpregu.90581.2008

Cuesta, A., Meseguer, J. and Esteban, M. Á. (2008). The antimicrobial peptide hepcidin exerts an important role in the innate immunity against bacteria in the bony fish gilthead seabream. Mol. Immunol. 45, 2333-2342. https://doi.org/10.1016/j.molimm.2007.11.007

Dalziel, A. C., Moyes, C. D., Fredriksson, E. and Lougheed, S. C. (2006). Molecular evolution of cytochrome c oxidase in high-performance fish (Teleostei: Scombroidei). J. Mol. Evol. 62, 319-331. https://doi.org/10.1007/s00239-005-0110-7

Das, S. and Sahoo, P. K. (2018). Ceruloplasmin, a moonlighting protein in fish. Fish Shellfish Immunol. 82, 460-468. https://doi.org/10.1016/j.fsi.2018.08.043

Davis, D. A. and Gatlin, D. M. (1996). Dietary mineral requirements of fish and marine crustaceans. Rev. Fish. Sci. 4, 75-99. https://doi.org/10.1080/10641269609388579

De Boeck, G., De Wachter, B., Vlaeminck, A. and Blust, R. (2003a). Effect of cortisol treatment and/or sublethal copper exposure on copper uptake and heat shock protein levels in common carp*, Cyprinus carpio*. Environ. Toxicol. Chem. 22, 1122-1126. https://doi.org/10.1002/etc.5620220521

De Boeck, G., Ngo, T. T. H., Van Campenhout, K. and Blust, R. (2003b). Differential metallothionein induction patterns in three freshwater fish during sublethal copper exposure. Aquat. Toxicol. 65, 413-424. https://doi.org/10.1016/S0166-445X(03)00178-4

Deforest, D. K. and Meyer, J. S. (2015). Critical review: toxicity of dietborne metals to aquatic organisms. Crit. Rev. Environ. Sci. Technol. 45, 1176-1241. https://doi.org/10.1080/10643389.2014.955626

de Souza, P. C. and Bonilla-Rodriguez, G. O. (2007). Fish hemoglobins. Brazilian J. Med. Biol. Res. 40, 769-778. https://doi.org/10.1590/s0100-879x2007000600004

Do, J. W., Saravanan, M., Nam, S. E., Lim, H. J. and Rhee, J. S. (2019). Waterborne manganese modulates immunity, biochemical, and antioxidant parameters in the blood of red seabream and black rockfish. Fish Shellfish Immunol. 88, 546-555. https://doi.org/10.1016/j.fsi.2019.03.020

Donovan, A., Brownlie, A., Zhou, Y., Shepard, J., Pratt, S. J., Moynihan, J., Paw, B. H., Drejer, A., Barut, B., Zapata, A.et al. (2000). Positional cloning of zebrafish ferroportin1 identifies a conserved vertebrate iron exporter. Nature 403, 776-781. https://doi.org/10.1038/35001596

Donovan, A., Brownlie, A., Dorschner, M. O., Zhou, Y., Pratt, S. J., Paw, B. H., Phillips, R. B., Thisse, C., Thisse, B., Zon, L. I. (2002). The zebrafish mutant gene chardonnay (*cdy*) encodes divalent metal transporter 1 (DMT1). Blood 100, 4655-4659. https://doi.org/10.1182/blood-2002-04-1169

Donovan, A., Lima, C. A., Pinkus, J. L., Pinkus, G. S., Zon, L. I., Robine, S. and Andrews, N. C. (2005). The iron exporter ferroportin/Slc40a1 is essential for iron homeostasis. Cell Metab. 1, 191-200. https://doi.org/10.1016/j.cmet.2005.01.003

Drakesmith, H. and Prentice, A. M. (2012). Hepcidin and the iron-infection axis. Science (80-.) 338, 768-772. https://doi.org/10.1126/science.1224577

Dymowska, A. K., Boyle, D., Schultz, A. G. and Goss, G. G. (2015). The role of acid-sensing ion channels in epithelial Na^+ uptake in adult zebrafish (*Danio rerio*). J. Exp. Biol. 218, 1244-1251. https://doi.org/10.1242/jeb.113118

Eisenstein, R. S. (2000). Iron regulatory proteins and the molecular control of mammalian iron metabolism. Annu. Rev. Phys. Chem. 51, 355-380. https://doi.org/10.1146/annurev.physchem.51.1.355

Elvitigala, D. A. S., Premachandra, H. K. A., Whang, I., Oh, M. J., Jung, S. J., Park, C. J. and Lee, J. (2013). A teleostean counterpart of ferritin M subunit from rock bream (*Oplegnathus fasciatus*): an active constituent in iron chelation and DNA protection against oxidative damage, with a modulated expression upon pathogen stress. Fish Shellfish Immunol. 35, 1455-1465. https://doi.org/10.1016/j.fsi.2013.08.012

Fadhlaoui, M. and Couture, P. (2016). Combined effects of temperature and metal exposure on the fatty acid composition of cell membranes, antioxidant enzyme activities and lipid peroxidation in yellow perch (*Perca flavescens*). Aquat. Toxicol. 180, 45-55. https://doi.org/10.1016/j.aquatox.2016.09.005

Fraenkel, P. G., Traver, D., Donovan, A., Zahrieh, D. and Zon, L. I. (2005). Ferroportin1 is required for normal iron cycling in zebrafish. J. Clin. Invest. 115, 1532-1541. https://doi.org/10.1172/jci23780

Fraenkel, P. G., Gibert, Y., Holzheimer, J. L., Lattanzi, V. J., Burnett, S. F., Dooley, K. A., Wingert, R. A. and Zon, L. I. (2009). Transferrin-a modulates hepcidin expression in zebrafish embryos. Blood 113, 2843-2850. https://doi.org/10.1182/blood-2008-06-165340

Gagnon, A., Jumarie, C. and Hontela, A. (2006). Effects of Cu on plasma cortisol and cortisol secretion by adrenocortical cells of rainbow trout (*Oncorhynchus mykiss*). Aquat. Toxicol. 78, 59-65. https://doi.org/10.1016/j.aquatox.2006.02.004

Gallaugher, P., Thorarensen, H. and Farrell, A. P. (1995). Hematocrit in oxygen transport and swimming in rainbow trout (*Oncorhynchus mykiss*). Respir. Physiol. 102, 279-292. https://doi.org/10.1016/0034-5687(95)00065-8

Gansner, J. M., Mendelsohn, B. A., Hultman, K. A., Johnson, S. L. and Gitlin, J. D. (2007). Essential role of lysyl oxidases in notochord development. Dev. Biol. 307, 202-213. https://doi.org/10.1016/j.ydbio.2007.04.029

Ganz, T. (2013). Systemic iron homeostasis. Physiol. Rev. 93, 1721-1741. https://doi.org/10.1152/physrev.00008.2013

Garrick, M. D., Dolan, K. G., Horbinski, C., Ghio, A. J., Higgins, D., Porubcin, M., Moore, E. G., Hainsworth, L. N., Umbreit, J. N., Conrad, M. E.et al. (2003). DMT1: A mammalian transporter for multiple metals. Biometals 16, 41-54. https://doi.org/10.1023/A:1020702213099

Glover, C. N. and Wood, C. M. (2008). Absorption of copper and copper-histidine complexes across the apical surface of freshwater rainbow trout intestine. J. Comp. Physiol. B Biochem. Syst. Environ. Physiol. 178, 101-109. https://doi.org/10.1007/s00360-007-0203-2

Glover, C. N., Bury, N. R. and Hogstrand, C. (2003). Zinc uptake across the apical membrane of freshwater rainbow trout intestine is mediated by high affinity, low affinity, and histidine-facilitated pathways. Biochim. Biophys. Acta Biomembr. 1614, 211-219.

Glover, C. N., Niyogi, S., Blewett, T. A. and Wood, C. M. (2016). Iron transport across the skin and gut epithelia of Pacific hagfish: kinetic characterisation and effect of hypoxia. Comp. Biochem. Physiol. A Mol. Integr. Physiol. 199, 1-7. https://doi.org/10.1016/j.cbpa.2016.04.018

Grillo, A. S., SantaMaria, A. M., Kafina, M. D., Cioffi, A. G., Huston, N. C., Han, M., Seo, Y. A., Yien, Y. Y., Nardone, C., Menon, A. V.et al. (2017). Restored iron transport by a small molecule promotes absorption and hemoglobinization in animals. Science (80-.) 356, 608-616. https://doi.org/10.1126/science.aah3862

Grosell, M. and Wood, C. M. (2002). Copper uptake across rainbow trout gills: mechanisms of apical entry. J. Exp. Biol. 205, 1179-1188. https://doi.org/10.1242/jeb.205.8.1179

Guh, Y.-J., Lin, C.-H. and Hwang, P.-P. (2015). Osmoregulation in zebrafish: ion transport mechanisms and functional regulation. EXCLI J. 14, 627-659.

Gunshin, H., Mackenzie, B., Berger, U. V., Gunshin, Y., Romero, M. F., Boron, W. F., Nussberger, S., Gollan, J. L. and Hediger, M. A. (1997). Cloning and characterization of a

mammalian proton-coupled metal-ion transporter. Nature 388, 482-488. https://doi.org/10.1038/41343

Guo, Z., Zhang, W., Du, S., Green, I., Tan, Q. and Zhang, L. (2016). Developmental patterns of copper bioaccumulation in a marine fish model *Oryzias melastigma*. Aquat. Toxicol. 170, 216-222. https://doi.org/10.1016/j.aquatox.2015.11.026

Guo, Y. L., Wu, P., Jiang, W. D., Liu, Y., Kuang, S. Y., Jiang, J., Tang, L., Tang, W. N., Zhang, Y. A., Zhou, X. Q.et al. (2018a). The impaired immune function and structural integrity by dietary iron deficiency or excess in gill of fish after infection with Flavobacterium columnare: regulation of NF-κB, TOR, JNK, p38MAPK, Nrf2 and MLCK signalling. Fish Shellfish Immunol. 74, 593-608. https://doi.org/10.1016/j.fsi.2018.01.027

Guo, S. N., Zheng, J. L., Yuan, S. S. and Zhu, Q. L. (2018b). Effects of heat and cadmium exposure on stress-related responses in the liver of female zebrafish: Heat increases cadmium toxicity. Sci. Total Environ. 618, 1363-1370. https://doi.org/10.1016/j.scitotenv.2017.09.264

Haller, G., McCall, K., Jenkitkasemwong, S., Sadler, B., Antunes, L., Nikolov, M., Whittle, J., Upshaw, Z., Shin, J., Baschal, E.et al. (2018). A missense variant in SLC39A8 is associated with severe idiopathic scoliosis. Nat. Commun. 9, 4171. https://doi.org/10.1038/s41467-018-06705-0

Handy, R. D., Musonda, M. M., Phillips, C. and Falla, S. J. (2000). Mechanisms of gastrointestinal copper absorption in the African walking catfish: copper dose-effects and a novel anion-dependent pathway in the intestine. J. Exp. Biol. 203, 2365-2377. https://doi.org/10.1242/jeb.203.15.2365

Handy, R. D., Eddy, F. B. and Baines, H. (2002). Sodium-dependent copper uptake across epithelia: a review of rationale with experimental evidence from gill and intestine. Biochim. Biophys. Acta Biomembr 1566, 104-115.

Harris, E. D. (1992). Copper as a cofactor and regulator of copper,zinc superoxide dismutase. J. Nutr. 122, 636-640. https://doi.org/10.1093/jn/122.suppl_3.636

Hashemi, S., Kunwar, P. S., Blust, R. and De Boeck, G. (2008). Differential metallothionein induction patterns in fed and starved carp (*Cyprinus carpio*) during waterborne copper exposure. Environ. Toxicol. Chem. 27, 2154-2158. https://doi.org/10.1897/07-502.1

Hassan, A. T. and Kwong, R. W. M. (2020). The neurophysiological effects of iron in early life stages of zebrafish. Environ. Pollut. 267, 115625. https://doi.org/10.1016/j.envpol.2020.115625

Hellman, N. E. and Gitlin, J. D. (2002). Ceruloplasmin metabolism and function. Annu. Rev. Nutr. 22, 439-458. https://doi.org/10.1146/annurev.nutr.22.012502.114457

Illing, A. C., Shawki, A., Cunningham, C. L. and Mackenzie, B. (2012). Substrate profile and metal-ion selectivity of human divalent metal-ion transporter-1. J. Biol. Chem. 287, 30485-30496. https://doi.org/10.1074/jbc.M112.364208

Ishizaki, H., Spitzer, M., Wildenhain, J., Anastasaki, C., Zeng, Z., Dolma, S., Shaw, M., Madsen, E., Gitlin, J., Marais, R.et al. (2010). Combined zebrafish-yeast chemical-genetic screens reveal gene–copper-nutrition interactions that modulate melanocyte pigmentation. Dis. Model. Mech. 3, 639-651. https://doi.org/10.1242/dmm.005769

Iyengar, V., Pullakhandam, R. and Nair, K. M. (2009). Iron-zinc interaction during uptake in human intestinal Caco-2 cell line: kinetic analyses and possible mechanism. Indian J. Biochem. Biophys. 46, 299-306.

Jiang, X. F., Liu, Z. F., Lin, A. F., Xiang, L. X. and Shao, J. Z. (2017). Coordination of bactericidal and iron regulatory functions of hepcidin in innate antimicrobial immunity in a zebrafish model. Sci. Rep. 7, 4265. https://doi.org/10.1038/s41598-017-04069-x

Jiang, Y., Chen, B., Yan, Y. and Zhu, G. X. (2019). Hepcidin protects against iron overload-induced inhibition of bone formation in zebrafish. Fish Physiol. Biochem. 45, 365-374. https://doi.org/10.1007/s10695-018-0568-z

Kamińska-Gibas, T., Szczygieł, J., Jurecka, P. and Irnazarow, I. (2020). The many faces of transferrin: does genotype modulate immune response? Fish Shellfish Immunol. 102, 511-518. https://doi.org/10.1016/j.fsi.2020.05.001

Kaplan, J. H. and Maryon, E. B. (2016). How mammalian cells acquire copper: an essential but potentially toxic metal. Biophys. J. 110, 7-13. https://doi.org/10.1016/j.bpj.2015.11.025

Krasnići, N., Dragun, Z., Erk, M. and Raspor, B. (2013). Distribution of selected essential (Co, Cu, Fe, Mn, Mo, Se, and Zn) and nonessential (Cd, Pb) trace elements among protein fractions from hepatic cytosol of European chub (*Squalius cephalus* L.). Environ. Sci. Pollut. Res. 20, 2340-2351. https://doi.org/10.1007/s11356-012-1105-8

Kumar, N., Krishnani, K. K., Kumar, P., Jha, A. K., Gupta, S. K. and Singh, N. P. (2017). Dietary zinc promotes immuno-biochemical plasticity and protects fish against multiple stresses. Fish Shellfish Immunol. 62, 184-194. https://doi.org/10.1016/j.fsi.2017.01.017

Kwok, M. L. and Chan, K. M. (2019). Functional characterization of copper transporters zCtr1, zAtox1, zAtp7a and zAtp7b in zebrafish liver cell line ZFL. Metallomics 11, 1532-1546. https://doi.org/10.1039/C9MT00159J

Kwong, R. W. M. and Niyogi, S. (2008). An in vitro examination of intestinal iron absorption in a freshwater teleost, rainbow trout (*Oncorhynchus mykiss*). J. Comp. Physiol. B Biochem. Syst. Environ. Physiol. 178, 963-975. https://doi.org/10.1007/s00360-008-0279-3

Kwong, R. W. M. and Niyogi, S. (2009). The interactions of iron with other divalent metals in the intestinal tract of a freshwater teleost, rainbow trout (*Oncorhynchus mykiss*). Comp. Biochem. Physiol. C 150, 442-449.

Kwong, R. W. M., Andrés, J. A. J. A. and Niyogi, S. (2010). Molecular evidence and physiological characterization of iron absorption in isolated enterocytes of rainbow trout (*Oncorhynchus mykiss*): Implications for dietary cadmium and lead absorption. Aquat. Toxicol. 99, 343-350. https://doi.org/10.1016/j.aquatox.2010.05.012

Kwong, R. W. M., Hamilton, C. D. C. D. and Niyogi, S. (2013). Effects of elevated dietary iron on the gastrointestinal expression of Nramp genes and iron homeostasis in rainbow trout (*Oncorhynchus mykiss*). Fish Physiol. Biochem. 39, 363-372. https://doi.org/10.1007/s10695-012-9705-2

Kwong, R. W. M., Auprix, D. and Perry, S. F. (2014). Involvement of the calcium-sensing receptor in calcium homeostasis in larval zebrafish exposed to low environmental calcium. Am. J. Physiol. Integr. Comp. Physiol. 306, R211-R221. https://doi.org/10.1152/ajpregu.00350.2013

Kwong, R. W. M., Kumai, Y. and Perry, S. F. (2016a). Neuroendocrine control of ionic balance in zebrafish. Gen. Comp. Endocrinol. 234, 40-46. https://doi.org/10.1016/j.ygcen.2016.05.016

Kwong, R. W. M., Kumai, Y., Tzaneva, V., Azzi, E., Hochhold, N., Robertson, C., Pelster, B. and Perry, S. F. (2016b). Inhibition of calcium uptake during hypoxia in developing zebrafish is mediated by hypoxia-inducible factor. J. Exp. Biol. 219, 3988-3995. https://doi.org/10.1242/jeb.148700

LaRochelle, O., Gagné, V., Charron, J., Soh, J. W. and Séguin, C. (2001). Phosphorylation is involved in the activation of metal-regulatory transcription factor I in response to metal ions. J. Biol. Chem. 276, 41879-41888. https://doi.org/10.1074/jbc.M108313200

Leung, K. P., Chen, D. and Chan, K. M. (2014). Understanding copper sensitivity in zebrafish (*Danio rerio*) through the intracellular localization of copper transporters in a hepatocyte cell-line ZFL and the tissue expression profiles of copper transporters. Metallomics 6, 1057-1067. https://doi.org/10.1039/C3MT00366C

Li, L. and Yang, X. (2018). The essential element manganese, oxidative stress, and metabolic diseases: links and interactions. Oxid. Med. Cell. Longev. 2018, 7580707.

Lin, C. H. and Hwang, P. P. (2016). The control of calcium metabolism in zebrafish (*Danio rerio*). Int. J. Mol. Sci. 17, 1783. https://doi.org/10.3390/ijms17111783

Liu, H., Peatman, E., Wang, W., Abernathy, J., Liu, S., Kucuktas, H., Terhune, J., Xu, D. H., Klesius, P. and Liu, Z. (2011). Molecular responses of ceruloplasmin to *Edwardsiella ictaluri* infection and iron overload in channel catfish (*Ictalurus punctatus*). Fish Shellfish Immunol. 30, 992-997. https://doi.org/10.1016/j.fsi.2010.12.033

Long, Y., Yan, J., Song, G., Li, X., Li, X., Li, Q. and Cui, Z. (2015). Transcriptional events co-regulated by hypoxia and cold stresses in Zebrafish larvae. BMC Genomics 16, 385. https://doi.org/10.1186/s12864-015-1560-y

Mackenzie, N. C., Brito, M., Reyes, A. E. and Allende, M. L. (2004). Cloning, expression pattern and essentiality of the high-affinity copper transporter 1 (*ctr1*) gene in zebrafish. Gene 328, 113-120. https://doi.org/10.1016/j.gene.2003.11.019

Madejczyk, M. S. and Ballatori, N. (2017). The iron transporter ferroportin can also function as a manganese exporter. Biochim. Biophys. Acta 1818, 651-657. https://doi.org/10.1016/j.bbamem.2011.12.002

Makwinja, R. and Geremew, A. (2020). Roles and requirements of trace elements in tilapia nutrition: review. Egypt. J. Aquat. Res. 46, 281-287. https://doi.org/10.1016/j.ejar.2020.05.001

Martínez, D., Oyarzún, R., Vargas-Lagos, C., Pontigo, J. P., Soto-Dávila, M., Saravia, J., Romero, A., Núñez, J. J., Yáñez, A. J. and Vargas-Chacoff, L. (2017). Identification, characterization and modulation of ferritin-H in the sub-Antarctic notothenioid *Eleginops maclovinus* challenged with *Piscirickettsia salmonis*. Dev. Comp. Immunol. 73, 88-96. https://doi.org/10.1016/j.dci.2017.03.015

Mathews, T. and Fisher, N. S. (2009). Dominance of dietary intake of metals in marine elasmobranch and teleost fish. Sci. Total Environ. 407, 5156-5161. https://doi.org/10.1016/j.scitotenv.2009.06.003

McCann, S., Amadó, M. P. and Moore, S. E. (2020). The role of iron in brain development: a systematic review. Nutrients 12, 2001. https://doi.org/10.3390/nu12072001

McDonald, S., Hassell, K. and Cresswell, T. (2021). Effect of short-term dietary exposure on metal assimilation and metallothionein induction in the estuarine fish Pseudogobius sp. Sci. Total Environ. 772, 145042. https://doi.org/10.1016/j.scitotenv.2021.145042

Mebane, C. A., Chowdhury, M. J., De Schamphelaere, K. A. C., Lofts, S., Paquin, P. R., Santore, R. C. and Wood, C. M. (2020). Metal bioavailability models: current status, lessons learned, considerations for regulatory use, and the path forward. Environ. Toxic. Chem. 39, 60-84. https://doi.org/10.1002/etc.4560

Mendelsohn, B. A., Yin, C., Johnson, S. L., Wilm, T. P., Solnica-Krezel, L. and Gitlin, J. D. (2006). Atp7a determines a hierarchy of copper metabolism essential for notochord development. Cell Metab. 4, 155-162. https://doi.org/10.1016/j.cmet.2006.05.001

Mi, X., Li, Z., Yan, J., Li, Y., Zheng, J., Zhaung, Z., Yang, W., Gong, L. and Shi, J. (2020). Activation of HIF-1 signaling ameliorates liver steatosis in zebrafish *atp7b* deficiency (Wilson's disease) models. Biochim. Biophys. Acta Mol. Basis Dis. 1866, 165842. https://doi.org/10.1016/j.bbadis.2020.165842

Moazenzadeh, K., Rajabi Islami, H., Zamini, A. and Soltani, M. (2020). Effect of dietary inorganic copper on growth performance and some hematological indices of Siberian sturgeon *Acipenser baerii* juveniles. N. Am. J. Aquac. 82, 200-207. https://doi.org/10.1002/naaq.10145

Muraina, I. A., Maret, W., Bury, N. R. and Hogstrand, C. (2020). Hatching gland development and hatching in zebrafish embryos: a role for zinc and its transporters Zip10 and Znt1a. Biochem. Biophys. Res. Commun. 528, 698-705. https://doi.org/10.1016/j.bbrc.2020.05.131

Nadella, S. R., Grosell, M. and Wood, C. M. (2007). Mechanisms of dietary Cu uptake in freshwater rainbow trout: evidence for Na-assisted Cu transport and a specific metal carrier in the intestine. J. Comp. Physiol. B Biochem. Syst. Environ. Physiol. 177, 433-446. https://doi.org/10.1007/s00360-006-0142-3

Nadella, S. R., Hung, C. C. Y. and Wood, C. M. (2011). Mechanistic characterization of gastric copper transport in rainbow trout. J. Comp. Physiol. B Biochem. Syst. Environ. Physiol. 181, 27-41. https://doi.org/10.1007/s00360-010-0510-x

Nemeth, E., Tuttle, M. S., Powelson, J., Vaughn, M. D., Donovan, A., Ward, D. M. V., Ganz, T. and Kaplan, J. (2004). Hepcidin regulates cellular iron efflux by binding to ferroportin and inducing its internalization. Science (80-.). 306, 2090-2093. https://doi.org/10.1126/science.1104742

Neves, J. V., Wilson, J. M. and Rodrigues, P. N. S. (2009). Transferrin and ferritin response to bacterial infection: The role of the liver and brain in fish. Dev. Comp. Immunol. 33, 848-857. https://doi.org/10.1016/j.dci.2009.02.001

Neves, J. V., Ramos, M. F., Moreira, A. C., Silva, T., Gomes, M. S. and Rodrigues, P. N. S. (2017). Hamp1 but not Hamp2 regulates ferroportin in fish with two functionally distinct hepcidin types. Sci. Rep. 7, 14793. https://doi.org/10.1038/s41598-017-14933-5

Niyogi, S. and Wood, C. M. (2006). Interaction between dietary calcium supplementation and chronic waterborne zinc exposure in juvenile rainbow trout, *Oncorhynchus mykiss*. Comp. Biochem. Physiol. C Toxicol. Pharmacol. 143, 94-102. https://doi.org/10.1016/j.cbpc.2005.12.007

Ong, S. T., Shan Ho, J. Z., Ho, B. and Ding, J. L. (2006). Iron-withholding strategy in innate immunity. Immunobiology 211, 295-314. https://doi.org/10.1016/j.imbio.2006.02.004

Pan, T.-C., Liao, B.-K., Huang, C.-J., Lin, L.-Y. and Hwang, P.-P. (2005). Epithelial $Ca2^{+}$ channel expression and $Ca2^{+}$ uptake in developing zebrafish. Am. J. Physiol. Integr. Comp. Physiol. 289, R1202-R1211. https://doi.org/10.1152/ajpregu.00816.2004

Pantopoulos, K. (2004). Iron metabolism and the IRE/IRP regulatory system: an update. Ann. N. Y. Acad. Sci. 1012, 1-13. https://doi.org/10.1196/annals.1306.001

Pelster, B. and Egg, M. (2018). Hypoxia-inducible transcription factors in fish: expression, function and interconnection with the circadian clock. J. Exp. Biol. 221, 163709. https://doi.org/10.1242/jeb.163709

Pilehvar, A., Town, R. M. and Blust, R. (2019). The effect of thermal pre-incubation and exposure on sensitivity of zebrafish (*Danio rerio*) to copper and cadmium single and binary exposures. Aquat. Toxicol. 213, 105226. https://doi.org/10.1016/j.aquatox.2019.105226

Pillet, M., Castaldo, G., Rodgers, E. M., Poleksić, V., Rašković, B., Bervoets, L., Blust, R. and De Boeck, G. (2021). Physiological performance of common carp (*Cyprinus carpio*, L., 1758) exposed to a sublethal copper/zinc/cadmium mixture. Comp. Biochem. Physiol. C Toxicol. Pharmacol. 242, 108954. https://doi.org/10.1016/j.cbpc.2020.108954

Pouil, S., Oberhänsli, F., Bustamante, P. and Metian, M. (2018). Investigations of temperature and pH variations on metal trophic transfer in turbot (*Scophthalmus maximus*). Environ. Sci. Pollut. Res. 25, 11219-11225. https://doi.org/10.1007/s11356-017-8691-4

Prasad, A. S. (2008). Zinc in human health: effect of zinc on immune cells. Mol. Med. 14, 353. https://doi.org/10.2119/2008-00033.Prasad

Puar, P., Niyogi, S. and Kwong, R. W. M. (2020). Regulation of metal homeostasis and zinc transporters in early-life stage zebrafish following sublethal waterborne zinc exposure. Aquat. Toxicol. 225, 105524. https://doi.org/10.1016/j.aquatox.2020.105524

Puig, S., Ramos-Alonso, L., Romero, A. M. and Martínez-Pastor, M. T. (2017). The elemental role of iron in DNA synthesis and repair. Metallomics 9, 1483-1500. https://doi.org/10.1039/C7MT00116A

Pyle, G. G., Kamunde, C. N., McDonald, D. G. and Wood, C. M. (2003). Dietary sodium inhibits aqueous copper uptake in rainbow trout (*Oncorhynchus mykiss*). J. Exp. Biol. 206, 609-618. https://doi.org/10.1242/jeb.00114

Qiu, A. and Hogstrand, C. (2004). Functional characterisation and genomic analysis of an epithelial calcium channel (ECaC) from pufferfish, *Fugu rubripes*. Gene 342, 113-123. https://doi.org/10.1016/j.gene.2004.07.041

Rae, T. D., Schmidt, P. J., Pufahl, R. A., Culotta, V. C. and O'Halloran, T. V. (1999). Undetectable intracellular free copper: The requirement of a copper chaperone for superoxide dismutase. Science 284, 805-808. https://doi.org/10.1126/science.284.5415.805

Rejitha, V. and Peter, M. C. S. (2013). Adrenaline and triiodothyronine modify the iron handling in the freshwater air-breathing fish Anabas testudineus Bloch: role of ferric reductase in iron acquisition. Gen. Comp. Endocrinol. 181, 130-138. https://doi.org/10.1016/j.ygcen.2012.11.008

Renassia, C. and Peyssonnaux, C. (2019). New insights into the links between hypoxia and iron homeostasis. Curr. Opin. Hematol. 26, 125-130. https://doi.org/10.1097/MOH.0000000000000494

Riggio, M., Filosa, S., Parisi, E. and Scudiero, R. (2003). Changes in zinc, copper and metallothionein contents during oocyte growth and early development of the teleost *Danio rerio* (zebrafish). Comp. Biochem. Physiol. C Toxicol. Pharmacol. 135, 191-196. https://doi.org/10.1016/S1532-0456(03)00107-8

Rørvik, K. A., Dehli, A., Thomassen, M., Ruyter, B., Steien, S. H. and Salte, R. (2003). Synergistic effects of dietary iron and omega-3 fatty acid levels on survival of farmed Atlantic salmon, *Salmo salar* L., during natural outbreaks of furunculosis and cold water vibriosis. J. Fish Dis. 26, 477-485. https://doi.org/10.1046/j.1365-2761.2003.00482.x

Sahoo, P. K., Das, S., Mahapatra, K. D., Saha, J. N., Baranski, M., Ødegård, J. and Robinson, N. (2013). Characterization of the ceruloplasmin gene and its potential role as an indirect marker for selection to *Aeromonas hydrophila* resistance in rohu, *Labeo rohita*. Fish Shellfish Immunol. 34, 1325-1334. https://doi.org/10.1016/j.fsi.2013.02.020

Scudiero, R., Trinchella, F., Riggio, M. and Parisi, E. (2007). Structure and expression of genes involved in transport and storage of iron in red-blooded and hemoglobin-less *Antarctic notothenioids*. Gene 397, 1-11. https://doi.org/10.1016/j.gene.2007.03.003

Seo, Y. A. and Wessling-Resnick, M. (2015). Ferroportin deficiency impairs manganese metabolism in flatiron mice. FASEB J. 29, 2726-2733. https://doi.org/10.1096/fj.14-262592

Shaw, G. C., Cope, J. J., Li, L., Corson, K., Hersey, C., Ackermann, G. E., Gwynn, B., Lambert, A. J., Wingert, R. A., Traver, D.et al. (2006). Mitoferrin is essential for erythroid iron assimilation. Nature 440, 96-100. https://doi.org/10.1038/nature04512

Shawki, A. and Mackenzie, B. (2010). Interaction of calcium with the human divalent metal-ion transporter-1. Biochem. Biophys. Res. Commun. 393, 471-475. https://doi.org/10.1016/j.bbrc.2010.02.025

Shawki, A., Anthony, S. R., Nose, Y., Engevik, M. A., Niespodzany, E. J., Barrientos, T., Öhrvik, H., Worrell, R. T., Thiele, D. J. and Mackenzie, B. (2015). Intestinal DMT1 is critical for iron absorption in the mouse but is not required for the absorption of copper or manganese. Am. J. Physiol. Gastrointest. Liver Physiol. 309, G635-G647. https://doi.org/10.1152/ajpgi.00160.2015

Shi, J. and Camus, A. C. (2006). Hepcidins in amphibians and fishes: antimicrobial peptides or iron-regulatory hormones? Dev. Comp. Immunol. 30, 746-755. https://doi.org/10.1016/j.dci.2005.10.009

Shike, H., Lauth, X., Westerman, M. E., Ostland, V. E., Carlberg, J. M., Van Olst, J. C., Shimizu, C., Bulet, P. and Burns, J. C. (2002). Bass hepcidin is a novel antimicrobial peptide induced by bacterial challenge. Eur. J. Biochem. 269, 2232-2237. https://doi.org/10.1046/j.1432-1033.2002.02881.x

Smirnova, I. V., Bittel, D. C., Ravindra, R., Jiang, H. and Andrews, G. K. (2000). Zinc and cadmium can promote rapid nuclear translocation of metal response element-binding transcription factor-1. J. Biol. Chem. 275, 9377-9384. https://doi.org/10.1074/jbc.275.13.9377

Soma, S., Latimer, A. J., Chun, H., Vicary, A. C., Timbalia, S. A., Boulet, A., Rahn, J. J., Chan, S. S. L., Leary, S. C., Kim, B. E.et al. (2018). Elesclomol restores mitochondrial function in genetic models of copper deficiency. Proc. Natl. Acad. Sci. USA 115, 8161-8166. https://doi.org/10.1073/pnas.1806296115

Song, Z. X., Jiang, W. D., Liu, Y., Wu, P., Jiang, J., Zhou, X. Q., Kuang, S. Y., Tang, L., Tang, W. N., Zhang, Y. A.et al. (2017). Dietary zinc deficiency reduced growth performance, intestinal immune and physical barrier functions related to NF-κB, TOR, Nrf2, JNK and MLCK signaling pathway of young grass carp (*Ctenopharyngodon idella*). Fish Shellfish Immunol. 66, 497-523. https://doi.org/10.1016/j.fsi.2017.05.048

Stevenson, M. J., Uyeda, K. S., Harder, N. H. O. and Heffern, M. C. (2019). Metal-dependent hormone function: The emerging interdisciplinary field of metalloendocrinology. Metallomics 11, 85-110. https://doi.org/10.1039/C8MT00221E

Sundh, H., Kvamme, B. O., Fridell, F., Olsen, R. E., Ellis, T., Taranger, G. L. and Sundell, K. (2010). Intestinal barrier function of Atlantic salmon (*Salmo salar* L.) post smolts is reduced by common sea cage environments and suggested as a possible physiological welfare indicator. BMC Physiol. 10, 1-13. https://doi.org/10.1186/1472-6793-10-22

Tapia, L., González-Agüero, M., Cisternas, M. F., Suazo, M., Cambiazo, V., Uauy, R. and González, M. (2004). Metallothionein is crucial for safe intracellular copper storage and cell survival at normal and supra-physiological exposure levels. Biochem. J. 378, 617-624. https://doi.org/10.1042/bj20031174

Tarifeño-Saldivia, E., Aguilar, A., Contreras, D., Mercado, L., Morales-Lange, B., Márquez, K., Henríquez, A., Riquelme-Vidal, C. and Boltana, S. (2018). Iron overload is associated with

oxidative stress and nutritional immunity during viral infection in fish. Front. Immunol. 9, 1296. https://doi.org/10.3389/fimmu.2018.01296

Tellis, M. S., Alsop, D. and Wood, C. M. (2012). Effects of copper on the acute cortisol response and associated physiology in rainbow trout. Comp. Biochem. Physiol. C Toxicol. Pharmacol. 155, 281-289. https://doi.org/10.1016/j.cbpc.2011.09.008

Tennant, J., Stansfield, M., Yamaji, S., Srai, S. and Sharp, P. (2002). Effects of copper on the expression of metal transporters in human intestinal Caco-2 cells. FEBS Lett. 527, 239-244. https://doi.org/10.1016/S0014-5793(02)03253-2

Thompson, B. A. V., Sharp, P. A., Elliott, R. and Fairweather-Tait, S. J. (2010). Inhibitory effect of calcium on non-heme iron absorption may be related to translocation of DMT-1 at the apical membrane of enterocytes. J. Agric. Food Chem. 58, 8414-8417. https://doi.org/10.1021/jf101388z

Thomason, R. T., Pettiglio, M. A., Herrera, C., Kao, C., Gitlin, J. D. and Bartnikas, T. B. (2017). Characterization of trace metal content in the developing zebrafish embryo. PLoS One 12, e0179318. https://doi.org/10.1371/journal.pone.0179318

Tuschl, K., Meyer, E., Valdivia, L. E., Zhao, N., Dadswell, C., Abdul-Sada, A., Hung, C. Y., Simpson, M. A., Chong, W. K., Jacques, T. S.et al. (2016). Mutations in SLC39A14 disrupt manganese homeostasis and cause childhood-onset parkinsonism-dystonia. Nat. Commun. 7, 11601. https://doi.org/10.1038/ncomms11601

Van Campenhout, K., Bervoets, L. and Blust, R. (2007). Assimilation efficiencies of Cd and Zn in the common carp (*Cyprinus carpio*): effects of metal concentration, temperature and prey type. Environ. Pollut. 145, 905-914. https://doi.org/10.1016/j.envpol.2006.05.002

Viegas, M. N., Salgado, M. A., Aguiar, C., Almeida, A., Gavaia, P. and Dias, J. (2021). Effect of dietary manganese and zinc levels on growth and bone status of Senegalese sole (*Solea senegalensis*) post-larvae. Biol. Trace Elem. Res. 199, 2012-2021. https://doi.org/10.1007/s12011-020-02307-4

Wang, J.-J. and Sun, L. (2015). Ferritin M of Paralichthys olivaceus possesses antimicrobial and antioxidative properties. Fish Physiol. Biochem. 41, 951-959. https://doi.org/10.1007/s10695-015-0060-y

Wang, J. and Wang, W.-X. (2016). Novel insights into iron regulation and requirement in marine medaka *Oryzias melastigma*. Sci. Rep. 6, 26615. https://doi.org/10.1038/srep26615

Wang, W.-C., Mao, H., Ma, D.-D. and Yang, W.-X. (2014). Characteristics, functions, and applications of metallothionein in aquatic vertebrates. Front. Mar. Sci. 1, 34. https://doi.org/10.3389/fmars.2014.00034

Wang, Y., Wu, Y., Li, T., Wang, X. and Zhu, C. (2019). Iron metabolism and brain development in premature infants. Front. Physiol. 10, 463. https://doi.org/10.3389/fphys.2019.00463

Watanabe, T., Kiron, V. and Satoh, S. (1997). Trace minerals in fish nutrition. Aquaculture 151, 185-207. https://doi.org/10.1016/S0044-8486(96)01503-7

Wessels, I., Maywald, M. and Rink, L. (2017). Zinc as a gatekeeper of immune function. Nutrients 9, 1286. https://doi.org/10.3390/nu9121286

Wichmann, L. and Althaus, M. (2020). Evolution of epithelial sodium channels: current concepts and hypotheses. Am. J. Physiol. Regul. Integr. Comp. Physiol. 319, R387-R400. https://doi.org/10.1152/ajpregu.00144.2020

Wood, C. M., Farrell, A. P. and Brauner, C. J. (2011). Homeostasis and Toxicology of Essential Metals. Academic Press.

Wyman, S., Simpson, R. J., McKie, A. T. and Sharp, P. A. (2008). Dcytb (Cybrd1) functions as both a ferric and a cupric reductase in vitro. FEBS Lett. 582, 1901-1906. https://doi.org/10.1016/j.febslet.2008.05.010

Xia, Z., Wei, J., Li, Y., Wang, J., Li, W., Wang, K., Hong, X., Zhao, L., Chen, C., Min, J.et al. (2017). Zebrafish slc30a10 deficiency revealed a novel compensatory mechanism of *Atp2c1* in maintaining manganese homeostasis. PLoS Genet. 13, 1-29.

Xue, Y., Gao, S. and Liu, F. (2015). Genome-wide analysis of the zebrafish Klf family identifies two genes important for erythroid maturation. Dev. Biol. 403, 115-127. https://doi.org/10.1016/j.ydbio.2015.05.015

Yamaji, S., Tennant, J., Tandy, S., Williams, M., Singh Srai, S. K. and Sharp, P. (2001). Zinc regulates the function and expression of the iron transporters DMT1 and IREG1 in human intestinal Caco-2 cells. FEBS Lett. 507, 137-141. https://doi.org/10.1016/S0014-5793(01)02953-2

Yan, G., Zhang, Y., Yu, J., Yu, Y., Zhang, F., Zhang, Z., Wu, A., Yan, X., Zhou, Y. and Wang, F. (2012). Slc39a7/zip7 plays a critical role in development and zinc homeostasis in zebrafish. PLoS ONE 7, e42939. https://doi.org/10.1371/journal.pone.0042939

Zafar, N. and Khan, M. A. (2019). Growth, feed utilization, mineralization and antioxidant response of stinging catfish *Heteropneustes fossilis* fed diets with different levels of manganese. Aquaculture 509, 120-128. https://doi.org/10.1016/j.aquaculture.2019.05.022

Zafar, N. and Khan, M. A. (2020). Effects of dietary iron on growth, haematology, oxidative stress and hepatic ascorbic acid concentration of stinging catfish *Heteropneustes fossilis*. Aquaculture 516, 734642. https://doi.org/10.1016/j.aquaculture.2019.734642

Zhang, T., Guan, P. P., Liu, W. Y., Zhao, G., Fang, Y. P., Fu, H., Gui, J. F., Li, G. L. and Liu, J. X. (2020). Copper stress induces zebrafish central neural system myelin defects via WNT/NOTCH-hoxb5b signaling and pou3f1/fam168a/fam168b DNA methylation. Biochim. Biophys. Acta Gene Regul. Mech. 1863, 194612. https://doi.org/10.1016/j.bbagrm.2020.194612

Zhao, L., Xia, Z. and Wang, F. (2014). Zebrafish in the sea of mineral (iron, zinc, and copper) metabolism. Front. Pharmacol. 5, 33. https://doi.org/10.3389/fphar.2014.00033

Zimmer, A. M., Dymowska, A. K., Kumai, Y., Goss, G. G., Perry, S. F. and Kwong, R. W. M. (2018). Assessing the role of the acid-sensing ion channel ASIC4b in sodium uptake by larval zebrafish. Comp. Biochem. Physiol. A Mol. Integr. Physiol. 226, 1-10. https://doi.org/10.1016/j.cbpa.2018.06.012

Zimmer, A. M., Pan, Y. K., Chandrapalan, T., Kwong, R. W. M. and Perry, S. F. (2019). Loss-of-function approaches in comparative physiology: is there a future for knockdown experiments in the era of genome editing? J. Exp. Biol. 222, jeb175737. https://doi.org/10.1242/jeb.175737

Chapter 2

Intergenerational Effects of Dietary Iron on Swimming and Metabolic Performance in Zebrafish

This chapter has been published and reproduced with permission.

Chandrapalan, T., Walia, S., and Kwong, R. W. M. (2025). Intergenerational effects of dietary iron on swimming and metabolic performance in zebrafish. *Front Physiol 16*, 1693900. doi: 10.3389/FPHYS.2025.1693900

2.1 Summary

Iron is an essential trace metal required for various physiological processes, yet both deficiency and excess can disrupt metal homeostasis and compromise fitness. In this study, we investigated how dietary iron availability influences physiological performance across generations in zebrafish (*Danio rerio*). Fish were fed diets spanning a gradient from deficiency to supplementation (Low Fe, 11 mg Fe/kg; Medium Fe, 420 mg Fe/kg; and High Fe, 2300 mg Fe/kg), and effects on growth, metal homeostasis, swimming performance, energy metabolism, and reproduction were assessed. Following reproductive assays, offspring were raised under control conditions and subsequently challenged with the same dietary iron treatments (Low Fe, Medium Fe, and High Fe as parents) in adulthood. Sub-acute exposure (20 days) to elevated dietary iron enhanced aerobic scope, maximum metabolic rate, and critical swimming speed, alongside improved reproductive output as measured by embryo survival and early development. However, sub-chronic exposure (40 days) to High Fe diminished swimming performance benefits and was also associated with tissue iron loading. Notably, zebrafish tolerated sub-chronic exposure to Low Fe without significant impacts on condition factor or energetic performance. Interestingly, the difference in swimming and metabolic performance between high and low iron treatments was more pronounced in the offspring, suggesting an intergenerational effect of parental iron status. Together, these findings suggest that dietary iron availability can shape both immediate and inherited performance phenotypes, underscoring its dual role as a nutritional requirement and a regulator of ecological fitness.

2.2 **Introduction**

Iron is an essential micronutrient for all fish; it is a vital component of a multitude of protein complexes, a cofactor for many enzymes, and is involved in various biochemical and metabolic

processes such as oxygen transport, energy metabolism, and development (Wood et al., 2011; Chandrapalan and Kwong, 2021). However, imbalances in iron levels, both deficiency and overload, can negatively impact fish health, leading to physiological impairments such as reduced growth, disrupted oxygen transport, oxidative stress, and metal accumulation (Watanabe et al., 1997; Lall and Kaushik, 2021). In freshwater environments, iron concentrations are usually low (<1 mg/L), but hypoxia, acidification, and anthropogenic activities (mining and industrial discharge) can substantially elevate levels and increase availability (Peuranen et al., 1994; Xing and Liu, 2011; Kwong, 2024). Within physiologically safe concentrations, iron supplementation can be important for the maintenance of fish health, including growth, feed utilization, and immune function (Wang et al., 2023). While diet is considered the predominant route of iron acquisition, the effects of dietary iron exposure have been far less studied than waterborne uptake, leaving critical gaps in our understanding of how dietary iron availability impacts fish physiological performance (Andersen, 1997; Bury, 2003; Jee et al., 2004; Lappivaara and Marttinen, 2005; Wang, 2013; Saha et al., 2015). In general, dietary iron overload is linked to iron loading in tissues, which can catalyze the Fenton reaction and the production of reactive oxygen species and oxidative stress, whereas dietary iron deficiency impairs hemoglobin synthesis, oxygen transport capacity, and reduces energetic performance in fish (Gallaugher et al., 1995; Andersen et al., 1996; Galbraith et al., 2019). However, no study has comprehensively examined how dietary iron deficiency and supplementation influence key survival traits such as sustained swimming performance, metabolic capacity, and reproductive success, and whether such effects can extend to subsequent generations.

Swimming performance is an integrative measure of physiological capacity because it incorporates oxygen transport, energy metabolism, and muscle function (Martínez et al., 2003; Rubio-Gracia et al., 2020). Ecologically, swimming ability is crucial for avoiding predation,

foraging for food, migration, and mating success, making it a key determinant of fitness (Tudorache et al., 2008; Cano-Barbacil et al., 2020). Consequently, swimming assays are widely used as sensitive biomarkers of environmental and nutritional stress (Little and Finger, 1990). Previous studies on other metals or metalloids have demonstrated that exposure to elevated levels of copper, selenium, and cadmium can impair swimming ability and alter metabolic rates in multiple species (minnows, trout, and sturgeon) (Massé et al., 2013; McPhee and Janz, 2014; Cunningham and McGeer, 2016; Puglis et al., 2019). In contrast, one study on iron supplementation (~1500 mg Fe/kg) reported improved burst swimming activity in masu salmon (*Oncorhynchus masou*) (Mizuno et al., 2007). Nonetheless, sustained swimming activities are energetically costly and are underpinned by metabolic capacity. Fish partition energy among basal maintenance, locomotion, and reproduction, and this balance is strongly influenced by nutrient availability (Ohlberger et al., 2006; Mcbride et al., 2015; Chabot et al., 2016). Since iron is directly involved in mitochondrial respiration and enzymatic activities, dietary iron levels have the potential to affect metabolic rates and energy balance (Judge and Dodd, 2020; Chandrapalan and Kwong, 2021). However, whether dietary iron deficiency or supplementation can also alter swimming performance remains largely unexplored.

Beyond swimming and metabolic performance, iron exposure may also affect reproductive success and influence intergenerational fitness. Intergenerational effects occur when parental environments shape offspring traits via altered nutrient provisioning, direct metal transfer to gametes, or epigenetic reprogramming (Thomas and Janz, 2014; Beaver et al., 2017; Domínguez-Petit et al., 2022). Such effects are increasingly recognized as critical for understanding population responses to environmental stressors, including metals. In fish, parental exposure to metals has been linked to metal accumulation in reproductive tissues and altered reproductive performance,

including fecundity, egg quality, and hatching success (Taslima et al., 2022). Most oviparous fishes, like zebrafish (*Danio rerio*), rely on maternally supplied yolk nutrients during early development and can be particularly vulnerable to these parental influences (Beaver et al., 2017; Thomason et al., 2017). Moreover, swimming performance in zebrafish has been shown to have a heritable component, and parental metal exposure was linked to persistent changes in offspring swimming ability and metabolism (Thomas and Janz, 2015; Wakamatsu et al., 2019). Investigating whether dietary iron availability affects reproductive performance and shapes offspring physiology is therefore essential to evaluate the ecological and intergenerational consequences of micronutrient stress.

In addition, iron exposure may have broader implications beyond its direct physiological roles, as iron is known to compete with or facilitate the uptake of other trace metals and major ions. Consequently, dietary iron deficiency or supplementation may disrupt systemic trace metal and ion homeostasis, with effects extending beyond iron regulation alone. These interactions between metals and metal transport pathways are further reflected in tissue-specific responses. For example, the brain is a highly metabolically active site and is sensitive to iron-induced oxidative stress; the intestine is the primary site of dietary metal absorption; the liver functions as the central hub for iron storage and metabolic regulation; and the ovaries represent a direct link between metal bioaccumulation to reproductive success, and potential maternal transfer (Kwong and Niyogi, 2008; Anderson and Shah, 2013; Thomas and Janz, 2015; Hassan and Kwong, 2020). Thus, understanding how dietary iron exposure affects the accumulation of metals and ions across these key tissues provides crucial insight into the mechanistic pathways by which iron may shape physiological performance and reproductive outcomes.

In the present study, we tested the hypothesis that dietary iron levels influence swimming performance by altering metabolic capacity and energy use, and affect reproductive success. We further hypothesized that these effects extend across generations and alter offspring performance. To address these questions, the freshwater teleost, zebrafish, with well-characterized physiology, tractability for dietary manipulation, and validated assays for swimming, metabolism, and reproduction, was chosen as the model species. Adult zebrafish were fed an iron-deficient (11 mg Fe/kg; Low Fe), adequate (420 mg Fe/kg; Medium Fe), or iron-enriched (2300 mg Fe/kg; High Fe) diet for 20 or 40 days. The concentrations of iron in the Low Fe, Medium Fe, and High Fe diets were selected to reflect fluctuating iron levels in the environment that span a biologically relevant gradient from deficiency, to adequacy, to supplementation. The Medium Fe diet was considered nutritionally adequate as it meets the baseline recommended levels in aquaculture (~30-170 mg Fe/kg) while also closely resembling the composition of commercial zebrafish diet (e.g., Zeigler) commonly used in laboratory rearing (Watanabe et al., 1997). To capture both early and longer-term responses, we examined 20-day (sub-acute) and 40-day (sub-chronic) exposures. These durations align with toxicological testing windows (~14–30 days), typical zebrafish nutritional trials (~3–10 weeks), and are ecologically relevant given the species' rapid life cycle and sexual maturation at ~3 months (Cooper et al., 2006; Singleman and Holtzman, 2014; Beaver et al., 2017; Chandrapalan and Kwong, 2020). We assessed: i) trace metal and major ion accumulation in the brain, intestine, liver, and ovaries, ii) swimming and metabolic performance, and iii) reproductive output. To evaluate potential intergenerational effects, the offspring of iron-exposed parent fish were raised under control conditions to adulthood before being challenged with the same dietary iron treatments as their parents. By integrating organ-specific metal analyses

with performance-based assessments across two generations, this study provides novel insight into the role of dietary iron in regulating metabolism, reproduction, and intergenerational fitness in fish.

2.3 **Material and Methods**

2.3.1 *Animals and experimental design*

Adult zebrafish (Tüpfel long-fin strain) were housed in recirculating systems (Aquaneering, CA, USA) and maintained at 28°C with a 14h light: 10h dark photoperiod at York University's zebrafish vivarium. They were fed brine shrimp in the morning and commercial zebrafish pellets to satiation in the afternoon (Zeigler, PA, USA; comprised of 55% protein; 15% fat; 1.5% fiber; 12% ash; 1.5% phosphorus; 2.78% calcium; and 0.37% sodium). During weekends, they were fed once a day with pellets. The measured trace metal content in the Zeigler diet was 309.00 mg Fe/kg, 208.00 mg Zn/kg, 57.00 mg Mn/kg, 40 mg Cu/kg, 0.41mg Co/kg, and 1.19 mg I/kg. All animal work was conducted in accordance with the Canadian Council for Animal Care and approved by the York University Animal Care Committee (2017-2 R2).

A total of 150 adult zebrafish (~12 months of age) were used in this study, and 25 fish were allocated per treatment group. Each group of 25 was split into two tanks (2.8 L) with an approximately equal ratio of males to females (12-13 fish per tank). In brief, the fish were subjected to a feeding trial (Section 2.2), physiological assessments (Section 2.3), and respirometry trials (Section 2.4). Throughout the dietary iron exposure, the fish also participated in repeated breeding trials (Section 2.5), and offspring from Day 15 were used to assess the potential intergenerational effects of parental dietary exposure. A schematic illustrating the experimental design is shown in Figure 2-1**.**

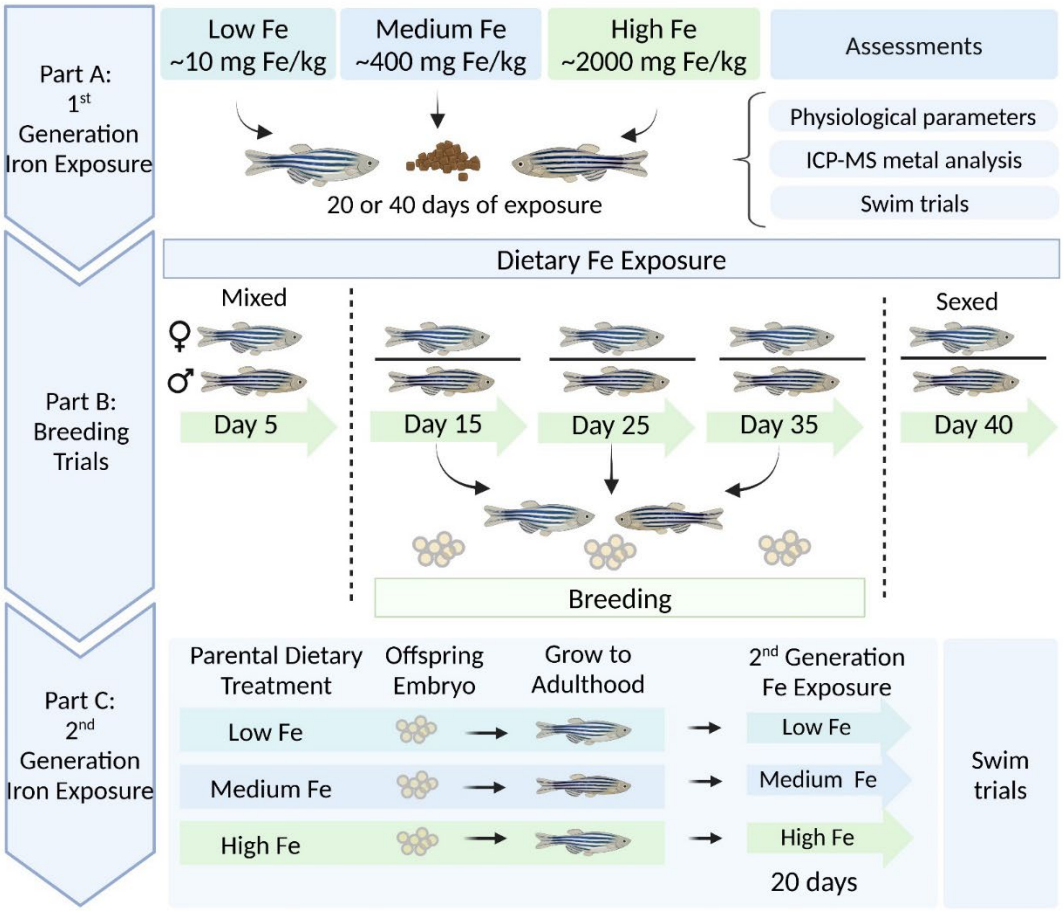

Figure 2-1. Schematic overview of dietary (parent and offspring) iron exposure, breeding trials, and intergenerational swim performance trials in zebrafish. Part A: Adult zebrafish were exposed to three experimental diets differing in iron content (Low Fe, Medium Fe, and High Fe) for 20 or 40 days. Following exposure, fish were assessed for physiological parameters, tissue metal accumulation, and swim performance. Part B: Concurrent breeding trials were conducted at 10-day intervals between days 5 and 40 of exposure. Fertilized embryos were collected from each dietary treatment group. Part C: Offspring from Day 15 breeding session were raised to adulthood under standard conditions, then exposed for 20 days to the same dietary iron treatment as their parents.

Swim performance was examined in parent and offspring generations to assess intergenerational effects of dietary iron exposure. Created with BioRender.com.

2.3.2 *Preparation of experimental diets and dietary treatment*

Three experimental diets ranging in iron content were prepared as described previously (Kwong et al., 2013; Chandrapalan and Kwong, 2020), with some modifications. A purified low-iron zebrafish diet (Dyets Inc; nutritional composition listed in Table 2-S1) was formulated by replacing high-iron protein sources (i.e., casein, wheat gluten, and egg white) with purified L-amino acids and ingredients lower in iron content (i.e., microcrystalline cellulose). Inductively coupled plasma mass spectrometry (ICP-MS) analysis (Water Quality Center, Trent University) determined the iron concentration in this purified diet to be 7.5 ± 0.2 mg Fe/kg (mean ± SEM, n=4). To prepare the Medium and High Fe diets, an appropriate amount of iron (as $FeSO_4 \cdot 7H_2O$) was dissolved in deionized water and mixed with the purified diet. The resulting paste was dehydrated at 65°C for 2 days. The food was then portioned into edible sizes (~1mm) and stored at 4°C until use. The Low Fe diet was prepared in the same manner but without the addition of $FeSO_4$. The final iron concentrations in the three diets were 11 ± 1 (Low Fe), 419 ± 46 (Medium Fe), and 2280 ± 75 (High Fe) mg Fe/kg (Table 2-1). The elemental composition of the purified diet and experimental diets are reported in Table 2-S2. Among the three dietary iron levels, the Medium Fe diet was considered the control, as its iron content was similar to that of the commercial zebrafish diet (i.e., Zeigler) used for routine zebrafish rearing alongside brine shrimp supplementation, although brine shrimp were not provided during the experimental feeding period.

Table 2-1. Measured Fe concentration (mg Fe/kg) in experimental diets and the daily dose of Fe (µg Fe/g fish wt/day). Data are mean ± SEM; n = 3.

Dietary treatment	**Fe concentration** (mg Fe/kg)	**Daily Fe dose** (µg Fe/g fish wt/day)
Low Fe	11 ± 0.8	0.17
Medium Fe	420 ± 50	6.3
High Fe	2300 ± 80	35

At the start of the feeding trials, all fish were acclimated to the Medium Fe diet for one week to ensure adjustment to the new feeding regime and experimental diet. Thereafter, the fish were divided into six groups: one group of three received a 20-day dietary exposure, while the other three groups received a 40-day exposure. The fish were fed the Low, Medium, or High Fe diets twice daily (totaling 5% of body weight) on weekdays and once daily on weekends. During feeding, the recirculating system (Aquaneering, CA, USA) was turned off, and the water in each tank was continuously flushed for one hour. To assess potential iron leaching from the diet, water samples were collected after feeding, and ICP-MS analysis indicated negligible leaching, with measured iron concentration of 2.03 ± 0.85 µg Fe/L (n=4). The iron concentration in the water of the recirculating system was approximately 1.2 µg Fe/L.

2.3.3 *Physiological parameters, tissue metal loading, and energy reserves*

Physiological parameters such as standard body length (SL; the distance from the tip of the snout to the base of the caudal peduncle) (cm), wet weight (g), and condition factor [100 x weight (g)/length^3 (cm)] were measured at the start and end of all feeding trials (Day 20 or 40). Hepatosomatic index [HSI; 100 x (liver weight (g)/body weight (g)] and gonadosomatic index [GSI; 100 x (gonad weight (g)/body weight (g)] were measured at the completion of feeding trials.

The fish were fasted for 24 h to clear the gut contents prior to euthanasia with an overdose of tricaine methanesulfonate (MS-222) buffered with sodium bicarbonate to pH 7 (0.4 g/L MS-222) and tissue collection. Brain, intestine, liver, and ovaries were collected, and organs from 3-5 fish from each experimental group were pooled to form one replicate. A total of 3-4 replicates were collected for each organ, and all tissue samples were dehydrated at 65°C overnight and then digested with 6N HNO_3 for 48h. The samples were diluted in 2% HNO_3, filtered (0.45 µm), and analyzed for metal concentrations using ICP-MS (Agilent, 8800 ICP-QQQ-MS, CA, USA) at the Water Quality Centre, Trent University (ON, CA). NIST SRM 1640a (Trace Elements in Natural Water) was used for QA/QC, and the measured concentrations were within 5% of the certified values.

Following organ extraction, fish carcasses were weighed, flash-frozen in liquid nitrogen, and stored at -80°C until use. Glycogen and triglyceride, which are primary energy sources utilized during burst and sustained swimming activities, were quantified in the carcass using colorimetric kits from Abcam following the manufacturer's instructions (Ab169558 and Ab65336).

2.3.4 Swimming and metabolic performance

Two Loligo miniswim tunnel respirometers (Loligo® Systems, Viborg, Denmark) with 170 mL swim tunnels were used for all intermittent-flow respirometry trials. Each Loligo system was connected to a recirculating system with a flush pump (Eheim Universal 1046 pump) and externally mixed to ensure homogenous oxygen distribution. Oxygen and velocity calibrations were conducted before the onset of the swim trials. The external water bath with a submersible aquarium heater was used to maintain a constant temperature (28°C), and both chambers were visually isolated using opaque shielding to minimize external disturbances and reduce stress to

fish. The lighting conditions were maintained constant throughout the experiment, and all trials were conducted during the daytime.

Oxygen saturation (%) was monitored continuously using oxygen probes (Dipping probe mini sensor, Loligo® Systems) connected to an oxygen meter (Witrox 4, Loligo® Systems). Readings were recorded at a frequency of approximately 1 Hz, and saturation was maintained above 85%. Chamber temperature was maintained at 28°C ± 0.5°C and monitored with a temperature probe (Temperature sensor Pt1000, Loligo® Systems) connected to the Witrox 4 system. AutoResp^{TM} 2 software (Loligo® Systems) was used to automate the intermittent-flow respirometry cycles and measure oxygen consumption. Each cycle consisted of a flush phase (1min 30s), a wait phase (30s), and a measurement phase (3min).

For critical swimming speed (Ucrit) tests (Figure 2-2), fish were transferred into the Loligo swim tunnel (inner swim chamber) quickly to minimize handling stress and allowed to acclimate to the new environment for 30 minutes at a velocity of 3.5 cm/s, or until their oxygen consumption rates stabilized. After 30 minutes, the critical swim test began, during which the water velocity was increased by 3.5 cm/s every 5 minutes until the fish reached fatigue, defined as consistent failure to swim against the current and resting against the back of the swim tunnel. Once the swim test concluded, the velocity was reset to the acclimation speed to allow the fish to rest briefly (~5 minutes) before being removed from the swim tunnel. The fish were then sacrificed to measure physiological indices and collect tissue for metal analysis and energy storage assays (as described above). Oxygen consumption (MO_2), cost of transport (COT), standard metabolic rate (SMR), maximum metabolic rate (MMR), aerobic scope (AS), and U_{crit} (body lengths/second, BL/s; the average length of the fish was 3.2 cm) were determined. SMR was calculated using linear regression analysis to extrapolate MO_2 values to 0 swimming speed. COT was calculated by

multiplying MO_2 by an oxycaloric value of 14.1 J/mg O_2 and then dividing by the corresponding swimming speed (m/s) (Videler, 1993). U_{crit} was calculated as follows:

$$U_{crit} = U_f + \left(T_f / T_i\right) \times U_i$$

U_f is the highest velocity (cm/s) maintained by the fish for a whole interval (5 min). T_f is the time elapsed at fatigue (min), and T_i is the prescribed time interval (min). U_i is the prescribed velocity increment (cm/s). U_{crit} was corrected for the body length of the fish (BL/s).

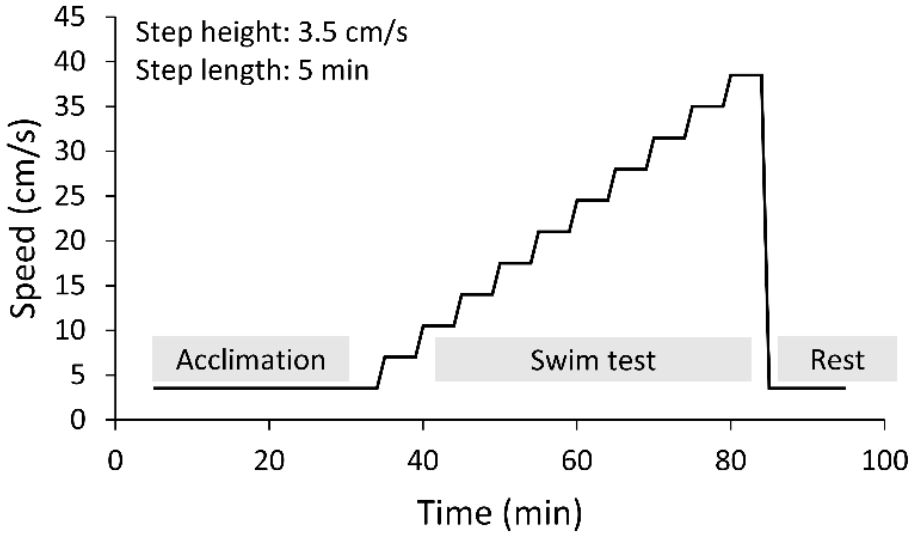

Figure 2-2. Critical swim test protocol used to assess swimming performance in zebrafish. Fish were acclimated at 3.5 cm/s for 30 minutes followed by a stepwise increase in swimming speed of 3.5 cm/s every 5 minutes until fatigue. Fish were allowed to rest (~5 minutes) at the end of swimming test.

2.3.5 Reproductive capacity and subsequent responses of the offspring to iron challenges

The breeding capacity of zebrafish was examined at 15, 25, and 35 days of dietary iron treatment. Before the onset of breeding trials, all fish were pre-bred once and maintained in mixed-sex groups to allow embryo release. At day 5 of iron treatment, males and females were separated, and this separation was maintained for 10 days between each breeding session on days 15, 25, and 35. This timeline ensured that both sexes were isolated for an equal duration (10 days) between breeding sessions. Eight breeding pairs were established for each dietary iron treatment group (Low Fe, Medium Fe, and High Fe), consisting of one male and one female per pair. Breeding pairs were set up in separate breeding tanks overnight and bred in the morning. Following breeding, the sexes were returned to their original tanks. All embryos were collected and transferred to 50 mL Petri dishes (20 embryos per dish) to quantify total embryo production. Eighty embryos (20 embryos per replicate, n=4 per treatment) were collected for ICP-MS analysis (as described previously for tissue samples; section 2.3). Survival rate at 1 day post-fertilization (dpf) for each breeding session (Day 15; n=28-29, Day 25 n=6-32, and Day 35 n=3-12) (each replicate consists of 20 embryos) and standard body length at 5 dpf were measured (n =4–10). All remaining embryos were euthanized, except those from the Day 15 breeding session, which were raised into adulthood for the next part of the study (intergenerational iron exposure).

To assess how the offspring of iron-exposed parents (F_1 generation) responded to dietary iron treatment compared to their parents (F_0), embryos from the Day 15 breeding session were raised to adulthood (under standard dietary regimes; section 2.1) and then re-exposed to the same experimental conditions (Low Fe, Medium Fe, or High Fe; section 2.2) as their parents for 20 days. The feeding and respirometry trials were conducted using the same protocols as for the parent generation (as outlined above). Physiological parameters (SL, weight, and condition factor) were

measured at the start and end of the dietary iron exposure. All fish were fasted for 24 h and subjected to the critical swim test.

2.3.6 *Statistical analysis*

Statistical analyses were performed using R (Version 4.1.3). Normality and homogeneity of data were assessed using the Shapiro-Wilk and Brown-Forsythe tests prior to all parametric tests. Two-way analysis of variance (ANOVA) or two-way repeated measures ANOVA followed by a Holm-Sidak multiple comparisons test was utilized to determine any statistical significance ($p<0.05$) of the dietary iron treatment and duration of iron exposure on multiple physiological parameters (tissue metal accumulation, swimming performance, and offspring development). One-way ANOVA followed by a Holm-Sidak multiple comparisons test was utilized to determine any statistical significance ($p<0.05$) within dietary treatments or exposure duration (physiological parameters of parents, offspring swim performance, and fatigue measurements). Permutation-based two-way ANOVA (10,000 iterations), followed by pairwise permutation tests (FDR-adjusted, $p < 0.05$), was used when assumptions were not met to compare group differences (average embryo survival). All graphs were constructed in R using the package ggplot2. Boxplots show the mean (central yellow diamond), median (horizontal line), upper and lower quartiles, and 1.5× interquartile range.

2.4 **Results**

2.4.1 *Physiological indices*

The effects of three different diets with low (11 mg Fe/kg), medium (420 mg Fe/kg), and high (2300 mg Fe/kg) levels of iron were assessed over two exposure periods: 20 days and 40 days. Physiological parameters, including condition factor, HSI, and GSI, were analysed separately

for each sex (Table 2-2). Following both 20- and 40-day exposures, there were no statistically significant differences in various physiological indices (condition factor, HSI (%), and GSI (%)) among the dietary iron treatment groups. Additionally, dietary iron treatments did not affect zebrafish survival as only one mortality was recorded, occurring on Day 34 in the Low Fe treatment group (Day 40 trial; data not shown).

However, there were significant differences between the duration of iron exposure (Day 20 and Day 40) within each diet (Table 2-2). Specifically, condition factor, HSI, and GSI were generally higher in fish from the Day 20 group compared to those from the Day 40 group, across all treatments in males except for GSI within the High Fe group. In females, condition factor and HSI were stable in Low and Medium Fe groups, but not in the High Fe group, and the GSI of the Low Fe group. Only females in the Medium Fe group maintained condition factor, HSI, and GSI at both sampling time points.

Consistent with the generally higher physiological indices observed in the Day 20 group, the body weight of fish used in the Day 20 experiment was also higher than that of the Day 40 group, both pre- and post-exposure (Table 2-3). Likewise, concurrent and repeated breeding trials may have resulted in temporal variation, as reflected by significantly lower GSI values within the Day 40 groups.

Table 2-2. Condition factor (g/cm^3), hepatosomatic index (HSI), and gonadosomatic index (GSI) of male and female zebrafish exposed to different dietary iron treatments (Low, Medium, and High Fe) for 20 or 40 days. Lowercase letters denote statistically significant differences between exposure durations within each dietary treatment and sex (Student's t-test, $p < 0.05$). Data are mean ± SEM; n=9-13.

		Condition factor (g/cm^3)		HSI (%)		GSI (%)	
Sex	**Diet**	Day 20	Day 40	Day 20	Day 40	Day 20	Day 40
Male	Low Fe	1.7±0.05^a	1.4±0.09^b	0.84±0.09^a	0.59±0.09^b	0.64±0.09^a	0.31±0.07^b
	Medium Fe	1.6±0.06^a	1.3±0.07^b	0.91±0.09^a	0.71±0.1^b	0.77±0.2^a	0.31±0.06^b
	High Fe	1.8±0.07^a	1.4±0.04^b	1.3±0.2^a	0.84±0.1^b	0.69±0.09^a	0.56±0.1^a
Female	Low Fe	1.7±0.05^a	1.7±0.07^a	1.9±0.2^a	1.2±0.1^a	8.1±1 ^{a}	2.5±0.4^b
	Medium Fe	1.8±0.08^a	1.6±0.08^a	1.4±0.1^a	1.1±0.1^a	5.6±1^a	3.6±0.6^a
	High Fe	1.9±0.06^a	1.6±0.06^b	1.9±0.3^a	1.4±0.1^b	8.2±1^a	3.5±0.4^b

Table 2-3. Weight (g) of male and female zebrafish exposed to Low, Medium, and High Fe diet for a duration of 20 and 40 days. Data are mean ± SEM, n=9-13 (per sex, per treatment). One-way ANOVA, $p < 0.05$. Lowercase letters denote statistical significance between pre- and post-exposure within timepoint and within sex.

Day	Sex	Pre-exposure (g)	Post-exposure (g)		
			Low Fe	Medium Fe	High Fe
20	Male	0.62±0.02^{a}	0.54±0.03^{ab}	0.51±0.02^{b}	0.52±0.02^{b}
	Female	0.74±0.02^{a}	0.64±0.02^{b}	0.59±0.03^{b}	0.60±0.02^{b}
40	Male	0.48±0.02^{a}	0.48±0.03^{a}	0.45±0.02^{a}	0.46±0.02^{a}
	Female	0.54±0.03^{a}	0.53±0.02^{a}	0.51±0.02^{a}	0.55±0.02^{a}

2.4.2 *Tissue burden of trace metals and major ions*

Tissue samples from the brain, intestine, liver, and ovaries were collected for trace metal and major ion analysis. A bar chart showing trace metal concentrations across tissues and dietary iron treatments (Low, Medium, High Fe) is presented in Figure 2-3, with summarized heatmaps in Figure 2-S1. The liver consistently exhibited the highest iron concentrations across all dietary treatments. Iron levels in various organs were influenced by both dietary iron levels and the exposure duration. Specifically, intestinal iron concentrations in the High Fe group increased significantly from Day 20 to Day 40 ($p<0.001$). Significant increases in iron accumulation were also observed in the brain ($p<0.001$), liver ($p<0.05$), and ovaries ($p<0.01$) after 40 days of High Fe exposure.

Zinc concentrations in the ovaries also increased at Day 40, but this effect was independent of dietary treatment (Figure 2-3; Figure 2-S1). At Day 40, an increase in intestinal zinc levels was also observed in fish from the High Fe group ($p<0.01$). Manganese, nickel, and cobalt levels in the

liver and ovaries were largely unaffected by dietary iron levels. However, nickel and cobalt concentrations in the intestine increased between Day 20 and Day 40 in the High Fe group. Within the Medium Fe group, manganese and cobalt showed elevated levels in the intestine and brain, respectively. Copper levels were measured but showed no significant treatment effects (data not shown).

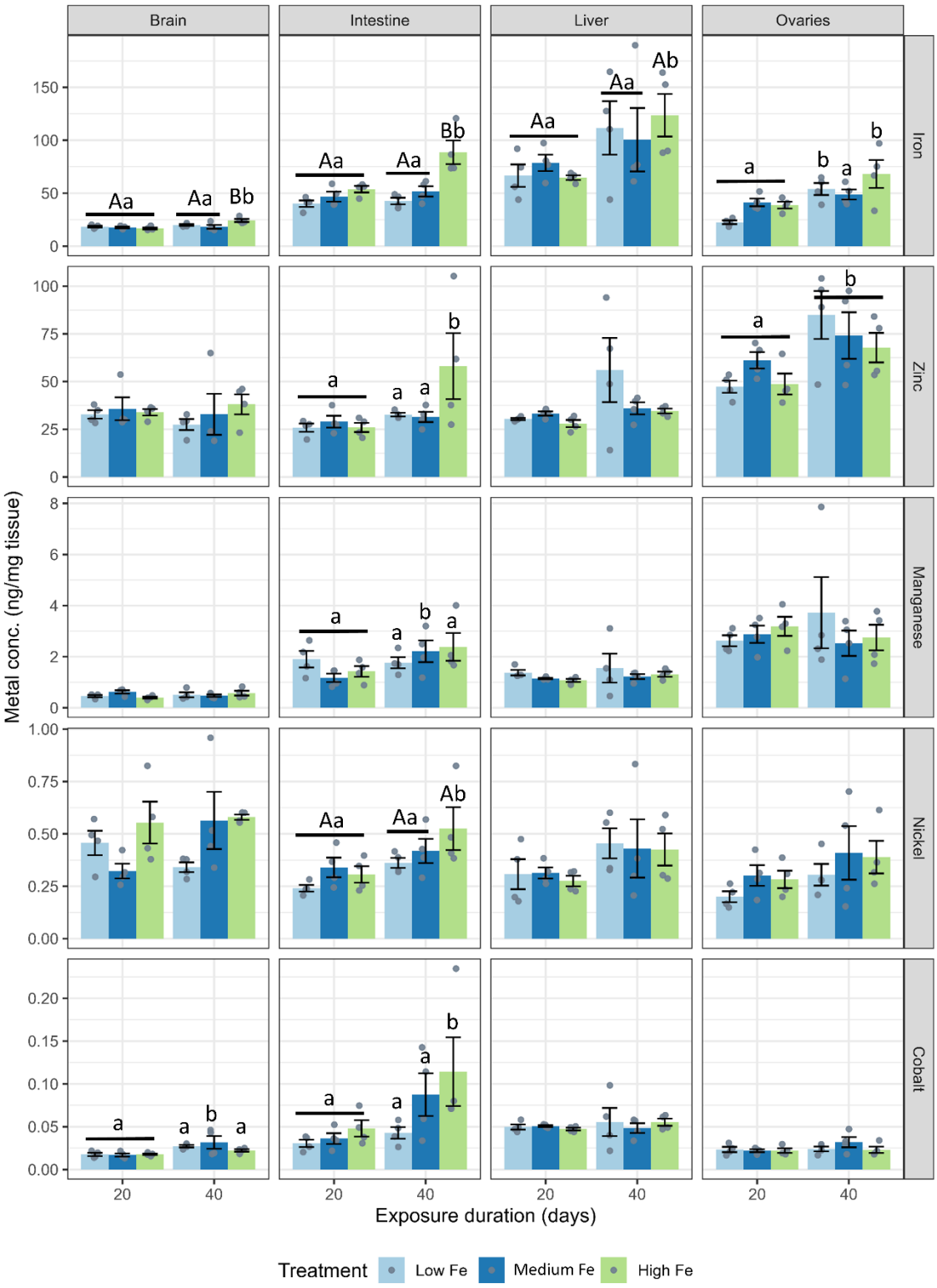

Figure 2-3. (caption on next page)

Figure 2-3. Tissue-specific accumulation of iron and other divalent metals in zebrafish following dietary iron exposure. Concentrations of iron, zinc, manganese, nickel, and cobalt (ng/mg tissue) were measured in the brain, intestine, liver, and ovaries after 20 or 40 days of exposure to Low Fe, Medium Fe, or High Fe diets. Data are mean ± SEM; n = 3–4 (each replicate consisted of a pooled tissue sample from 3–5 fish). Differing uppercase letters denote statistically significant differences among dietary iron treatments within an exposure timepoint. Differing lowercase letters indicate differences between exposure durations within the same dietary iron treatment. Two-way ANOVA followed by a post hoc Holm–Sidak test; $p < 0.05$.

For major ions, dietary iron treatments did not have significant effects across most organs (Figure 2-4; Figure 2-S1). Instead, major ion levels appeared to fluctuate from Day 20 to Day 40 within dietary Fe treatments. At Day 40, hepatic calcium levels were higher in fish fed the low and medium Fe diet when compared with fish fed the high Fe diet ($p<0.01$ in both dietary iron groups).

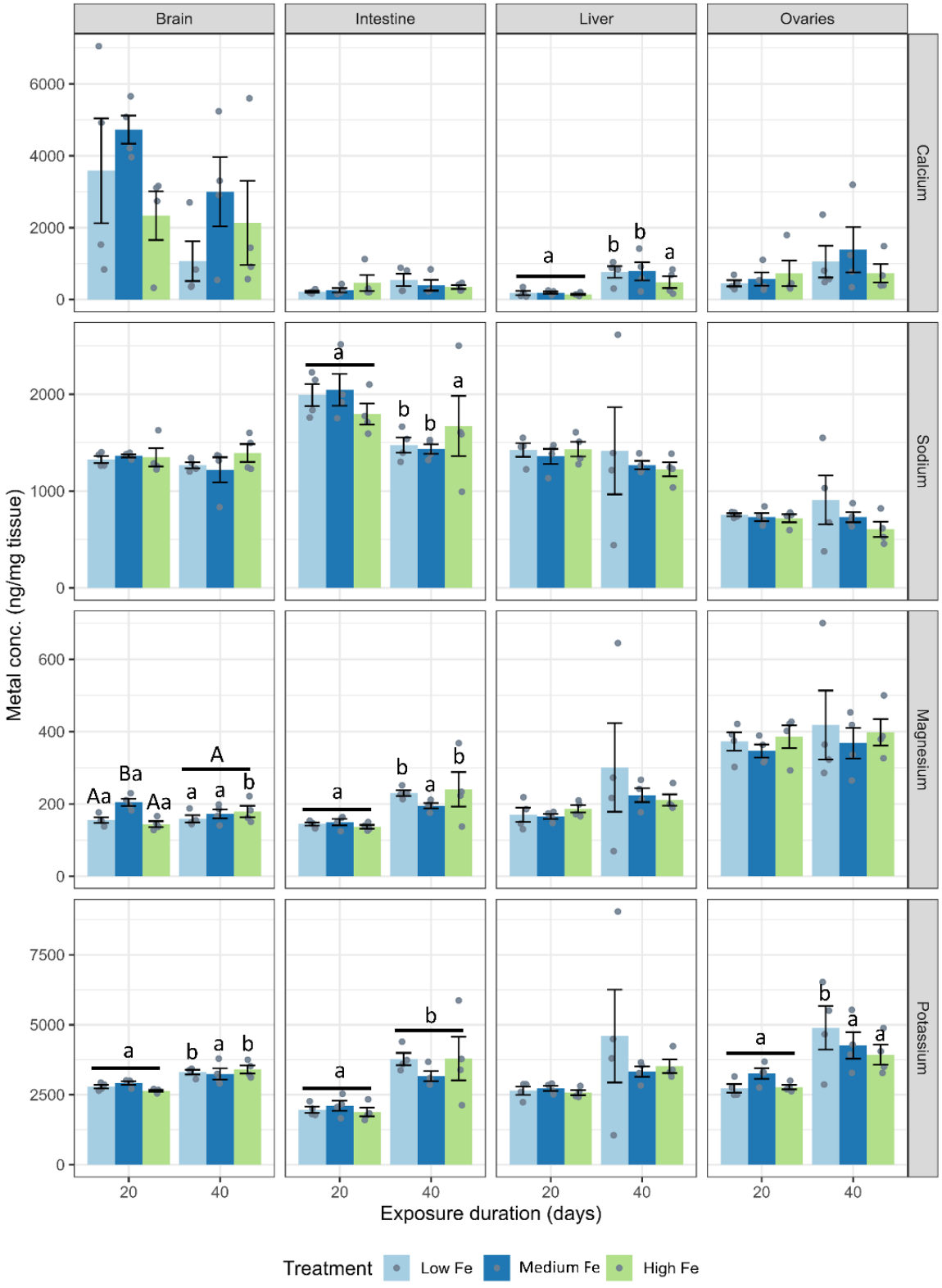

Figure 2-4. (caption next page)

Figure 2-4. Effects of dietary iron exposure on concentrations of major ions in zebrafish tissues. Calcium, sodium, potassium, and magnesium concentrations (ng/mg tissue) were measured in the brain, intestine, liver, and ovaries after 20 or 40 days of exposure to Low Fe, Medium Fe, and High Fe diets. Data are mean ± SEM; n = 3–4 (each replicate consisted of a pooled sample from 3–5 fish). Differing uppercase letters indicate statistically significant differences among dietary iron treatments within an exposure duration. Lowercase letters indicate differences between exposure durations within the same dietary iron treatment. Two-way ANOVA followed by a post hoc Holm–Sidak test; $p < 0.05$.

2.4.3 *Swimming capacity and energy metabolism*

On both Day 20 and Day 40, the High Fe groups consistently outperformed the other two dietary treatment groups in terms of swimming endurance during the critical swim test, often lasting 1–3 cycles longer (Figure 2-5A, B). MMR, AS, Ucrit, and COT, but not SMR, were positively affected by higher dietary iron levels following 20 days of exposure (Figure 2-5C–F; Figure 2-S2). However, by Day 40, some of these positive effects appeared to diminish. At that time point, fish fed the Low and Medium Fe diets showed increases in Ucrit and MMR, respectively.

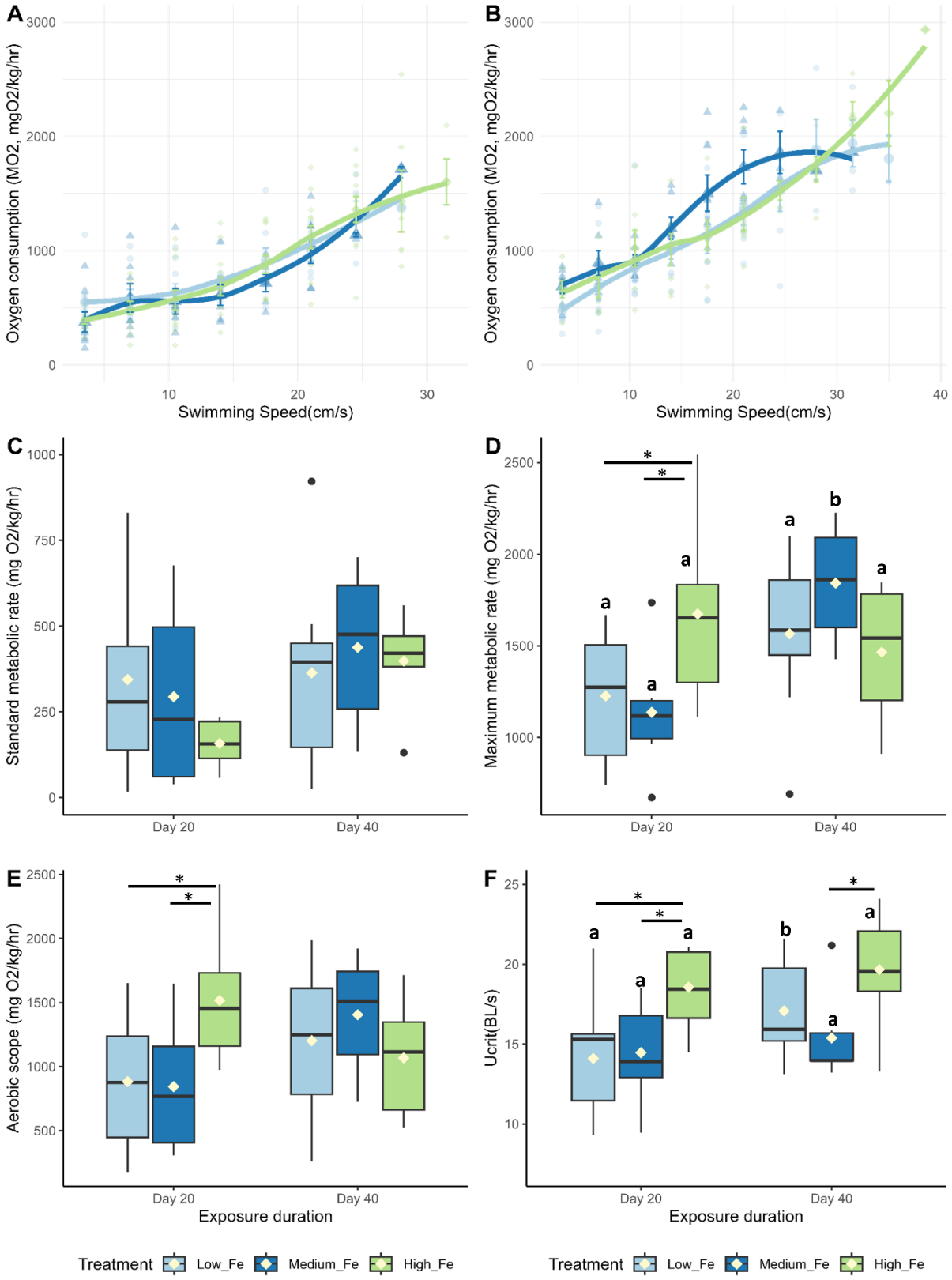

Figure 2-5. (caption next page)

Figure 2-5. Effects of dietary iron exposure on swimming performance and metabolic rates of adult zebrafish exposed to dietary iron. Oxygen consumption rates (MO_2, mgO_2/kg/hr) during a critical swim test following (A) 20 or (B) 40 days of Low Fe, Medium Fe, and High Fe treatment. Data are mean ± SEM; n=7-12 fish at starting speeds and n=1-3 fish at ending speeds. Each data point represents an individual measurement, with different symbols/colors indicating different dietary iron groups. Non-linear regression lines were fitted using locally estimated scatterplot smoothing (LOESS) to illustrate trends in metabolic demand across swimming speeds. Statistical differences were assessed using a two-way repeated-measures ANOVA, followed by post hoc Holm-Sidak test, $p < 0.05$. (C) Standard metabolic rate, (D) maximum metabolic rate, (E) critical swimming speed, and (F) aerobic scope of adult zebrafish exposed to dietary iron treatment for 20 or 40 days. Asterisks denote statistical significance (*p<0.05) among dietary iron treatments (Low, Medium, and High Fe) within exposure duration, and lowercase letters denote significant differences between exposure durations (Day 20 vs Day 40) within the same dietary iron treatment. Two-way ANOVA; p<0.05, n=7-9 fish.

There were no statistically significant differences in glycogen or triglyceride levels among zebrafish fed Low, Medium, or High Fe diets (Table 2-4). However, within the Low Fe group, glycogen levels appeared elevated at Day 40, and triglyceride levels appeared elevated at Day 20.

Table 2-4. Glycogen and triglyceride concentrations (mg/g) in the carcass of adult zebrafish exposed to different dietary iron treatments. Data are mean ± SEM; n=3-4. No statistical difference noted following one-way ANOVA, $p<0.05$.

Diet	Glycogen (mg/g)		Triglyceride (mg/g)	
	Day 20	Day 40	Day 20	Day 40
Low Fe	3.99±0.9	9.46±3	17.8±4	10.9±2
Medium Fe	5.15±3	3.40±0.7	8.57±1	9.89±3
High Fe	3.82±0.8	4.99±1	7.93±3	13.0±2

2.4.4 Reproductive performance

Adult fish exposed to Low, Medium, and High dietary iron treatments were bred every 10 days to assess fertility. Of the eight breeding pairs (1 male:1 female) per treatment group, 2-7 pairs successfully bred during each session (Figure 2-6A). Embryo production per breeding pair varied considerably, with no significant differences among treatment groups ($p > 0.05$). However, the Medium Fe group showed the highest breeding success at Day 15, with 7 of 8 pairs producing embryos. With repeated breeding, the number of successful breeding pairs decreased on Day 35 (from 7-3 at Day 15 to 2-3 at Day 35). Although embryo production varied widely between breeding sessions with no statistical differences, the High Fe group produced the most cumulative

embryos (total embryos collected on Days 15, 25, and 35) (Figure 2-S3). This group produced approximately 300 more embryos than the Medium Fe group and 500 more than the Low Fe group.

Embryos from parents exposed to 35 days of High Fe exhibited the highest survival rate compared to the other treatment groups ($p<0.01$) (Figure 2-6B). No significant differences in survival were observed in embryos collected from parents exposed to 25 days of Fe.

Offspring of parent fish exposed to 15 days of High Fe treatment had the lowest SL (Figure 2-6C). In contrast, longer parental High Fe exposure led to significant increases in larval SL. An increase in SL was also observed in the Medium Fe group following 35 days of parental iron exposure. The duration of Low Fe exposure did not affect the SL of the offspring.

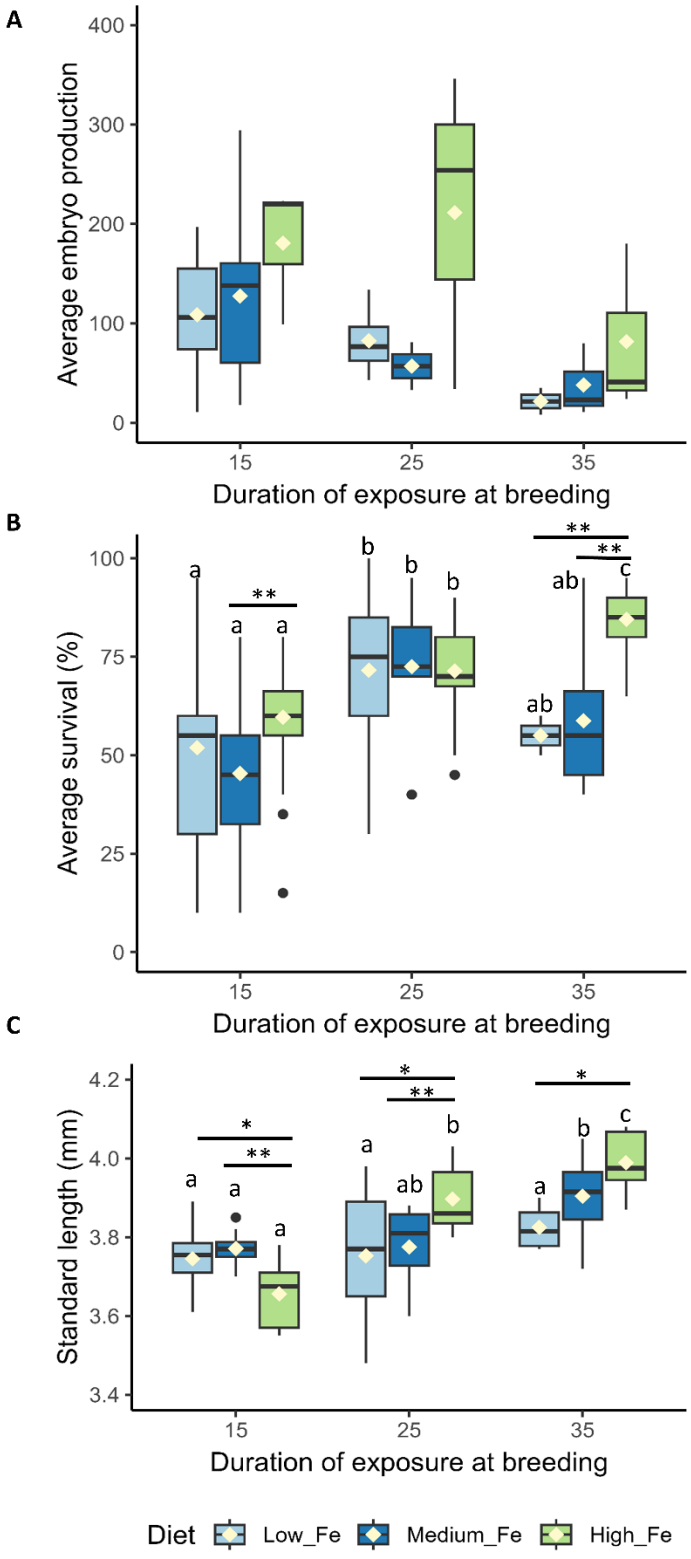

Figure 2-6. (caption next page)

Figure 2-6. Reproductive performance and offspring quality in zebrafish following parental dietary iron exposure. (A) Average embryo production per breeding pair (n=2-7 successful breeding pairs per session). (B) Percentage embryo survival 1 day post-fertilization (n=28-29 replicates for Day 15, n=6-32 for Day 25, and n=3-12 for Day 35 per dietary treatment; each replicate consists of 20 embryos). (C) Standard length (SL) of larvae at 5 days post-fertilization, derived from parents exposed to Low Fe, Medium Fe, or High Fe diets for 15, 25, or 35 days. Asterisks indicate significant (*p<0.05, **p<0.01) differences among dietary iron treatments within an exposure period; lowercase letters indicate significant differences between exposure periods within the same dietary iron treatment. Statistical analysis for average embryo production and percentage embryo survival was performed using a permutation-based two-way ANOVA (10,000 iterations), followed by pairwise permutation tests (FDR-adjusted, $p < 0.05$) to compare group differences. Two-way ANOVA followed by a post hoc Holm-Sidak test was used to compare SL between treatment groups; p<0.05 (n=4-10 fish per treatment).

During the Day 15 and Day 35 breeding sessions, embryos were collected for trace metal and major ion analysis (Figure 2-7 and Figure 2-S4). Iron was the most abundant trace metal in embryos from the Day 15 parental exposure group. Interestingly, zinc appeared to be more abundant in embryos in the Day 35 exposure group. Also, at Day 15, copper levels in embryos from High Fe treated parents were significantly higher than those from Low Fe groups. In embryos from the Day 35 exposure group, major ions such as calcium, magnesium, and sodium were significantly higher in the High Fe group compared to the Low Fe group. Apart from selenium at Day 35, all other metals and ions measured were not different between the Low and Medium Fe groups.

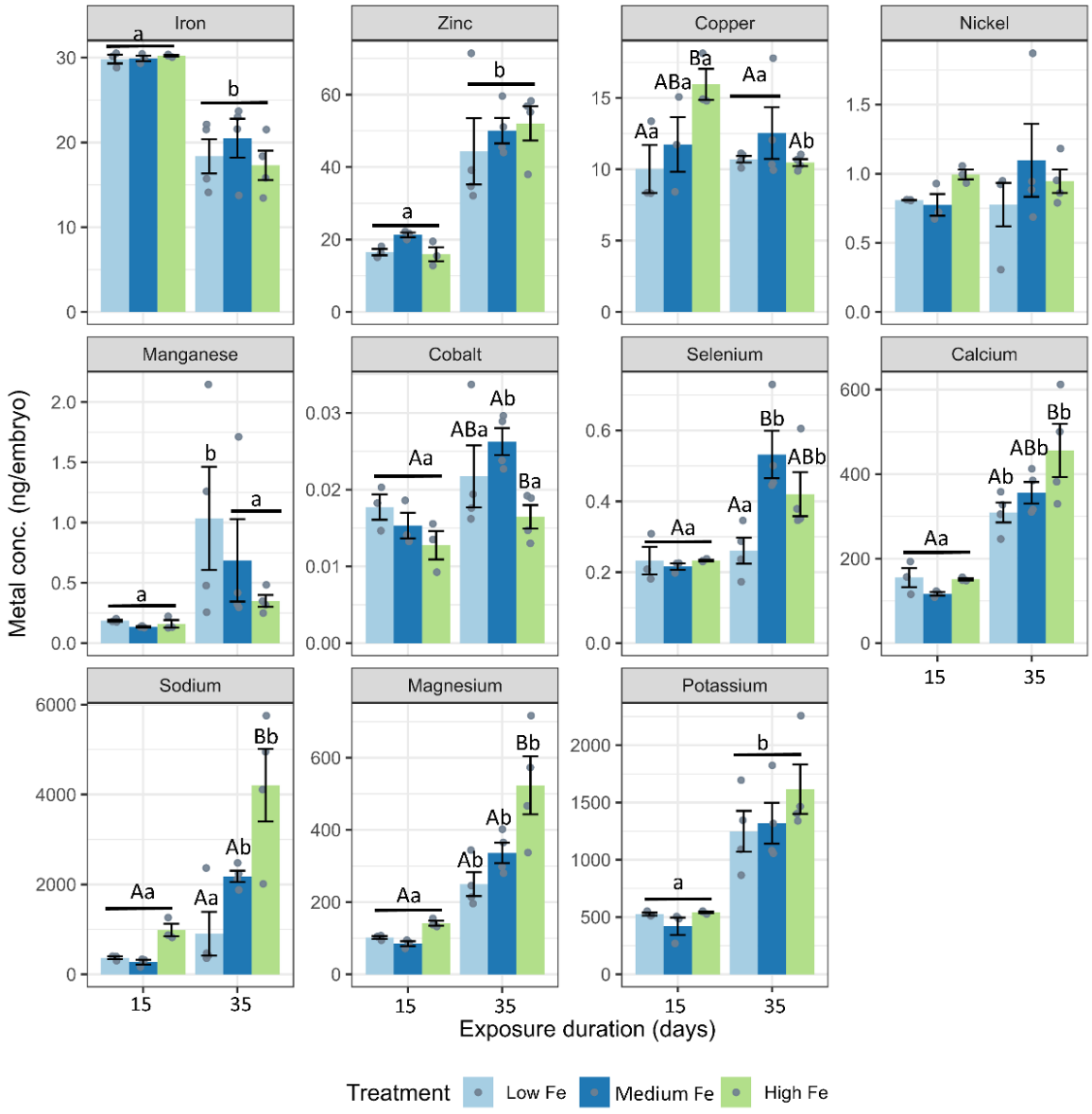

Figure 2-7. Elemental composition of zebrafish embryos derived from parents exposed to dietary iron treatments. Concentrations of iron, zinc, copper, nickel, manganese, cobalt, selenium, calcium, sodium, magnesium, and potassium (ng/embryo) in embryos collected at 15 and 35 days of parental exposure to Low Fe, Medium Fe, and High Fe diets. Data are mean ± SEM, n=3-4 (each replicate consisted of a pooled sample from 10-20 fish). Two-way ANOVA followed by a post hoc Holm-Sidak test, $p < 0.05$. Uppercase letters indicate

significant differences among dietary iron treatments within an exposure duration; lowercase letters indicate differences between exposure durations within the same dietary treatment.

2.4.5 *Physiological condition, swimming performance, and metabolic rate of the offspring*

2.4.5.1 Physiological condition

Embryos from the parental iron treatment groups were raised to adulthood and were treated with the same dietary iron regimen as their parents. There were no significant differences in weight, SL, or condition factor among the three offspring groups following dietary Fe exposure (Table 2-5). Condition factor was also comparable between the offspring groups and their respective parent groups at Day 20 (Table 2-2).

Table 2-5. Body weight (g), standard body length (cm), and condition factor (g/cm^3) of male and female offspring exposed for 20 days to the same dietary iron treatments (Low, Medium, and High Fe) as their parents. Data are mean ± SEM; n=10-13. No statistical difference noted following one-way ANOVA, $p<0.05$.

Diet	Body weight (g)	Standard body length (cm)	Condition factor (g/cm^3)
Low Fe	0.69±0.05	3.3±0.1	1.8±0.1
Medium Fe	0.54±0.02	3.2±0.0	1.7±0.0
High Fe	0.63±0.04	3.3±0.1	1.7±0.1

2.4.5.2 Swim and metabolic parameters

Offspring exposed to Low, Medium, or High Fe diets for 20 days exhibited similar trends in swimming and metabolic performance as their parents at Day 20 (Figure 2-8; Figure 2-S5). Offspring from the High Fe group showed significant improvement in swimming performance, with maximum sustained swimming speeds reaching 35 cm/s in High Fe offspring, compared to 24.5 cm/s in Low Fe fish (Figure 2-8A). Metabolic parameters including MMR, AS, and Ucrit were also elevated in the High Fe group (Figure 2-8B, C).

The difference in Ucrit between Low and High Fe groups was most pronounced in the offspring ($p<0.001$), exceeding the disparity observed in Day 20 ($p<0.01$) and Day 40 ($p>0.05$) parents (Figure 2-8; Figure 2-5). A similar pattern was observed for time to fatigue, which differed significantly between Low and High Fe offspring ($p < 0.001$) but not in parents (Figure 2-9). The offspring group displayed the largest increases in MMR, Ucrit, and fatigue time between Low and High Fe treatments when compared with their parents.

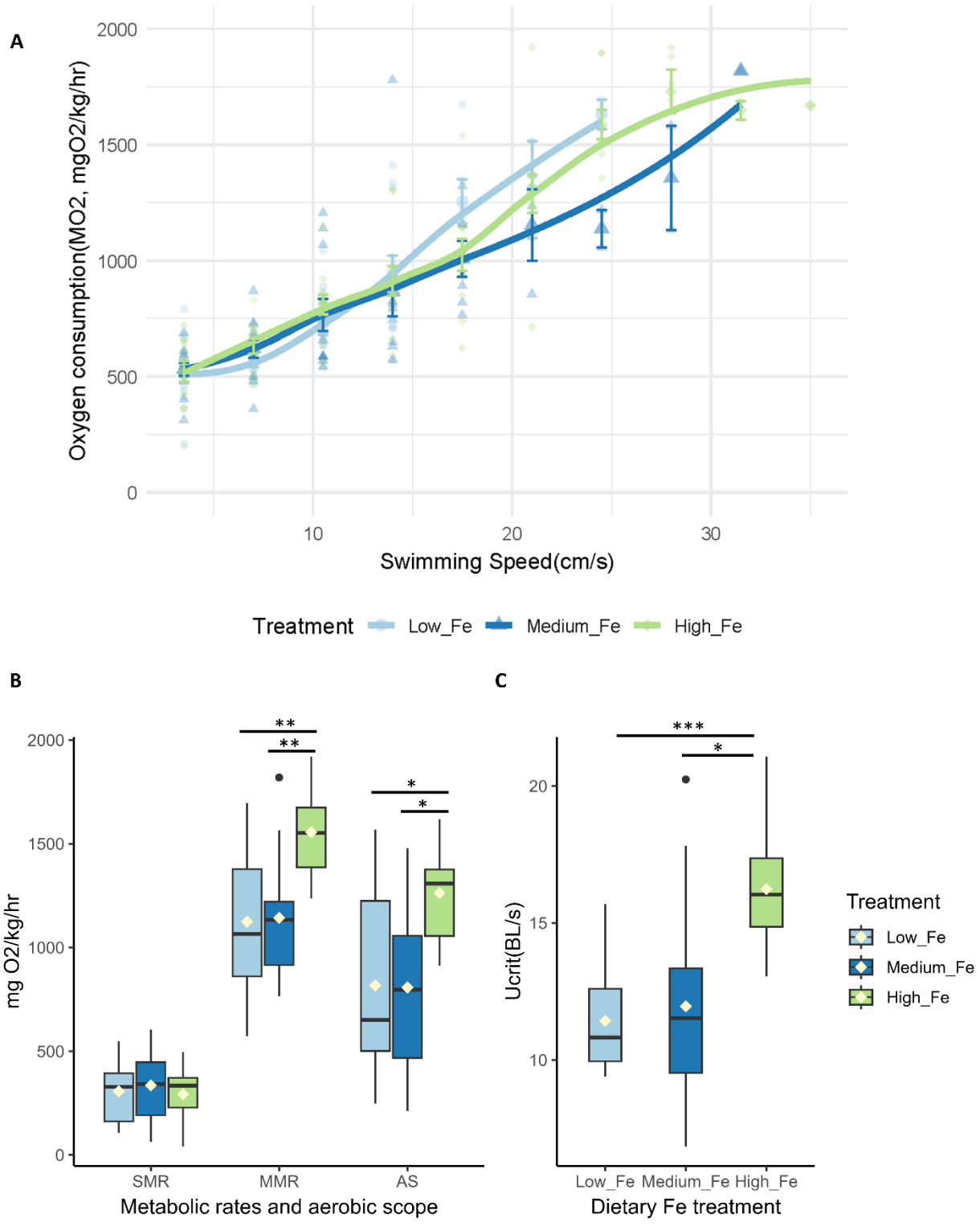

Figure 2-8. (caption next page)

Figure 2-8. Intergenerational effects of parental dietary iron exposure on swimming performance and metabolism in offspring. (A) Oxygen consumption rates (MO_2, $mgO_2/kg/hr$) during a critical swim test in adult offspring (F_1) exposed for 20 days to the same dietary iron treatment as their parents (Low Fe, Medium Fe, or High Fe). Each data point represents an individual measurement (n=12-13 fish at starting speed and n=1-2 fish at ending speed), with different symbols/colors indicating different experimental groups. Non-linear regression lines were fitted using locally estimated scatterplot smoothing (LOESS) to illustrate trends in metabolic demand across swimming speeds. Statistical differences were assessed using a two-way repeated-measures ANOVA, followed by post hoc Holm-Sidak test, $p < 0.05$. (B) Standard metabolic rate (SMR), maximum metabolic rate (MMR), and aerobic scope (AS) (n=11-12 fish per treatment group). (C) Critical swimming speed (body lengths/s; n=11-12 fish per treatment group). Asterisks denote statistical significance (*p<0.05, **p<0.01, ***p<0.001) among dietary iron groups; (One-way ANOVA; p<0.05).

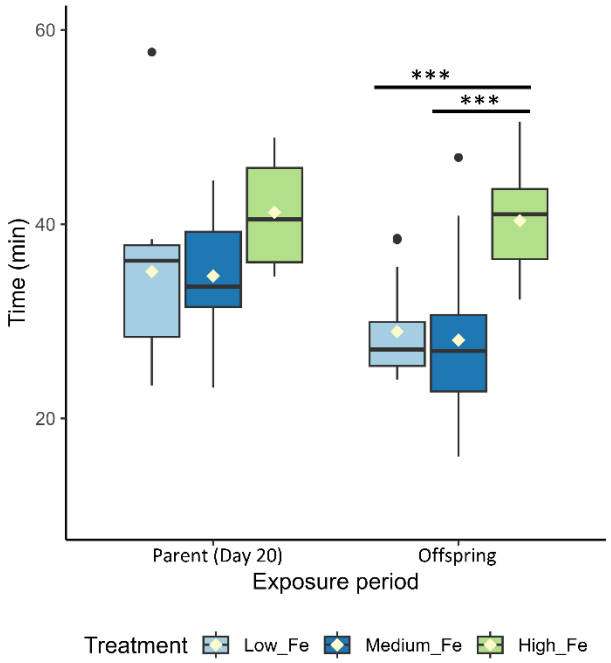

Figure 2-9. Endurance performance in parent and offspring zebrafish following dietary iron exposure. Time (min) to fatigue during a critical swim test in adult zebrafish exposed to dietary iron treatments (Low Fe, Medium Fe, and High Fe). Groups include Parent (Day 20) and Offspring (exposed for 20 days to the same dietary treatment as their parents). Asterisks indicate significant differences (***p<0.001) among dietary iron treatments within an exposure period (One-way ANOVA; p<0.05, n=7-13 per treatment group).

2.5 **Discussion**

2.5.1 *Overview and physiological responses of adult zebrafish to dietary iron levels*

Fish need to tightly regulate iron balance to meet metabolic requirements while also avoiding excessive accumulation under changing dietary iron availability. In the present study, zebrafish were fed diets representing iron deficiency (11 mg Fe/kg), adequate/control levels (420 mg Fe/kg), and iron-enriched (2300 mg Fe/kg), to reflect environmentally relevant differences in dietary iron availability. Although precise dietary requirements for zebrafish remain undefined, the three diets represented a gradient from below sufficiency to excess. The Low Fe diet contained approximately three times less iron than the lowest recommended dietary level reported for fish (Andersen et al., 1996). Here, we observed that there was no significant difference in weight, body length, condition factor, and HSI as a result of dietary iron concentrations. Our data indicate that zebrafish tolerated sub-chronic exposure to low dietary Fe without major physiological deficits, which is possibly buffered by pre-existing iron reserves. While the acclimation period (7 days) to the Medium Fe diet may have been insufficient to stabilize iron reserves in the Low Fe group, it is likely that the pre-exposure diets (~300 mg Fe/kg daily during regular rearing) could have facilitated the accumulation of sufficient iron reserves for the duration of this experiment. In a similar study, no adverse effects were reported in zebrafish fed a diet containing 33 mg Fe/kg, although a decline in body weight became apparent after ten weeks of exposure (Cooper et al., 2006).

Despite no difference among dietary groups, condition factor, HSI, and GSI were generally higher at Day 20 than Day 40. These changes coincided with the initial differences in body weight between Day 20 and Day 40 fish groups, leading to the higher physiological indices observed within the Day 20 group. The variation between Day 20 and 40 was further magnified by

reproductive demands such as repeated spawning, reflected in the significantly lower GSI observed at Day 40. In particular, female zebrafish can release hundreds of eggs, which may have also contributed to weight fluctuations during the trial. A decrease in GSI of up to 5% has been reported in females following consecutive breeding sessions (Hoo et al., 2016). Nonetheless, all parameters remained within ranges that were considered normal, and there were no other overt changes in their feeding activity (Frederickson et al., 2021). Only the females from the Medium Fe group showed no change in physiological metrics throughout the exposure duration. The iron level in this Medium Fe diet was the most similar to their pre-exposure conditions and was likely the most nutritionally optimal of the three experimental diets for maintaining all physiological indices. Furthermore, there were no apparent benefits of high iron supplementation to general physiological conditions, and both the condition factor and HSI were decreased in both sexes within this group during prolonged exposure.

2.5.2 *Tissue burden of trace metals and major ions*

Dietary iron is absorbed in the intestine and distributed throughout the body for storage and metabolic use. Iron and its transport pathways are known to interact with multiple other metals, including zinc, copper, nickel, and calcium, and dietary iron exposure has been shown to modulate the expression of zinc (Zrt- and Irt-like protein; *zip8* and *zip14*) and copper (copper transport 1; *ctr1*) transporters, and calcium (epithelial calcium channel; *ecac*) channel (Gunshin et al., 1997; Qiu and Hogstrand, 2004; Kwong and Niyogi, 2009; Chandrapalan and Kwong, 2020). In particular, the highly conserved major iron transporter, divalent metal transporter 1 (DMT1), was found to have broad specificity to multiple divalent metals (iron, zinc, manganese, cobalt, cadmium, copper, nickel, and lead) in mammals (Gunshin et al., 1997; Garrick et al., 2003). These studies suggest potential interactions among metal uptake mechanisms and multi-metal

homeostasis. In the present study, we found that dietary iron altered tissue metal burdens, most notably increasing iron in the intestine and brain. While the deleterious effects of iron in the intestine are less understood, the accumulation in the brain may have functional implications, consistent with earlier reports of neurobehavioral sensitivity to iron (Hassan and Kwong, 2020). Although we observed tissue iron accumulation, we did not directly measure biomarkers of oxidative stress (e.g., lipid peroxidation, ROS production, antioxidant enzyme activity) or tissue-level pathology, which would be important indicators of iron toxicity (Pereira et al., 2016; Chowdhury and Saikia, 2022; Formicki et al., 2025). While iron toxicity is not the scope of this study, future work incorporating these endpoints would be useful to understand whether the elevated iron burdens translate into cellular or organ-level damage. Nonetheless, among all organs examined, the intestine was the most affected by dietary Fe treatment, with almost all measured metals/ions (excluding calcium) showing significant changes either across exposure duration or between dietary treatment. Notably, there did not appear to be a consistent trend, likely reflecting complex metal–metal interactions in the intestine via DMT1 and other shared metal transport pathways (e.g., ZIPs and ECaC) (Pinilla-Tenas et al., 2011; Kondaiah et al., 2019; Chandrapalan and Kwong, 2020).

Furthermore, fish exposed to the Low Fe treatment maintained iron levels comparable to the Medium Fe group. It is possible that the Low Fe diet with deficient iron content, along with pre-existing iron reserves, was sufficient to mitigate iron dysregulation in these zebrafish.

2.5.3 *Swimming capacity and energy metabolism*

We demonstrated the nutritional benefits of sub-acute iron supplementation, as fish showed enhanced capacity for sustained swimming and exhibited higher metabolic rates. Fish fed the High

Fe diet had significantly higher Ucrit (~1.5x of the Medium Fe group), surpassing the reported average for wildtype zebrafish (~12.5 BL/s) (Plaut, 2000). These results provide evidence that iron supplementation enhances both aerobic scope and endurance capacity and may better meet the higher energetic demands during sustained swimming activities. Despite improvements in swimming performance, there were no changes in glycogen and triglyceride (primary energy sources for swimming) levels among the three dietary Fe groups. Notably, elevated ATP and hemoglobin levels were previously reported in iron-treated masu salmon (Mizuno et al., 2007), and incorporating similar measures into zebrafish studies would be valuable going forward. Since iron levels undermine ATP and hemoglobin production, iron supplementation and corresponding increases in body iron reserves may help to sustain the increase in energy and oxygen transport demands associated with enhanced swimming performance. Indeed, fish experiencing anemia and hypoxia display reduced swimming performance from limited oxygen carrying capacity and aerobic metabolic scope (Wagner and McKinley, 2004; Domenici et al., 2013).

The present study also showed signs of a potential plateau in swimming performance following sub-chronic supplementation with High Fe. Reductions in swimming performance are commonly observed in fish inhabiting metal-contaminated environments or experiencing persisting metal-induced stress (van der Oost et al., 2020; Gashkina, 2024). Previous studies also found that sublethal exposure to metals or metalloids disrupted metabolic enzymes and increased cortisol levels, impairing energy homeostasis (Handy et al., 1999; Almeida et al., 2001; Thomas and Janz, 2011; Javed and Usmani, 2015; Pettem et al., 2017). Similarly, masu salmon supplemented with 1500 but not 3000 mg Fe/kg for three months improved sprint swimming ability (Mizuno et al., 2007). Together, these results suggest a dual effect where sub-acute iron supplementation can enhance swimming capacity and metabolism, but prolonged exposure may

lead to toxicity, highlighting the narrow balance between benefit and toxicity. During prolonged exposure to high levels of iron, a threshold may exist where supplementation becomes metal stress. Fish in these circumstances require metabolic trade-offs, often diverting their energy toward detoxification (e.g., hepatic clearance) and reestablishing homeostasis, thereby limiting the energy available for other activities, including locomotion (Handy et al., 1999). Since sub-chronic exposure to High Fe was also associated with iron accumulation in organs like the brain and intestine, possible toxicity may underlie observed declines in swimming performance over time. It is also important to acknowledge the potential of repeated handling stress on swimming performance during concurrent breeding trials. As such, measuring biomarkers of oxidative stress (as mentioned above) and cortisol could help understand whether these effects lead to functional impairments in swimming performance (Clark et al., 2011; Formicki et al., 2025).

2.5.4 *Reproductive output and early development*

Our study showed that dietary iron supplementation improved reproductive output, embryo survival, and early larval growth. Zebrafish fed the High Fe diet consistently produced more embryos across all three breeding events. Zebrafish are known for their high fecundity, and within the course of the 20-day breeding period, they produced 900-1400 embryos. However, the reproductive output in zebrafish can be inherently variable, both among individuals and across breeding sessions. This variability is influenced by factors such as age, spawning frequency, and environmental conditions. Although our statistical analyses accounted for treatment effects, such variability may mask subtle differences among dietary groups. Future work should consider larger sample sizes or mixed-effect models that better accommodate repeated breeding events and individual-level variation (Hoo et al., 2016; Wafer et al., 2016). The total number of eggs produced per session also generally declined over time, possibly from the stress of repeated breeding

sessions. As oviparous fish, zebrafish embryos also rely on maternally supplied yolk nutrients (Reading et al., 2018). Interestingly, trace metal content in embryos appeared to vary inversely with the number of eggs produced at the time of breeding. Embryos from the final breeding event (Day 35) appeared to have higher metal content except for iron, copper, and nickel, but this session also produced the fewest eggs. Although these effects were non-specific to dietary treatment, they were most likely reflecting maternal depletion or selective allocation of nutrients. Previous studies have reported that maternal metal/metalloid exposure can influence offspring metal/metalloid content, including the transfer of zinc and selenium (Beaver et al., 2017; Thomas and Janz, 2015). In contrast, our findings suggested that parental iron exposure did not lead to increased iron content in the embryos. Interestingly, in embryos collected on Day 35, we observed a reduction in manganese content, but increases in calcium, sodium, and magnesium contents with increasing parental dietary Fe exposure. It seems that parental iron status may influence the deposition of certain trace metals and major ions in embryos.

2.5.5 *Offspring physiological responses and swimming performance*

Previous studies of parental exposure to waterborne metals have primarily demonstrated intergenerational effects through altered embryonic metal loads or disrupted developmental processes. For example, early life exposure to zinc was found to disrupt metal homeostasis in adult zebrafish and their offspring, with persistent alterations in genes involved in metal regulation (Zheng et al., 2022). Similarly, parental copper exposure has been linked to altered developmental processes in the next generation through epigenetic mechanisms (Tai et al., 2022). One of the most compelling findings of our study is the observation that not only waterborne exposures, but dietary exposure to iron can also elicit intergenerational effects on offspring performance. In particular, offspring of the sub-acute High Fe parents exhibited significant improvements in aerobic scope

and swimming performance, traits that are closely linked to ecological fitness. Importantly, the differences in Ucrit and fatigue resistance between the Low and High Fe groups were even more pronounced in the offspring generation. The exact mechanism underlying these intergenerational effects would be an important area to address in future studies, particularly to identify whether the enhanced offspring performance results from direct maternal iron transfer to gametes and/or epigenetic reprogramming. While we did not observe differences in iron content among the embryos from the three dietary iron groups, recent advances in epigenetic research suggested that exposure to environmental stressors can induce changes in DNA methylation, histone modification, and small RNA expression, leading to persisting transgenerational effects (Cecere, 2021; Pierron et al., 2022; Pham et al., 2023; Abdelnour et al., 2024). Incorporating such epigenetic analyses in future studies on iron exposure could provide mechanistic insight into any observed intergenerational effects.

Nonetheless, the intergenerational physiological adjustment to repeated dietary iron exposure highlights the importance of parental iron status and its lasting effects on offspring fitness. These findings reveal that dietary iron not only shapes immediate metabolic and performance outcomes in adults but can also program offspring traits with potential ecological consequences. In natural ecosystems, fluctuations in dietary iron availability, driven by environmental stressors such as hypoxia, acidification, or mining runoff, may have the potential to alter predatory-prey dynamics, foraging efficiency, and reproductive success by influencing both parental condition and offspring swimming capacity. By demonstrating that dietary iron has potential intergenerational effects on traits directly tied to survival and fitness, our study highlights the complex ecological consequences of dietary iron availability.

2.6 Conclusion and future directions

The present study reveals a complex relationship between dietary iron exposure, metal homeostasis, and swimming performance in zebrafish. We found that zebrafish tolerated both sub-acute and sub-chronic exposure to deficient and high levels of dietary iron without apparent detriments to general health; however, tissue-specific iron accumulation was observed in the High Fe treatment group following prolonged exposure. Notably, a 20-day exposure to high dietary iron led to enhanced critical swimming speed, aerobic scope, and maximum metabolic rate, as well as improved endurance capacity. These performance improvements were even more pronounced in the offspring, underscoring the potential intergenerational effects of dietary iron exposure. Together, our findings demonstrate that dietary iron availability can shape both parental and offspring performance.

From an ecological perspective, our results highlight the importance of iron levels in freshwater habitats, where natural fluctuations and anthropogenic activities can influence iron concentrations and potentially affect the fitness of wild fish populations. Additionally, understanding how parental iron nutrition impacts offspring performance could inform aquaculture practices, where optimizing feed formulations may enhance survival, growth, and resilience in subsequent generations. Future studies should focus on elucidating the molecular and physiological mechanisms underlying these intergenerational effects, with particular emphasis on iron and energy metabolism, as well as the potential roles of epigenetic modifications, transporter regulation, and interactions with other trace metals.

2.7 **Reference**

Abdelnour, S. A., Naiel, M. A. E., Said, M. Ben, Alnajeebi, A. M., Nasr, F. A., Al-Doaiss, A. A., et al. (2024). Environmental epigenetics: Exploring phenotypic plasticity and transgenerational adaptation in fish. *Environ Res* 252, 118799. doi: 10.1016/J.ENVRES.2024.118799

Almeida, J. A., Novelli, E. L. B., Alves, R., and Dal Pai Silva, M. (2001). Environmental cadmium exposure and metabolic responses of the Nile tilapia, *Oreochromis niloticus*. *Environmental Pollution* 114, 169–175. doi: 10.1016/S0269-7491(00)00221-9

Andersen, F., Maage, A., and Julshamn, K. (1996). An estimation of dietary iron requirement of Atlantic salmon, *Salmo solar* L., parr. *Aquac Nutr* 2, 41–47. doi: 10.1111/j.1365-2095.1996.tb00006.x

Andersen, Ø. (1997). Accumulation of waterborne iron and expression of ferritin and transferrin in early developmental stages of brown trout (*Salmo trutta*). Available at: https://link.springer.com/content/pdf/10.1023/A:1007729900376.pdf (Accessed April 23, 2019).

Anderson, E. R., and Shah, Y. M. (2013). Iron homeostasis in the liver. *Compr Physiol* 3, 315–330. doi: 10.1002/cphy.c120016

Beaver, L. M., Nkrumah-Elie, Y. M., Truong, L., Barton, C. L., Knecht, A. L., Gonnerman, G. D., et al. (2017). Adverse effects of parental zinc deficiency on metal homeostasis and embryonic development in a zebrafish model ☆. *J Nutr Biochem* 43, 78–87. doi: 10.1016/j.jnutbio.2017.02.006

Bury, N. (2003). Iron acquisition by teleost fish. *Comparative Biochemistry and Physiology Part C:* 135, 97–105. doi: 10.1016/S1532-0456

Cano-Barbacil, C., Radinger, J., Argudo, M., Rubio-Gracia, F., Vila-Gispert, A., and García-Berthou, E. (2020). Key factors explaining critical swimming speed in freshwater fish: a review and statistical analysis for Iberian species. *Sci Rep* 10, 1–12. doi: 10.1038/s41598-020-75974-x

Cecere, G. (2021). Small RNAs in epigenetic inheritance: from mechanisms to trait transmission. *FEBS Lett* 595, 2953. doi: 10.1002/1873-3468.14210

Chabot, D., Steffensen, J. F., and Farrell, A. P. (2016). The determination of standard metabolic rate in fishes. *J Fish Biol* 88, 81–121. doi: 10.1111/jfb.12845

Chandrapalan, T., and Kwong, R. W. M. (2020). Influence of dietary iron exposure on trace metal homeostasis and expression of metal transporters during development in zebrafish. *Environmental pollution* 261, 114159. doi: 10.1016/j.envpol.2020.114159

Chandrapalan, T., and Kwong, R. W. M. (2021). Functional significance and physiological regulation of essential trace metals in fish. *J Exp Biol* 224, jeb243834. doi: 10.1242/JEB.238790

Chandrapalan, T., Walia, S., and Kwong, R. W. (n.d.). Intergenerational Effects of Dietary Iron on Swimming and Metabolic Performance in Zebrafish. *Front Physiol* 16, 1693900. doi: 10.3389/FPHYS.2025.1693900

Chowdhury, S., and Saikia, S. K. (2022). Use of Zebrafish as a Model Organism to Study Oxidative Stress: A Review. *https://home.liebertpub.com/zeb* 19, 165–176. doi: 10.1089/ZEB.2021.0083

Clark, K. J., Boczek, N. J., and Ekker, S. C. (2011). Stressing Zebrafish for Behavioral Genetics. *Rev Neurosci* 22, 49. doi: 10.1515/RNS.2011.007

Cooper, C. A., Handy, R. D., and Bury, N. R. (2006). The effects of dietary iron concentration on gastrointestinal and branchial assimilation of both iron and cadmium in zebrafish (*Danio rerio*). *Aquatic Toxicology* 79, 167–175. doi: 10.1016/j.aquatox.2006.06.008

Cunningham, J. L., and McGeer, J. C. (2016). The effects of chronic cadmium exposure on repeat swimming performance and anaerobic metabolism in brown trout (*Salmo trutta*) and lake whitefish (Coregonus clupeaformis). *Aquatic toxicology* 173, 9–18. doi: 10.1016/j.aquatox.2015.12.003

Domenici, P., Herbert, N. A., Lefrançois, C., Steffensen, J. F., and McKenzie, D. J. (2013). The effect of hypoxia on fish swimming performance and behaviour. *Swimming Physiology of Fish: Towards Using Exercise to Farm a Fit Fish in Sustainable Aquaculture*, 129–159. doi: 10.1007/978-3-642-31049-2_6/FIGURES/8

Domínguez-Petit, R., García-Fernández, C., Leonarduzzi, E., Rodrigues, K., and Macchi, G. J. (2022). Parental Effects and Reproductive Potential of Fish and Marine Invertebrates: Cross-Generational Impact of Environmental Experiences. *Fishes 2022, Vol. 7, Page 188* 7, 188. doi: 10.3390/FISHES7040188

Formicki, G., Goc, Z., Bojarski, B., and Witeska, M. (2025). Oxidative Stress and Neurotoxicity Biomarkers in Fish Toxicology. *Antioxidants* 14, 939. doi: 10.3390/ANTIOX14080939

Frederickson, S. C., Steinmiller, M. D., Blaylock, T. R., Wisnieski, M. E., Malley, J. D., Pandolfo, L. M., et al. (2021). Comparison of juvenile feed protocols on growth and spawning in zebrafish. *J Am Assoc Lab Anim Sci* 60, 298–305. doi: 10.30802/AALAS-JAALAS-20-000105

Galbraith, E. D., Mézo, P. Le, Hernandez, G. S., Bianchi, D., and Kroodsma, D. (2019). Growth limitation of marine fish by low iron availability in the open ocean. *Front Mar Sci* 6, 28. doi: 10.3389/fmars.2019.00509

Gallaugher, P., Thorarensen, H., and Farrell, A. P. (1995). Hematocrit in oxygen transport and swimming in rainbow trout (*Oncorhynchus mykiss*). *Respir Physiol* 102, 279–292.

Garrick, M. D., Dolan, K. G., Horbinski, C., Ghio, A. J., Higgins, D., Porubcin, M., et al. (2003). DMT1: A mammalian transporter for multiple metals., in *BioMetals*, 41–54. doi: 10.1023/A:1020702213099

Gashkina, N. A. (2024). Metal toxicity: Effects on energy metabolism in fish. *Int J Mol Sci* 25, ijms25095015. doi: 10.3390/IJMS25095015

Gunshin, H., Mackenzie, B., Berger, U. V., Gunshin, Y., Romero, M. F., Boron, W. F., et al. (1997). Cloning and characterization of a mammalian proton-coupled metal-ion transporter. *Nature* 388, 482–488. doi: 10.1038/41343

Handy, R. D., Sims, D. W., Giles, A., Campbell, H. A., and Musonda, M. M. (1999). Metabolic trade-off between locomotion and detoxification for maintenance of blood chemistry and growth parameters by rainbow trout (*Oncorhynchus mykiss*) during chronic dietary exposure to copper. *Aquatic Toxicology* 47, 23–41. doi: 10.1016/S0166-445X(99)00004-1

Hassan, A. T., and Kwong, R. W. M. (2020). The neurophysiological effects of iron in early life stages of zebrafish. *Environmental Pollution* 267, 115625. doi: 10.1016/j.envpol.2020.115625

Hoo, J. Y., Kumari, Y., Shaikh, M. F., Hue, S. M., and Goh, B. H. (2016). Zebrafish: A versatile animal model for fertility research. *Biomed Res Int* 2016, 9732780. doi: 10.1155/2016/9732780

Javed, M., and Usmani, N. (2015). Impact of heavy metal toxicity on hematology and glycogen status of fish: A review. *Proc Natl Acad Sci India Sect B Biol Sci* 85, 889–900. doi: 10.1007/s40011-014-0404-x

Jee, J., Kim, S., and Kang, J. (2004). Effects of waterborne iron on serum iron concentration and iron bidning capacity of olive flounder. *J Fish Sci Technol* 7, 23–28. doi: 10.1017/CBO9781107415324.004

Judge, A., and Dodd, M. S. (2020). Metabolism. *Essays Biochem* 64, 607–647. doi: 10.1042/EBC20190041

Kondaiah, P., Singh Yaduvanshi, P., Sharp, P. A., and Pullakhandam, R. (2019). Iron and zinc homeostasis and interactions: Does enteric zinc excretion cross-talk with intestinal iron absorption? *Nutrients* 11, nu11081885. doi: 10.3390/nu11081885

Kwong, R. W. M. (2024). Trace metals in the teleost fish gill: biological roles, uptake regulation, and detoxification mechanisms. *J Comp Physiol B* 194, 1–15. doi: 10.1007/S00360-024-01565-1

Kwong, R. W. M., Hamilton, C. D., and Niyogi, S. (2013). Effects of elevated dietary iron on the gastrointestinal expression of Nramp genes and iron homeostasis in rainbow trout (*Oncorhynchus mykiss*). *Fish Physiol Biochem* 39, 363–372. doi: 10.1007/s10695-012-9705-2

Kwong, R. W. M., and Niyogi, S. (2008). An in vitro examination of intestinal iron absorption in a freshwater teleost, rainbow trout (*Oncorhynchus mykiss*). *J Comp Physiol B* 178. doi: 10.1007/s00360-008-0279-3

Kwong, R. W. M., and Niyogi, S. (2009). The interactions of iron with other divalent metals in the intestinal tract of a freshwater teleost, rainbow trout (*Oncorhynchus mykiss*). *Comp Biochem Physiol C Toxicol Pharmacol* 150, 442–449. doi: 10.1016/j.cbpc.2009.06.011

Lall, S. P., and Kaushik, S. J. (2021). Nutrition and Metabolism of Minerals in Fish. *Animals* 11, 2711. doi: 10.3390/ANI11092711

Lappivaara, J., and Marttinen, S. (2005). Effects of waterborne iron overload and simulated winter conditions on acute physiological stress response of whitefish, *Coregonus lavaretus*. *Ecotoxicol Environ Saf* 60, 157–168. doi: 10.1016/j.ecoenv.2004.01.003

Little, E. E., and Finger, S. E. (1990). Swimming behavior as an indicator of sublethal toxicity in fish. *Environ Toxicol Chem* 9, 13–19. doi: 10.1002/ETC.5620090103

Martínez, M., Guderley, H., Dutil, J. D., Winger, P. D., He, P., and Walsh, S. J. (2003). Condition, prolonged swimming performance and muscle metabolic capacities of cod *Gadus morhua*. *Journal of Experimental Biology* 206, 503–511. doi: 10.1242/JEB.00098

Massé, A. J., Thomas, J. K., and Janz, D. M. (2013). Reduced swim performance and aerobic capacity in adult zebrafish exposed to waterborne selenite. *Comp Biochem Physiol C Toxicol Pharmacol* 157, 266–271. doi: 10.1016/j.cbpc.2012.12.004

Mcbride, R. S., Somarakis, S., Fitzhugh, G. R., Albert, A., Yaragina, N. A., Wuenschel, M. J., et al. (2015). Energy acquisition and allocation to egg production in relation to fish reproductive strategies. *Fish and Fisheries* 16, 23–57. doi: 10.1111/FAF.12043

McPhee, D. L., and Janz, D. M. (2014). Dietary selenomethionine exposure alters swimming performance, metabolic capacity and energy homeostasis in juvenile fathead minnow. *Aquatic Toxicology* 155, 91–100. doi: 10.1016/j.aquatox.2014.06.012

Mizuno, S., Misaka, N., Ando, D., Torao, M., Urabe, H., and Kitamura, T. (2007). Effects of diets supplemented with iron citrate on some physiological parameters and on burst swimming velocity in smoltifying hatchery-reared masu salmon (*Oncorhynchus masou*). *Aquaculture* 273, 284–297. doi: 10.1016/J.AQUACULTURE.2007.10.011

Ohlberger, J., Staaks, G., and Hölker, F. (2006). Swimming efficiency and the influence of morphology on swimming costs in fishes. *J Comp Physiol B* 176, 17–25. doi: 10.1007/s00360-005-0024-0

Pereira, T. C. B., Campos, M. M., and Bogo, M. R. (2016). Copper toxicology, oxidative stress and inflammation using zebrafish as experimental model. *Journal of Applied Toxicology* 36, 876–885. doi: 10.1002/JAT.3303

Pettem, C. M., Weber, L. P., and Janz, D. M. (2017). Cardiac and metabolic effects of dietary selenomethionine exposure in adult zebrafish. *Toxicological sciences* 159, 449–460. doi: 10.1093/toxsci/kfx149

Peuranen, S., Vourinen, P. J., Vourinen, M., and Hollender, A. (1994). The effects of iron, humic acids and low pH on the gills and physiology of Brown Trout. *Ann Zool Fennici* 31, 389–396. doi: 10.2307/23735677

Pham, K., Ho, L., D'Incal, C. P., De Cock, A., Berghe, W. Vanden, and Goethals, P. (2023). Epigenetic analytical approaches in ecotoxicological aquatic research. *Environmental Pollution* 330, 121737. doi: 10.1016/J.ENVPOL.2023.121737

Pierron, F., Heroin, D., Daffe, G., Daramy, F., Barré, A., Bouchez, O., et al. (2022). Genetic and epigenetic interplay allows rapid transgenerational adaptation to metal pollution in zebrafish. *Environ Epigenet* 8. doi: 10.1093/EEP/DVAC022

Pinilla-Tenas, J. J., Sparkman, B. K., Shawki, A., Illing, A. C., Mitchell, C. J., Zhao, N., et al. (2011). Zip14 is a complex broad-scope metal-ion transporter whose functional properties support roles in the cellular uptake of zinc and nontransferrin-bound iron. *Am J Physiol Cell Physiol* 301, 862–871. doi: 10.1152/ajpcell.00479.2010.-Recent

Plaut, I. (2000). Effects of fin size on swimming performance, swimming behaviour and routine activity of zebrafish *Danio rerio*. *J Exp Biol* 203, 813–820. doi: 10.1242/jeb.203.4.813

Puglis, H. J., Calfee, R. D., and Little, E. E. (2019). Behavioral effects of copper on larval white sturgeon. *Environ Toxicol Chem* 38, 132–144. doi: 10.1002/etc.4293

Qiu, A., and Hogstrand, C. (2004). Functional characterisation and genomic analysis of an epithelial calcium channel (ECaC) from pufferfish, *Fugu rubripes*. *Gene* 342, 113–123. doi: 10.1016/j.gene.2004.07.041

Reading, B. J., Andersen, L. K., Ryu, Y.-W., Mushirobira, Y., Todo, T., and Hiramatsu, N. (2018). Oogenesis and egg quality in finfish: Yolk formation and other factors influencing female fertility. *Fishes* 3, fishes3040045. doi: 10.3390/fishes3040045

Rubio-Gracia, F., Garci´a, E., Garci´a-Berthou, G., Guasch, H., Zamora, L., and Vila-Gispert, A. (2020). Size-related effects and the influence of metabolic traits and morphology on swimming performance in fish. *Curr Zool* 66, 493–503. doi: 10.1093/cz/zoaa013

Saha, R. K., Saha, H., Debnath, M., and Kamilya, D. (2015). Effects of waterborne iron on fry of *Catla catla* (Ham.), *Labeo rohita* (Ham.) and *Cirrhinus mrigala* (Ham.). *Article in Indian Journal of Animal Research* 49, 210–217. doi: 10.5958/0976-0555.2015.00106.5

Singleman, C., and Holtzman, N. G. (2014). Growth and Maturation in the Zebrafish, *Danio Rerio* : A Staging Tool for Teaching and Research. *Zebrafish* 11, 396–406. doi: 10.1089/zeb.2014.0976

Tai, Z., Guan, P., Zhang, T., Liu, W., Li, L., Wu, Y., et al. (2022). Effects of parental environmental copper stress on offspring development: DNA methylation modification and responses of differentially methylated region-related genes in transcriptional expression. *J Hazard Mater* 424, 127600. doi: 10.1016/J.JHAZMAT.2021.127600

Taslima, K., Al-Emran, M., Rahman, M. S., Hasan, J., Ferdous, Z., Rohani, M. F., et al. (2022). Impacts of heavy metals on early development, growth and reproduction of fish – A review. *Toxicol Rep* 9, 858–868. doi: 10.1016/j.toxrep.2022.04.013

Thomas, J. K., and Janz, D. M. (2011). Dietary selenomethionine exposure in adult zebrafish alters swimming performance, energetics and the physiological stress response. *Aquatic Toxicology* 102, 79–86. doi: 10.1016/j.aquatox.2010.12.020

Thomas, J. K., and Janz, D. M. (2014). In ovo exposure to selenomethionine via maternal transfer increases developmental toxicities and impairs swim performance in F1 generation zebrafish (*Danio rerio*). *Aquatic Toxicology* 152, 20–29. doi: 10.1016/j.aquatox.2014.03.022

Thomas, J. K., and Janz, D. M. (2015). Developmental and persistent toxicities of maternally deposited selenomethionine in zebrafish (*Danio rerio*). *Environ Sci Technol* 49, 10182–10189. doi: 10.1021/acs.est.5b02451

Thomason, R. T., Pettiglio, M. A., Herrera, C., Kao, C., Gitlin, J. D., and Bartnikas, T. B. (2017). Characterization of trace metal content in the developing zebrafish embryo. *PLoS One* 12, 0179318. doi: 10.1371/journal.pone.0179318

Tudorache, C., Viaene, P., Blust, R., Vereecken, H., and De Boeck, G. (2008). A comparison of swimming capacity and energy use in seven European freshwater fish species. *Ecol Freshw Fish* 17, 284–291. doi: 10.1111/J.1600-0633.2007.00280.X

van der Oost, R., McKenzie, D. J., Verweij, F., Satumalay, C., van der Molen, N., Winter, M. J., et al. (2020). Identifying adverse outcome pathways (AOP) for Amsterdam city fish by integrated field monitoring. *Environ Toxicol Pharmacol* 74, 103301. doi: 10.1016/j.etap.2019.103301

Videler, J. J. (1993). “The costs of swimming,” in *Fish Swimming*, (Springer, Dordrecht), 185–205. doi: 10.1007/978-94-011-1580-3_9

Wafer, L. N., Jensen, V. B., Whitney, J. C., Gomez, T. H., Flores, R., and Goodwin, B. S. (2016). Effects of Environmental Enrichment on the Fertility and Fecundity of Zebrafish (*Danio*

rerio). *J Am Assoc Lab Anim Sci* 55, 291. Available at: https://pmc.ncbi.nlm.nih.gov/articles/PMC4865689/ (Accessed September 10, 2025).

Wagner, G. N., and McKinley, R. S. (2004). Anaemia and salmonid swimming performance: The potential effects of sub-lethal sea lice infection. *J Fish Biol* 64, 1027–1038. doi: 10.1111/J.1095-8649.2004.0368.X

Wakamatsu, Y., Ogino, K., and Hirata, H. (2019). Swimming capability of zebrafish is governed by water temperature, caudal fin length and genetic background. *Sci Rep* 9, 16307. doi: 10.1038/s41598-019-52592-w

Wang, W. X. (2013). Dietary toxicity of metals in aquatic animals: Recent studies and perspectives. *Chinese Science Bulletin* 58, 203–213. doi: 10.1007/s11434-012-5413-7

Wang, Z., Li, X., Lu, K., Wang, L., Ma, X., Song, K., et al. (2023). Effects of dietary iron levels on growth performance, iron metabolism and antioxidant status in spotted seabass (*Lateolabrax maculatus*) reared at two temperatures. *Aquaculture* 562, 738717. doi: 10.1016/J.AQUACULTURE.2022.738717

Watanabe, T., Kiron, V., and Satoh, S. (1997). Trace minerals in fish nutrition. *Aquaculture* 151, 185–207. doi: 10.1016/S0044-8486(96)01503-7

Wood, C. M., Farrell, A. P., and Brauner, C. J. (2011). *Homeostasis and toxicology of essential metals*. Academic Press. doi: 10.1016/S1546-5098(11)31010-2

Xing, W., and Liu, G. (2011). Iron biogeochemistry and its environmental impacts in freshwater lakes. *Fresenius Environ Bull* 20, 1339–1345. Available at:

http://sourcedb.cas.cn/sourcedb_wbg_cas/yw/rckyw/201002/W020120116564991205836.pdf

Zheng, J. L., Zhu, Q. L., Hu, X. C., Parsons, D., Lawson, R., and Hogstrand, C. (2022). Transgenerational effects of zinc in zebrafish following early life stage exposure. *Sci Total Environ* 828, 154443. doi: 10.1016/J.SCITOTENV.2022.154443

2.8 Supplementary Tables and Figures

Table 2-S 1. Nutritional composition of purified zebrafish diet deficient in Fe used to prepare the experimental diets.

Ingredient	Concentration (g/Kg)
Cornstarch	329
Dyetrose*	110
Microcrystalline Cellulose	190
Soybean Oil	30.0
Menhaden Oil	30.0
Ethoxyquin (0.1%)	0.060
L-Amino Acid mix	239
Salt Mix #295004 (Rx, no Fe)	40.0
Sodium Bicarbonate	14.3
Vitamin Mix #390015	10.0
L-Methionine	6.12
Choline Chloride	1.67

* Depolymerized cornstarch which aids in the pelleting process.

Table 2-S 2. Elemental composition (mg/kg) in the purified iron deficient diet purchased from Dyets Inc. and the experimental diets (Low Fe, Medium Fe, and High Fe). Data are mean ± SEM; n = 4 (Dyets) and n =9 (Experimental diets).

Element	Purified base diet	Experimental diets
Zn	48 ± 2	61 ± 5
Cu	36 ± 9	34 ± 7
Ni	0.42 ± 0.01	0.29 ± 0.06
Mn	67 ± 20	66 ± 2
Co	0.24 ± 0.02	0.31 ± 0.01
Se	0.052 ± 0.002	0.08 ± 0.0048
Ca	7200 ± 200	6800 ± 200
Na	5500 ± 70	5500 ± 270
Mg	190 ± 40	310 ± 8
K	3800 ± 500	4000 ± 200

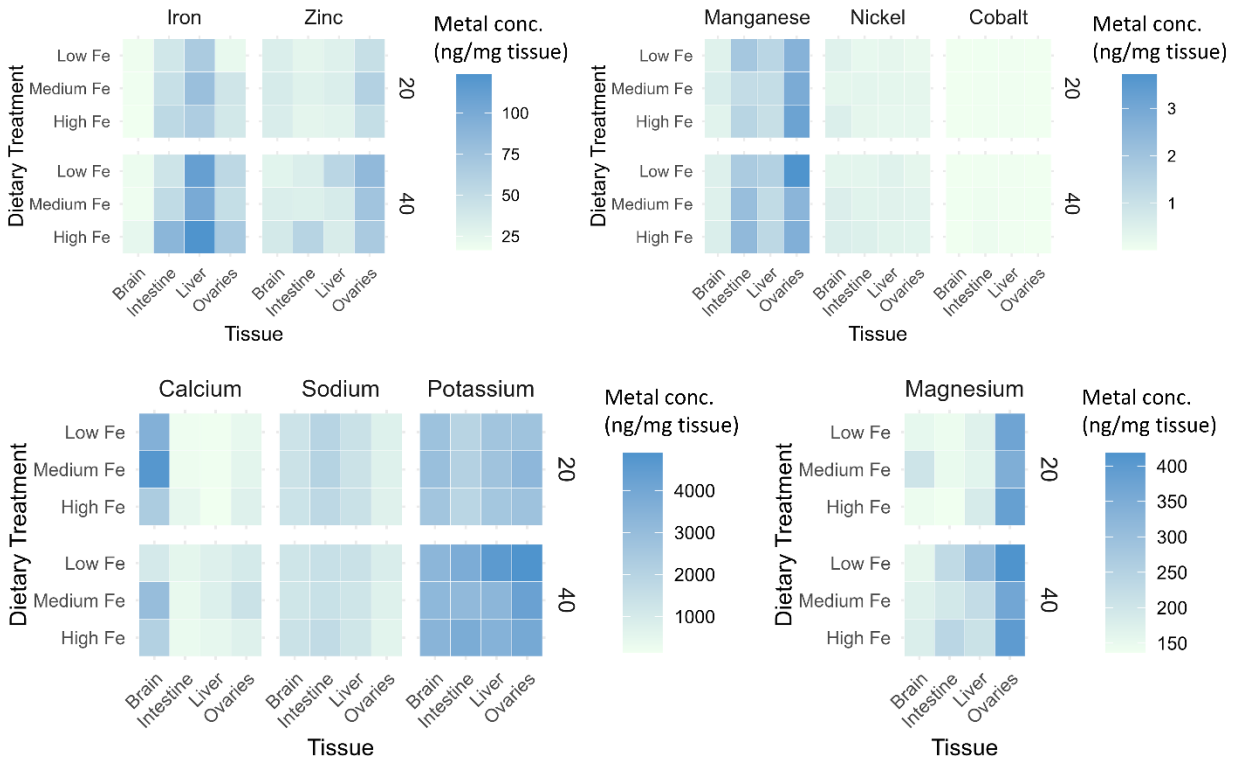

Figure 2-S 1. Tissue specific accumulation of trace metals and major ions in zebrafish following dietary iron exposure. Heatmaps showing the concentrations (ng/mg tissue) of trace metals and major ions in various organs of zebrafish exposed to different dietary iron treatments (Low, Medium, and High Fe) for 20 or 40 days. Concentrations are represented by a color gradient, with darker shades indicating higher concentrations. Data are mean; n=3-4 (each replicate consisted of a pooled sample from 3-5 fish).

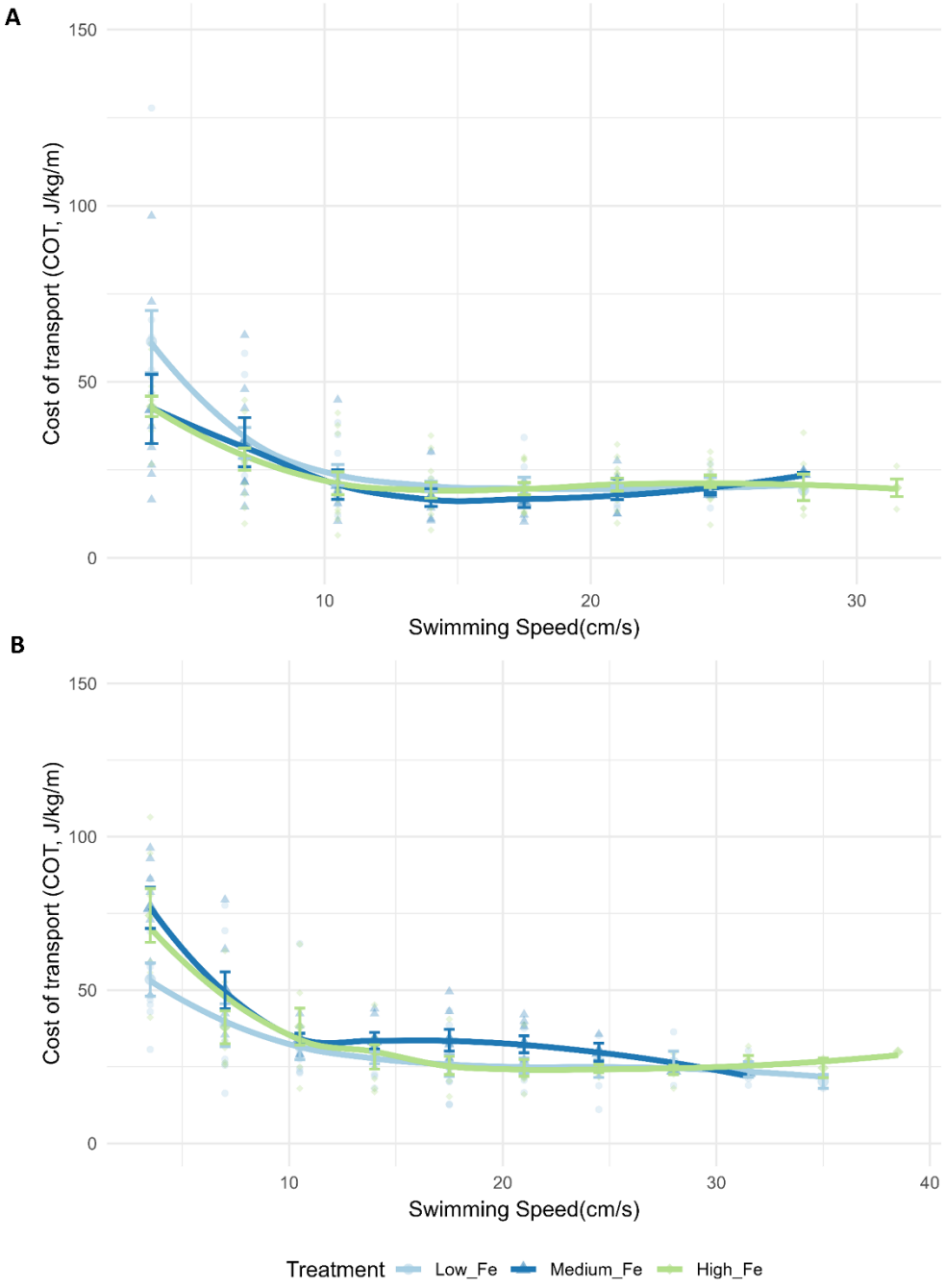

Figure 2-S 2. Cost of transport in zebrafish exposed to dietary iron. Cost of transport (COT, J/kg/m) during a critical swim test in zebrafish exposed to different dietary iron treatments for (A) 20 and (B) 40 days. Each data point represents an individual measurement, with different symbols/colors indicating different experimental groups. Non-linear regression lines were fitted using locally estimated scatterplot smoothing (LOESS)

to illustrate trends in metabolic demand across swimming speeds. Data are mean ± SEM, n=7-12 fish per treatment. Statistical differences were assessed using a two-way repeated-measures ANOVA, followed by post hoc Holm-Sidak test, $p < 0.05$.

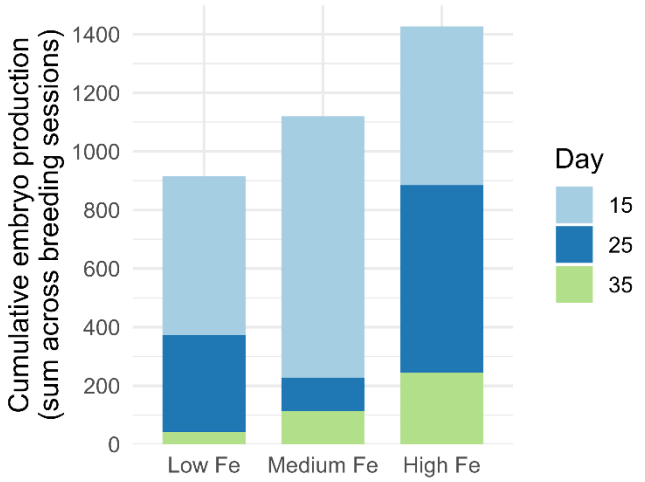

Figure 2-S 3. Cumulative embryo production following dietary iron exposure. Stacked bars show the total number of embryos produced across three breeding sessions (Day 15, 25 and 35) for each dietary iron treatment (Low, Medium, and High Fe). Two-way linear model (Embryo production ~ Diet + Day) with pairwise comparison among treatments obtained from estimated marginal means (Sidak-adjusted) found no significant differences (p>0.05). N=10-12 breeding pairs per dietary iron treatment with 2-7 successful breeding pairs per breeding session.

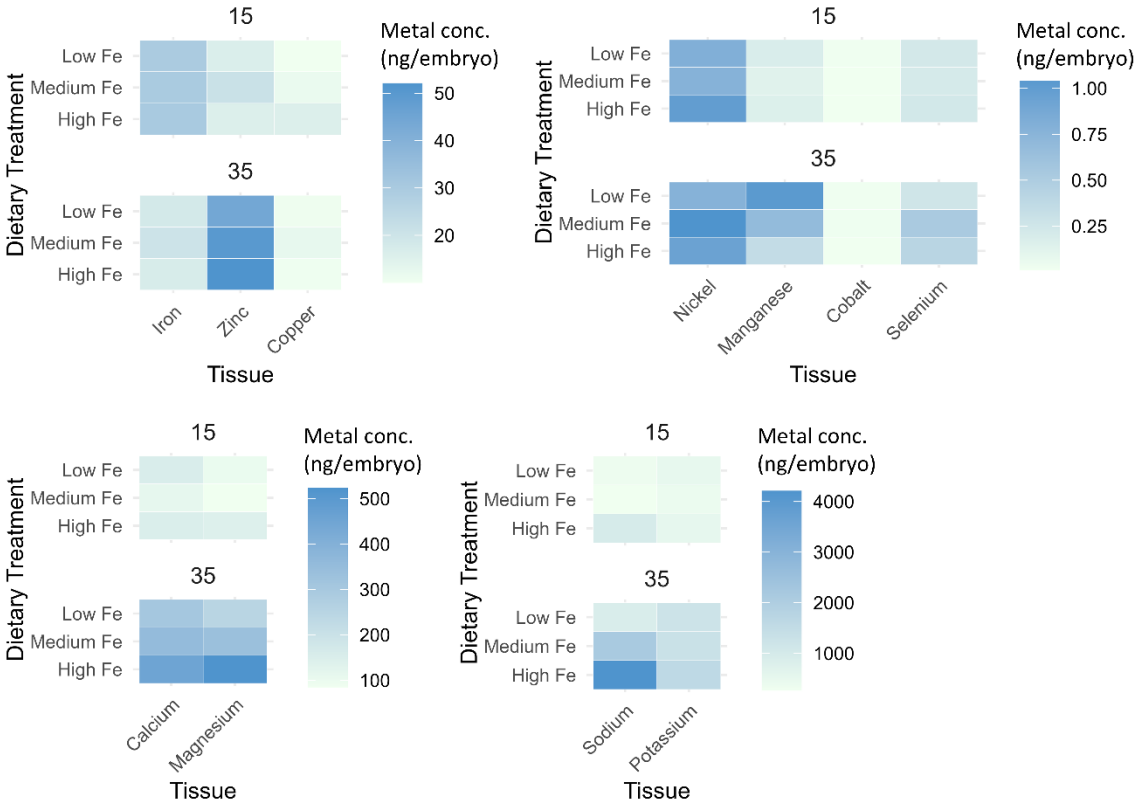

Figure 2-S 4. Elemental composition of zebrafish embryos following parental dietary iron exposure. Heatmaps showing the concentrations (ng) of trace metals, minerals, and major ions in embryos collected from zebrafish exposed to different dietary iron treatments for 15 and 35 days. Concentration is represented by a color gradient, with darker shades indicating higher concentrations of metals. Data are mean; n=3-4 (each replicate consisted of a pooled sample of 10-20 embryos).

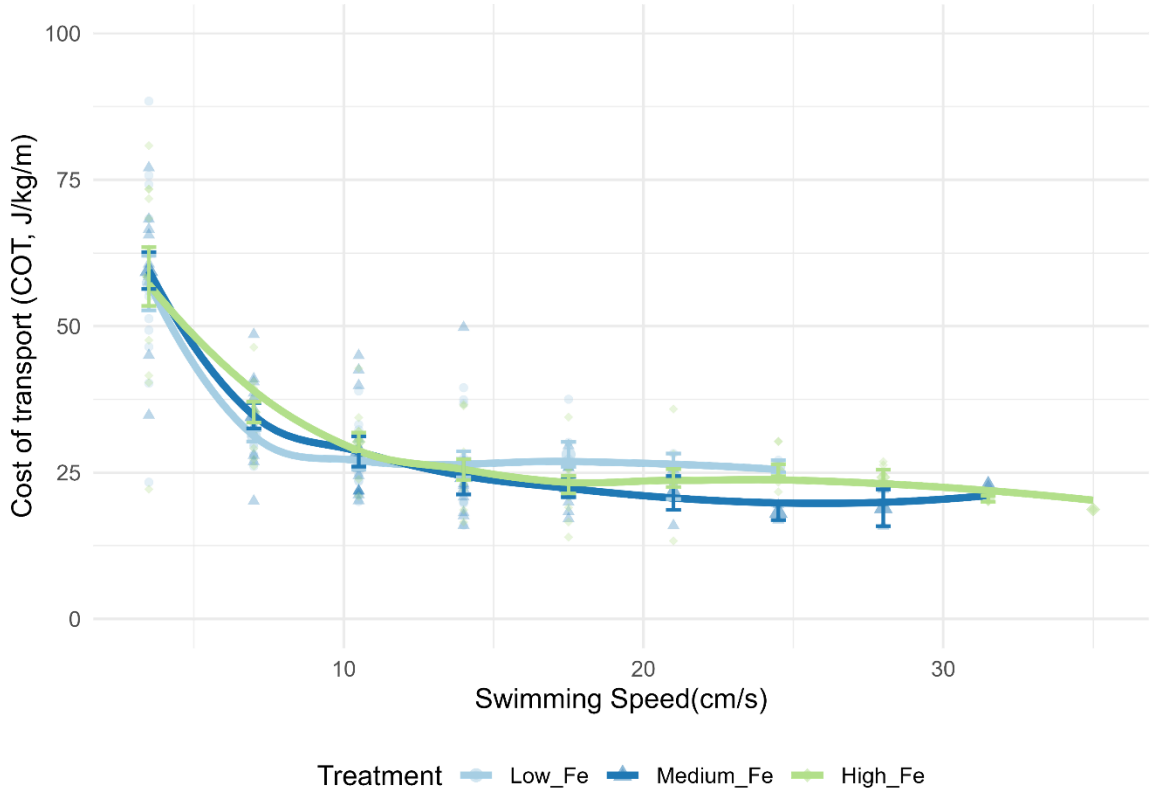

Figure 2-S 5. Cost of transport in zebrafish offspring following parental dietary iron exposure. Cost of transport (COT, J/kg/m) during a critical swim test in offspring of parents exposed to different dietary iron levels and subsequently fed the same dietary iron treatments for 20 days. Each data point represents an individual measurement, with different symbols/colors indicating different experimental groups. Nonlinear regression lines were fitted using locally estimated scatterplot smoothing (LOESS) to illustrate trends in metabolic demand across swimming speeds. Data are presented as mean ± SEM; n = 12–13 fish per treatment. Statistical differences were assessed using a two-way repeated-measures ANOVA, followed by post hoc Holm-Sidak test, $p < 0.05$.

Chapter 3

CRISPR-Cas9 Mediated Knock Out of Major Iron Transporter Affects Homeostasis of Multiple Essential Metals

3.1 Summary

Divalent metal transporter 1 (DMT1) is thought to be the primary route for non-heme iron absorption in vertebrates, but its systemic role remains poorly understood. Using CRISPR-Cas9 gene editing, we generated a DMT1 knockout (*dmt1*$^{-/-}$) zebrafish line to examine the developmental and physiological consequences of DMT1 loss. Phenotypic and hematological assessments were performed alongside measurements of whole-body and tissue-specific metal concentrations. Further, to identify potential compensatory pathways during DMT1 loss, the expression profile of candidate metal transporters or ion channels (*hcp1*, *zip4*, *zip8*, *zip14*, and *ecac*) was quantified using droplet digital PCR (ddPCR). *Dmt1*$^{-/-}$ larvae exhibited delayed development, anemia, and had broad disruption in multiple trace elements (iron, zinc, manganese, cobalt, and selenium). Gene expression analysis during early development revealed adjustments in several transporters, suggesting possible compensatory responses to maintain metal homeostasis during DMT1 loss. Although viable to adulthood, the mutants had persisting iron dysregulation and red blood cell abnormalities. This study provides the first *in vivo* evidence of the physiological role of DMT1 in multi-metal balance in fish and offers new insight into compensatory mechanisms underlying DMT1 loss.

3.2 Introduction

Iron (Fe) is an essential trace element that coordinates a wide range of biological processes in vertebrates, including oxygen transport, energy production, DNA synthesis, and cellular respiration (Cairo et al., 2006; Chandrapalan and Kwong, 2021). Fe is an integral component of hemoglobin and forms various metalloenzymes, but at the same time, high levels of Fe can lead to oxidative stress and cell damage (Galaris et al., 2019; Meneghini, 1997). Accordingly, maintaining systemic Fe levels within physiologically safe limits is essential for optimal health.

A key protein responsible for the uptake and internal regulation of Fe is divalent metal transporter 1 (DMT1, also known as SLC11A2) (Fleming et al., 1997; Gunshin et al., 1997). Although DMT1 is the major route for non-heme bound Fe absorption, this protein has previously been reported to facilitate the transport of several other divalent cations including zinc (Zn), manganese (Mn), cobalt (Co), and nickel (Ni), which play critical roles in development, antioxidant defense, and cellular signaling (Garrick et al., 2003; Gunshin et al., 1997; Zhao et al., 2014). DMT1 is also important for the intracellular transport of Fe via endosomes (Garrick et al., 2003; Yanatori and Kishi, 2019). Furthermore, the function of DMT1 in Fe transport appears to be highly conserved among vertebrates (Neves et al., 2011; Zhao et al., 2014). Consistent with this, human and mouse DMT1 share 89% protein identity, while the zebrafish homolog is about 71-73% identical to mammalian DMT1 (Zhao et al., 2014). In mammalian models, mutations in *Slc11a2* result in severe microcytic anemia, impaired erythropoiesis, and disrupted Fe distribution (Fleming et al., 1998; Gunshin et al., 2005; Veuthey and Wessling-Resnick, 2014). As such, these properties of DMT1 highlight the integral role of this transporter in metal homeostasis and overall organismal health.

While DMT1 has been quite well characterized in mammals, its functional involvement in fishes remains less investigated, particularly with respect to its *in vivo* significance in multi-metal regulation and broader systemic roles. Importantly, potential compensatory regulation of other metal transporters during DMT1 deficiency is yet to be determined. The *chardonnay* (*cdy*) zebrafish, which carries a mutation in *dmt1* induced by treatment with N-ethyl-N-nitrosourea, exhibited hypochromic microcytic anemia but remained viable (Donovan et al., 2002). This finding suggests possible compensation by alternate iron uptake pathways. Notably, the heme carrier protein 1 (HCP1; also known as SLC46A1), Zrt- and Irt-like family of transporters (ZIP4,

ZIP8, and ZIP14), and the epithelium calcium channel (ECaC), have been implicated in Fe transport/homeostasis (Dufner-Beattie et al., 2003; Geiser et al., 2012; Pinilla-Tenas et al., 2011; Qiu and Hogstrand, 2004; van Raaij et al., 2019; Wang et al., 2012). These proteins represent potential alternative or compensatory pathways for iron uptake in the absence of DMT1.

In fishes, Fe can be taken up through the apical membrane of the intestinal epithelium from the diet and across the gill lamellae directly from the surrounding water (Bury, 2003a; Kwong, 2024; Kwong and Niyogi, 2009; Okazaki, 2023). Coordinating Fe uptake from these two routes requires precise regulatory mechanisms, especially under variable environmental conditions and fluctuating Fe availability (Norman et al., 2014; Xing and Liu, 2011). Nonetheless, fishes exhibit remarkable physiological plasticity, adjusting transporter expression profiles and prioritizing uptake pathways depending on Fe source and demand (Chandrapalan and Kwong, 2020; Wang and Wang, 2016). Despite these insights, the systemic and developmental roles of the major iron transporter in fish have yet to be fully characterized.

In the present study, CRISPR-Cas9 gene editing was employed to perform targeted mutagenesis, generating a *dmt1*$^{-/-}$ knockout (KO) zebrafish line to assess the phenotypic, hematological, and physiological consequences of DMT1 loss at different developmental stages. We assessed trace metal and major ion concentrations in whole-body and specific tissues using inductively coupled plasma mass spectrometry (ICP-MS) to understand the effects of DMT1 KO on metal homeostasis. In addition, we investigated the mRNA expression of potential candidate genes (*hcp1*, *zip4*, *zip8*, *zip14*, and *ecac*) for compensatory responses during DMT1 loss using droplet digital PCR (ddPCR). We hypothesized that DMT1 is essential for maintaining metal homeostasis and, as such, i) DMT1 KO will result in the dysregulation of metals, including Fe and potentially other divalent metals, and ii) DMT1 KO fish will exhibit modulation in the expression

of other transporters as a means to compensate for this dysregulation. To our knowledge, this is the first study employing targeted CRISPR-Cas9 mutagenesis to investigate the systemic roles of DMT1 in fish, revealing novel developmental and adaptive mechanisms underlying multi-metal regulation following DMT1 loss.

3.3 Material and Methods

3.3.1 Animals

Zebrafish (*Danio rerio;* Tüpfel long fin strain) were housed at York University's vivarium, and all animal experiments were carried out in accordance with the Canadian Council for Animal Care and approved by the York University Animal Care Committee (2017-2 R2). Adult zebrafish were maintained in recirculatory systems (Aquaneering, CA, USA) at 28°C with a 14h light: 10h dark photoperiod. Fish were kept in mixed sex groups at a density of 25-30 fish per 2.8 L tanks. Adult fish were fed brine shrimp each morning (weekdays) and commercial zebrafish pellets (Zeigler, PA, USA) daily in the afternoon. The trace metal composition of the Zeigler diet was approximately: 309.00 mg Fe/kg, 208.00 mg Zn/kg, 57.00 mg Mn/kg, 40 mg Cu/kg, 0.41mg Co/kg, and 1.19 mg I/kg.

Prior to breeding, zebrafish were separated by sex for one week and bred in the morning for embryo collection. The embryos were then transferred to 50 mL Petri dishes (20 embryos per dish) containing 0.5 ppm methylene blue in system water and grown to 5 days post fertilization (dpf). From the onset of exogenous feeding (~5 dpf) to early juvenile development (~10-15 dpf), fish were raised in a polyculture with rotifer before gradually transitioning to brine shrimp and dry feed (about 1 month post-fertilization).

3.3.2 Microinjection and generation of targeted mutation

The DMT1 knockout (KO) line (*dmt1*$^{-/-}$) was generated in-house using the CRISPR-Cas9 system (Figure 3-1) (Jao et al., 2013). Potential CRISPR target sites were identified using CHOPCHOP, and a synthetic single guide RNA (sgRNA; 5'-CCGACGCCCCGUCUCGAGGU-3') targeting exon 5 of *dmt1* (gene ID: 678623) was purchased from Synthego Corporation (CA, USA) (Figure 3-1A and B). On the *Danio rerio* chromosome 11 (NC_007122.7) GRCz11 (GCF_000002035.6) gene assembly, the site of mutation is located between 285,669 - 285,682 bp. Synthesized gRNA was diluted (200 ng/µL) and stored at -80°C. Cas9 protein (EnGen® Spy Cas9 NLS) was purchased from NEB (MA, USA) and stored at -20°C until use.

The injection solution was prepared on the day of use and consisted of 50 ng/µL sgRNA, 5 µM Cas9 protein, 0.3 M KCl, 0.05% phenol red, and nuclease-free water. Control injections excluded sgRNA. Approximately 2 nL of solution was microinjected into one-cell stage embryos using a WPI picopump pv830 (FL, USA) to establish the founding generation (F_0).

3.3.3 Mutagenesis analysis and generation of homozygous mutants

At 1 dpf, ten injected embryos were randomly sampled for genomic DNA extraction and mutation screening. Total DNA from individual embryos was extracted by incubation in 50 mM NaOH for 10 minutes at 95°C, followed by vortexing for tissue disruption and release of genetic material. Samples were neutralized (1:10) with 1 M Tris-HCl (pH 8.0) prior to polymerase chain reaction (PCR) analysis using the One*Taq*® DNA polymerase kit (New England Biolabs, MA, USA). CHOPCHOP was used to identify regions flanking the target site and was used to design the sequencing primers (Labun et al., 2016). To test for successful mutation, RT-PCR was performed using primers for exon 5 (genotyping primer; Table 3-1). The PCR protocol was: 30 s

initial denaturation at 94°C, 35 cycles of 94°C for 30 s, 55°C for 60 s, 68°C for 45 s, and a final extension at 68°C for 5 min. Amplicons were resolved on a 5% agarose gel with RedSafe nucleic acid staining solution (FroggaBio, ON, CA) and imaged using Invitrogen iBright™ CL1500 imager (ThermoFisher Scientific, ON, CA). Heteroduplex banding patterns indicated potential mutagenesis in mosaic (F_0) and heterozygous (F_1) individuals (Zhu et al., 2014). In F_2 homozygous mutants, a reduced PCR product size (from 555 bp in WT fish) indicated a putative deletion. PCR products were purified (Monarch PCR & DNA Cleanup Kit, New England Biolabs) and sequenced (The Centre for Applied Genomics, The Hospital for Sick Children, Toronto, ON) to confirm the mutations.

Table 3-1. Primer sets used for RT-PCR and droplet digital PCR.

Gene	Accession Number	Primer sequence
dmt1 (genotyping)	NC_007122.7	F: 5'- TATGTGGATATTGCGGAGCA-3' R: 5'- ATCCACACACCTCCATCACA-3'
dmt1	NM_001040370.1	F: 5'-CTGCGCTCTACATCTGGGCT-3' R: 5'-CTGCACGTCCTGAAACACGG-3'
hcp1	NM_200285.1	F: 5'-TGGCATTATTGGGGGCTTGG-3' R: 5'-TGAGTTGTACATGCGTCCCT-3'
zip4	XM_073931343.1 & XM_073931344.1	F: 5'-TGGCAGACATGCTTCCTACG-3' R: 5'-TTCCCCAGCCGCTTAAAAGT-3'
zip8	XM_009307205.4	F: 5'-TGGAAGATGAAGGCAATCCGC-3' R: 5'-CTGACACTGACCACAGAAGCG-3'
zip14	NM_001326699.1	F: 5'-GCAGAGGGGTTGGAGAAGAC-3' R: 5'-TGCCGATGTCAGAGTAAGCC-3'
ecac	XM_005173469.3	F: 5'-GTCTCGGTGTCCTCCTGAAATC-3' R: 5'-GCATTGTTCTCCTTAGTGGCGG-3'
ef1α	AM422110.2	F: 5'-CCTCTTGGTCGCTTTGCTGT-3' R: 5'-GAGGTTGGGAAGAACACGCC-3'

Gene	Accession Number	Primer sequence
rpl13	NM_001326699.1	F: 5'- GTATTTGGCTTCCTCCGCA-3'
		R: 5'- ACCATGCGCTTTCTCTTGTC-3'
rps18	NM_001320405.1	F: 5'- CCCTCGTCATCCCAGAGAAGT-3'
		R: 5'- CGCCTTCCAACACCCTTAATA-3'

dmt1, divalent metal transporter 1; *hcp1*, heme carrier protein 1; *zip4*, Zrt- and Irt-like protein 4; *zip8*, Zrt- and Irt-like protein 8; *zip14*, Zrt- and Irt-like protein 14; *ecac*, epithelial calcium channel; *ef1a*, elongation factor 1 alpha; *rpl13*, ribosomal protein L13; *rps18*, ribosomal protein S18.

3.3.4 Generation of homozygous mutants

The generation of heterozygous and homozygous mutants is illustrated in Figure 3-1C. In brief, F_0 embryos (Founder) were grown to 90 dpf (reproductive maturity) and outcrossed with WT fish to generate heterozygous F_1 offspring (*dmt1*$^{+/-}$). The F_1 offspring were similarly screened for a mutation (as described above), and positive fish were identified and in-crossed to establish F_2 homozygous mutants. Genotyping of adult fish was performed using tailfin clipping, and gDNA was extracted similarly to 1 dpf samples. Homozygous mutants were bred again to obtain the subsequent generations of *dmt1*$^{-/-}$ used for all downstream experiments involving the mutants. For each generation of mutants, a corresponding WT control generation was also established. F_1 control fish were generated by in-crossing F_0 fish microinjected with a control injection (lacking sgRNA). WT controls were in-crossed to produce all subsequent generations, and these fish will be referred to as WT hereafter.

3.3.5 Physiological parameters of DMT1 mutants and Fe metabolism

To evaluate the physiological condition of mutants, rates of survival (24 hour post fertilization; hpf), morphology, standard body length (SL; mm), and weight (g) were monitored

from embryo to the juvenile stage of development. Images of developing fish were captured using a camera-equipped stereomicroscope (Leica Microsystems, ON, Canada) with LAS X software. Adult fish were euthanized with buffered tricaine (0.4 g/L MS-222) for measurements of SL, weight, condition factor [K = 100 x (weight (g)/length^3 (cm))], gonadosomatic index [GSI = 100 x (gonad weight (g)/body weight (g))], hepatosomatic index [HSI = 100 x (liver weight (g)/body weight (g))], and intestinal somatic index [ISI = 100 x (intestinal weight (g)/body weight (g))].

3.3.6 Haematology

Adult zebrafish were anesthetized with MS-222, and blood samples were collected using a heparin-coated syringe (Elimedical Inc., ON, CA) via caudal venipuncture targeting the dorsal aorta and posterior cardinal vein (Zang et al., 2015). 1-2 drops of blood were used to prepare blood smears, which were air-dried and fixed in methanol. Slides were also stained using modified Wright-Giemsa stain (Sigma-Aldrich, MO, USA), rinsed with phosphate-buffered saline followed by deionized water, and stored at 4°C until use. Slides were imaged using a Panthera compound microscope and the Motic Images Plus 2.0 software (Motic®, BC, CA).

3.3.7 Trace metal analysis

Whole body samples of developing fish (0, 5, 14, and 28 dpf) and adult tissues (gill, intestine, liver, and the remaining carcass) were collected for inductively coupled plasma mass spectrometry (ICP-MS) analysis. Each replicate consisted of 20 embryos or larvae (0, 5, and 14 dpf), 10 juveniles (28 dpf), or pooled tissues from 5 adults. Carcasses were analyzed individually. A total of 3-4 replicates (n=3-4) were collected for each sample group. Tissue preparation for ICP-MS analysis included overnight dehydration at 65°C, followed by digestion in 6N HNO_3 for 48 h. The samples were diluted in 2% HNO_3 and filtered (0.45 µm) before measurement of metal

concentrations with Agilent 8800 ICP-QQQ-MS (Water Quality Centre, Trent University). Quality assurance and control were performed using NIST SRM 1640a (Trace Elements in Natural Water), with measured concentrations within 5% of the certified values.

3.3.8 Droplet digital PCR analysis

Pooled larvae at 5 dpf (20 per sample) and 14 dpf (15 per sample) were used for RNA extraction (Monarch RNA Extraction kit, New England Biolabs), with 3 to 4 replicates collected for each sample group (n=3-4). Total RNA (1 μg) was reverse transcribed using the iScript™ cDNA synthesis kit (Bio-Rad). This cDNA was used to quantify transcript levels of *dmt1, hcp1, zip4, zip8, zip14, ecac.* Elongation factor 1 alpha (*ef1α*), ribosomal protein L13 (*rpl13*), and ribosomal protein S18 (*rps18*) were used as reference genes. All primer sets are listed in Table 3-1.

Droplet digital PCR (ddPCR) analysis was performed using the QX200 Droplet Digital™ PCR System (Bio-Rad) with EvaGreen® Supermix, as described previously (Chandrapalan and Kwong, 2020). PCR cycling conditions were: 5 min enzyme activation at 95°C, followed by 40 cycles of 30 sec denaturation at 95°C and 1 min annealing/extension at 60°C. Signal stabilization was performed at the end of the cycle (4°C for 5 min and then 90°C for 5 min). Droplets were read using the QX200 Droplet Reader and analyzed in QuantaSoft™ (Bio-Rad). All data were normalized to the geometric mean expression of the housekeeping genes *ef1α*, *rpl13*, and *rps18*.

3.3.9 Statistical analysis

Statistical analyses were performed using R (Version 4.4.2). Two-way analysis of variance (ANOVA) followed by Tukey's post hoc test was used to evaluate the effects of genotype and

developmental stage on physiological parameters and tissue metal levels. Student's t-test was employed to compare adult physiological indices and relative gene expression between WT and KO fish. Three-way ANOVA followed by a Tukey's post hoc test was utilized to determine any statistical significance of gene, genotype, and timepoint on mRNA expression. Non-parametric data were arcsine square root transformed prior to analysis. Welch's t-test was used to compare survival rates and *dmt1* expression between WT and KO groups. Differing letters and asterisks were used to denote statistical significance (*p<0.05, **p<0.01, ***p<0.001). All statistical tests were performed at $\alpha = 0.05$. Graphs were constructed using the ggplot2 package in R.

3.4 Results

3.4.1 Generation of dmt1$^{-/-}$ mutants

CRISPR-Cas9 genome editing was used to successfully generate a DMT1 KO (*dmt1*$^{-/-}$) model in zebrafish (Figure 3-1). From several candidates, a line carrying a 14 bp deletion was selected for this study (Figure 3-1D). This mutation in the DNA sequence produced a frameshift mutation as well as a premature stop codon in the protein sequence, resulting in a truncated protein (Figure 3-1E). mRNA expression of *dmt1* was reduced by one-third in the mutants ($p<0.001$) (Figure 3-1F). Homozygosity and gene KO were confirmed by Sanger sequencing. Effects of the functional KO of DMT1 were examined through phenotypic characterization and analysis of metal homeostasis (discussed below).

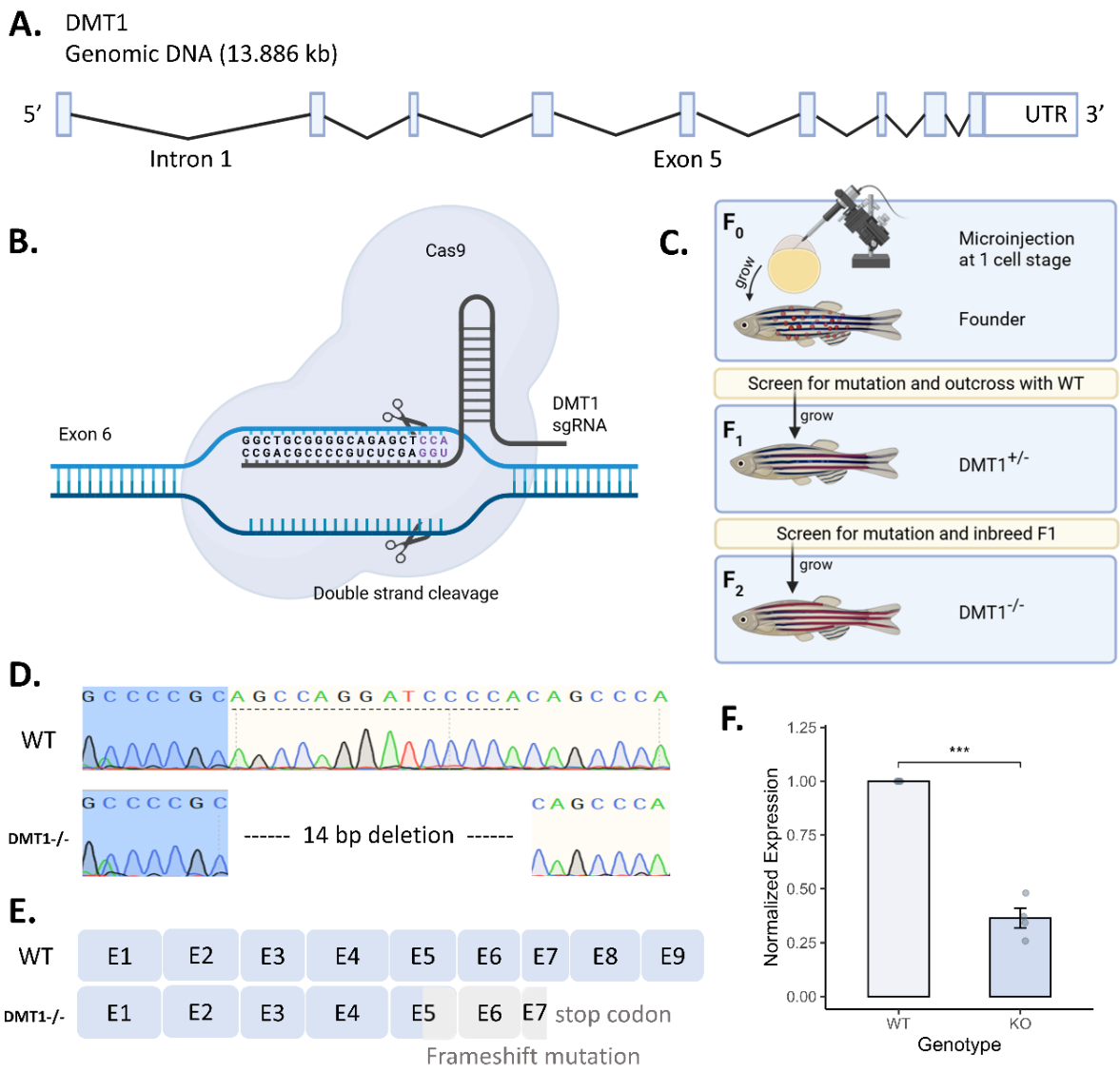

Figure 3-1. Summary of CRISPR-Cas9 mediated knockout (KO) of *dmt1* and the generation of *dmt1*$^{-/-}$ zebrafish mutants. A) Exon 5 of *dmt1* gene was selected for targeted mutagenesis using B) custom designed *dmt1* sgRNA. C) Microinjection was performed at the 1-cell stage of development and carriers of the mutation were screened and bred to obtain homozygous mutants. D) Sanger sequencing was used to identify a 14bp deletion at target site in the mutants. E) Mutants have a truncated protein with a premature stop codon on exon 7 (E7). F) Normalized mRNA expression level of *dmt1* in KO mutants is significantly reduced when compared with the wildtype (WT) fish at 5 dpf. Data are mean

± SEM, n=4. Welch's t-test, $p<0.05$ was used to determine statistical significance between groups (WT and DMT1 KO fish) and is denoted with an asterisk. BioRender was used to create Figure 3-1A-C.

3.4.2 Phenotype during early development

At 24 hpf, *dmt1*$^{-/-}$ KO mutants exhibited significantly (p=0.034) lower survival rates compared to WT embryos (Figure 3-2A). The average SL of KO fish was also lower than WT fish (Figure 3-2B). In both WT and KO fish, SL and weight increased throughout development from 0 and 5 dpf to 28 dpf (Figure 3-2B and C). Morphologically, both WT and KO embryos appeared similar at the start of development (Figure 3-2D i, ii). At 2 dpf, WT larvae displayed normal development with clear pigmentation, well-formed eyes, yolk sac, and visible blood circulation (Figure 3-2D iii). In KO larvae, overall morphology and pigmentation were similar to WT, but blood circulation appeared reduced, particularly in the heart and caudal tail regions (black arrows) (Figure 3-2D iv). The KO fish lacked the characteristic red hue of the red blood cells (RBCs), which were clearly visible in the peripheral blood flow in the tail region of WT fish (Figure 3-2D v, vi). This phenotypic difference persisted throughout early development until the fish were no longer transparent for direct examination.

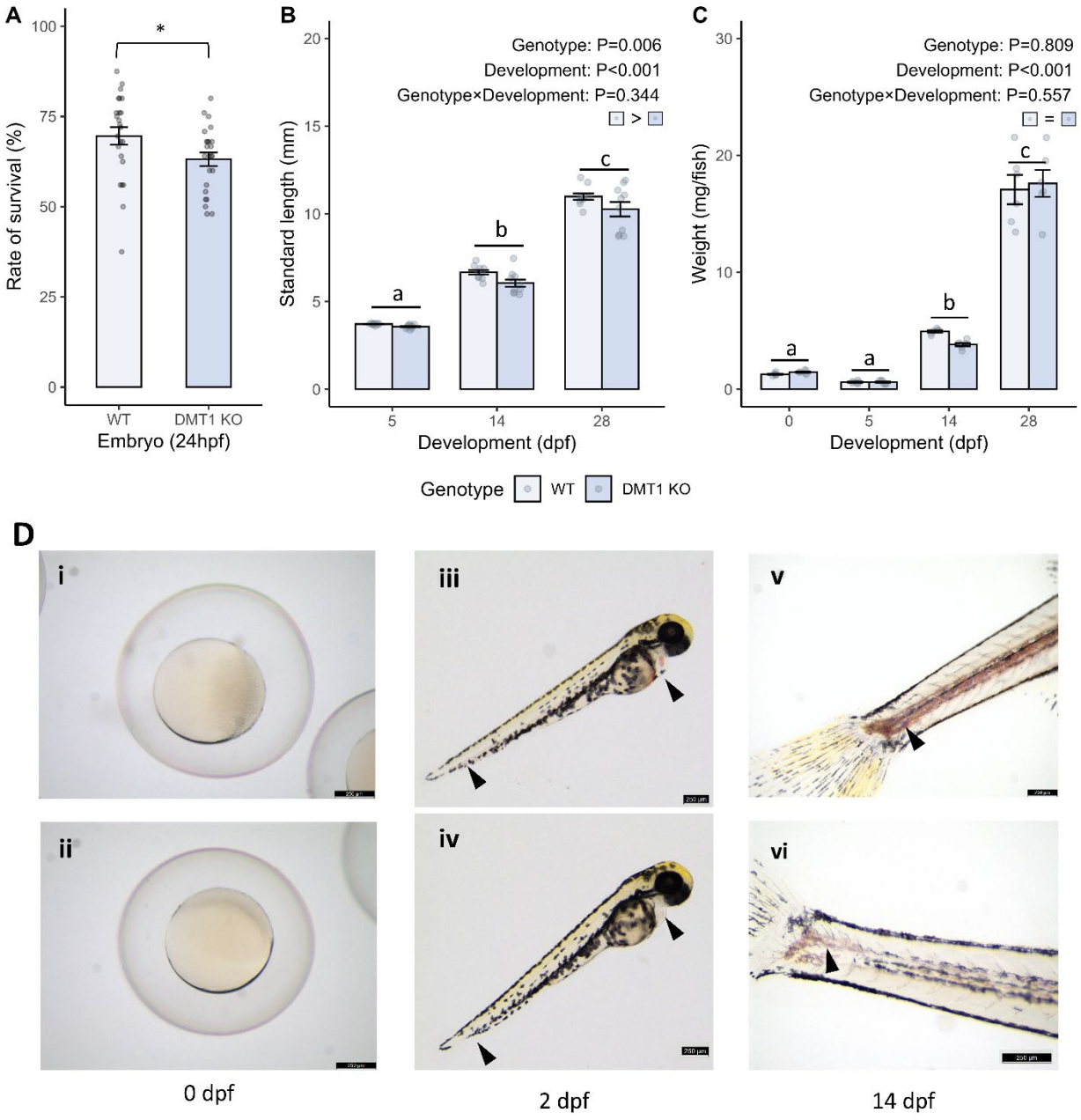

Figure 3-2. Physiological and morphological comparison of wildtype (WT; control) and DMT1 knockout (KO) zebrafish during development. A) Rate of survival (%) in embryos 24 hours post fertilization (hpf). Data are mean ± SEM, n=24. Data was arcsine square root transformed prior to a Welch's t-test and statistically significant effect of genotype is denoted with an asterisk. B) Standard length (mm, n=10) and C) weight

(mg/fish, n=6) over development (days post fertilization, dpf). Data are mean ± SEM. Statistical significance over development within each genotype is denoted with different lowercase letters. Overall effect of genotype when interaction effect is insignificant is depicted by the colored boxes at the top right-hand corner. Two-way ANOVA followed by Tukey's test, $p<0.05$. D) Comparison of morphology in WT (i, iii, v) and DMT1 KO (ii, iv, vi) mutants during development (0 dpf; i and ii), 2 dpf (iii and iv), and 14 dpf (v and vi). The arrows are used to highlight the difference in the visible blood circulation at the heart and tail end of the fish. Scale bars are 250 μm.

3.4.3 Trace metal homeostasis during early development

Five out of the seven trace elements analyzed were significantly altered in the KO fish. The two most abundant metals in the body, Fe and Zn, were also the most significantly impacted by the KO in developing fish (Figure 3-3 and 3-4). At 0 dpf, Fe concentrations were more than two-fold lower in the KO embryos. From 0 to 5 dpf, Fe levels increased in both WT and KO fish, but Fe levels remained significantly lower in KO fish at 5 dpf ($p < 0.01$ at 0 and 5 dpf). As development progressed, Fe levels in KO fish became comparable to WT levels ($p > 0.05$ at 14 and 28 dpf). ($p<0.01$ at 0 and 5 dpf; $p>0.05$ at 14 and 28 dpf). Similarly, Zn levels were initially reduced in KO embryos ($p=0.009$) at 0 dpf but increased to WT levels by 5 dpf and exceeded WT levels at 14 dpf ($p=0.017$). Like Fe, Zn levels in both WT and KO fish significantly increased from 0 to 5 dpf (Figure 3-4A).

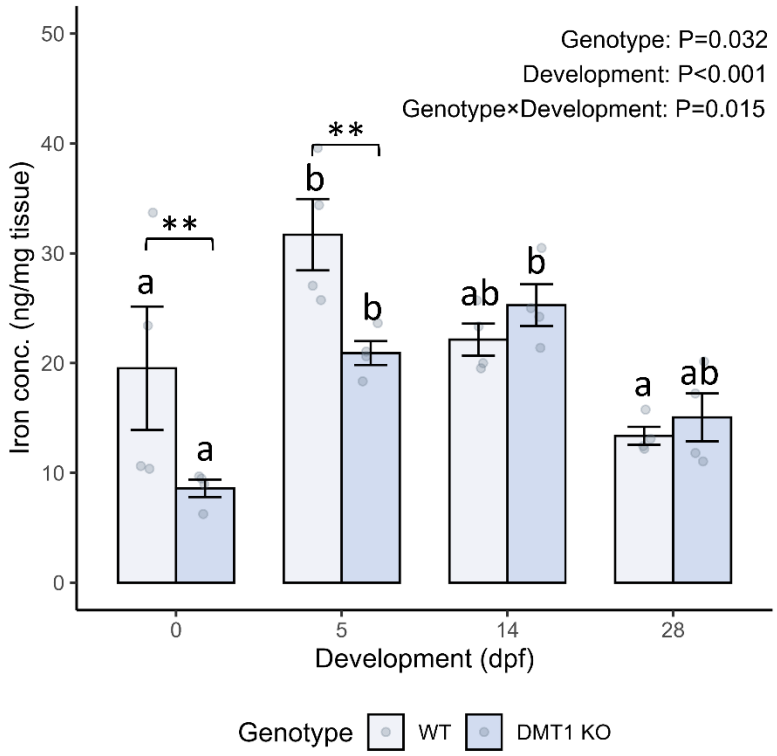

Figure 3-3. Developmental changes in whole-body iron levels in wildtype (WT; control) and DMT1 knockout (KO) zebrafish. Iron concentration (ng Fe/mg tissue) were measured at 0, 5, 14, and 28 days post fertilization (dpf). Data are mean ± SEM (n=4 per group). Two-way ANOVA revealed significant effects of genotype, development, and their interaction. Different letters above bars indicate significant differences among developmental stages within each genotype (Tukey's post hoc test, $p<0.05$). Asterisks denote significance pairwise differences between genotypes at the same developmental stage (**$p<0.01$).

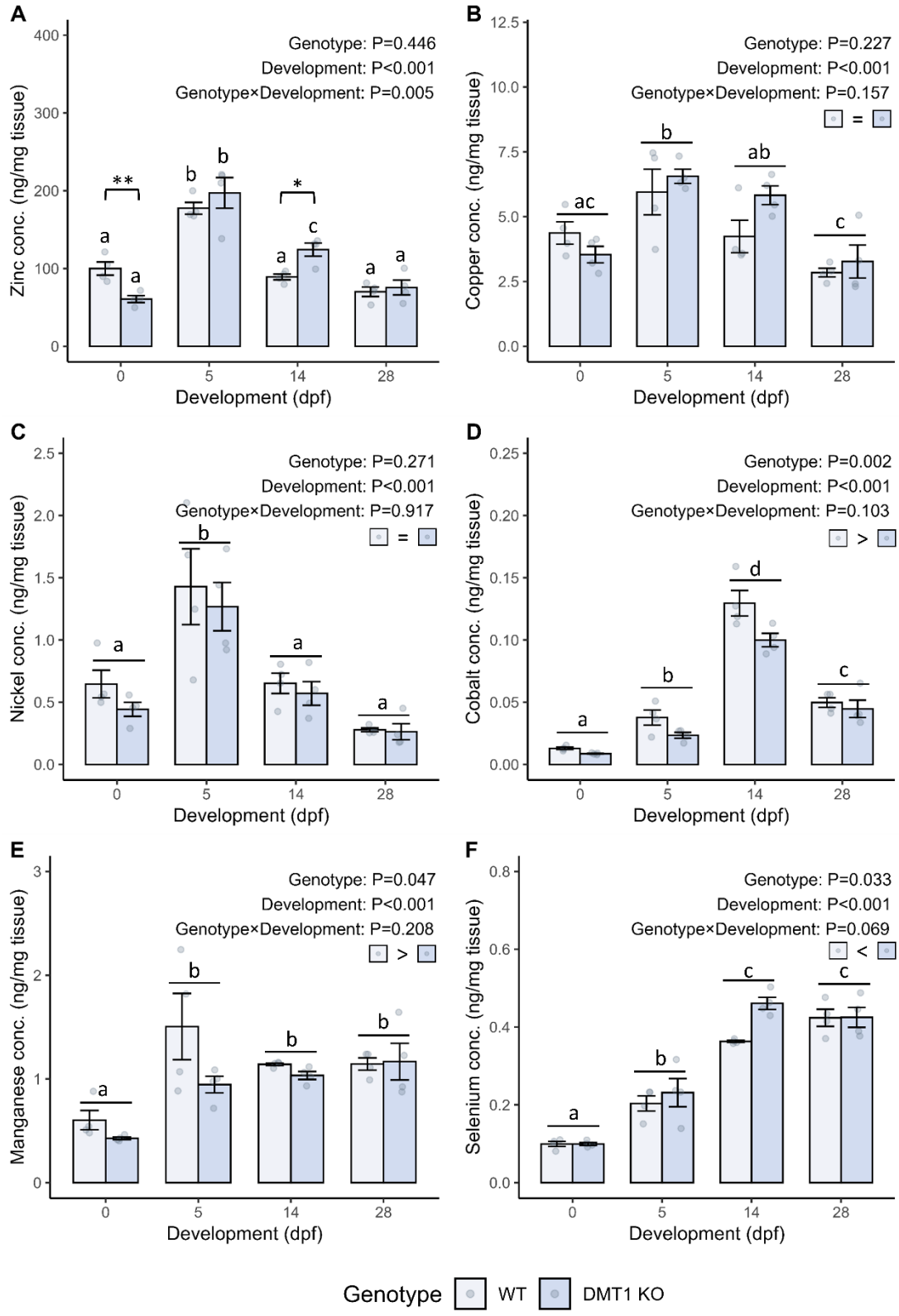

Figure 3-4. (caption on next page)

Figure 3-4. Developmental changes in whole-body trace element levels in wildtype (WT; control) and DMT1 knockout (KO) zebrafish. Concentrations (ng/mg tissue) of (A) zinc, (B) copper, (C) nickel, (D) cobalt, (E) manganese, and (F) selenium in WT and DMT1 KO zebrafish at 0, 5, 14, and 28 days post fertilization (dpf). Data are mean ± SEM (n=4 per group). Two-way ANOVA revealed significant main effects of genotype, development, and/or their interaction, as indicated in each panel. Different letters above bars indicate significant differences among developmental stages within each genotype (Tukey's post hoc test, $p<0.05$). Asterisks denote significant pairwise differences between genotypes at the same developmental stage (*$p<0.05$, **$p<0.01$). Bars lacking asterisks indicate no significant genotype effect at developmental stage. When the genotype x development interaction was not significant, the overall effect of genotype is depicted by the colored squares in the top right-hand corner of each panel.

In addition to Fe and Zn, Co, Mn, and Se were also affected by DMT1 KO (Figure 3-4). Results from two-way ANOVA suggested that Co ($p<0.01$) and Mn ($p<0.05$) levels were significantly lower in KO fish compared to WT fish. Conversely, Se levels were elevated in the KO fish ($p<0.05$). Cu and Ni levels varied throughout development and did not appear to be influenced by the KO. Additionally, the levels of major ions such as Ca, Mg, and K were not significantly affected by DMT1 KO (Figure 3-5), although Na level was elevated in KO fish at 14 dpf ($p=0.043$). Concentrations of all major ions increased from 0 to 5 dpf, with Ca continuing to rise until 28 dpf.

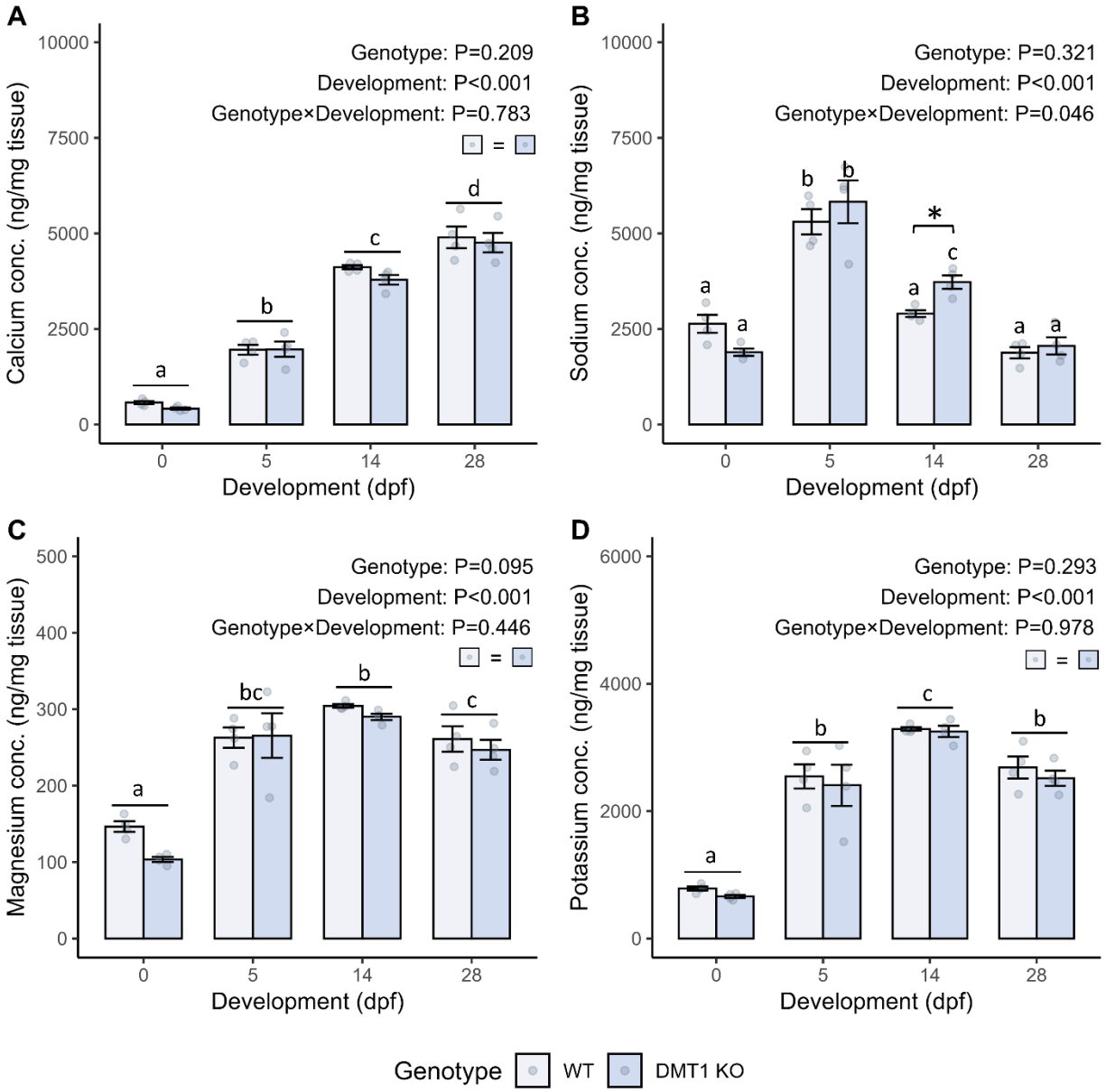

Figure 3-5. Concentrations (ng metal/mg tissue) of major ions, (A) calcium, (B) sodium, (C) magnesium, and (D) potassium in wildtype (WT; control) and DMT1 knockout (KO) zebrafish at 0, 5, 14, and 28 days post fertilization (dpf). Data are mean ±SEM (n=4 per group). Two-way ANOVA revealed significant main effects of genotype, development, and/or their interaction, as indicated in each panel. Different letters above bars indicate significant differences among developmental stages within each genotype (Tukey's post hoc test, $p<0.05$). Asterisks denote significant pairwise differences between genotypes at

the same developmental stage (*p<0.05). Bars lacking asterisks indicate no significant genotype effect at developmental stage. When the genotype x development interaction was not significant, the overall effect of genotype is depicted by the colored squares in the top right-hand corner of each panel.

3.4.4 Physiological and hematological parameters in adult fish

Adult KO fish appeared visibly paler than their WT counterparts (Figure 3-6A-D). The gills of KO fish are also much paler in comparison to WT gills (Figure 3-6E and F). However, no significant differences were observed in any of the morphometric and physiological indices measured (SL, weight, K, GSI, HSI, and ISI) (Table 3-2).

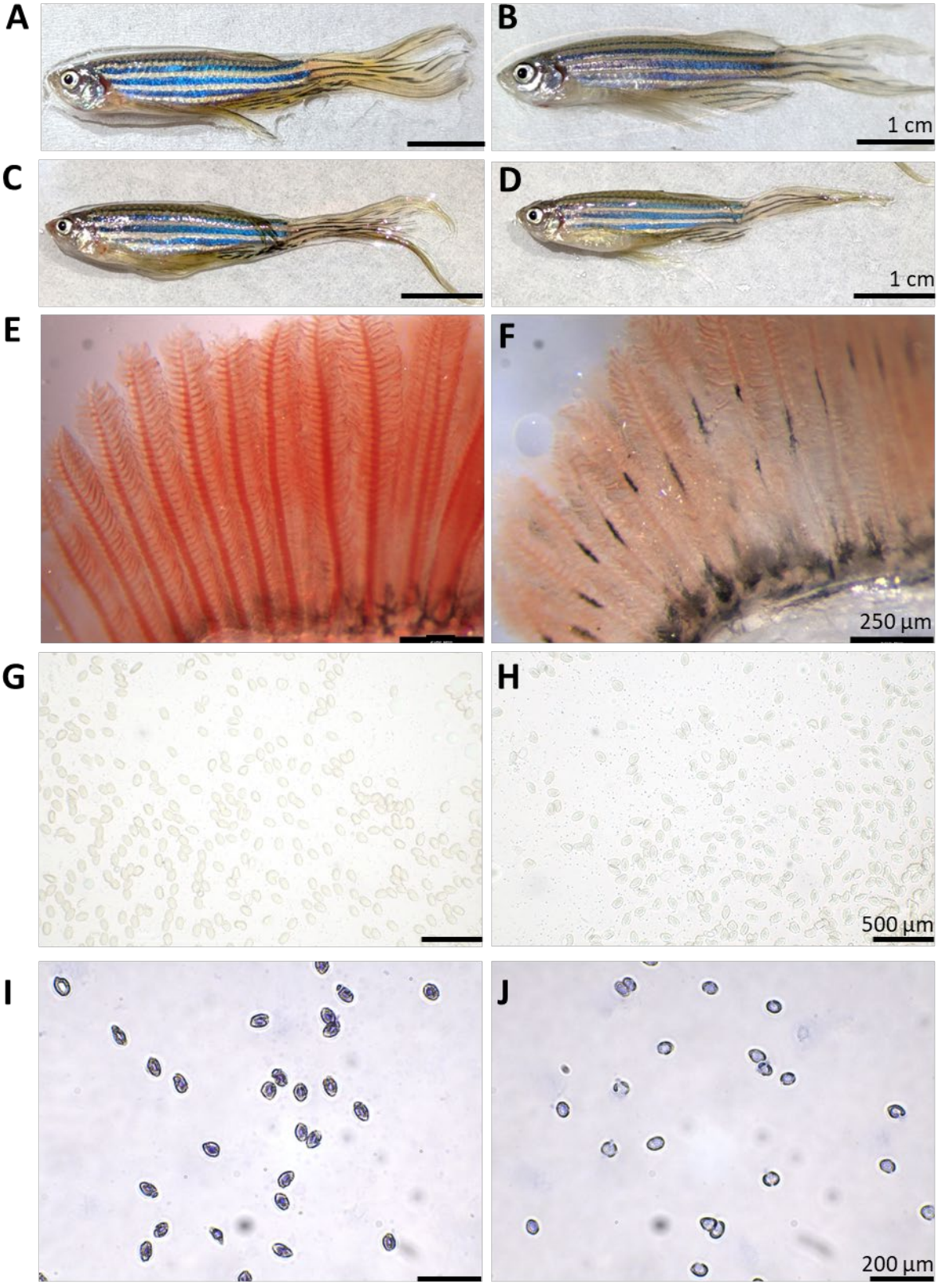
A
B
1 cm
C
D
1 cm
E
F
250 µm
G
H
500 µm
I
J
200 µm

Figure 3-6. Morphological and hematological comparison of adult wildtype (WT; control) and DMT1 knockout (KO) zebrafish. WT male (A) and female (C) zebrafish appear vibrant and healthy. DMT1 KO male (B) and female (D) zebrafish appear paler in body coloration compared to WT. Gills of WT (E) fish are bright red while mutants (F) appear pale. Representative blood smears showing comparable red blood cell (RBC) abundance and morphology between WT (G) and KO (H) fish. Wright-Giemsa staining of blood smear appears to have reduced hemoglobin staining intensity in KO fish (J) relative to WT (I). Scale bars are shown in black.

Table 3-2. Physiological parameters of adult WT (wildtype) and DMT1 KO (mutant) zebrafish. Data are mean ± SEM. Standard length (SL), weight, condition factor (K), gonadosomatic index (GSI), hepatosomatic index (HSI), and intestinal somatic index (ISI) were measured. Student's t-test finds no statistical difference (p>0.05) in SL, weight, and K between WT (control) and DMT1 KO fish, with n=3-18, depending on the specific measurement. GSI, HSI, and ISI were arcsine square root transformed prior to t-test.

Physiological indices	WT	DMT1 KO
SL (cm)	2.5 ± 0.06	2.5 ± 0.04
Weight (g)	0.30 ± 0.02	0.27 ± 0.02
K	1.8 ± 0.06	1.8 ± 0.05
GSI (%) in Females	8.2 ± 1	5.6 ± 1
GSI (%) in Males	1.1 ± 0.1	1.1 ± 0.08
HIS (%)	1.1 ± 0.08	1.6 ± 0.3
ISI (%)	2.4 ± 0.3	2.9 ± 0.2

Upon hematological examination, the RBC morphology appeared to be comparable between both genotypes (Figure 3-6E-F). However, Wright-Giemsa staining revealed notable differences in RBC coloration. RBCs from KO fish exhibited a paler and bluish hue compared to pink in WT fish (Figure 3-6G-H), potentially owing to altered hemoglobin content or cellular staining properties.

3.4.5 Trace metal homeostasis in adults

In adults, results from two-way ANOVA revealed that Fe levels across different tissues were significantly lower in KO fish when compared to WT fish (p<0.05) (Figure 3-7). However, subsequent pairwise comparisons within individual tissues showed no statistically significant differences between genotypes.

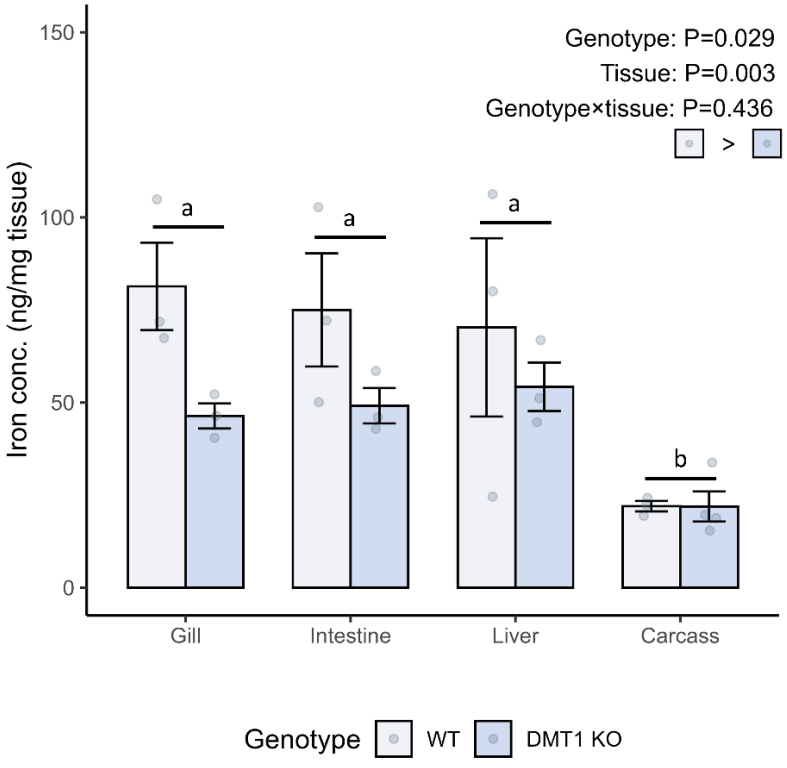

Figure 3-7. (caption on next page)

Figure 3-7. Tissue-specific iron concentrations in adult wildtype (WT; control) and DMT1 knockout (KO) zebrafish. Iron concentrations (ng Fe/mg tissue) in different tissues (gill, intestine, liver, and carcass). Data are mean ± SEM (n=3-4 per group). Two-way ANOVA revealed significant effects of genotype and tissue. Different letters above bars indicate significant differences among tissues within each genotype (Tukey's post hoc test, $p<0.05$). The overall effect of genotype is depicted by the colored squares in the top right-hand corner.

In contrast to developing fish, metal homeostasis was less impacted by DMT1 KO in adults than in larvae (Figure 3-8 and 3-9). Out of the 11 trace metals and major ions measured, Cu, Se, and Ca were significantly altered by DMT1 KO. Specifically, in KO fish, Cu and Se levels were elevated in the liver, while Ca levels were increased in the gills ($p<0.001$ for all three).

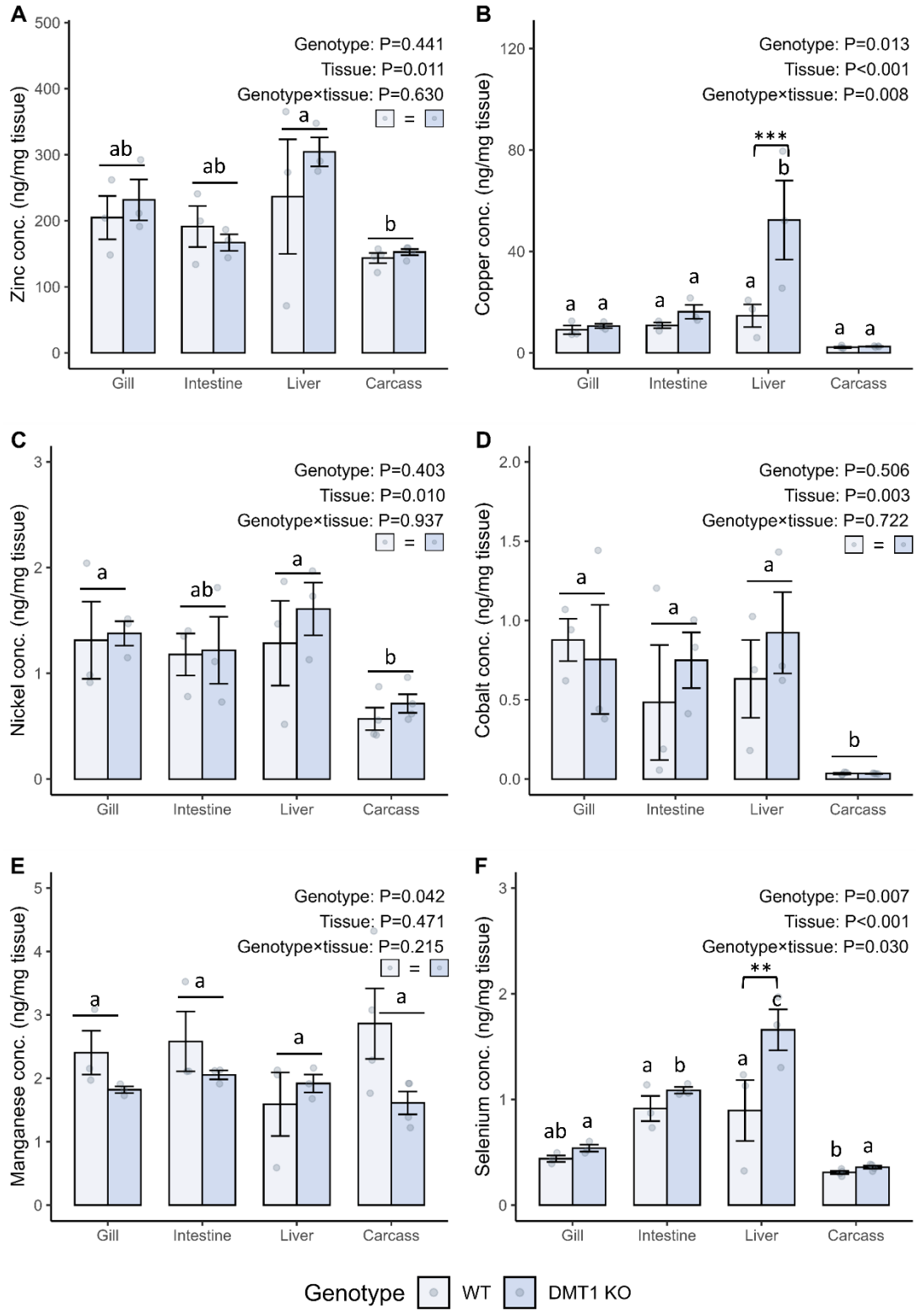

Figure 3-8. (caption on next page)

Figure 3-8. Tissue-specific trace element concentrations in adult wildtype (WT; control) and DMT1 knockout (KO) zebrafish. Concentrations of (A) zinc, (B) copper, (C) nickel, (D) cobalt, (E) manganese, and (F) selenium (ng/mg tissue) in different tissues (gill, intestine, liver, and carcass). Data are mean ± SEM (n=3-4 per group). Two-way ANOVA revealed significant main effects of genotype, tissue, and/or their interaction, as indicated in each panel. Different letters above bars indicate significant differences among tissues within each genotype (Tukey's post hoc test, $p<0.05$). Asterisks denote significant pairwise differences between genotypes within the same tissue (***$p<0.001$). Bars lacking asterisks indicate no significant genotype effect for that tissue. When the genotype x tissue interaction was not significant, the overall effect of genotype is depicted by the colored squares in the top right-hand corner of each panel.

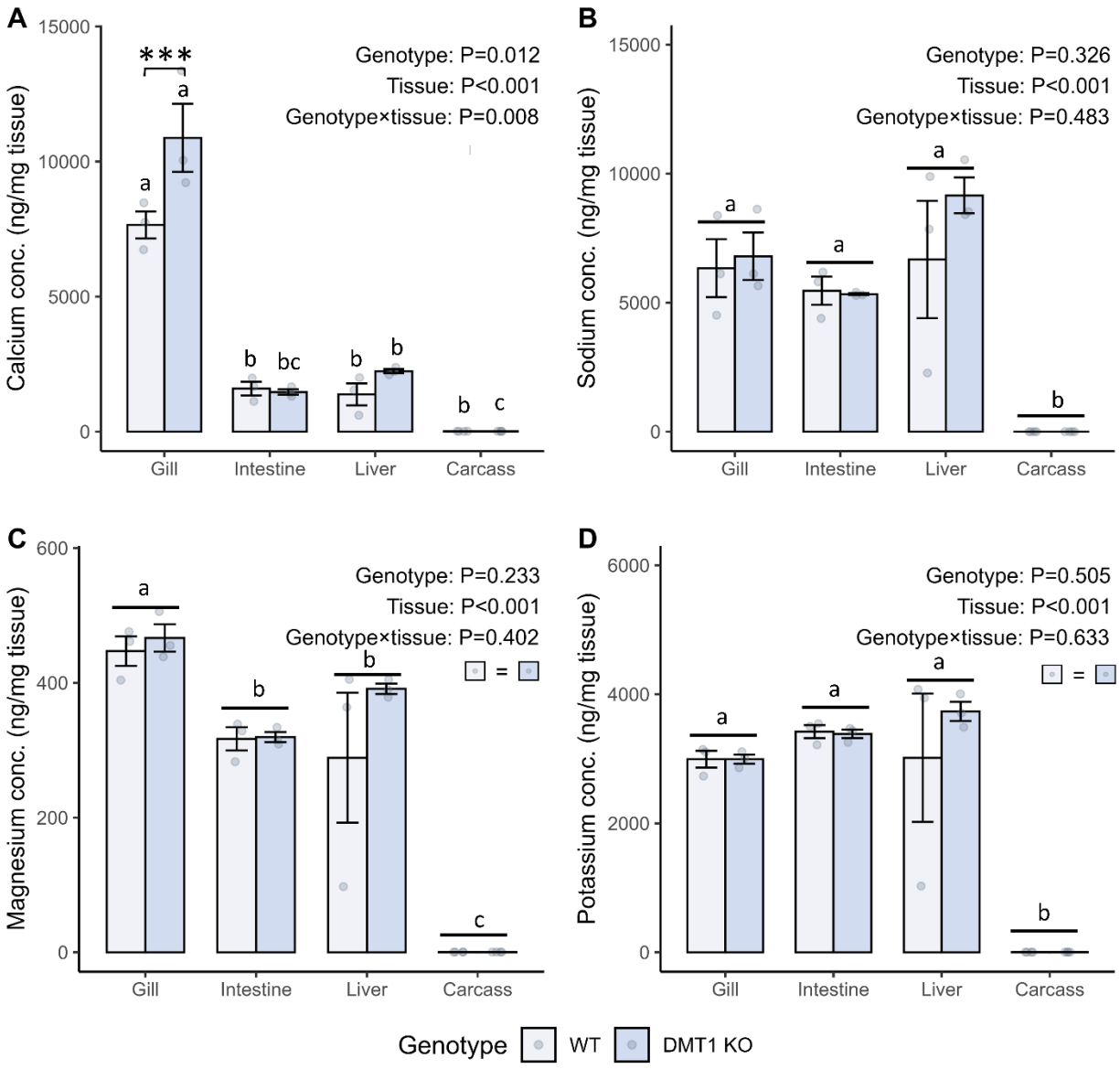

Figure 3-9. Concentrations (ng/mg tissue) of the major ions, (A) calcium, (B) sodium, (C) magnesium, and (D) potassium in different tissues (gill, intestine, liver, and carcass) of adult wildtype (WT; control) and DMT1 knockout (KO) zebrafish. Data are mean ± SEM (n=3-4 per group). Two-way ANOVA revealed significant main effects of genotype, tissue, and/or their interaction, as indicated in each panel. Different letters above bars indicate significant differences among tissues within each genotype (Tukey's post hoc test, $p<0.05$). Asterisks denote significant pairwise differences between genotypes within the

same tissue (***p<0.001). Bars lacking asterisks indicate no significant genotype effect for that tissue. When the genotype x tissue interaction was not significant, the overall effect of genotype is depicted by the colored squares in the top right-hand corner of each panel.

3.4.6 Metal transporter expression in developing fish

Results from ddPCR suggested that *hcp1* and *zip4* exhibited two- to three-fold higher mRNA expression levels (p<0.001) compared to *zip8*, *zip14*, and *ecac* (Figure 3-10A). Additionally, significant gene- and developmental age-specific differences were observed between WT and DMT1 KO fish. Specifically, *hcp1* expression was significantly higher (p=0.01) in KO fish at 14 dpf, while *zip4* expression was reduced in KO fish at both 5 dpf (p=0.02) and 14 dpf (p=0.04). When mRNA expression levels were assessed relative to 5 dpf WT fish, three-way ANOVA suggested significant interactive effects between genotype and developmental age (p<0.01) (Figure 3-10B). The mRNA expression profiles of all five genes were initially comparable between the two genotypes at 5 dpf but diverged as development progressed. In WT fish, most genes (except *zip4*) were significantly downregulated from 5 to 14 dpf. This developmental decline was more pronounced in WT fish than in KO fish. Notably, *hcp1* and *zip8* expression levels remained elevated in KO fish at 14 dpf relative to 5 dpf KO fish.

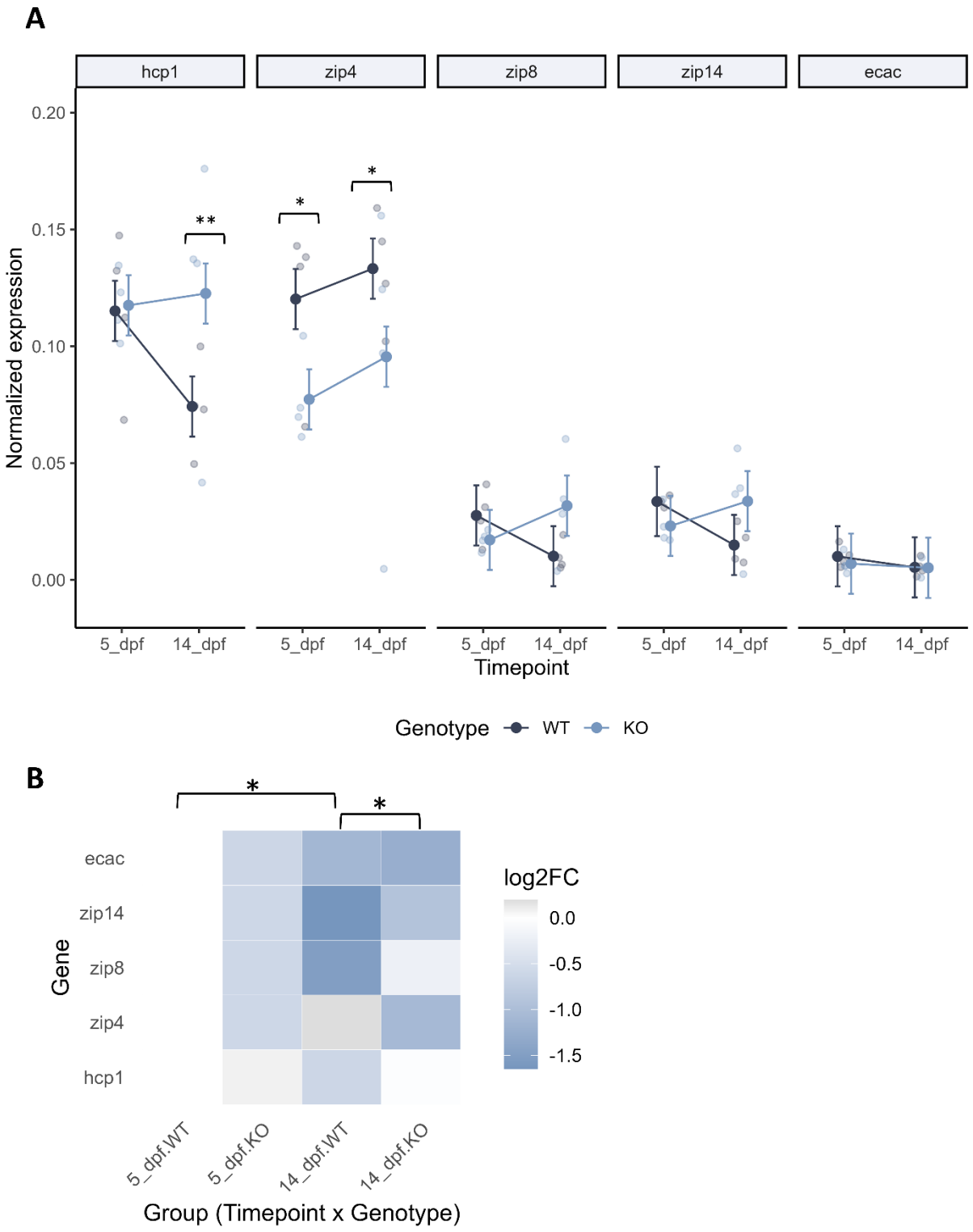

Figure 3-10. (caption on the next page)

Figure 3-10. Gene expression of iron-related metal transporters in wildtype (WT; control) and DMT1 knockout (KO) zebrafish during development. Gene expression was measured at 5 and 14 days post fertilization (dpf) (n=3-4 per group). A) Absolute quantification of *hcp1*, *zip4*, *zip8*, *zip14*, and *ecac* normalized to housekeeping genes (*ef1a*, *rpl13*, *rps18*). Data are model estimated means ± SE. Three-way ANOVA followed by Tukey-adjusted post-hoc ($p<0.05$) test. Asterisks denote significant difference between WT and KO within each timepoint for each gene (*$p<0.05$, **$p<0.01$). Samples lacking asterisks indicate no significant difference. B) Heatmap of relative gene expression (log_2 fold change) to 5 dpf WT fish. Three-way ANOVA identified a significant timepoint x genotype interaction ($p=0.018$). Tukey's post hoc test revealed that WT fish exhibited lower overall gene expression (*ecac*, *zip14*, *zip8*, *zip4*, and *hcp1*) at 14 dpf compared to 5 dpf ($p=0.044$), and KO fish had higher expression than WT at 14 dpf ($p=0.032$). No other pairwise differences were significant. Asterisks denote significant pairwise differences between groups (Timepoint x Genotype) (*$p<0.05$).

3.5 Discussion

The present study characterized the first *in vivo* $dmt1^{-/-}$ knockout zebrafish model generated using targeted mutagenesis via CRISPR-Cas9 technology, revealing the critical role of this transporter in regulating Fe and other trace metal homeostasis during development and adulthood. The $dmt1^{-/-}$ KO line was used to systematically evaluate the physiological, hematological, and molecular effects of DMT1 loss. Our findings highlight developmental-age specific impacts of DMT1 KO, with pronounced impairments observed during early development, including reduced survival rates, slower growth, likely lowered hemoglobin content in RBCs, and disrupted metal

homeostasis. Adults exhibited a persistent phenotype of anemia (morphologically paler, RBCs with less hemoglobin, and lower Fe content), but these impairments were more subtle and potentially mitigated by compensatory regulation.

3.5.1 Fe deficiency and hypochromic anemia in developing dmt1$^{-/-}$ fish

As early as the embryonic stage, *dmt1*$^{-/-}$ embryos were deficient in Fe, with less than half the Fe content of WT. During this time, developing zebrafish are solely dependent on the yolk nutrients before the onset of exogenous feeding (about 5 dpf) and external Fe acquisition (Wallace et al., 2005). Fe is exported through the yolk syncytial layer to the developing fish independent of DMT1 via the Fe exporter, iron regulated transporter 1 (IREG1; slc40a1) (Donovan et al., 2000; Fraenkel et al., 2005). *Weissherbst* (*Weh*) zebrafish mutants lacking IREG1 exhibit an inability to obtain Fe from the yolk and die during early development (Donovan et al., 2000). Furthermore, it is not until at least two weeks post-fertilization that the gills are fully developed and begin to contribute to ion exchange and possibly waterborne Fe uptake (Bury, 2003b, 2003a; Rombough, 2002). Thus, the impaired Fe balance observed at 0 and 5 dpf in the KO mutants was likely resulting from inadequate maternal Fe deposition.

As Fe is essential for a multitude of developmental processes that onset during early development, including DNA replication, mitochondrial respiration, hemoglobin synthesis, and oxygen transport, insufficient Fe levels during this critical stage can lead to developmental delays and even compromise survival (Chandrapalan and Kwong, 2021; Wood et al., 2011). Likewise, the Fe deficiency observed during early development in *dmt1*$^{-/-}$ larvae was associated with reduced survival and growth. The KO mutants also exhibited visible abnormalities in their RBC morphology consistent with hypochromic anemia. This is similar to the phenotype of the *cdy*

mutants, which presented microcytic hypochromic anemia during *dmt1* loss (Donovan et al., 2002). In the present study, we observed that the RBC shape and size were not affected in *dmt1*$^{-/-}$ fish, and the hypochromia observed in the mutants was likely linked to impaired hemoglobin synthesis, as both whole-body Fe levels and hemoglobin staining in the RBCs were diminished. Furthermore, although Fe levels appeared comparable to WT later in development, overall Fe content in adult *dmt1*$^{-/-}$ fish remained lower, and the hypochromia in RBCs persisted into adulthood. These adverse effects highlight the importance of DMT1 in supporting Fe transport and RBC development in zebrafish.

3.5.2 Broader disruption in trace metal homeostasis

In addition to its role in Fe transport, DMT1 KO led to significant changes in the whole-body levels of several other trace elements in developing zebrafish, including Zn, Co, Mn, and Se. These findings support previous literature on mammalian models, including the Belgrade (*b*) rat and microcytic anemia (*mk*) mice, both of which not only developed microcytic anemia but also showed impaired Mn and Co transport (Fleming et al., 1998, 1997). In fishes, the importance of DMT1 in multi-metal uptake and the interaction between Fe and other metals have generally been inferred through *in vitro* techniques examining competitive inhibition of Fe absorption and *in vivo* Fe exposure studies (Chandrapalan and Kwong, 2020, 2020; Cooper et al., 2007; Kwong and Niyogi, 2009). The present study represents one of the first direct *in vivo* evidence showing that the loss of DMT1 can broadly affect trace metal homeostasis, leading to early-life dysregulation in multiple metals (decreases in Zn, Co, Mn, and increases in Se) and a persisting reduction in Fe in adults.

Notably, findings on the specific divalent metals thought to be substrates for DMT1 vary across studies (Cooper et al., 2007; Garrick et al., 2003; Gunshin et al., 1997; Illing et al., 2012). For mammalian DMT1, heterologous expression studies in *Xenopus* oocytes demonstrated that although Fe, Mn, and Co were the preferred substrates of DMT1, it is less physiologically significant for Cu, Ni, and Zn transport (Illing et al., 2012). Likewise, in the present study, Cu and Ni levels remained unaffected in the developing KO mutants, but not Zn. Zn homeostasis in zebrafish is thought to be largely regulated by specific Zn transporters (ZIP and ZnT families) (Feeney et al., 2005; Zhao et al., 2014). The changes in Zn homeostasis observed in developing *dmt1*$^{-/-}$ fish were possibly due to Fe-Zn interactions such as competitive metal uptake, regulatory feedback mechanisms, or modulation of Zn transporters during DMT1 loss, rather than inhibition of Zn transport via DMT1. Nonetheless, the observation that Zn levels were nearly halved in *dmt1*$^{-/-}$ embryos at 0 dpf highlights the significant role of DMT1 in Zn homeostasis during early development. On the other hand, the homeostasis of major ions remained largely unchanged across genotypes, suggesting that DMT1 plays little or no role in their systemic regulation.

3.5.3 Partial phenotypic recovery in adulthood

Despite early developmental differences in survival, growth, and trace metal homeostasis, adult *dmt1*$^{-/-}$ zebrafish exhibited near-normal morphology and body condition indices. This suggests that over time, zebrafish may be able to partially compensate for DMT1 loss, particularly under dietary metal sufficiency. In this study, the diets of adult *dmt1*$^{-/-}$ fish comprised of both dry feed (commercial zebrafish pellets) and live food (brine shrimp), providing access to both heme- and non-heme sources of Fe. Accordingly, the non-heme sources could support DMT1-independent Fe uptake, possibly via heme Fe transport pathways (HCP1). In particular, heme-bound Fe is considered more bioavailable and readily absorbed than non-heme Fe (Standal et al.,

1999; Wheal et al., 2016), which could help meet the nutritional Fe requirements of the *dmt1*$^{-/-}$ mutants. Additionally, there is no known regulated excretory pathway for Fe (Bury, 2003b). As a result, most of the Fe accumulated in the body is likely stored intracellularly in labile pools, bound to ferritin, or sequestered in the liver (Mackenzie et al., 2008). Therefore, it is possible that over development, *dmt1*$^{-/-}$ fish accumulate sufficient Fe reserves to support growth and physiological functions.

3.5.4 Tissue-specific trace metal patterns in adults

The present study demonstrated tissue-specific alterations in metal homeostasis in adult *dmt1*$^{-/-}$ fish. Apart from Fe, which appeared to remain consistently lower across tissues, an elevation in Cu and Se levels was observed in the liver, and Ca was increased in the gills. Co and Mn, which were significantly lower in the developing mutants, were not different in adults. These shifts in homeostasis may reflect underlying changes in metal transporter expression or redistribution of metal pools in response to chronic DMT1 loss. Metal homeostasis is tightly regulated through complex interactions between metal availability and the expression of metal transporters (Chandrapalan and Kwong, 2020; Kondaiah et al., 2019; Kwong and Niyogi, 2009; Puar et al., 2021; Shawki and Mackenzie, 2010; Yamaji et al., 2001). Interactions between metals can modulate transporter activity and abundance. For example, in response to a deficiency, fish may upregulate specific transporters to restore metal balance. Thus, the elevated levels of certain metals observed in adult *dmt1*$^{-/-}$ fish may result from compensatory regulation.

3.5.5 Developmental plasticity and temporal gene regulation

The *dmt1*$^{-/-}$ mutants exhibited developmental plasticity in trace metal regulation, characterized by a transition from significant metal imbalance at 0 and 5 dpf to an apparent onset

of rebalance at 14 dpf. To investigate the molecular mechanisms underlying this recovery, we analyzed the temporal expression of candidate heme/metal transporters and ion channel implicated in apical Fe uptake. One candidate was *hcp1* (also known as proton-coupled folate transporter, PCFT), which is reported to function primarily in high affinity folate transport but also has low-affinity heme transport function (Qiu et al., 2006; Shayeghi et al., 2005). HCP1 is localized to the apical membrane of polarized epithelial cells and contributes to dietary heme assimilation, making it a relevant candidate for compensation in the absence of DMT1 (Laftah et al., 2008; Radziejewska et al., 2020; Yanatori et al., 2010). In addition, we also examined the mRNA expression levels of *zip8*, *zip14*, *zip4*, and *ecac*; transporters proposed to have permeability to Fe and other divalent cations such as Zn, Mn, and Ca (Geiser et al., 2012; Jenkitkasemwong et al., 2012; Liuzzi et al., 2006; Pinilla-Tenas et al., 2011; Qiu and Hogstrand, 2004). While ZIP4 is primarily recognized as an intestinal Zn transporter, evidence from mammalian models shows that the loss of intestinal ZIP4 reduces intestinal iron content by nearly half, suggesting potential importance in Fe homeostasis (Geiser et al., 2012; Zhang et al., 2016). Collectively, these five transporters/channel were selected based on their broad substrate specificity and prior evidence supporting their roles in Fe homeostasis.

Our results reveal that *hcp1* transcripts were significantly elevated in *dmt1*$^{-/-}$ larvae during the developmental window when exogenous feeding begins and iron acquisition from dietary heme becomes essential (Andersen, 1997; Bury, 2003b). In WT larvae, although a general decline in metal transporter expression was observed, *zip4* expression remained elevated, likely reflecting its importance and critical role in sustaining zinc uptake during this developmental window. In contrast, sustained expression of Fe transport-related genes in developing *dmt1*$^{-/-}$ larvae coincided with a significant increase in whole-body Zn content by 14 dpf, surpassing levels in WT fish.

Considering the broad permeability of ZIP8 and ZIP14, which can facilitate the uptake of Zn, Mn, and Fe, their prolonged expression likely represents a compensatory mechanism as alternate pathways to partially restore metal balance during DMT1 loss (Pasquadibisceglie et al., 2023; Pinilla-Tenas et al., 2011). These findings highlight the importance of temporal regulation in metal transporter networks for coordinating trace metal rebalance from early-life metal dysregulation. Furthermore, the divergence in gene expression between WT and mutants suggests that developmental plasticity and differential expression of transporters may buffer the physiological consequences of impaired DMT1 function. These temporal readjustments may represent a broader adaptive strategy in vertebrate metal homeostasis, whereby the redundancy and flexibility within transporter networks safeguard against stressors and environmental changes.

3.6 Conclusion and perspectives

This study underscores the critical role of DMT1 in early Fe uptake and systemic trace metal homeostasis in fish. The viability of zebrafish during DMT1 loss, albeit with developmental delays, highlights the involvement of alternate uptake mechanisms and a remarkable degree of physiological resilience. Our findings demonstrate the developmental plasticity of zebrafish larvae to dynamically adjust metal transporter expression to maintain physiological function despite genetic disruption of a key Fe transporter. However, the persistence of whole-body Fe imbalance and RBC pathology in adult fish shows that compensatory pathways cannot fully substitute for DMT1, reaffirming its importance in Fe homeostasis. Loading of other trace elements like Cu and Se during DMT1 loss also requires further investigation.

At the same time, additional confirmation of gene disruption in terms of functional validation of DMT1 loss at the protein level and transport function (e.g., western blotting and electrophysiology) can strengthen the interpretation of the observed phenotype and metal

imbalance in *dmt1*$^{-/-}$ fish. Incorporation of biomarkers of iron imbalance such as ferritin abundance and hepcidin expression can also provide a more comprehensive assessment of systemic iron status in the mutants.

Beyond fundamental physiology, the *dmt1*$^{-/-}$ mutants are also a valuable model to assess the toxicological significance of DMT1 in non-essential metal uptake, like Cd and Pb in fish, and to investigate the molecular mechanisms underlying Fe-related disorders, such as iron deficiency anemia or impaired erythropoiesis, and to explore the evolutionary strategies of metal homeostasis in vertebrates. By integrating molecular, physiological, and ecological perspectives, this work not only advances our understanding of Fe regulation in zebrafish but also establishes a foundation for broader comparative studies across vertebrates, with implications for aquaculture, environmental toxicology, and human health.

3.7 Reference

Andersen, Ø., 1997. Accumulation of waterborne iron and expression of ferritin and transferrin in early developmental stages of brown trout (*Salmo trutta*). Fish Physiology and Biochemistry 16, 223–231. https://doi.org/10.1023/A:1007729900376

Bury, N.R., 2003a. Waterborne iron acquisition by a freshwater teleost fish, zebrafish *Danio rerio*. Journal of Experimental Biology 206, 3529–3535. https://doi.org/10.1242/jeb.00584

Bury, N.R., 2003b. Iron acquisition by teleost fish. Comparative Biochemistry and Physiology Part C: 135, 97–105. https://doi.org/10.1016/S1532-0456

Cairo, G., Bernuzzi, F., Recalcati, S., 2006. A precious metal: Iron, an essential nutrient for all cells. Genes & Nutrition 1, 25–39. https://doi.org/10.1007/BF02829934

Chandrapalan, T., Kwong, R.W.M., 2021. Functional significance and physiological regulation of essential trace metals in fish. The Journal of experimental biology 224, jeb243834. https://doi.org/10.1242/JEB.238790

Chandrapalan, T., Kwong, R.W.M., 2020. Influence of dietary iron exposure on trace metal homeostasis and expression of metal transporters during development in zebrafish. Environmental pollution 261, 114159. https://doi.org/10.1016/j.envpol.2020.114159

Cooper, C.A., Shayeghi, M., Techau, M.E., Capdevila, D.M., MacKenzie, S., Durrant, C., Bury, N.R., 2007. Analysis of the rainbow trout solute carrier 11 family reveals iron import ≤ pH 7.4 and a functional isoform lacking transmembrane domains 11 and 12. FEBS Letters 581, 2599–2604. https://doi.org/10.1016/j.febslet.2007.04.081

Donovan, A., Brownlie, A., Dorschner, M.O., Zhou, Y., Pratt, S.J., Paw, B.H., Phillips, R.B., Thisse, C., Thisse, B., Zon, L.I., 2002. The zebrafish mutant gene chardonnay (*cdy*) encodes divalent metal transporter 1 (DMT1). Blood 100, 4655–4659. https://doi.org/10.1182/blood-2002-04-1169

Donovan, A., Brownlie, A., Zhou, Y., Shepard, J., Pratt, S.J., Moynihan, J., Paw, B.H., Drejer, A., Barut, B., Zapata, A., Law, T.C., Brugnara, C., Lux, S.E., Pinkus, G.S., Pinkus, J.L., Kingsley, P.D., Palis, J., Fleming, M.D., Andrews, N.C., Zon, L.I., 2000. Positional cloning of zebrafish ferroportin1 identifies a conserved vertebrate iron exporter. Nature 403, 776–781. https://doi.org/10.1038/35001596

Dufner-Beattie, J., Wang, F., Kuo, Y.M., Gitschier, J., Eide, D., Andrews, G.K., 2003. The Acrodermatitis Enteropathica Gene ZIP4 Encodes a Tissue-specific, Zinc-regulated Zinc Transporter in Mice. Journal of Biological Chemistry 278, 33474–33481. https://doi.org/10.1074/JBC.M305000200

Feeney, G.P., Zheng, D., Kille, P., Hogstrand, C., 2005. The phylogeny of teleost ZIP and ZnT zinc transporters and their tissue specific expression and response to zinc in zebrafish. Biochimica et Biophysica Acta (BBA) - Gene Structure and Expression 1732, 88–95. https://doi.org/10.1016/j.bbaexp.2005.12.002

Fleming, M.D., Romano, M.A., Su, M.A., Garrick, L.M., Garrick, M.D., Andrews, N.C., 1998. *Nramp2* is mutated in the anemic Belgrade (*b*) rat: evidence of a role for Nramp2 in endosomal iron transport. Proceedings of the National Academy of Sciences of the United States of America 95, 1148–53.

Fleming, M.D., Trenor, C.C., Su, M.A., Foernzler, D., Beier, D.R., Dietrich, W.F., Andrews, N.C., 1997. Microcytic anaemia mice have a mutation in *Nramp2*, a candidate iron transporter gene. Nature Genetics 16, 383–386. https://doi.org/10.1038/ng0897-383

Fraenkel, P.G., Traver, D., Donovan, A., Zahrieh, D., Zon, L.I., 2005. Ferroportin1 is required for normal iron cycling in zebrafish. Journal of Clinical Investigation 115, 1532–1541. https://doi.org/10.1172/JCI23780

Galaris, D., Barbouti, A., Pantopoulos, K., 2019. Iron homeostasis and oxidative stress: An intimate relationship ☆. https://doi.org/10.1016/j.bbamcr.2019.118535

Garrick, M.D., Dolan, K.G., Horbinski, C., Ghio, A.J., Higgins, D., Porubcin, M., Moore, E.G., Hainsworth, L.N., Umbreit, J.N., Conrad, M.E., Feng, L., Lis, A., Roth, J.A., Singleton, S., Garrick, L.M., 2003. DMT1: A mammalian transporter for multiple metals, in: BioMetals. pp. 41–54. https://doi.org/10.1023/A:1020702213099

Geiser, J., Venken, K.J.T., Lisle, R.C.D., Andrews, G.K., 2012. A Mouse Model of Acrodermatitis Enteropathica: Loss of Intestine Zinc Transporter ZIP4 (Slc39a4) Disrupts the Stem Cell Niche and Intestine Integrity. PLOS Genetics 8, e1002766. https://doi.org/10.1371/journal.pgen.1002766

Gunshin, H., Fujiwara, Y., Custodio, A.O., DiRenzo, C., Robine, S., Andrews, N.C., 2005. Slc11a2 is required for intestinal iron absorption and erythropoiesis but dispensable in placenta and liver. The Journal of Clinical Investigation 115, 1258–1266. https://doi.org/10.1172/JCI24356

Gunshin, H., Mackenzie, B., Berger, U.V., Gunshin, Y., Romero, M.F., Boron, W.F., Nussberger, S., Gollan, J.L., Hediger, M.A., 1997. Cloning and characterization of a mammalian proton-coupled metal-ion transporter. Nature 388, 482–488. https://doi.org/10.1038/41343

Illing, A.C., Shawki, A., Cunningham, C.L., Mackenzie, B., 2012. Substrate profile and metal-ion selectivity of human divalent metal-ion transporter-1. Journal of Biological Chemistry 287, 30485–30496. https://doi.org/10.1074/jbc.M112.364208

Jao, L.-E., Wente, S.R., Chen, W., 2013. Efficient multiplex biallelic zebrafish genome editing using a CRISPR nuclease system. Proceedings of the National Academy of Sciences 110, 13904–13909. https://doi.org/10.1073/pnas.1308335110

Jenkitkasemwong, S., Wang, C.Y., MacKenzie, B., Knutson, M.D., 2012. Physiologic implications of metal-ion transport by ZIP14 and ZIP8. BioMetals 25, 643–655. https://doi.org/10.1007/s10534-012-9526-x

Kondaiah, P., Yaduvanshi, P.S., Sharp, P.A., Pullakhandam, R., 2019. Iron and zinc homeostasis and interactions: Does enteric zinc excretion cross-talk with intestinal iron absorption? Nutrients 11, nu11081885. https://doi.org/10.3390/nu11081885

Kwong, R.W.M., 2024. Trace metals in the teleost fish gill: biological roles, uptake regulation, and detoxification mechanisms. Journal of comparative physiology. B, Biochemical, systemic, and environmental physiology. 194, 1–15. https://doi.org/10.1007/S00360-024-01565-1

Kwong, R.W.M., Niyogi, S., 2009. The interactions of iron with other divalent metals in the intestinal tract of a freshwater teleost, rainbow trout (*Oncorhynchus mykiss*). Comparative biochemistry and physiology. Toxicology & pharmacology : CBP. 150, 442–449. https://doi.org/10.1016/j.cbpc.2009.06.011

Labun, K., Montague, T.G., Gagnon, J.A., Thyme, S.B., Valen, E., 2016. CHOPCHOP v2: a web tool for the next generation of CRISPR genome engineering. Nucleic Acids Research 44. https://doi.org/10.1093/nar/gkw398

Laftah, A.H., Latunde-Dada, G.O., Fakih, S., Hider, R.C., Simpson, R.J., McKie, A.T., 2008. Haem and folate transport by proton-coupled folate transporter/haem carrier protein 1 (SLC46A1). British Journal of Nutrition 101, 1150–1156. https://doi.org/10.1017/S0007114508066762

Liuzzi, J.P., Aydemir, F., Nam, H., Knutson, M.D., Cousins, R.J., 2006. Zip14 (Slc39a14) mediates non-transferrin-bound iron uptake into cells. Proc Natl Acad Sci U S A 103, 13612–13617. https://doi.org/10.1073/pnas.0606424103

Mackenzie, E.L., Iwasaki, K., Tsuji, Y., 2008. Intracellular iron transport and storage: From molecular mechanisms to health implications. Antioxidants and Redox Signaling 10, 997–1030. https://doi.org/10.1089/ars.2007.1893

Meneghini, R., 1997. Iron homeostasis, oxidative stress, and DNA damage. Free Radical Biology and Medicine 23, 783–792. https://doi.org/10.1016/S0891-5849(97)00016-6

Neves, J.V., Wilson, J.M., Kuhl, H., Reinhardt, R., Castro, L.F.C., Rodrigues, P.N., 2011. Natural history of SLC11 genes in vertebrates: Tales from the fish world. BMC Evolutionary Biology 11. https://doi.org/10.1186/1471-2148-11-106

Norman, L., Cabanes, D.J.E., Blanco-Ameijeiras, S., Moisset, S.A.M., Hassler, C.S., 2014. Iron biogeochemistry in aquatic systems: From source to bioavailability. Chimia 68, 764–771. https://doi.org/10.2533/chimia.2014.764

Okazaki, Y., 2023. Iron from the gut: the role of divalent metal transporter 1. Journal of Clinical Biochemistry and Nutrition 74, 1. https://doi.org/10.3164/JCBN.23-47

Pasquadibisceglie, A., Bonaccorsi di Patti, M.C., Musci, G., Polticelli, F., 2023. Membrane Transporters Involved in Iron Trafficking: Physiological and Pathological Aspects. Biomolecules 13, 1172. https://doi.org/10.3390/biom13081172

Pinilla-Tenas, J.J., Sparkman, B.K., Shawki, A., Illing, A.C., Mitchell, C.J., Zhao, N., Liuzzi, J.P., Cousins, R.J., Knutson, M.D., Mackenzie, B., 2011. Zip14 is a complex broad-scope metal-ion transporter whose functional properties support roles in the cellular uptake of zinc and nontransferrin-bound iron. American Journal of Physiology-Cell Physiology 301, C862–C871. https://doi.org/10.1152/ajpcell.00479.2010

Puar, P., Naderi, M., Niyogi, S., Kwong, R.W.M., 2021. Using zebrafish as a model to assess the individual and combined effects of sub-lethal waterborne and dietary zinc exposure during development ☆. Environmental Pollution 284, 117377. https://doi.org/10.1016/j.envpol.2021.117377

Qiu, A., Hogstrand, C., 2004. Functional characterisation and genomic analysis of an epithelial calcium channel (ECaC) from pufferfish, *Fugu rubripes*. Gene 342, 113–123. https://doi.org/10.1016/j.gene.2004.07.041

Qiu, A., Jansen, M., Sakaris, A., Min, S.H., Chattopadhyay, S., Tsai, E., Sandoval, C., Zhao, R., Akabas, M.H., Goldman, I.D., 2006. Identification of an Intestinal Folate Transporter and the Molecular Basis for Hereditary Folate Malabsorption. Cell 127, 917–928. https://doi.org/10.1016/j.cell.2006.09.041

Radziejewska, A., Suliburska, J., Kołodziejski, P., Chmurzynska, A., 2020. Simultaneous supplementation with iron and folic acid can affect Slc11a2 and Slc46a1 transcription and metabolite concentrations in rats. British Journal of Nutrition 123, 264–272. https://doi.org/10.1017/S0007114519002721

Rombough, P., 2002. Role of gills in developing zebrafish. The Journal of Experimental Biology 205, 1787–1794.

Shawki, A., Mackenzie, B., 2010. Interaction of calcium with the human divalent metal-ion transporter-1. Biochemical and Biophysical Research Communications 393, 471–475. https://doi.org/10.1016/j.bbrc.2010.02.025

Shayeghi, M., Latunde-Dada, G.O., Oakhill, J.S., Laftah, A.H., Takeuchi, K., Halliday, N., Khan, Y., Warley, A., McCann, F.E., Hider, R.C., Frazer, D.M., Anderson, G.J., Vulpe, C.D., Simpson, R.J., McKie, A.T., 2005. Identification of an intestinal heme transporter. Cell 122, 789–801. https://doi.org/10.1016/j.cell.2005.06.025

Standal, H., Dehli, A., Rørvik, K.A., Andersen, 1999. Iron status and dietary levels of iron affect the bioavailability of haem and nonhaem iron in Atlantic salmon *Salmo salar*. Aquaculture Nutrition 5, 193–198. https://doi.org/10.1046/J.1365-2095.1999.00105.X

van Raaij, S.E.G., Srai, S.K.S., Swinkels, D.W., van Swelm, R.P.L., 2019. Iron uptake by ZIP8 and ZIP14 in human proximal tubular epithelial cells. BioMetals 32, 211–226. https://doi.org/10.1007/s10534-019-00183-7

Veuthey, T., Wessling-Resnick, M., 2014. Pathophysiology of the Belgrade rat. Frontiers in Pharmacology 5, 1–13. https://doi.org/10.3389/fphar.2014.00082

Wallace, K.N., Akhter, S., Smith, E.M., Lorent, K., Pack, M., 2005. Intestinal growth and differentiation in zebrafish. Mechanisms of Development 122, 157–173. https://doi.org/10.1016/j.mod.2004.10.009

Wang, C.Y., Jenkitkasemwong, S., Duarte, S., Sparkman, B.K., Shawki, A., Mackenzie, B., Knutson, M.D., 2012. ZIP8 is an iron and zinc transporter whose cell-surface expression is up-regulated by cellular iron loading. Journal of Biological Chemistry 287, 34032–34043. https://doi.org/10.1074/jbc.M112.367284

Wang, J., Wang, W.-X., 2016. Novel insights into iron regulation and requirement in marine medaka O*ryzias melastigma*. Scientific Reports 6, 26615. https://doi.org/10.1038/srep26615

Wheal, M.S., Decourcy-Ireland, E., Bogard, J.R., Thilsted, S.H., Stangoulis, J.C.R., 2016. Measurement of haem and total iron in fish, shrimp and prawn using ICP-MS:

Implications for dietary iron intake calculations. Food Chemistry 201, 222–229. https://doi.org/10.1016/J.FOODCHEM.2016.01.080

Wood, C.M., Farrell, A.P., Brauner, C.J., 2011. Homeostasis and toxicology of essential metals, Fish Physiology. Academic Press. https://doi.org/10.1016/S1546-5098(11)31010-2

Xing, W., Liu, G., 2011. Iron biogeochemistry and its environmental impacts in freshwater lakes. Fresenius Environmental Bulletin 20, 1339–1345.

Yamaji, S., Tennant, J., Tandy, S., Williams, M., Singh Srai, S.K., Sharp, P., 2001. Zinc regulates the function and expression of the iron transporters DMT1 and IREG1 in human intestinal Caco-2 cells. FEBS Letters 507, 137–141. https://doi.org/10.1016/S0014-5793(01)02953-2

Yanatori, I., Kishi, F., 2019. DMT1 and iron transport. Free Radical Biology and Medicine 133, 55–63. https://doi.org/10.1016/J.FREERADBIOMED.2018.07.020

Yanatori, I., Tabuchi, M., Kawai, Y., Yasui, Y., Akagi, R., Kishi, F., 2010. Heme and non-heme iron transporters in non-polarized and polarized cells. BMC Cell Biology 11, 1–11. https://doi.org/10.1186/1471-2121-11-39/FIGURES/7

Zang, L., Shimada, Y., Nishimura, Y., Tanaka, T., Nishimura, N., 2015. Repeated Blood Collection for Blood Tests in Adult Zebrafish. Journal of Visualized Experiments : JoVE 2015, 53272. https://doi.org/10.3791/53272

Zhang, T., Sui, D., Hu, J., 2016. Structural insights of ZIP4 extracellular domain critical for optimal zinc transport. Nat Commun 7, 11979. https://doi.org/10.1038/ncomms11979

Zhao, L., Xia, Z., Wang, F., 2014. Zebrafish in the sea of mineral (iron, zinc, and copper) metabolism. Frontiers in Pharmacology 5, 1–23. https://doi.org/10.3389/fphar.2014.00033

Zhu, X., Xu, Y., Yu, S., Lu, L., Ding, M., Cheng, J., Song, G., Gao, X., Yao, L., Fan, D., Meng, S., Zhang, X., Hu, S., Tian, Y., 2014. An efficient genotyping method for genome-modified animals and human cells generated with CRISPR/Cas9 system. Scientific Reports 4, 6420. https://doi.org/10.1038/srep06420

Chapter 4

Transcriptomic Analysis of DMT1 Mutant Zebrafish: Comparative Insights from the Gill and Gut

4.1 Summary

The divalent metal transporter 1 (DMT1, *slc11a2*) is a central player in vertebrate iron uptake and homeostasis, but the consequences of DMT1 loss on systemic iron balance and potential compensatory pathways in iron transport remain unresolved in fish. In this study, we combined CRISPR-Cas9 mutagenesis with RNA sequencing to characterize the transcriptomic remodeling in the gill and intestine of zebrafish (*Danio rerio*) during DMT1 loss. Differential expression, enrichment analysis, and functional profiling were used to evaluate shared and tissue-specific responses employed by *dmt1*$^{-/-}$ fish. Notably, DMT1 knockout (KO) produced a broad reprogramming of iron transport and metabolism and also affected many secondary pathways. While *dmt1* expression was strongly suppressed in the mutants, upregulations in ferric reductase (*cybrd1*), transferrin receptors (*tfr1a* and *tfr1b*), and hemoglobin/erythropoiesis-related genes (*alas2*, *gata1a*, and *tal1*) were consistent with an attempt to increase iron assimilation and preserve oxygen transport function during iron deficiency. The suppression of hepcidin/BMP-Smad signaling also aligned with systemic iron deficiency in the mutants. In particular, tissue-specific induction of two potential compensatory routes, including *zip4* in the intestine and *ecac* in the gill, was evident. Broader physiological implications of *dmt1* loss included an upregulation of vesicle transport, membrane remodeling, and immunity/redox adjustments. Gill-specific remodeling emphasized barrier tightening, ion regulation, and autophagy, whereas the intestine highlighted transferrin-mediated uptake, xenobiotic/lipid metabolism, and selective downregulation of apical solute transport. Nonetheless, the loss of DMT1 not only reveals its integral role in iron homeostasis but also the plasticity and highly coordinated transport network in zebrafish. Although these adjustments buffer systemic iron imbalance, they do not fully rescue iron deficiency in the mutants who exhibit persistent hypochromic phenotypes. Ecophysiologically, the plasticity in

metal homeostatic pathways may enhance survival in environments with fluctuating iron, zinc, and calcium availability, while, comparatively, zebrafish display both conserved (transferrin-ferritin-hepcidin) and distinct (*ecac*, *cybrd1*) pathways of iron regulation. Together, these findings establish zebrafish as a powerful comparative model for studying vertebrate iron metabolism and related disorders.

4.2 Introduction

Iron is an essential micronutrient required for fundamental processes, including oxygen transport, energy metabolism, and cellular proliferation (Cairo et al., 2006; Wood et al., 2011; Chandrapalan and Kwong, 2021). However, both iron deficiency and iron overload are associated with impaired growth, disrupted redox balance, and compromised survival (Meneghini, 1997; Andrews, 2000b; Sevcikova et al., 2011). To mitigate the risks of iron imbalance, vertebrates have evolved highly coordinated mechanisms of iron uptake, storage, and distribution, which help to maintain iron levels within a physiologically safe range (Lall and Kaushik, 2021; Galy et al., 2024). A central player in this regulatory framework is the divalent metal transporter 1 (DMT1; also known as SLC11A2) (Fleming et al., 1997; Gunshin et al., 1997). DMT1 is the principal importer of ferrous iron across cellular membranes; it facilitates the absorption of dietary non-heme iron at the intestinal epithelium and the endosomal release of transferrin-bound iron during erythropoiesis (Bury et al., 2003; Gunshin et al., 2005; Mackenzie and Garrick, 2005; Yanatori and Kishi, 2019). In addition to iron, DMT1 is proposed to have broad substrate specificity to multiple divalent metals, including zinc, manganese, cobalt, nickel, cadmium, and lead (Gunshin et al., 1997; Garrick et al., 2003). DMT1 may therefore have broader physiological significance and influence the homeostasis of multiple metals.

The structure and function of DMT1 are highly conserved across vertebrates, with human and mouse orthologs sharing ~89% similarity and the zebrafish homolog showing ~71-73% amino acid similarity to its mammalian counterparts (Zhao et al., 2014). Across multiple vertebrate models, including the microcytic anemia (*mk*) mouse, Belgrade (*b*) rats, and the chardonnay (*cdy*) zebrafish, gene disruption to *dmt1* is characterized by the consistent development of severe anemia and systemic iron deficiency, further highlighting the conserved and nonredundant role of DMT1 in maintaining iron balance (Fleming et al., 1997, 1998; Andrews, 2000a; Donovan et al., 2002; Shawki et al., 2012). However, the viability of these models also indicates that DMT1-independent mechanisms exist, potentially involving heme absorption or alternative non-heme transporters such as members of the ZRT-, IRT-like protein (ZIP) family (ZIP8 and ZIP14) and the epithelial calcium channel (ECaC; also known as transient receptor potential cation channel 6 (TRPV6)), which may provide sufficient iron uptake required for survival (Qiu and Hogstrand, 2004; Yanatori et al., 2010; Pinilla-Tenas et al., 2011; Wang et al., 2012). Nonetheless, compensatory mechanisms of iron uptake and the relative importance of alternate iron uptake pathways remain unresolved, particularly in non-mammalian vertebrates, including teleosts, where iron regulation is less understood.

Fish in particular face a unique challenge in iron regulation compared to terrestrial vertebrates because iron can be absorbed not only through the intestine but also directly across the gills from the aquatic environment (Bury, 2003). In zebrafish, DMT1 expression is conserved in the intestine and erythroid cells, suggesting evolutionary conservation of function (Donovan et al., 2002). However, the gill represents an additional and ecologically relevant site of iron uptake in teleosts, raising important questions about how systemic and tissue-specific iron homeostasis is maintained when DMT1 is disrupted. While the intestine is the primary site of dietary iron

absorption, the gills are multifunctional organs engaged in ionoregulation, gas exchange, and chemosensing, which make it a secondary but significant route for iron acquisition (Evans et al., 2005; Grosell et al., 2010; Kwong, 2024; Leonard et al., 2024). Radiotracer studies in zebrafish demonstrate that branchial uptake of iron is sufficient to offset daily iron losses and can meet up to 85% of the iron demand in developing rainbow trout (Bury, 2003; Cooper and Bury, 2007). Fish integrate intestinal and branchial pathways to meet iron demands, but the compensatory roles of these tissues and how this dual system adjusts to DMT1-deficient conditions are unclear.

While previous studies have characterized the expression and function of DMT1 in fish, the broader transcriptional consequences of its loss across different organs remain largely unexplored (Cooper et al., 2006; Kwong et al., 2010; Neves et al., 2011; Chandrapalan and Kwong, 2020). High-throughput transcriptomics provides a powerful tool to uncover these effects by identifying genome-wide transcriptional changes (Wang et al., 2009). Such analyses can identify not only the conserved iron-handling pathways but also potential compensatory mechanisms and secondary processes involving signalling, metabolism, and stress responses which may accompany DMT1 loss. Focusing on the gill and the gut as major sites of iron uptake also provides comparative insight into how iron transport pathways are coordinated across distinct physiological interfaces in fish. The extent to which gill and intestinal responses diverge, overlap, or interact under DMT1 deficiency remains unclear. These insights are particularly valuable in zebrafish, a widely used model in developmental biology, genetics, and environmental physiology (Hwang et al., 2013; Roper and Tanguay, 2018; Srivastava et al., 2025). Moreover, the high degree of evolutionary conservation across vertebrates supports the use of zebrafish as a tractable model to elucidate the molecular basis of iron transport and homeostasis (Zhao et al., 2014).

In this study, we employed RNA sequencing to investigate the transcriptomic consequences of DMT1 loss in adult zebrafish, focusing on the gill and intestine as two critical sites of iron uptake. By comparing wild-type and CRISPR-Cas9 generated *dmt1*$^{-/-}$ fish, we aimed to identify differentially expressed genes, enriched pathways, and potential compensatory transport mechanisms that emerge in the absence of this major iron importer. This approach provides the first tissue-specific transcriptomic assessment of DMT1 function in a vertebrate model, extending our understanding of how iron homeostasis is maintained when conserved transport pathways are disturbed. More broadly, the findings of this study will provide critical insight into how fish regulate iron transport and their ability to maintain metal homeostasis during challenging conditions. By advancing the zebrafish as a model system, this work not only deepens our understanding of the molecular basis of iron metabolism and its integration with other essential trace metals but also establishes a framework for investigating iron-related disorders in vertebrates and environmental stressors like metal pollution in teleosts.

4.3 Materials and Methods

4.3.1 Animals

All experimental work involving the handling and use of fish in this study were carried out in accordance with the Canadian Council for Animal Care and approved by the York University Animal Care Committee (2017-2 R2). Zebrafish (Tüpfel long-fin strain) were housed at York University's vivarium and adult fish were maintained in recirculatory systems (Aquaneering, CA, USA) at 28°C with a 14h light: 10h dark photoperiod. Fish were kept in 2.8 L tanks with a density of 25-30 fish per tank. They were fed brine shrimp each morning (weekdays) and commercial zebrafish pellets (Zeigler, PA, USA) daily in the afternoon.

4.3.2 CRISPR-Cas9 generated dmt1$^{-/-}$ fish

A DMT1 knockout (KO) line (*dmt1*$^{-/-}$) was established in-house using the CRISPR-Cas9 system. Homozygous mutants have a 14 bp deletion in the DNA sequence located (285,669 - 285,682 bp) on the *Danio rerio* chromosome 11 (NC_007122.7) GRCz11 (GCF_000002035.6) gene assembly. Single guide RNA (sgRNA; 5'-CCGACGCCCCGUCUCGAGGU-3') targeting site of mutation was purchased from Synthego Corporation (CA, USA) and Cas9 protein (EnGen® Spy Cas9 NLS) was purchased from NEB (MA, USA). In brief, zebrafish embryos at the one-cell stage were microinjected (WPI picopump pv830, FL, USA) with 50 ng/µL sgRNA, 5 µM Cas9 protein, 0.3 M KCl, 0.05% phenol red, and nuclease-free water to generate the founding generation (F_0). F_0 fish carrying a mutation were grown to adulthood (reproductive maturity) and outcrossed with wildtype (WT) fish to generate heterozygous F_1 offspring (*dmt1*$^{+/-}$). F_1 mutants were in-crossed to breed for F_2 homozygous (*dmt1*$^{-/-}$) mutants. For each generation of mutants (F_0, F_1, and F_2), a corresponding control genotype (referred to as WT going forward) was established. WT fish were microinjected with a control injection (lacking sgRNA) and grown to adulthood and the resulting F_0 WT fish were bred similarly to the mutants to obtain subsequent F_1 and F_2 WT generations. Homozygosity and gene KO were confirmed through Sanger sequencing (The Center for Applied Genomics, The Hospital for Sick Children). (Further details on the generation of *dmt1*$^{-/-}$ mutants and mutagenesis analysis can be found on Chapter 3.)

4.3.3 Tissue collection and RNA sequencing

Adult *dmt1*$^{-/-}$ (~12 months) and WT fish were fasted for 24 h to clear gut contents prior to tissue collection. Fish were euthanized with an overdose of tricaine methanesulfonate (MS-222, 0.4 g/L) buffered with sodium bicarbonate to pH 7 (Sigma-Aldrich, MO, USA). Tissues from the

gill and intestine were collected for RNA sequencing. Each tissue sample consisted of pooled tissue from 4-5 adults. A total of 3 replicates were collected per tissue per genotype. RNA was extracted and DNase I treatment was performed using the Monarch RNA Extraction kit (New England Biolabs, ON, CA) following manufacturer's protocol. RNA quality was measured using the BioTek Synergy LX multimode reader (Agilent Technologies, CA, USA) to ensure OD 260/280 ratios ~2 (Gen5 version 3.17.17, Agilent Technologies). RNA samples were also checked on an agarose gel prior to sample submission. RNA samples were stored at -80°C until use.

RNA-seq libraries were prepared using the NEBNext Ultra II Directional polyA mRNA Library Prep Kit and sequenced on an Illumina NovaSeq X with 150 bp paired-end reads at the TCAG Sequencing Facility at the Centre for Applied Genomics (Toronto, Canada). The target sequencing depth was 20 million reads per sample.

4.3.4 RNA-seq data alignment and quantification

Raw paired-end RNA-seq reads were trimmed with Trimmomatic v0.39 to remove adapters and low-quality bases (ILLUMINACLIP:TruSeq3-PE-2.fa:2:30:10, LEADING:10, TRAILING:10, SLIDINGWINDOW:4:15, MINLEN:36), followed by fastp v0.23.2 for trimming poly-G (NovaSeq artifacts) and poly-X (poly-A tails) with a minimum read length of 30 bp. Read quality before and after trimming was assessed using FastQC v0.11.9. Filtered reads were aligned to the *Danio rerio* GRCz11 reference genome (NCBI GCF_000002035.6) using STAR v2.7.11b, with alternate loci included. Alternate loci are distinct versions of defined genomic regions, representing variations such as haplotypes or structural variants. Genes from alternate loci share the same gene symbol as their counterparts in the primary assembly but are denoted by an

underscore suffix in their RefSeq gene IDs (genome annotation release 106). Unless otherwise indicated, analyses used gene ID-level data.

Gene-level quantification on exon-mapped reads was performed using featureCounts v2.0.6, with fractional counting for multi-mapping reads and for reads in overlapping gene regions. Exon-level counts were obtained separately using DEXSeq's dexseq_count.py script for differential exon usage analysis. The 14 bp deletion in *dmt1* in the KO group (NC_007122.7:285,669-285,682) was confirmed by visualizing read alignments from STAR in IGV.

4.3.5 Differential expression analysis

To assess gene-level differential expression between the wildtype (WT) and *dmt1* (DMT1) knockout (KO) fish in the gill and intestine, we used edgeR v4.4.2 (Chen et al., 2025). We filtered out lowly expressed genes using the filterByExpr function (min.count=10, min.total.count=15), normalized library sizes using the trimmed mean of M-values (TMM) method, and estimated dispersion. Negative binomial generalized linear models were fitted to each gene. The design matrix included tissue, genotype, and interaction (model: tissue + genotype + tissue:genotype). Three contrasts were tested for each gene: WT vs KO (KO − WT) in intestine, WT vs KO in gill, and interaction. P-values were corrected for multiple testing using the Benjamini-Hochberg method, and genes with a false discovery rate (FDR) < 0.05 were considered significantly differentially expressed. Sample clustering by gene expression was visualized using multidimensional scaling (MDS) in edgeR, based on leading log-fold-changes, producing a principal coordinate (PCoA) plot. For visualizing gene expression, expression values were converted to $\log_2$ counts per million (logCPM) using edgeR's *cpm* function (with a prior count of 0.25), scaled by the normalized library sizes.

4.3.6 Functional analysis

Overrepresentation analysis (ORA) of differentially expressed genes (DEGs) (edgeR intestine, gill, and interaction contrasts) was performed using g:Profiler (Ensembl release 113) and clusterProfiler v4.14.6 (Kolberg et al., 2023; Xu et al., 2024). As required for functional mapping, gene IDs from alternate loci were merged by gene symbol. For g:Profiler, GO Biological Process, KEGG, Reactome, and Human Phenotype Ontology (orthology-mapped) terms were tested against the *Danio rerio* reference gene set, with g:SCS multiple testing correction (Padj < 0.05). For clusterProfiler, GO Biological Process ORA was then conducted separately for upregulated and downregulated DEGs against the annotation database org.Dr.eg.db (Bioconductor v3.20), using the Benjamini-Hochberg method for multiple testing correction (Padj < 0.05) (Huber et al., 2015). To facilitate interpretation and visualization, significant GO terms were simplified based on semantic similarity using the simplify function in clusterProfiler.

To visualize the functional profiles of DEGs in word clouds, we retrieved GO Biological Process annotations for each gene ID by its gene symbol from the GO Consortium (release 2024-11-04) (Ashburner et al., 2000; Consortium et al., 2023). The DEGs were partitioned into four non-overlapping categories to distinguish between tissue-specific from shared responses: (i) DEGs with significant tissue × genotype interactions, and, among genes without interactions, (ii) DEGs significant in both tissues, (iii) gill-specific DEGs, and (iv) intestine-specific DEGs. For each category, we used simplifyEnrichment v2.0.0 with Fisher's exact test to identify overrepresented words in the set of GO term names relative to the background GO terms in the database (Gu and Hübschmann, 2023). These categorizations were used solely for visualization and not for ORA results.

4.4 Results

4.4.1 RNA-Seq quality and gene knockout

Sequencing yielded an average of 26.0 million paired-end reads per library (range: 20.4 to 30.6 million). Following trimming and filtering, 93.7% (88.8-95.7%) of reads were used for alignment to the zebrafish reference genome. On average, 79.9% (78.2-81.7%) of the reads were uniquely mapped, and 15.3% (14.3-16.6%) mapped to multiple loci. Multidimensional clustering of expression profiles showed a clear separation of samples by tissue (gill vs. intestine) and genotype (WT vs. DMT1 KO), with tight clustering of biological replicates (Figure 4-1).

Figure 4-1. Multidimensional scaling (MDS) plot of RNA-seq samples. Sample clustering was visualized using MDS in edgeR, based on leading log-fold-changes in gene expression. The first dimension (dim 1, 80 variance) separates samples by tissue type (gill vs. intestine). Second dimension (dim 2, 5% variance) separates samples by genotype (wildtype (WT)

vs. DMT1 knockout (KO)). Each point represents one biological replicate (n=3, pooled from 4-5 fish), colour-coded by tissue and genotype.

Sequence alignment confirmed a 14 bp deletion in exon 5 of *dmt1* (slc11a2; gene ID: 678623), located within a conserved iron-binding motif (285,669 - 285,682 bp; Figure 4-S1). This deletion produced a frameshift mutation and premature stop codon expected to produce a truncated, non-functional transcript, and abolished protein function (refer to Chapter 3 for more information).

4.4.2 Alterations in DMT1- and iron-related genes

After filtering out low-expressed genes, 26985 gene IDs were retained for analysis. A total of 2774, 2881, and 376 DEGs (FDR < 0.05; all with $|\log_2$ fold-change$| > 0.487$) between WT and *dmt1* KO fish were identified in the intestine, in the gill, and for genotype × tissue interaction, respectively, for simplicity the top 1.5% of DEGs in each category are summarized in Table 4-S1). After merging alternate locus IDs by gene symbol, these corresponded to 2475, 2573, and 347 genes. In the intestine, 1542 DEGs were upregulated and 1232 downregulated in KO fish compared to WT; in the gill, 1744 were upregulated and 1137 downregulated.

Dmt1 (*slc11a2*) expression was significantly reduced in KO fish in both tissues (gill: FDR<0.01; intestine: FDR<0.001; Figure 4-2 and Table 4-S2) and also displayed significant genotype x tissue interaction (FDR<0.01). In WT fish, *dmt1* expression was higher in the intestine than in the gill, but not in the mutants. Expression of cytochrome b reductase 1 (*cybrd1*), a ferric reductase, was significantly upregulated in the gills (FDR<0.05) of *dmt1*$^{-/-}$ fish (Figure 4-2; Table 4-S2). No difference was observed in intestinal *cybrd1* expression in both WT and KO fish.

A number of other iron-related genes were also differentially expressed (Table 4-S2). Iron storage (*fth1a*) and uptake (*tfr1a*) were upregulated in both tissues, as well as oxygen transport (*hbaa1*). Tissue-specific upregulation was observed in the paralogs *tfr1b* and *hbba1* in the intestine. Increased *hephl1b* (ferroxidase) was present in the gills. Conversely, transcripts related to hepcidin and BMP/Smad signaling (*hamp*, *smad1*, *bmpr1ab*, *bmpr2a*, and *bmpr2b*) were downregulated. Genes involved in erythropoiesis (*alas2*, *gata1a*, and *tal1*) were also significantly induced in KO fish.

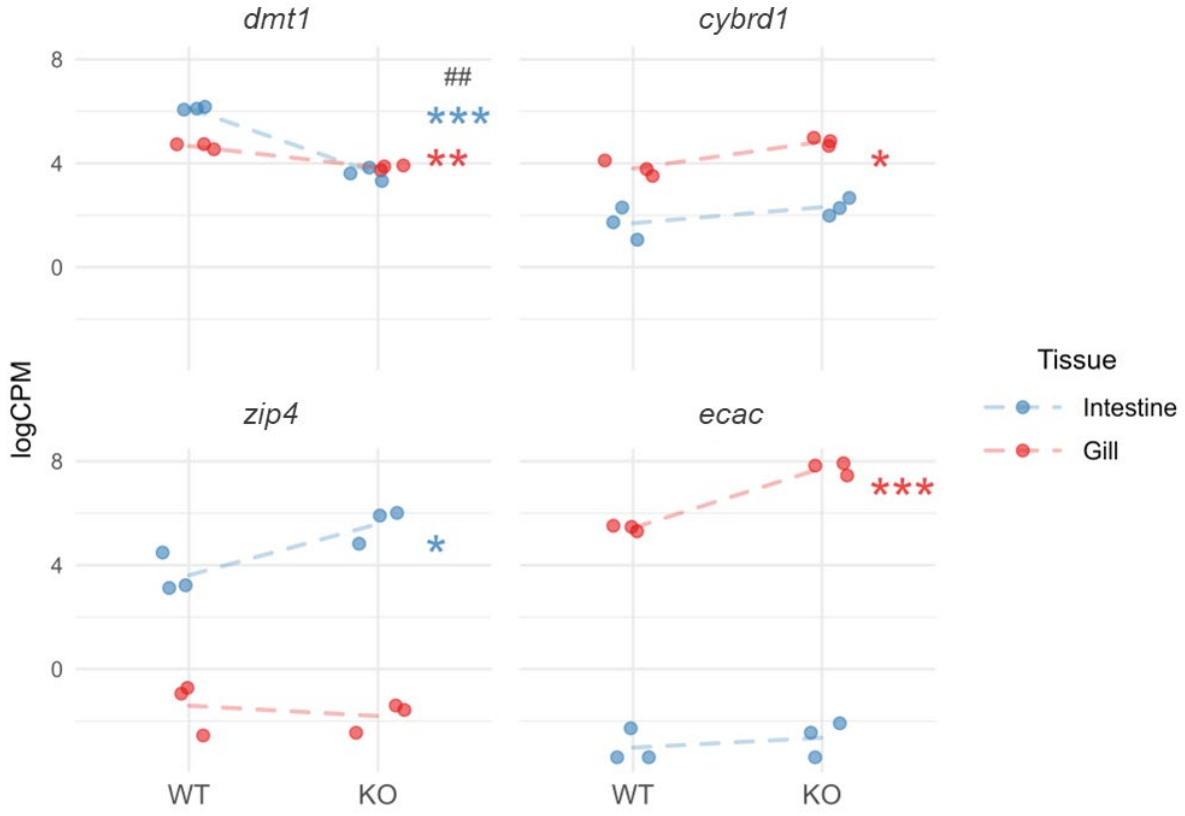

Figure 4-2. (caption on next page)

Figure 4-2. Expression levels of *dmt1*, *cybrd1*, *zip4*, and *ecac* in the gill and intestine of wildtype and DMT1 knockout (KO) zebrafish. Transcript abundance (log_2 counts per million, logCPM) was computed by edgeR with normalized library sizes (n=3, each pooled

from 4-5 fish). Dashed lines connect group means. Significant difference between WT and DMT1 KO within tissues are indicated by asterisks with colours matching the respective tissue: * FDR < 0.05; ** FDR < 0.01; *** FDR < 0.001 (edgeR quasi F-tests). Significant genotype x tissue interaction: ## FDR < 0.01.

4.4.3 Differential expression of solute carrier (SLC) genes and alternate metal uptake pathways

A total of 93 DEGs were assigned to 31 SLC families, but only one SLC transporter, the ZIP family member *zip4* (*slc39a4*), was related to metal uptake (Table 4-S2 and 4-S3). *Zip4* transcripts were significantly elevated in the intestine (FDR<0.05) of *dmt1*$^{-/-}$ fish, while gill expression remained unchanged (Figure 4-2). Other transporters related to iron, including the dietary heme transporter *slc46a1* (heme carrier protein 1, *hcp1*), the basolateral iron exporter *slc40a1* (*ferroportin1*), and the zinc/divalent metal transporters *slc39a8* (*zip8*) and *slc39a14* (*zip14*), were unaltered. Remaining SLC-related DEGs were classified into seven functional groups encompassing sugar transport, mitochondrial processes, organic and inorganic ion transport, vitamin uptake, amino acid transport, and other metabolic solutes (Figure 4-3).

An alternate metal uptake pathway, the calcium channel *ecac* (*trpv6*), was strongly upregulated in the gills (FDR<0.001) of KO fish but remained unchanged in the intestine (Figure 4-2; Table 4-S2).

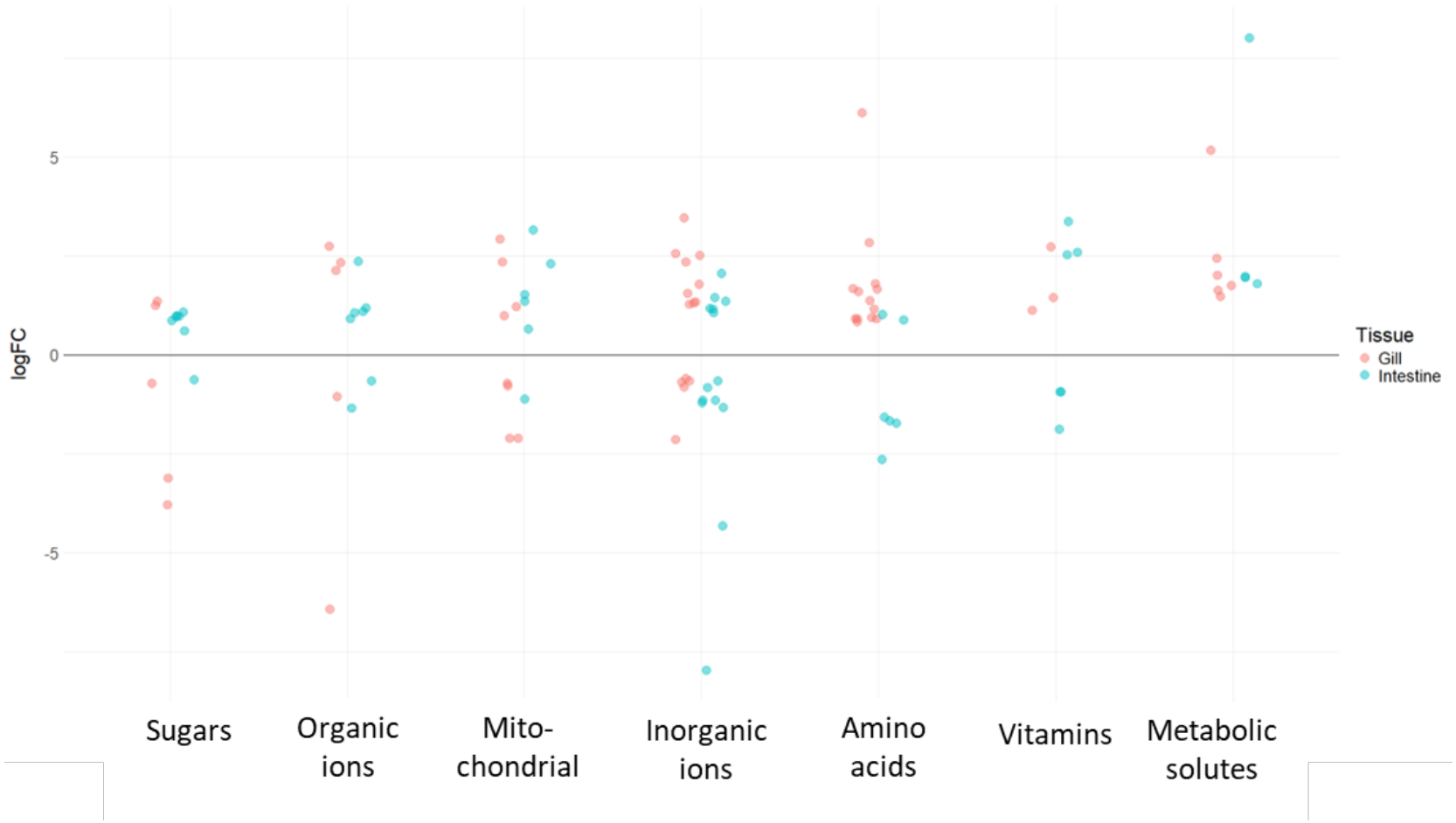

Figure 4-2. Differentially expressed solute carrier (SLC) genes in the gill and intestine of DMT1 knockout zebrafish. A total of 93 differentially expressed genes (DEGs) were identified across 31 SLC families and grouped into seven functional categories based on substrate (sugar transport, mitochondrial processes, organic and inorganic ion transport, vitamin uptake, amino acid transport, and metabolic solutes). Data are shown as $\log_2$ fold change ($\log_2$FC) for gill (pink dots) and intestine (blue dots).

4.4.4 Shared transcriptional responses to DMT1 loss

Expression pattern and functional profiles of the top 1.5% DEGs ranked by FDR were visualized in a heatmap (Figure 4-4). The DEGs were grouped into four distinct (non-overlapping) categories: interaction, both tissues, gill-only, and intestine-only (Table 4-S1). Adjacent word clouds summarize the functional profiles of the full DEG sets in each category, highlighting keywords overrepresented in the names of their associated GO terms. The most prominent keyword across categories was “signalling”, followed by “development” and “transport”.

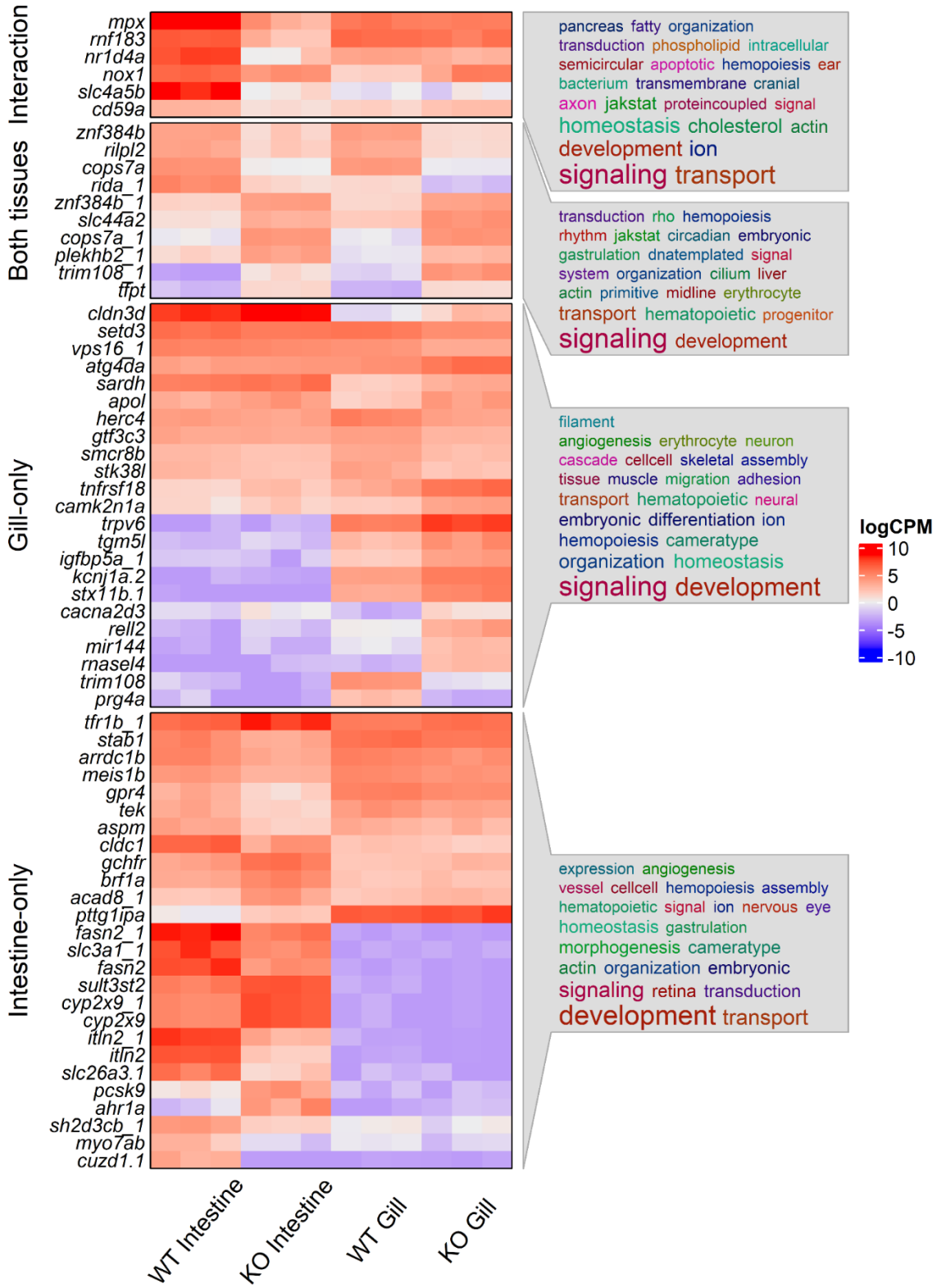

Figure 4-4. (caption on next page)

Figure 4-4. Heatmap of DEGs and associated GO terms in wildtype (WT) and DMT1 knockout (KO) zebrafish. The heatmap shows the top 1.5% of DEGs (FDR ≤ 0.05), ranked by FDR within each category (defined below). Each row is a DEG and each column is a pooled sample of four to five fish (three pools per genotype x tissue). Genes without recognizable gene symbols or GO Biological Process annotations are excluded for clarity. Genes with an underscore (e.g., "_1") indicate alternate loci in the reference genome (see Methods). Tiles are coloured by expression values (log_2 counts per million, logCPM) as computed by edgeR with normalized library sizes. Differential expression was assessed with quasi F-tests for three contrasts: WT vs KO in gill, WT vs KO in intestine, and the interaction term. DEGs are grouped into non-overlapping categories: "Interaction" - genes with a significant interaction term, reflecting differential response to DMT1 KO between tissues; "Both tissues" - response in both tissues without significant interaction; "Gill-only" and "Intestine-only" - response in only one tissue without significant interaction. To the right, the word cloud shows up to 25 enriched keywords in GO term names from the full DEG sets (not just the genes shown) for each category, with font size proportional to keyword enrichment significance. The generic, prevalent term "pathway" has been excluded for clarity.

Interaction-specific (significant genotype x tissue interaction) DEGs showed divergent tissue responses (Figure 4-4, interaction panel). In the KO intestine, genes related to host defense and redox balance, including *mpx* (myeloid-specific peroxidase) and *nox1* (NADPH oxidase 1), were strongly downregulated. *Cd59a* (CD59 molecule a), an inhibitor of complement membrane attack complex (MAC) for protection against cell injury, was also repressed in the intestine. Other

suppressed genes included *nr1d4a* (nuclear receptor), *rnf183* (E3 ubiquitin ligase), and *slc4a5b* (bicarbonate transporter). Enriched interaction-specific GO terms were related to signaling, ion transport, and development.

A second subset of DEGs was consistently altered in the same manner within the gill and intestine (Figure 4-4, "Both tissues"). Many genes associated with mRNA handling and ciliary trafficking (*rida* and *rilpl2*) were downregulated in KO fish. However, select genes related to zinc-finger transcription factors and COP9 (constitutive photomorphogenesis 9) signalosome assembly were differentially altered depending on alternative gene splicing. While *Znf38b* and *cops7a*_1 decreased at one locus, *znf384b*_1 and *cops7a* increased at another. Conversely, genes related to transport and membrane organization (*slc44a2*, *plekhb2*, *trim108*, and *tfpt* were strongly induced. Enriched GO terms in this DEG category emphasized transport, signaling, development, and protein/vesicle trafficking.

4.4.5 Tissue-specific transcriptional responses to DMT1 loss

Gill-specific DEGs pertained to remodeling of epithelial barriers, ion transport, and immune/autophagy activities in *dmt1*$^{-/-}$ fish (Figure 4-4, "Gill-only). Upregulated genes include c*ldn3d* (tight-junction assembly), *trpv6* (*ecac*), *cacna2d3* (calcium channel subunit), *igfbp5a* (insulin-like growth factor binding protein), and *kcnj1a.2* (potassium channel). Membrane trafficking/exocytosis-related *stx11b.1* and *tnfrsf18* were also increased in the mutants. Genes associated with autophagy (*atg4da*) and metabolism (*sardh* and *apol*) were induced, whereas *vps16* and *smcr8b* were reduced. Several transcriptional regulators (*setd3*, *stk38l*, *herc4*) were downregulated, while small RNA defense (*rnasel4*) was activated. Enriched GO terms related to epithelial organization, homeostasis, signaling, and development.

In contrast, intestine-specific DEGs emphasized iron acquisition, epithelial transport, lipid/xenobiotic metabolism, and mucosal defense (Figure 4-4, "Intestine-only"). *Tfr1b* (transferrin receptor 1b) was strongly upregulated in *dmt1*$^{-/-}$ fish. Barrier and transport genes (*slc26a3.1* and *slc3a1*) were downregulated along with innate immune lectin (*itln2*). Lipogenesis and lipid metabolism-related genes (*fasn2*, *pcsk9*, and *stab1*) were also altered in the mutants. Additional upregulated DEGs pertained to xenobiotic metabolism (*ahr1a*), heme binding (*cyp2x9*), and sulfotransferase activity (*sult3st2*), transcription/translation (*brf1a*), cofactor metabolism (*gchfr*), fatty acid β-oxidation (*acad8*), and nuclear import (*pttg1ipa*). Whereas, signaling and angiogenic regulators (*tek*, *meis1b*, *gpr4*), vesicle/cytoskeletal components (*arrdc1b* and *myo7ab*), and endopeptidase/endonuclease (*cuzd1*) related genes were downregulated.

4.4.6 Functional enrichment of differentially expressed genes

Over-representation analysis (ORA) was performed using g:Profiler for all DEGs (Table 4-S4.) and clusterProfiler for up- and down-regulated DEGs separately (Figure 4-5 and S2, Table 4-S5.). ORA revealed limited overlap (adjusted $P<0.05$) between terms overrepresented in the intestine and gills and largely comprised of tissue-specific enrichment profiles. In the intestine, upregulated DEGs were enriched for metabolic and redox processes, transport and binding functions (including iron, heme, and ammonium binding/transport), glycosyltransferase activity, and apoptotic/DNA-related processes. Downregulated terms included SMAD binding, fibroblast growth factor binding, and GTPase binding, suggesting reduced receptor-mediated signaling.

Figure 4-5. (caption on next page)

Figure 4-5. Comparison of functional enrichment in up- and down-regulated DEGs in wildtype (WT) and DMT1 (KO) zebrafish. Over-representation analysis of GO Biological Process terms was performed separately for up- and down-regulated DEGs identified from three contrasts (gill KO vs. WT, intestine KO vs WT, and interaction; quasi F-tests, FDR < 0.05) (n=3, pooled from 4-5 fish). Significant terms (adjusted P < 0.05) were simplified based on semantic similarity by clusterProfiler and are shown on the y-axis. The direction of regulation is defined by the difference in expression levels in the DMT1 KO group relative to WT group. Bubble color represents the Benjamini-Hochberg adjusted P-value (p.adjust) of term enrichment; bubble size (GeneRatio) indicates the proportion of DEGs annotated with a term, reflecting enrichment strength.

In the gill, upregulated terms were primarily associated with signaling and receptor-mediated processes, including actin binding, MAP kinase phosphatase activity, peptidase activity, and fibroblast growth factor binding. Functional annotations related to downregulated DEGs were significantly enriched (p.adjust <0.01) in categories related to molecular and enzyme inhibitor activity, protein folding chaperone function, ferric iron binding, semaphorin receptor binding, hydrolase, and endopeptidase activities.

There were only a limited number of significant interaction-enriched terms, including ATP-dependent chaperon activity and GTPase regulator activities. Steroid binding was uniquely enriched in the interaction category and diverged between tissues.

4.5 Discussion

This study provides the first transcriptomic characterization of *dmt1*$^{-/-}$ zebrafish and offers novel insights into how the gill and intestine, two critical sites of iron uptake in fish, respond to

disruption of a major iron transporter. By combining CRISPR-Cas9 gene editing with RNA sequencing, we demonstrate that the loss of *dmt1* induces widespread transcriptional reprogramming across both sites of iron uptake. These changes not only encompass iron-related pathways but also broader processes linked to cellular signaling, development, transport, and homeostasis. Tissue-specific and shared adjustments in *dmt1*$^{-/-}$ fish highlight the complexity of compensatory mechanisms that underlie the coordination of systemic iron homeostasis.

4.5.1 Effects of dmt1 loss on established pathways of iron uptake

DMT1 allows for the dual uptake of dietary and waterborne iron in teleosts (Bury, 2003; Bury et al., 2003). In the intestine, DMT1 mediates the uptake of dietary non-heme iron through saturable, proton-dependent kinetics and affinities comparable to those observed in mammalian enterocytes (Kwong et al., 2010; Okazaki, 2023). In parallel, branchial DMT1 supports the waterborne acquisition of iron, which is a particularly important pathway under conditions of low dietary iron availability and during early development, when systemic iron requirements are high (Bury, 2003; Cooper et al., 2006). Consistent with this dual role, previous studies have shown that *dmt1* transcript abundance is strongly regulated by iron status, where low dietary iron availability can induce expression levels in both the intestine and gills, whereas excess iron suppresses expression (Kwong et al., 2013; Wang and Wang, 2016). In WT zebrafish, intestinal expression of *dmt1* exceeds that in the gill, reflecting its primary role in dietary absorption. In contrast, *dmt1*$^{-/-}$ mutants display a generalized reduction of transcripts in both the gills and intestine, abolishing this heterogeneous pattern. *Dmt1*$^{-/-}$ fish therefore exhibit a loss of function in line with the gene knockout of *dmt1*.

Interestingly, *dmt1* loss was also associated with altered ferric reductase expression, specifically cytochrome b reductase 1 (*cybrd1*). Iron transport via DMT1 and other ferrous iron transporters (e.g., ZIP family) relies on the reduction of ferric iron to the ferrous form by ferric reductases. At circumneutral pH, iron forms hydroxides and oxyhydroxides and is most commonly found in the insoluble ferric (Fe^{3+}) form, making reductase activity a critical and often a rate-limiting step in iron transport (Stumm and Morgan, 1996; Bury et al., 2001; Bury, 2003). While ferric reductase activities have been reported in fishes and shown to positively correlate with iron transport and tissue accumulation, little is known about teleost *cybrd1*, particularly its expression and function in the gills (Bury et al., 2001; Carriquiriborde, 2003; Rejitha and Peter, 2013). The mammalian ortholog (also known as duodenal cytochrome b, Dcytb) localizes to the brush border membrane of enterocytes and functions in the ascorbate-dependent reduction of iron (Lane et al., 2015). *Dcytb* is upregulated by iron deficiency and anemia and is thought to be important for iron homeostasis (McKie et al., 2001; McKie, 2008). *Cybrd1* transcripts were higher in the gills than in the intestine in both WT and *dmt1*$^{-/-}$ zebrafish and were significantly elevated in the gills of mutants. This pattern suggests that *cybrd1* may be more functionally relevant to branchial iron acquisition than previously recognized. The upregulation of *cybrd1* in *dmt1*$^{-/-}$ fish may also be a compensatory response to chronic systemic iron deficiency in the mutants. Nonetheless, enhanced ferric reductase activity could increase the pool of ferrous iron available for uptake, potentially offsetting the impaired transport capacity caused by the loss of DMT1. These findings further strengthen the established relationship between ferric reductases and iron transport and suggest that branchial *cybrd1* may represent an important compensatory mechanism during impaired intestinal iron absorption.

4.5.2 Effects of dmt1 loss on established pathways of iron metabolism

As expected, a number of genes related to iron metabolism were modulated by DMT1-deficient conditions and comprise a coordinated transcriptional reprogramming across the gill and intestine to facilitate iron transport, storage, and regulation. In accordance with the increased need to compensate for impaired apical iron uptake, there was an associated increase in *tfr1a* (both tissues) and *tfr1b* (intestine), which can enhance transferrin-mediated iron acquisition. The upregulation of both transferrin receptors also indicates increased demand for both erythroid-specific (*tfr1a*) and non-erythroid (*tfr1b*) iron uptake in the mutants (Wingert et al., 2004). In parallel, *fth1a* was consistently upregulated in both tissues, which would support sequestration of labile iron to stabilize cellular iron pools, but it may also be an important antioxidant mechanism in the mutants (Fraenkel et al., 2005). The ferritin heavy chain has been increasingly recognized as an anti-ferroptotic factor because it prevents the accumulation of redox-active ferrous iron that can fuel lipid peroxidation (Tiwari et al., 2019; Lv and Liu, 2023). In the *dmt1*$^{-/-}$ mutants who exhibit both an iron-deficient phenotype (hypochromic RBCs with possible heme deficiency, refer to Chapter 3) and a systemic shift to increase iron assimilation, *fth1a* mediated iron sequestration would be critical to mitigate any redox stress during this iron dysregulation.

While *tfr1* and *fth1a* support cellular iron assimilation and accumulation, respectively, activation of key regulatory pathways that control iron export and circulation in the blood is also apparent. Although the iron exporter, *ferroportin1*, was not differentially expressed in the mutants, elevation of its associated ferroxidase may reinforce the basolateral iron-export/iron-cycling activities by promoting efficient conversion of ferrous iron to ferric iron required for transferrin-bound circulation in the blood (Vulpe et al., 1999; Chen et al., 2003; Galaris et al., 2019). Furthermore, another key regulatory pathway in iron metabolism via *hepcidin* and *BMP/Smad*

signaling was downregulated in the mutants. Hepcidin is a master regulator of systemic iron homeostasis and acts by modulating ferroportin1 localization/degradation to control iron absorption and iron release from body stores, whereas the BMP/Smad signaling pathway modulates hepcidin transcription (Xiao et al., 2020; Nemeth and Ganz, 2021; Kesharwani et al., 2025). The downregulation of both *hepcidin* and *BMP/Smad* signaling genes is consistent with iron-deficient conditions, which require increased iron absorption and mobilization; nonetheless, still restricted by the level of apical iron acquisition.

A strong upregulation of erythroid genes, *alas2* (rate-limiting step for heme synthesis) and hemoglobin (*hbaa1* and *hbba1*) in both tissues (logFC ≈2.6-2.7 for alas2 and ≈1.5-1.7 for globins) suggests an attempt to preserve oxygen transport functions while circulating iron levels are compromised (Astner et al., 2005; Kulkeaw and Sugiyama, 2012). Moreover, the induction of *gata1a* and *tal1* to enhance erythroid differentiation within the highly vascularized surface of the gills would be an important strategy to support the systemic requirements to increase hemoglobinization and oxygen delivery during DMT1 loss (Kassouf et al., 2010; Han et al., 2015; Tian et al., 2021). Regardless of these highly coordinated transcriptional reprogramming to re-establish iron homeostasis, the *dmt1*$^{-/-}$ fish still exhibit systemic iron imbalance and a definitive hypochromic RBC phenotype (refer to Chapter 3), asserting the integral role of DMT1 in the maintenance of iron homeostasis.

4.5.3 Compensatory regulation by alternate metal uptake pathways

The loss of *dmt1* was accompanied by selective upregulation of two alternate metal uptake pathways, highlighting potential remodeling of divalent cation transport networks. In the intestine, *zip4* expression was significantly elevated in the mutants. ZIP4 is best characterized as critical for

zinc absorption, and mutations to this gene have been linked to embryonic lethality in mice and the zinc deficiency disorder acrodermatitis enteropathica in humans (Feeney et al., 2005; Andrews, 2008). ZIP4 is localized to the apical membrane of enterocytes and mediates dietary zinc uptake. In zebrafish, *zip4* is highly expressed in the intestine compared to the gills and is modulated by zinc exposure (Feeney et al., 2005; Puar et al., 2021). While little is known about the role of ZIP4 in iron transport, mammalian studies suggest potential indirect interactions where intestinal *zip4* knockout transiently reduced iron content in the small intestine by half; at the same time, iron exposure did not inhibit zinc uptake through ZIP4 (Antala and Dempski, 2012; Geiser et al., 2012). In *dmt1*$^{-/-}$ zebrafish, it remains unclear whether the observed increase in *zip4* reflects a direct compensatory route for iron transport or a secondary adjustment to maintain zinc balance under conditions of altered metal homeostasis. Notably, ZIP8 and ZIP14 are capable of transporting both zinc and iron, which supports the possibility that a broad specificity ZIP transporter can be rerouted to meet iron transport demands. The functional interplay of cation transporters highlights the need for future studies to elucidate the substrate specificity and regulatory dynamics of teleost ZIP4.

Similarly, gill expression of *ecac* was significantly elevated in the mutants, suggesting potential crosstalk between calcium and iron transport pathways. ECaC is a key mediator of transcellular calcium uptake in vertebrates, and in fishes it serves as the primary route for waterborne calcium absorption through the gills (Hoenderop et al., 2002; Pan et al., 2005). Phylogenetic analyses indicate that teleosts possess a single *ecac* gene, distinct from mammalian TRPV5 and TRPV6 paralogs that arose from evolutionary divergence and gene duplication event in higher vertebrates (Hoenderop et al., 2003; Shahsavarani, 2006). Importantly, evidence from heterologous expression systems shows that the fugu ECaC, cloned from gill tissue of *Takifugu rubripes*, is capable of transporting not only calcium but also zinc and iron (Qiu and Hogstrand,

2004). Furthermore, dietary iron exposure to a high iron diet (~1795 mg Fe/kg) led to a significant increase in *ecac* expression, alongside *zip14* and *zip8*, and coincided with tissue iron loading in larval zebrafish (Chandrapalan and Kwong, 2020). The upregulation of *ecac* in *dmt1*$^{-/-}$ zebrafish, therefore, suggests that this channel may provide an alternate route for branchial iron uptake under conditions where DMT1-mediated transport is impaired.

Together, the interaction between iron, zinc, and calcium transport pathways emphasizes the plasticity within transporter networks. The possible compensatory roles of ZIP4 and ECaC, particularly in a tissue-specific manner, demonstrate how dual uptake (gill and intestine), overlapping substrate specificities, competitive interactions, and adaptive regulatory responses may buffer essential metal homeostasis despite genetic disruption to *dmt1*. This functional redundancy may also represent an important evolutionary mechanism to increase survival during fluctuating environments where iron, zinc, and calcium levels can vary drastically.

4.5.4 Broader physiological consequences encompassing tissue-specific and shared transcriptional responses

Beyond iron transport and metabolism, tissue-specific and shared remodeling of several secondary pathways were observed in *dmt1*$^{-/-}$ fish. Notably, a subset of DEGs with significant interaction (genotype x tissue) was related to immunity and oxidative stress, both of which are closely linked to iron metabolism (Guo et al., 2018; Tarifeño-Saldivia et al., 2018). In the intestine of mutants, there was evident repression of *mpx* and *nox1*, which are central to reactive oxygen species production and antibacterial defense (Lieschke et al., 2001; Nauseef, 2008). *Nox1* induces ROS production in zebrafish during bacterial infection to promote immunoreaction and host defense, and repression of this gene may compromise fish immunity (Wu and Chang, 2025). In

contrast, the gills exhibited stable expression of both *mpx* and *nox1*, which may highlight the greater importance of DMT1-mediated iron transport in intestinal immune and redox metabolism. Particularly, the immunomodulatory effects of dietary iron were highlighted during iron exposure in Nile tilapia (*Oreochromis niloticus*), which exhibited heightened complement activity and enhanced fish immunity during supplementation with organic iron (Hermes et al., 2024). Aligning with the repression of *cd59a*, a complement inhibitor with bacterial-binding and inhibiting activities, observed in the iron compromised intestine of KO fish (Sun et al., 2013). This divergence in function was also reflected during functional enrichment analysis, whereby oxidative stress and immune-related GO terms were prominent in the interaction category.

Nonetheless, the gills and intestine also shared many conserved transcriptional responses to DMT1 KO, suggesting the presence of common compensatory adjustments to restore systemic iron imbalance in the mutants. In particular, the upregulation of *slc44a2* and *plekhb2*, along with chromatin and apoptosis regulators (*tfpt* and *trim108*), highlights enhanced lipid transport, vesicle trafficking, and transcriptional control activities in both tissues. *Slc44a2* encodes a choline/ethanolamine transporter and its induction points to remodeling of membrane phospholipid metabolism (Michel et al., 2006; Taylor et al., 2021). While membrane composition directly influences vesicle budding and receptor trafficking activities, the upregulation of *slc44a2* may facilitate any enhanced endocytosis and signal transduction activities that accompany rebalance of iron homeostasis. Similarly, *plekhb2* is associated with membrane dynamics and cell differentiation, and increased levels of *plekhb2* could also be linked to increased requirements for cytoskeletal membrane coupling and vesicle transport (Lemmon et al., 2002). There was also induction of nuclear factors, including *tfpt*, a transcriptional regulator of chromatin remodeling and apoptosis, consistent with the enriched GO terms for transcriptional regulation and apoptotic

signaling (Jin et al., 2005; Franchini et al., 2006). Conversely, the suppression of deaminase (*rida*), which regulates translation and mRNA stability, could imply a reduced protein synthesis capacity in the mutants, which is expected as many biosynthetic processes are dependent on iron availability (Irons et al., 2020). Likewise, downregulation of *rilpl2,* a protein involved in ciliary and endosomal trafficking, could also suggest a reduction in non-essential trafficking pathways and possibly a reprioritization of vesicle transport routes (i.e., transferrin-mediated) (Schaub and Stearns, 2012; Johnson et al., 2024).

When tissue-specific remodeling was assessed, the gills exhibited a distinct pattern of transcriptional responses related to barrier reinforcement, ion regulation, and autophagy. Induction of *cldn3d* and genes related to calcium and potassium transport suggests that the KO gills tightened paracellular permeability to ions and to larger uncharged solutes while concomitantly increasing transcellular ion flux capacity (Milatz et al., 2010; Sakipov et al., 2017; Silic et al., 2022). Furthermore, ORA of downregulated gill DEGs display strong enrichment for enzyme inhibitor and cytoskeletal activities, while gProfiler highlighted pathways related to muscle contraction and multicellular movement. Collectively, these changes suggest a gill-specific strategy that involves structural and ionoregulatory adaptation and remodeling of trafficking and contractile processes, which can help to buffer external homeostatic challenges.

In contrast, the intestine appears to prioritize alternative mechanisms of iron acquisition and metabolic detoxification. Notably, the strong induction of *tfr1b* indicates a shift towards transferrin-mediated cellular iron uptake, aligning with ORA enrichment terms related to receptor-mediated endocytosis and vesicle trafficking (Gammella et al., 2021). Nonetheless, there was also suppression of epithelial anion and amino acid exchange (*slc26a3* and *slc3a1*) and a downregulation of *itln2* lections important for mucosal defense (Dugan et al., 2025). The intestine

also showed alterations in lipid metabolism (*fasn2*, *stab1*, and *pcsk9*) and was associated with enriched terms relating to xenobiotic and metabolic processes (*ahr1a*, *cyp2x9*). During systemic iron imbalance, compensatory shifts to increase iron uptake can elevate intracellular free iron levels, promoting oxidative stress. At the same time, efficient lipid metabolism is necessary to prevent lipid accumulation, which can amplify this vulnerability by exacerbating potential ferroptosis (Yao et al., 2024). Similarly, during iron-deficient conditions, a focus on xenobiotic processes would be an important host defense mechanism under iron deficiency linked immune system is compromised (Eide et al., 2021).

4.6 Conclusion and future directions

This study provides the first systems-level view of how DMT1 loss reshapes iron homeostasis at two principal iron uptake epithelia in teleosts. Gene knockout of *dmt1* highlights its integral role in iron homeostasis and was accompanied by shared and tissue-specific transcriptomic remodeling of iron metabolism, cellular trafficking, erythropoiesis, and host defense. Potential compensatory uptake routes, including *zip4* and *ecac*, along with the reprioritization of transferrin-mediated intracellular transport, were evident. The identification of these candidate pathways provides a foundation for identifying alternative iron uptake routes that may operate in parallel with or independently of DMT1. The distinct physiological niches of the gill and intestine were demonstrated in their divergence of function, whereby the gills exhibited barrier tightening, ion conductance, and autophagy, while the intestine prioritized transferrin-mediated endocytosis, xenobiotic/lipid metabolism, and strategic reprioritization of transport functions.

Collectively, these results reveal the plasticity of metal homeostasis, which involves dual uptake tissues, broad specificity of transporter selectivity, along with the highly coordinated

network of transcriptional remodeling that buffers systemic iron imbalance during DMT1 loss. In an ecophysiological context, these inherent properties are likely adaptive for fishes as they encounter fluctuating dietary iron availability, variable waterborne iron speciation, and co-exposure to other metals among additional environmental stressors. Comparatively, many axes of regulation appear conserved with mammals (transferrin-TfR, ferritin buffering, hepcidin/BMP-Smad signaling), but there are also clear teleost-specific features (branchial *cybrd1* signaling, *ecac* upregulation with plausible multi-metal transport, and differential tissue compensation). The dmt1-/- fish provides a model for cross-taxonomic comparison which can help to dissect both conserved and lineage-specific mechanisms of iron transport, enabling transferrable results that can apply to vertebrate iron-related disorders (e.g., anemia, inflammation, iron-loading, etc.) and toxic metal uptake (e.g., lead and cadmium).

Nonetheless, while transcriptomics provides comprehensive insights into the complex and highly coordinated networks underlying iron homeostasis, functional validation is required to determine whether these transcriptional changes translate to altered protein abundance or transporter activities. Characterization of other organs, including the liver and kidney, central to systemic iron storage and mobilization, along with the integration of transcriptomic data with proteomics, metabolomics, and electrophysiology, would further our understanding of how fishes regulate iron and help identify potential biomarkers for iron imbalance and metal toxicity that can have ecological and biomedical implications. Together, this study advances our understanding of iron homeostasis in a dual-uptake vertebrate model, identifies potential alternative iron uptake routes, and provides comparative insights into vertebrate iron physiology with significance extending to nutritional physiology, environmental toxicology, and human health.

4.7 Reference

Andrews, G. K. (2008). Regulation and function of *Zip4*, the acrodermatitis enteropathica gene. *Biochem Soc Trans* 36, 1242. doi: 10.1042/BST0361242

Andrews, N. C. (2000a). Iron homeostasis: Insights from genetics and animal models. *Nat Rev Genet* 1, 208–217. doi: 10.1038/35042073

Andrews, N. C. (2000b). Iron metabolism: Iron deficiency and iron overload. *Annu Rev Genomics Hum Genet* 1, 75–98. doi: 10.1146/annurev.genom.1.1.75

Antala, S., and Dempski, R. E. (2012). The human ZIP4 transporter has two distinct binding affinities and mediates transport of multiple transition metals. *Biochemistry* 51, 963–973. doi: 10.1021/bi201553

Ashburner, M., Ball, C. A., Blake, J. A., Botstein, D., Butler, H., Cherry, J. M., et al. (2000). Gene ontology: Tool for the unification of biology. *Nat Genet* 25, 25–29. doi: 10.1038/75556;KWRD

Astner, I., Schulze, J. O., Van Den Heuvel, J., Jahn, D., Schubert, W. D., and Heinz, D. W. (2005). Crystal structure of 5-aminolevulinate synthase, the first enzyme of heme biosynthesis, and its link to XLSA in humans. *EMBO J* 24, 3166. doi: 10.1038/SJ.EMBOJ.7600792

Bury, N. R. (2003). Waterborne iron acquisition by a freshwater teleost fish, zebrafish *Danio rerio*. *Journal of Experimental Biology* 206, 3529–3535. doi: 10.1242/jeb.00584

Bury, N. R., Grosell, M., Wood, C. M., Hogstrand, C., Wilson, R. W., Rankin, J. C., et al. (2001). Intestinal iron uptake in the European flounder (*Platichthys flesus*). *Journal of Experimental Biology* 204, 3779–3787. doi: 10.1242/jeb.204.21.3779

Bury, N. R., Walker, P. A., and Glover, C. N. (2003). Nutritive metal uptake in teleost fish. *Journal of Experimental Biology* 206, 11–23. doi: 10.1242/jeb.00068

Cairo, G., Bernuzzi, F., and Recalcati, S. (2006). A precious metal: Iron, an essential nutrient for all cells. *Genes Nutr* 1, 25–39. doi: 10.1007/BF02829934

Carriquiriborde, P. (2003). Physiological modulation of iron metabolism in rainbow trout (*Oncorhynchus mykiss*) fed low and high iron diets. *Journal of Experimental Biology* 207, 75–86. doi: 10.1242/jeb.00712

Chandrapalan, T., and Kwong, R. W. M. (2020). Influence of dietary iron exposure on trace metal homeostasis and expression of metal transporters during development in zebrafish. *Environmental pollution* 261, 114159. doi: 10.1016/j.envpol.2020.114159

Chandrapalan, T., and Kwong, R. W. M. (2021). Functional significance and physiological regulation of essential trace metals in fish. *J Exp Biol* 224, jeb243834. doi: 10.1242/JEB.238790

Chen, H., Su, T., Attieh, Z. K., Fox, T. C., McKie, A. T., Anderson, G. J., et al. (2003). Systemic regulation of Hephaestin and Ireg1 revealed in studies of genetic and nutritional iron deficiency. *Blood* 102, 1893–1899. doi: 10.1182/blood-2003-02-0347

Chen, Y., Chen, L., Lun, A. T. L., Baldoni, P. L., and Smyth, G. K. (2025). edgeR v4: powerful differential analysis of sequencing data with expanded functionality and improved support for small counts and larger datasets. *Nucleic Acids Res* 53. doi: 10.1093/NAR/GKAF018

Consortium, T. G. O., Aleksander, S. A., Balhoff, J., Carbon, S., Cherry, J. M., Drabkin, H. J., et al. (2023). The Gene Ontology knowledgebase in 2023. *Genetics* 224. doi: 10.1093/GENETICS/IYAD031

Cooper, C. A., and Bury, N. R. (2007). The gills as an important uptake route for the essential nutrient iron in freshwater rainbow trout *Oncorhynchus mykiss*. *J Fish Biol* 71, 115–128. doi: 10.1111/j.1095-8649.2007.01474.x

Cooper, C. A., Handy, R. D., and Bury, N. R. (2006). The effects of dietary iron concentration on gastrointestinal and branchial assimilation of both iron and cadmium in zebrafish (*Danio rerio*). *Aquatic Toxicology* 79, 167–175. doi: 10.1016/j.aquatox.2006.06.008

Donovan, A., Brownlie, A., Dorschner, M. O., Zhou, Y., Pratt, S. J., Paw, B. H., et al. (2002). The zebrafish mutant gene chardonnay (*cdy*) encodes divalent metal transporter 1 (DMT1). *Blood* 100, 4655–4659. doi: 10.1182/blood-2002-04-1169

Dugan, A. E., Syangtan, D., Nonnecke, E. B., Chorghade, R. S., Peiffer, A. L., Yao, J. J., et al. (2025). Intelectin-2 is a broad-spectrum antimicrobial lectin. *bioRxiv*, 2025.06.09.658748. doi: 10.1101/2025.06.09.658748

Eide, M., Zhang, X., Karlsen, O. A., Goldstone, J. V., Stegeman, J., Jonassen, I., et al. (2021). The chemical defensome of five model teleost fish. *Sci Rep* 11, 1–13. doi: 10.1038/S41598-021-89948-0;SUBJMETA

Evans, D. H., Piermarini, P. M., and Choe, K. P. (2005). The Multifunctional Fish Gill: Dominant Site of Gas Exchange, Osmoregulation, Acid-Base Regulation, and Excretion of Nitrogenous Waste. doi: 10.1152/physrev.00050.2003.-The

Feeney, G. P., Zheng, D., Kille, P., and Hogstrand, C. (2005). The phylogeny of teleost ZIP and ZnT zinc transporters and their tissue specific expression and response to zinc in zebrafish. *Biochim Biophys Acta* 1732, 88–95. doi: 10.1016/j.bbaexp.2005.12.002

Fleming, M. D., Romano, M. A., Su, M. A., Garrick, L. M., Garrick, M. D., and Andrews, N. C. (1998). Nramp2 is mutated in the anemic Belgrade (*b*) rat: evidence of a role for Nramp2 in endosomal iron transport. *Proc Natl Acad Sci U S A* 95, 1148–53. Available at: http://www.pnas.org.ezproxy.library.yorku.ca/content/95/3/1148.full.pdf (Accessed November 30, 2017).

Fleming, M. D., Trenor, C. C., Su, M. A., Foernzler, D., Beier, D. R., Dietrich, W. F., et al. (1997). Microcytic anaemia mice have a mutation in *Nramp2*, a candidate iron transporter gene. *Nat Genet* 16, 383–386. doi: 10.1038/ng0897-383

Fraenkel, P. G., Traver, D., Donovan, A., Zahrieh, D., and Zon, L. I. (2005). Ferroportin1 is required for normal iron cycling in zebrafish. *Journal of Clinical Investigation* 115, 1532–1541. doi: 10.1172/JCI23780

Franchini, C., Fontana, F., Minuzzo, M., Babbio, F., and Privitera, E. (2006). Apoptosis promoted by up-regulation of TFPT (TCF3 fusion partner) appears p53 independent, cell type restricted and cell density influenced. *Apoptosis* 11, 2217–2224. doi: 10.1007/S10495-006-0195-5

Galaris, D., Barbouti, A., and Pantopoulos, K. (2019). Iron homeostasis and oxidative stress: An intimate relationship ☆. doi: 10.1016/j.bbamcr.2019.118535

Galy, B., Conrad, M., and Muckenthaler, M. (2024). Mechanisms controlling cellular and systemic iron homeostasis. *Nat Rev Mol Cell Biol* 25, 133–155. doi: 10.1038/S41580-023-00648-1;SUBJMETA

Gammella, E., Lomoriello, I. S., Conte, A., Freddi, S., Alberghini, A., Poli, M., et al. (2021). Unconventional endocytosis and trafficking of transferrin receptor induced by iron. Mol Biol Cell 32, 98-108. doi: 10.1091/mbc.e20-02-0129

Garrick, M. D., Dolan, K. G., Horbinski, C., Ghio, A. J., Higgins, D., Porubcin, M., et al. (2003). DMT1: A mammalian transporter for multiple metals., in *BioMetals*, 41–54. doi: 10.1023/A:1020702213099

Geiser, J., Venken, K. J. T., de Lisle, R. C., and Andrews, G. K. (2012). A Mouse Model of Acrodermatitis Enteropathica: Loss of Intestine Zinc Transporter ZIP4 (Slc39a4) Disrupts the Stem Cell Niche and Intestine Integrity. *PLoS Genet* 8, e1002766. doi: 10.1371/JOURNAL.PGEN.1002766

Grosell, M., Farrell, A. P., and Brauner, C. (2010). *Fish Physiology: The multifunctional gut of fish, 1st Edition*. doi: 10.1016/j.preteyeres.2009.12.002

Gu, Z., and Hübschmann, D. (2023). SimplifyEnrichment: A Bioconductor Package for Clustering and Visualizing Functional Enrichment Results. *Genomics Proteomics Bioinformatics* 21, 190–202. doi: 10.1016/J.GPB.2022.04.008

Gunshin, H., Fujiwara, Y., Custodio, A. O., DiRenzo, C., Robine, S., and Andrews, N. C. (2005). Slc11a2 is required for intestinal iron absorption and erythropoiesis but dispensable in placenta and liver. *J Clin Invest* 115, 1258–1266. doi: 10.1172/JCI24356

Gunshin, H., Mackenzie, B., Berger, U. V., Gunshin, Y., Romero, M. F., Boron, W. F., et al. (1997). Cloning and characterization of a mammalian proton-coupled metal-ion transporter. *Nature* 388, 482–488. doi: 10.1038/41343

Guo, Y. L., Wu, P., Jiang, W. D., Liu, Y., Kuang, S. Y., Jiang, J., et al. (2018). The impaired immune function and structural integrity by dietary iron deficiency or excess in gill of fish after infection with *Flavobacterium columnare*: Regulation of NF-κB, TOR, JNK, p38MAPK, Nrf2 and MLCK signalling. *Fish Shellfish Immunol* 74, 593–608. doi: 10.1016/j.fsi.2018.01.027

Han, G. C., Vinayachandran, V., Bataille, A. R., Park, B., Chan-Salis, K. Y., Keller, C. A., et al. (2015). Genome-Wide Organization of GATA1 and TAL1 Determined at High Resolution. *Mol Cell Biol* 36, 157. doi: 10.1128/MCB.00806-15

Hermes, L. B., Peixoto, N. C., Battisti, E. K., Schneider, T. L. S., and Lazzari, R. (2024). Dietary iron affect innate immunity, hematological and oxidative responses in Nile tilapia (*Oreochromis niloticus*). *Aquaculture International* 32, 3993–4007. doi: 10.1007/S10499-023-01361-8

Hoenderop, J. G. J., Nilius, B., and Bindels, R. J. M. (2002). ECaC: the gatekeeper of transepithelial $Ca2^{+}$ transport. *Biochimica et Biophysica Acta (BBA) - Proteins and Proteomics* 1600, 6–11. doi: 10.1016/S1570-9639(02)00438-7

Hoenderop, J. G. J., Nilius, B., Renø, ·, and Bindels, J. M. (2003). Epithelial calcium channels: from identification to function and regulation Tissue distribution of TRPV5 and TRPV6. *Pflugers Arch-Eur J Physiol* 446, 304–308. doi: 10.1007/s00424-003-1045-8

Huber, W., Carey, V. J., Gentleman, R., Anders, S., Carlson, M., Carvalho, B. S., et al. (2015). Orchestrating high-throughput genomic analysis with Bioconductor. *Nat Methods* 12, 115–121. doi: 10.1038/NMETH.3252;SUBJMETA

Hwang, W. Y., Fu, Y., Reyon, D., Maeder, M. L., Tsai, S. Q., Sander, J. D., et al. (2013). Efficient genome editing in zebrafish using a CRISPR-Cas system. *Nat Biotechnol* 31, 227–229. doi: 10.1038/nbt.2501

Irons, J. L., Hodge-Hanson, K., and Downs, D. M. (2020). RidA Proteins Protect against Metabolic Damage by Reactive Intermediates. *Microbiology and Molecular Biology Reviews* 84. doi: 10.1128/MMBR.00024-20

Jin, J., Cai, Y., Yao, T., Gottschalk, A. J., Florens, L., Swanson, S. K., et al. (2005). A mammalian chromatin remodeling complex with similarities to the yeast INO80 complex. *Journal of Biological Chemistry* 280, 41207–41212. doi: 10.1074/jbc.M509128200

Johnson, D., Colijn, S., Richee, J., Yano, J., Burns, M., Davis, A. E., et al. (2024). Angiogenesis is limited by LIC1-mediated lysosomal trafficking. *Angiogenesis* 27, 943–962. doi: 10.1007/S10456-024-09951-7

Kassouf, M. T., Hughes, J. R., Taylor, S., McGowan, S. J., Soneji, S., Green, A. L., et al. (2010). Genome-wide identification of TAL1's functional targets: Insights into its mechanisms of action in primary erythroid cells. *Genome Res* 20, 1064–1083. doi: 10.1101/GR.104935.110

Kesharwani, P., Dash, D., and Koiri, R. K. (2025). Deciphering the role of hepcidin in iron metabolism and anemia management. *Journal of Trace Elements in Medicine and Biology* 87, 127591. doi: 10.1016/J.JTEMB.2025.127591

Kolberg, L., Raudvere, U., Kuzmin, I., Adler, P., Vilo, J., and Peterson, H. (2023). g:Profiler—interoperable web service for functional enrichment analysis and gene identifier mapping (2023 update). *Nucleic Acids Res* 51, W207–W212. doi: 10.1093/NAR/GKAD347

Kulkeaw, K., and Sugiyama, D. (2012). Zebrafish erythropoiesis and the utility of fish as models of anemia. *Stem Cell Res Ther* 3, 1–11. doi: 10.1186/scrt146

Kwong, R. W. M. (2024). Trace metals in the teleost fish gill: biological roles, uptake regulation, and detoxification mechanisms. *J Comp Physiol B* 194, 1–15. doi: 10.1007/S00360-024-01565-1

Kwong, R. W. M., Andrés, J. A., and Niyogi, S. (2010). Molecular evidence and physiological characterization of iron absorption in isolated enterocytes of rainbow trout (*Oncorhynchus mykiss*): Implications for dietary cadmium and lead absorption. *Aquatic Toxicology* 99, 343–350. doi: 10.1016/j.aquatox.2010.05.012

Kwong, R. W. M., Hamilton, C. D., and Niyogi, S. (2013). Effects of elevated dietary iron on the gastrointestinal expression of *Nramp* genes and iron homeostasis in rainbow trout (Oncorhynchus mykiss). *Fish Physiol Biochem* 39, 363–372. doi: 10.1007/s10695-012-9705-2

Lall, S. P., and Kaushik, S. J. (2021). Nutrition and metabolism of minerals in fish. *Animals* 11. doi: 10.3390/ANI11092711

Lane, D. J. R., Bae, D. H., Merlot, A. M., Sahni, S., and Richardson, D. R. (2015). Duodenal cytochrome b (DCYTB) in Iron metabolism: An update on function and regulation. *Nutrients* 7, 2274–2296. doi: 10.3390/NU7042274

Lemmon, M. A., Ferguson, K. M., and Abrams, C. S. (2002). Pleckstrin homology domains and the cytoskeleton. *FEBS Lett* 513, 71–76. doi: 10.1016/S0014-5793(01)03243-4

Leonard, E. M., Porteus, C. S., Brink, D., and Milsom, W. K. (2024). Fish gill chemosensing: knowledge gaps and inconsistencies. *J Comp Physiol B* 194, 1–33. doi: 10.1007/S00360-024-01553-5/METRICS

Lieschke, G. J., Oates, A. C., Crowhurst, M. O., Ward, A. C., and Layton, J. E. (2001). Morphologic and functional characterization of granulocytes and macrophages in embryonic and adult zebrafish. *Blood* 98, 3087–3096. doi: 10.1182/blood.v98.10.3087

Lv, P., and Liu, F. (2023). Heme-deficient primitive red blood cells induce HSPC ferroptosis by altering iron homeostasis during zebrafish embryogenesis. *Development (Cambridge)* 150. doi: 10.1242/dev.201690/

Mackenzie, B., and Garrick, M. D. (2005). Iron Imports. II. Iron uptake at the apical membrane in the intestine. *Am J Physiol Gastrointest Liver Physiol* 289, 981–986. doi: 10.1152/ajpgi.00363.2005

McKie, A. T. (2008). The role of Dcytb in iron metabolism: an update. *Biochem Soc Trans* 36, 1239–1241. doi: 10.1042/BST0361239

McKie, A. T., Barrow, D., Latunde-Dada, G. O., Rolfs, A., Sager, G., Mudaly, E., et al. (2001). An iron-regulated ferric reductase associated with the absorption of dietary iron. *Science (1979)* 291, 1755–1759. doi: 10.1126/science.1057206

Meneghini, R. (1997). Iron homeostasis, oxidative stress, and DNA damage. *Free Radic Biol Med* 23, 783–792. doi: 10.1016/S0891-5849(97)00016-6

Michel, V., Yuan, Z., Ramsubir, S., and Bakovic, M. (2006). Choline Transport for Phospholipid Synthesis. *Exp Biol Med* 231, 490–504. doi: 10.1177/153537020623100503

Milatz, S., Krug, S. M., Rosenthal, R., Günzel, D., Müller, D., Schulzke, J. D., et al. (2010). Claudin-3 acts as a sealing component of the tight junction for ions of either charge and uncharged solutes. *Biochimica et Biophysica Acta (BBA) - Biomembranes* 1798, 2048–2057. doi: 10.1016/j.bbamem.2010.07.014

Nauseef, W. M. (2008). Biological Roles for the NOX Family NADPH Oxidases. *Journal of Biological Chemistry* 283, 16961–16965. doi: 10.1074/jbc.r700045200

Nemeth, E., and Ganz, T. (2021). Hepcidin-Ferroportin Interaction Controls Systemic Iron Homeostasis. *International Journal of Molecular Sciences 2021, Vol. 22, Page 6493* 22, 6493. doi: 10.3390/IJMS22126493

Neves, J. V, Wilson, J. M., Kuhl, H., Reinhardt, R., Castro, L. F. C., and Rodrigues, P. N. (2011). Natural history of SLC11 genes in vertebrates: Tales from the fish world. *BMC Evol Biol* 11. doi: 10.1186/1471-2148-11-106

Okazaki, Y. (2023). Iron from the gut: the role of divalent metal transporter 1. *J Clin Biochem Nutr* 74, 1. doi: 10.3164/jcbn.23-47

Pan, T. C., Liao, B. K., Huang, C. J., Lin, L. Y., and Hwang, P. P. (2005). Epithelial Ca2+ channel expression and $Ca2^{+}$ uptake in developing zebrafish. *Am J Physiol Regul Integr Comp Physiol* 289, 1202–1211. doi: 10.1152/ajpregu.00816.2004

Pinilla-Tenas, J. J., Sparkman, B. K., Shawki, A., Illing, A. C., Mitchell, C. J., Zhao, N., et al. (2011). Zip14 is a complex broad-scope metal-ion transporter whose functional properties

support roles in the cellular uptake of zinc and nontransferrin-bound iron. *American Journal of Physiology-Cell Physiology* 301, C862–C871. doi: 10.1152/ajpcell.00479.2010

Puar, P., Naderi, M., Niyogi, S., and Kwong, R. W. M. (2021). Using zebrafish as a model to assess individual and combined effects of waterborne and dietary zinc exposure during development. *Environmental Pollution*, 117377. doi: 10.1016/j.envpol.2021.117377

Qiu, A., and Hogstrand, C. (2004). Functional characterisation and genomic analysis of an epithelial calcium channel (ECaC) from pufferfish, *Fugu rubripes*. *Gene* 342, 113–123. doi: 10.1016/j.gene.2004.07.041

Rejitha, V., and Peter, M. C. S. (2013). Adrenaline and triiodothyronine modify the iron handling in the freshwater air-breathing fish *Anabas testudineus* Bloch: Role of ferric reductase in iron acquisition. *Gen Comp Endocrinol* 181, 130–138. doi: 10.1016/j.ygcen.2012.11.008

Roper, C., and Tanguay, R. L. (2018). Zebrafish as a model for developmental biology and toxicology. *Handbook of Developmental Neurotoxicology*, 143–151. doi: 10.1016/B978-0-12-809405-1.00012-2

Sakipov, S., Sobolevsky, A. I., and Kurnikova, M. (2017). Ion Permeation Mechanism in TRPV6 Ca 2^+ Channel. *Biophys J* 112, 466a. doi: 10.1016/j.bpj.2016.11.2498

Schaub, J. R., and Stearns, T. (2012). The Rilp-like proteins Rilpl1 and Rilpl2 regulate ciliary membrane content. *https://doi.org/10.1091/mbc.e12-08-0598* 24, 453–464. doi: 10.1091/MBC.E12-08-0598

Sevcikova, M., Modra, H., Slaninova, A., and Svobodova, Z. (2011). Metals as a cause of oxidative stress in fish: a review. *Vet Med (Praha)* 56, 537–546.

Shahsavarani, A. (2006). Characterization of a branchial epithelial calcium channel (ECaC) in freshwater rainbow trout (*Oncorhynchus mykiss*). *Journal of Experimental Biology* 209, 1928–1943. doi: 10.1242/jeb.02190

Shawki, A., Knight, P. B., Maliken, B. D., Niespodzany, E. J., and MacKenzie, B. (2012). H+-coupled divalent metal-ion transporter-1: Functional properties, physiological roles and therapeutics. *Curr Top Membr* 70, 169. doi: 10.1016/B978-0-12-394316-3.00005-3

Silic, M. R., Murata, S. H., Park, S. J., and Zhang, G. J. (2022). Evolution of inwardly rectifying potassium channels and their gene expression in zebrafish embryos. *Developmental Dynamics* 251, 687–713. doi: 10.1002/DVDY.425

Srivastava, R., Eswar, K., Ramesh, S. S. R., Prajapati, A., Sonpipare, T., Basa, A., et al. (2025). Zebrafish as a Versatile Model Organism: From Tanks to Treatment. *MedComm – Future Medicine* 4, e70028. doi: 10.1002/MEF2.70028

Stumm, W., and Morgan, J. J. (1996). Aquatic chemistry: chemical equilibria and rates in natural waters. *Choice Reviews Online* 33, 33-6312-33–6312. doi: 10.5860/choice.33-6312

Sun, C., Wu, J., Liu, S., Li, H., and Zhang, S. (2013). Zebrafish CD59 has both bacterial-binding and inhibiting activities. *Dev Comp Immunol* 41, 178–188. doi: 10.1016/j.dci.2013.05.008

Tarifeño-Saldivia, E., Aguilar, A., Contreras, D., Mercado, L., Morales-Lange, B., Márquez, K., et al. (2018). Iron overload is associated with oxidative stress and nutritional immunity during viral infection in fish. *Front Immunol* 9, 376176. doi: 10.3389/fimmu.2018.01296/bibtex

Taylor, A., Grapentine, S., Ichhpuniani, J., and Bakovic, M. (2021). Choline transporter-like proteins 1 and 2 are newly identified plasma membrane and mitochondrial ethanolamine transporters. *Journal of Biological Chemistry* 296. doi: 10.1016/j.jbc.2021.100604

Tian, Y., Sun, Y., Ou, M., Cui, X., Zhou, D., and Che, W. (2021). Cloning and expression analysis of GATA1 gene in *Carassius auratus* red var. *BMC Genom Data* 22, 1–13. doi: 10.1186/S12863-021-00966-3/

Tiwari, A., Upadhyay, A. D., Priyadarshi, H., Roy, A. K., Ghosh, R., Yambem, S., et al. (2019). Structural and functional analysis of ferritin heavy chain subunit in *Oryzias latipes*. *Journal of Advanced Research in Biotechnology* 4, 1–12. doi: 10.15226/2475-4714/4/1/00143

Vulpe, C. D., Kuo, Y. M., Murphy, T. L., Cowley, L., Askwith, C., Libina, N., et al. (1999). Hephaestin, a ceruloplasmin homologue implicated in intestinal iron transport, is defective in the sla mouse. *Nat Genet* 21, 195–199. doi: 10.1038/5979

Wang, C. Y., Jenkitkasemwong, S., Duarte, S., Sparkman, B. K., Shawki, A., Mackenzie, B., et al. (2012). ZIP8 is an iron and zinc transporter whose cell-surface expression is up-regulated by cellular iron loading. *Journal of Biological Chemistry* 287, 34032–34043. doi: 10.1074/jbc.M112.367284

Wang, J., and Wang, W.-X. (2016). Novel insights into iron regulation and requirement in marine medaka *Oryzias melastigma*. *Sci Rep* 6, 26615. doi: 10.1038/srep26615

Wang, Z., Gerstein, M., and Snyder, M. (2009). RNA-Seq: a revolutionary tool for transcriptomics. *Nat Rev Genet* 10, 57. doi: 10.1038/nrg2484

Wingert, R. A., Brownlie, A., Galloway, J. L., Dooley, K., Fraenkel, P., Axe, J. L., et al. (2004). The chianti zebrafish mutant provides a model for erythroid-specific disruption of transferrin receptor 1. *Development* 131, 6225–6235. doi: 10.1242/dev.01540

Wood, C. M., Farrell, A. P., and Brauner, C. J. (2011). *Homeostasis and toxicology of essential metals*. Academic Press. doi: 10.1016/S1546-5098(11)31010-2

Wu, X. M., and Chang, M. X. (2025). NOX1-ROS axis regulates the MAPK signaling pathway and activates caspase-1 to resist Edwardsiella piscicida infection. *Aquaculture* 609, 742784. doi: 10.1016/j.aquaculture.2025.742784

Xiao, X., Alfaro-Magallanes, V. M., and Babitt, J. L. (2020). Bone morphogenic proteins in iron homeostasis. *Bone* 138, 115495. doi: 10.1016/J.BONE.2020.115495

Xu, S., Hu, E., Cai, Y., Xie, Z., Luo, X., Zhan, L., et al. (2024). Using clusterProfiler to characterize multiomics data. *Nature Protocols 2024 19:11* 19, 3292–3320. doi: 10.1038/s41596-024-01020-z

Yanatori, I., and Kishi, F. (2019). DMT1 and iron transport. *Free Radic Biol Med* 133, 55–63. doi: 10.1016/j.freeradbiomed.2018.07.020

Yanatori, I., Tabuchi, M., Kawai, Y., Yasui, Y., Akagi, R., and Kishi, F. (2010). Heme and non-heme iron transporters in non-polarized and polarized cells. *BMC Cell Biol* 11, 1–11. doi: 10.1186/1471-2121-11-39/

Yao, H., Jiang, W., Liao, X., Wang, D., and Zhu, H. (2024). Regulatory mechanisms of amino acids in ferroptosis. *Life Sci* 351, 122803. doi: 10.1016/j.lfs.2024.122803

Zhao, L., Xia, Z., and Wang, F. (2014). Zebrafish in the sea of mineral (iron, zinc, and copper) metabolism. *Front Pharmacol* 5, 1–23. doi: 10.3389/fphar.2014.00033

4.8 Supplementary Tables and Figures

Table 4-S 1. Top 1.5% of differentially expressed genes (DEGs) identified in the gill and intestine of WT and DMT1 KO zebrafish used for heatmap visualization in Figure 4-4. Subset of the most significant DEGs (top 1.5%, FDR ≤ 0.05) identified from edgeR quasi-likelihood F-tests, ranked by FDR within each DEG category. For each gene, the table reports $\log_2$ fold-change (logFC), average expression (logCPM), F-statistic, raw and adjusted P-values, and normalized expression values (logCPM) across all wildtype (WT) and DMT1 knockout (KO) samples (n=3, pooled from 4-5 organs). Genes are grouped into four non-overlapping categories based on significance patterns across tissues: (A) Interaction – genes with a significant genotype × tissue interaction; (B) Gill-only – significant in gill only; (C) Intestine-only – significant in intestine only; and (D) Both tissues – significant in both gill and intestine without interaction. These DEGs correspond to the heatmap and word-cloud enrichment analysis shown in Figure 4-4.

Category	Gene ID	gene symbol	gene name	logFC KO	logCPM KO	F	PValue	FDR	logCPM WT Intestine	logCPM KO Intestine	logCPM WT Gill	logCPM KO Gill
Interaction	mpx	mpx	myeloid-specific peroxidase	-7.29	9.45	114.00	9.94E-08	0.000647	11.31	3.53	5.69	5.43
Interaction	rnf183	rnf183	ring finger protein 183	-3.84	5.98	73.89	1.15E-06	0.002341	6.87	2.45	6.22	5.74
Interaction	nr1d4a	nr1d4a	nuclear receptor subfamily 1, group D, member 4a	-5.66	5.75	75.10	1.06E-06	0.002341	7.54	0.76	3.75	3.04
Interaction	nox1	nox1	NADPH oxidase 1	-5.52	5.18	83.60	5.81E-07	0.001774	6.36	4.54	1.49	4.88
Interaction	slc4a5b	slc4a5b	solute carrier family 4 member 5b	-8.11	6.72	111.59	1.18E-07	0.000647	8.66	0.68	-0.45	-0.52
Interaction	cd59a	cd59a	CD59 molecule (CD59 blood group) a	-3.09	2.13	99.86	2.14E-07	0.000982	2.93	0.85	1.46	2.40
Gill only	cldn3d	cldn3d	claudin 3d	3.15	7.51	51.99	7.73E-06	0.000962	8.08	8.82	-0.64	2.18

Category	Gene ID	gene symbol	gene name	logFC KO	logCPM KO	F	PValue	FDR	logCPM WT Intestine	logCPM KO Intestine	logCPM WT Gill	logCPM KO Gill
Gill only	setd3	setd3	SET domain containing 3, actin histidine methyltransferase	-1.02	5.60	44.90	1.61E-05	0.001586	6.05	5.57	5.74	4.73
Gill only	vps16_1	vps16	VPS16 core subunit of CORVET and HOPS complexes	-1.05	4.61	53.99	6.23E-06	0.000869	5.21	4.84	4.44	3.39
Gill only	atg4da	atg4da	autophagy related 4D, cysteine peptidase a	1.50	4.94	54.40	5.99E-06	0.000844	3.84	4.17	4.54	6.03
Gill only	sardh	sardh	sarcosine dehydrogenase	1.70	4.90	62.75	2.81E-06	0.000499	5.47	5.92	1.71	3.36
Gill only	apol	apol	apolipoprotein L	2.36	3.59	61.14	3.22E-06	0.000561	3.26	4.10	1.77	4.10
Gill only	herc4	herc4	HECT and RLD domain	-1.48	4.32	52.31	7.35E-06	0.000939	4.00	3.68	5.20	3.74

Category	Gene ID	gene symbol	gene name	logFC KO	logCPM KO	F	PValue	FDR	logCPM WT Intestine	logCPM KO Intestine	logCPM WT Gill	logCPM KO Gill
			containing E3 ubiquitin protein ligase 4									
Gill only	gtf3c3	gtf3c3	general transcription factor IIIC, polypeptide 3	-1.07	3.49	41.79	2.31E-05	0.001918	3.54	3.41	3.93	2.87
Gill only	smcr8b	smcr8b	Smith-Magenis syndrome chromosome region, candidate 8b	-1.11	2.83	43.68	1.85E-05	0.001683	2.66	2.22	3.56	2.45
Gill only	stk38l	stk38l	serine/threonine kinase 38 like	-1.56	2.79	52.05	7.55E-06	0.000952	2.74	2.04	3.60	2.09
Gill only	tnfrsf18	tnfrsf18	tumor necrosis factor receptor	2.44	4.41	65.61	2.21E-06	0.000419	1.29	2.25	3.52	6.00

Category	Gene ID	gene symbol	gene name	logFC KO	logCPM KO	F	PValue	FDR	logCPM WT Intestine	logCPM KO Intestine	logCPM WT Gill	logCPM KO Gill
			superfamily, member 18									
Gill only	camk2n1a	camk2n1a	calcium/calmodulin-dependent protein kinase II inhibitor 1a	2.09	2.52	66.02	2.14E-06	0.000417	1.07	1.72	1.74	3.79
Gill only	trpv6	trpv6	transient receptor potential cation channel, subfamily V, member 6	2.32	6.03	66.04	1.13E-07	5.65E-05	-2.96	-2.65	5.44	7.75
Gill only	tgm5l	tgm5l	transglutaminase 5, like	2.12	3.00	57.19	2.14E-06	0.000417	-2.28	-1.44	2.53	4.59
Gill only	igfbp5a_1	igfbp5a	insulin-like growth factor binding protein 5a	2.22	2.31	67.78	1.14E-06	0.000271	-1.55	-2.10	1.76	3.93

Category	Gene ID	gene symbol	gene name	logFC KO	logCPM KO	F	PValue	FDR	logCPM WT Intestine	logCPM KO Intestine	logCPM WT Gill	logCPM KO Gill
Gill only	kcnj1a.2	kcnj1a.2	potassium inwardly rectifying channel subfamily J member 1a, tandem duplicate 2	1.65	3.95	48.38	1.30E-06	0.000297	-2.96	-2.85	3.88	5.53
Gill only	stx11b.1	stx11b.1	syntaxin 11b, tandem duplicate 1	1.90	3.56	73.36	7.48E-06	0.000952	-3.22	-3.34	3.30	5.17
Gill only	cacna2d3	cacna2d3	calcium channel, voltage dependent, alpha2/delta subunit 3	3.91	-0.04	52.92	5.47E-06	0.00079	-1.03	0.09	-2.28	0.97
Gill only	rell2	rell2	RELT like 2	3.74	1.87	91.35	5.97E-08	3.64E-05	-2.63	-1.54	0.04	3.57
Gill only	mir144	mir144	microRNA 144	3.16	0.85	85.83	4.97E-08	3.17E-05	-2.95	-2.17	-0.50	2.53

Category	Gene ID	gene symbol	gene name	logFC KO	logCPM KO	F	PValue	FDR	logCPM WT Intestine	logCPM KO Intestine	logCPM WT Gill	logCPM KO Gill
Gill only	rnasel4	rnasel4	ribonuclease like 4	5.70	0.77	184.72	1.33E-09	1.93E-06	-3.34	-2.50	-2.27	2.59
Gill only	trim108	trim108	tripartite motif containing 108	-5.29	2.54	212.88	2.52E-10	5.33E-07	-1.85	-3.02	4.43	-0.65
Gill only	prg4a	prg4a	proteoglycan 4a	-6.33	0.59	142.45	1.14E-09	1.79E-06	-2.28	-3.10	2.36	-2.69
Intestine only	tfr1b_1	tfr1b	transferrin receptor 1b	1.81	6.93	55.99	5.14E-06	0.000754	6.37	8.14	5.49	6.04
Intestine only	stab1	stab1	stabilin 1	-1.72	5.36	54.58	5.88E-06	0.000829	5.08	3.40	6.05	5.70
Intestine only	arrdc1b	arrdc1b	arrestin domain containing 1b	-1.59	4.76	51.11	8.29E-06	0.001044	5.03	3.47	5.24	4.64
Intestine only	meis1b	meis1b	Meis homeobox 1 b	-1.16	4.30	46.84	1.30E-05	0.001433	4.18	3.04	4.92	4.42
Intestine only	gpr4	gpr4	G protein-coupled receptor 4	-1.92	4.34	53.72	6.41E-06	0.000872	3.19	1.29	5.33	4.82

Category	Gene ID	gene symbol	gene name	logFC KO	logCPM KO	F	PValue	FDR	logCPM WT Intestine	logCPM KO Intestine	logCPM WT Gill	logCPM KO Gill
Intestine only	tek	tek	TEK tyrosine kinase, endothelial	-2.03	3.56	55.92	5.19E-06	0.000754	3.39	1.43	4.33	3.69
Intestine only	aspm	aspm	assembly factor for spindle microtubules	-2.13	3.02	48.40	1.10E-05	0.001292	3.68	1.60	3.19	2.77
Intestine only	cldc1	cldc1	C-type lectin domain containing 1	-2.31	4.90	49.28	1.00E-05	0.001197	6.52	4.07	2.18	1.71
Intestine only	gchfr	gchfr	GTP cyclohydrolase I feedback regulator	1.98	4.35	55.90	5.19E-06	0.000754	3.82	5.79	2.03	2.69
Intestine only	brf1a	brf1a	BRF1 RNA polymerase III transcription initiation factor subunit a	1.56	3.68	51.52	7.96E-06	0.001016	3.45	4.97	1.95	2.26

Category	Gene ID	gene symbol	gene name	logFC KO	logCPM KO	F	PValue	FDR	logCPM WT Intestine	logCPM KO Intestine	logCPM WT Gill	logCPM KO Gill
Intestine only	acad8_1	acad8	acyl-CoA dehydrogenase family, member 8	2.32	3.03	55.48	5.40E-06	0.000777	1.92	4.10	1.99	2.73
Intestine only	pttg1ipa	pttg1ipa	PTTG1 interacting protein a	2.01	6.24	45.94	1.45E-05	0.001521	-0.03	1.92	6.86	7.45
Intestine only	fasn2_1	fasn2	fatty acid synthase 2	-3.33	7.11	85.36	1.41E-07	6.59E-05	8.85	5.59	-3.00	-3.24
Intestine only	slc3a1_1	slc3a1	solute carrier family 3 member 1	-2.63	5.79	75.09	4.79E-08	3.06E-05	7.44	4.90	-3.02	-2.76
Intestine only	fasn2	fasn2	fatty acid synthase 2	-3.09	5.83	93.06	8.09E-08	4.19E-05	7.58	4.54	-3.00	-3.24
Intestine only	sult3st2	sult3st2	sulfotransferase family 3, cytosolic sulfotransferase 2	1.53	5.41	62.52	2.22E-06	0.00041	5.44	6.98	-2.67	-3.34
Intestine only	cyp2x9_1	cyp2x9	cytochrome P450, family 2, subfamily	2.21	5.38	78.68	1.98E-07	8.49E-05	4.88	7.07	-2.97	-3.24

Category	Gene ID	gene symbol	gene name	logFC KO	logCPM KO	F	PValue	FDR	logCPM WT Intestine	logCPM KO Intestine	logCPM WT Gill	logCPM KO Gill
			X, polypeptide 9									
Intestine only	cyp2x9	cyp2x9	cytochrome P450, family 2, subfamily X, polypeptide 9	2.21	5.37	78.53	2.00E-07	8.49E-05	4.88	7.07	-2.97	-3.24
Intestine only	itln2_1	itln2	intelectin 2	-4.63	5.84	193.42	1.06E-09	2.08E-06	7.76	3.06	-2.86	-3.30
Intestine only	itln2	itln2	intelectin 2	-5.33	5.10	561.50	1.39E-12	3.81E-08	7.07	1.75	-3.03	-3.30
Intestine only	slc26a3.1	slc26a3.1	solute carrier family 26 member 3	-4.32	3.99	82.66	7.24E-08	3.90E-05	5.83	1.53	-2.51	-2.86
Intestine only	pcsk9	pcsk9	proprotein convertase subtilisin/kexin type 9	3.64	2.36	75.69	5.72E-07	0.000169	0.65	4.15	-2.03	-2.33
Intestine only	ahr1a	ahr1a	aryl hydrocarbon receptor 1a	6.22	2.52	103.21	8.55E-08	4.35E-05	-1.49	4.26	-3.16	-2.08

Category	Gene ID	gene symbol	gene name	logFC KO	logCPM KO	F	PValue	FDR	logCPM WT Intestine	logCPM KO Intestine	logCPM WT Gill	logCPM KO Gill
Intestine only	sh2d3cb_1	sh2d3cb	SH2 domain containing 3Cb	-2.74	2.47	80.45	7.36E-07	0.000206	4.11	1.44	0.20	-0.39
Intestine only	myo7ab	myo7ab	myosin VIIAb	-4.12	1.05	54.69	5.99E-06	0.000839	2.61	-1.20	-0.29	-1.46
Intestine only	cuzd1.1	cuzd1.1	CUB and zona pellucida-like domains 1, tandem duplicate 1	-10.17	1.39	211.22	3.64E-09	4.54E-06	3.33	-3.30	-3.14	-3.14

Category	Geneid	gene symbol	gene name	logFC Gill	FDR Gill	logFC Intestine	FDR Intestine	logCPM WT Intestine	logCPM KO Intestine	logCPM WT Gill	logCPM KO Gill
Both tissues	znf384b	znf384b	zinc finger protein 384 b	-2.93	4.51E-05	-2.39	0.000224	3.79	1.36	3.96	1.08
Both tissues	rilpl2	rilpl2	Rab interacting lysosomal protein-like 2	-2.48	7.70E-05	-2.19	0.000213	3.67	1.51	3.45	1.03
Both tissues	cops7a	cops7a	COP9 constitutive photomorphogenic homolog subunit 7A	-4.76	1.00E-07	-4.90	1.15E-07	4.50	-0.31	4.20	-0.39
Both tissues	rida_1	rida	reactive intermediate imine deaminase A homolog	-3.77	2.21E-05	-4.00	5.85E-07	5.00	1.04	1.15	-2.02
Both tissues	znf384b_1	znf384b	zinc finger protein 384 b	2.67	2.99E-06	2.67	4.02E-06	1.40	4.02	1.21	3.83
Both tissues	slc44a2	slc44a2	solute carrier family 44 member 2 (CTL2 blood group)	2.72	2.99E-06	2.53	1.59E-05	0.67	3.13	1.83	4.52
Both tissues	cops7a_1	cops7a	COP9 constitutive photomorphogenic	5.34	1.65E-07	4.93	5.88E-07	-0.51	4.31	-0.67	4.47

Category	Geneid	gene symbol	gene name	logFC Gill	FDR Gill	logFC Intestine	FDR Intestine	logCPM WT Intestine	logCPM KO Intestine	logCPM WT Gill	logCPM KO Gill
			homolog subunit 7A								
Both tissues	plekhb2_1	plekhb2	pleckstrin homology domain containing, family B (evectins) member 2	3.51	8.12E-06	2.89	1.78E-05	1.00	3.84	-0.64	2.68
Both tissues	trim108_1	trim108	tripartite motif containing 108	5.77	2.06E-06	6.88	0.000247	-3.22	0.90	-1.08	4.39
Both tissues	tfpt	tfpt	TCF3 (E2A) fusion partner	4.49	5.44E-06	3.95	2.76E-05	-2.19	1.14	-2.50	1.04

Table 4-S 2. Iron-related differentially expressed genes (DEGs) identified in the gill and intestine of WT and DMT1 KO zebrafish. Subset of significant DEGs (FDR ≤ 0.05) identified from edgeR quasi-likelihood F-tests. For each gene, the table reports $\log_2$ fold-change (logFC), average expression (logCPM), F-statistic, raw and adjusted P-values, and normalized expression values (logCPM) across all wildtype (WT) and DMT1 knockout (KO) samples (n=3, pooled from 4-5 organs). Genes are grouped into non-overlapping categories based on significance patterns across tissues: Gill-only – significant in gill only; Intestine-only – significant in intestine only; and Interaction – genes with a significant genotype × tissue interaction.

Category	Geneid	Gene symbol	Gene name	logFC KO	logCPM KO	F	PValue	FDR	logCPM WT Intestine	logCPM KO Intestine	logCPM WT Gill	logCPM KO Gill
Intestine	slc11a2	slc11a2	solute carrier family 11 member 2	-2.52513	4.932633	227.4511	1.64E-09	2.82E-06	6.126396	3.590538	4.677755	3.852631
Intestine	slc39a4	slc39a4	solute carrier family 39 member 4	1.918613	4.017231	21.54847	0.000479	0.012315	3.629173	5.586306	-1.32577	-1.81892
Intestine	fth1a	fth1a	ferritin, heavy polypeptide 1a	1.001694	10.14392	22.28828	0.00042	0.011455	9.604802	10.58566	9.410027	10.53509
Intestine	tfr1a	tfr1a	transferrin receptor 1a	1.927194	5.973572	13.815	0.002676	0.03441	-0.13679	1.24464	5.594488	7.623539

Category	Geneid	Gene symbol	Gene name	logFC KO	logCPM KO	F	PValue	FDR	logCPM WT Intestine	logCPM KO Intestine	logCPM WT Gill	logCPM KO Gill
Intestine	tfr1b	tfr1b	transferrin receptor 1b	1.535323	6.036056	34.11358	6.21E-05	0.003784	5.594887	7.178466	4.867273	5.164921
Intestine	hbba1	hbba1	hemoglobin, beta adult 1	1.535726	10.61994	21.78206	0.000462	0.012061	5.323018	6.701605	10.7807	12.08662
Intestine	hamp	hamp	hepcidin antimicrobial peptide	-1.99456	3.112666	11.23401	0.004081	0.043926	4.696832	2.152513	-1.31284	-3.04164
Intestine	smad1	smad1	SMAD family member 1	-0.99947	3.063028	25.75729	0.000226	0.008182	1.922896	0.958442	3.853244	3.682696
Intestine	bmpr2a	bmpr2a	bone morphogenetic protein receptor, type II a (serine/threonine kinase)	-0.71702	5.371398	18.75558	0.00085	0.017567	3.441757	2.732663	6.109011	6.282466
Intestine	bmpr2b	bmpr2b	bone morphogenetic protein receptor, type II b	-1.19402	4.728968	13.40165	0.00296	0.036466	3.899399	2.593269	5.78102	4.806823

Category	Geneid	Gene symbol	Gene name	logFC KO	logCPM KO	F	PValue	FDR	logCPM WT Intestine	logCPM KO Intestine	logCPM WT Gill	logCPM KO Gill
			(serine/threonine kinase)									
Intestine	alas2	alas2	aminolevulinate, delta-, synthase 2	2.71829	6.971823	42.66484	2.09E-05	0.0019	0.642091	3.067	6.062059	8.710765
Gills	slc11a2	slc11a2	solute carrier family 11 member 2	-0.8303	4.932633	27.20008	0.000177	0.006692	6.126396	3.590538	4.677755	3.852631
Gills	cybrd1	cybrd1	cytochrome b reductase 1	1.028968	3.70792	15.34983	0.001826	0.026326	1.684068	2.367161	3.816495	4.853265
Gills	trpv6	trpv6	transient receptor potential cation channel, subfamily V, member 6	2.323037	6.028584	66.04236	1.13E-07	5.65E-05	-2.95981	-2.65459	5.437547	7.74726
Gills	fth1a	fth1a	ferritin, heavy polypeptide 1a	1.137551	10.14392	28.5929	0.000141	0.005867	9.604802	10.58566	9.410027	10.53509
Gills	tfr1a	tfr1a	transferrin receptor 1a	2.037162	5.973572	28.56654	0.000143	0.005908	-0.13679	1.24464	5.594488	7.623539

Category	Geneid	Gene symbol	Gene name	logFC KO	logCPM KO	F	PValue	FDR	logCPM WT Intestine	logCPM KO Intestine	logCPM WT Gill	logCPM KO Gill
Gills	hbba1	hbba1	hemoglobin, beta adult 1	1.310521	10.61994	16.39328	0.001429	0.022594	5.323018	6.701605	10.7807	12.08662
Gills	hephl1b	hephl1b	hephaestin-like 1b	1.887905	-0.29775	10.68412	0.005053	0.048823	-2.53929	-2.26759	-0.75985	0.945124
Gills	bmpr1ab	bmpr1ab	bone morphogenetic protein receptor, type IAb	-0.8154	4.470408	15.58006	0.001728	0.02549	3.360001	3.404285	5.417138	4.586264
Gills	alas2	alas2	aminolevulinate, delta-, synthase 2	2.659402	6.971823	56.0905	5.12E-06	0.000764	0.642091	3.067	6.062059	8.710765
Gills	gata1a	gata1a	GATA binding protein 1a	1.843909	2.004749	48.29738	1.17E-05	0.001278	-0.66111	-0.19421	1.635834	3.431628
Gills	tal1	tal1	T-cell acute lymphocytic leukemia 1	1.268417	3.471371	32.46113	8.05E-05	0.004134	-0.45402	0.320885	3.614869	4.867376
Interaction	slc11a2	slc11a2	solute carrier family 11 member 2	-1.694830172	4.932632556	56.06972339	5.10612E-06	0.004836727	6.126396208	3.590537792	4.677754868	3.852630729

Table 4-S 3. Differentially expressed solute carrier (SLC) families identified in DMT1 knockout zebrafish. Summary of solute carrier (*slc*) gene families represented among differentially expressed genes (DEGs; FDR < 0.05) in the gill and intestine. Families are listed by their standard Slc nomenclature, with corresponding family names and primary substrate categories based on known transport functions.

Slc family	Family name	Substrate
Slc1	Glutamate/neutral Amino acids transporters	Amino acids
Slc2	Hexose and sugar alcohol transporters	Sugars
Slc3	Heteromeric Amino acids transporters	Amino acids
Slc4	Bicarbonate transporters	Inorganic ions
Slc5	Sodium-dependent glucose transporters	Sugars
Slc6	Neurotransmitter transporters	Amino acids
Slc7	Cationic Amino acids transporters	Amino acids
Slc8	Sodium/calcium exchangers	Inorganic ions
Slc9	Sodium/hydrogen exchangers	Inorganic ions
Slc10	Sodium/bile acid cotransporters	Organic ions
Slc12	Sodium/potassium/chloride transporters	Inorganic ions
Slc13	Sodium-dependent sulphate/carboxylate transporters	Organic ions
Slc14	Urea transporters	Metabolic solutes
Slc16	Monocarboxylate transporters	Metabolic solutes

Slc family	Family name	Substrate
Slc19	Vitamin transporters	Vitamins
Slc20	Sodium-dependent phosphate transporters	Inorganic ions
Slc22	Organic anion/cation transporters	Organic ions
Slc23	Sodium-dependent ascorbic acid transporters	Vitamins
Slc25	Mitochondrial transporters	Mitochondrial
Slc26	Anion exchangers	Inorganic ions
Slc34	Type II Na^+-phosphate cotransporters	Inorganic ions
Slc35	Nucleotide sugar transporters	Sugars
Slc37	Phosphosugar/phosphate exchangers	Sugars
Slc38	Sodium-dependent neutral Amino acids transporters	Amino acids
Slc43	Na^+-independent, system-L-like amino acid transporters	Amino acids
Slc44	Choline-like transporters	Vitamins
Slc45	H^+/sugar cotransporters	Sugars
Slc47	Xenobiotic detox	Organic ions
Slc52	Riboflavin transporters	Vitamins
Slc66	Lysosomal Amino acids transporters	Amino acids
Slco2	Organic anion transporters	Organic ions

Table 4-S 4. Over-representation analysis (ORA) of enriched GO Biological Process terms identified by g:Profiler. Functional enrichment of differentially expressed genes (DEGs; FDR < 0.05) was performed using g:Profiler (Ensembl release 113) against the *Danio rerio* reference gene set with g:SCS multiple testing correction (Padj < 0.05). The table lists significantly enriched Gene Ontology Biological Process (GO:BP), KEGG pathway, and Human Phenotype Ontology (HP) terms for each contrast—gill, intestine, and interaction—along with their adjusted P-values (Padj). Bar shading represents enrichment strength, with darker colors (from yellow to green) indicating higher significance. Only terms with Padj < 0.05 in at least one contrast are shown.

GO:BP		Gill	Intestine	Interaction
Term Name	Term ID	p_adj	p_adj	p_adj
skeletal muscle contraction	GO:0003009	2.283×10^{-7}	1.000	1.000
muscle system process	GO:0003012	1.034×10^{-6}	1.000	1.000
musculoskeletal movement	GO:0050881	4.109×10^{-6}	1.000	1.000
multicellular organismal movement	GO:0050879	4.109×10^{-6}	1.000	1.000
striated muscle contraction	GO:0006941	1.051×10^{-5}	1.000	1.000
muscle contraction	GO:0006936	7.417×10^{-5}	1.000	1.000
response to oxidative stress	GO:0006979	1.000	2.038×10^{-4}	1.000
response to stimulus	GO:0050896	3.475×10^{-4}	6.986×10^{-3}	1.000
modified amino acid metabolic process	GO:0006575	3.599×10^{-4}	1.000	1.000
response to stress	GO:0006950	3.514×10^{-2}	6.325×10^{-4}	1.000
catabolic process	GO:0009056	1.000	7.160×10^{-4}	1.000
modified amino acid catabolic process	GO:0042219	7.647×10^{-4}	1.000	1.000
homeostatic process	GO:0042592	1.727×10^{-3}	3.330×10^{-3}	1.000
muscle structure development	GO:0061061	2.371×10^{-3}	1.000	1.000
regulation of programmed cell death	GO:0043067	3.791×10^{-3}	1.000	1.000
regulation of apoptotic process	GO:0042981	4.082×10^{-3}	7.065×10^{-1}	1.000
cardiac muscle contraction	GO:0060048	6.336×10^{-3}	1.000	1.000
cellular response to transforming growth factor beta stimulus	GO:0071560	1.000	6.487×10^{-3}	1.000
response to transforming growth factor beta	GO:0071559	1.000	6.487×10^{-3}	1.000
transforming growth factor beta receptor signaling pathway	GO:0007179	1.000	6.487×10^{-3}	1.000
anatomical structure development	GO:0048856	8.772×10^{-3}	1.000	1.000
response to decreased oxygen levels	GO:0036293	1.095×10^{-2}	1.000	1.000
response to hypoxia	GO:0001666	1.095×10^{-2}	1.000	1.000
developmental process	GO:0032502	1.425×10^{-2}	1.000	1.000
negative regulation of response to stimulus	GO:0048585	1.466×10^{-2}	1.000	1.000
chemical homeostasis	GO:0048878	1.538×10^{-2}	1.000	1.000
negative regulation of intracellular signal transduction	GO:1902532	7.278×10^{-2}	1.815×10^{-2}	1.000
muscle organ development	GO:0007517	1.940×10^{-2}	1.000	1.000
intracellular signal transduction	GO:0035556	2.027×10^{-2}	5.958×10^{-2}	1.000
animal organ development	GO:0048513	2.066×10^{-2}	1.000	1.000
apoptotic signaling pathway	GO:0097190	1.000	2.105×10^{-2}	1.000
Rho protein signal transduction	GO:0007266	2.870×10^{-1}	2.278×10^{-2}	1.000
neuromuscular process	GO:0050905	2.534×10^{-2}	1.000	1.000
negative regulation of cell communication	GO:0010648	2.618×10^{-2}	1.000	1.000
negative regulation of signaling	GO:0023057	2.618×10^{-2}	1.000	1.000
negative regulation of TORC1 signaling	GO:1904262	1.000	2.684×10^{-2}	1.000
response to oxygen levels	GO:0070482	2.746×10^{-2}	1.000	1.000
programmed cell death	GO:0012501	5.162×10^{-2}	2.765×10^{-2}	1.000
cell death	GO:0008219	5.162×10^{-2}	2.765×10^{-2}	1.000
lipid metabolic process	GO:0006629	1.000	2.889×10^{-2}	1.000
multicellular organismal-level homeostasis	GO:0048871	1.000	3.092×10^{-2}	1.000
regulation of plasma membrane bounded cell projection as...	GO:0120032	1.000	3.508×10^{-2}	1.000
negative regulation of signal transduction	GO:0009968	3.960×10^{-2}	4.414×10^{-1}	1.000
intracellular iron ion homeostasis	GO:0006879	4.340×10^{-2}	1.000	1.000
regulation of cell projection assembly	GO:0060491	1.000	4.454×10^{-2}	1.000
apoptotic process	GO:0006915	8.170×10^{-2}	4.504×10^{-2}	1.000
anatomical structure morphogenesis	GO:0009653	4.577×10^{-2}	3.102×10^{-1}	1.000
antigen processing and presentation of peptide antigen via ...	GO:0002474	1.000	4.890×10^{-2}	1.000
hemopoiesis	GO:0030097	4.967×10^{-2}	1.000	1.000

KEGG		Gill	Intestine	Interaction
Term Name	Term ID	p_adj	p_adj	p_adj
Ascorbate and aldarate metabolism	KEGG:00053	1.000	4.213×10^{-7}	1.000
Drug metabolism - other enzymes	KEGG:00983	1.000	4.343×10^{-4}	1.000
Drug metabolism - cytochrome P450	KEGG:00982	1.000	6.830×10^{-4}	2.234×10^{-1}
Pentose and glucuronate interconversions	KEGG:00040	1.000	8.825×10^{-4}	1.000
Steroid hormone biosynthesis	KEGG:00140	1.000	1.260×10^{-3}	1.000
Porphyrin metabolism	KEGG:00860	1.000	2.588×10^{-3}	1.000
Ferroptosis	KEGG:04216	3.750×10^{-3}	1.000	2.621×10^{-1}
ECM-receptor interaction	KEGG:04512	3.774×10^{-3}	1.000	3.670×10^{-1}
p53 signaling pathway	KEGG:04115	1.000	8.404×10^{-3}	1.000
Necroptosis	KEGG:04217	8.698×10^{-3}	1.000	6.471×10^{-1}
Metabolism of xenobiotics by cytochrome P450	KEGG:00980	1.000	9.098×10^{-3}	1.000
Biosynthesis of cofactors	KEGG:01240	1.000	1.086×10^{-2}	1.000
Retinol metabolism	KEGG:00830	1.000	3.995×10^{-2}	1.000

HP		Gill	Intestine	Interaction
Term Name	Term ID	p_adj	p_adj	p_adj
Abnormal erythrocyte physiology	HP:0020054	2.514×10^{-4}	1.000	1.000
Reticulocytosis	HP:0001923	1.207×10^{-3}	1.000	1.000
Hypertension	HP:0000822	1.000	3.947×10^{-3}	1.000
Increased red cell osmotic fragility	HP:0005502	9.527×10^{-3}	1.000	1.000
Hemolytic anemia	HP:0001878	1.405×10^{-2}	1.000	1.000
Anemia due to reduced life span of red cells	HP:0011895	1.582×10^{-2}	1.000	1.000
Poikilocytosis	HP:0004447	1.715×10^{-2}	1.000	1.000
Abnormal vascular physiology	HP:0030163	1.000	2.051×10^{-2}	1.000
Increased blood pressure	HP:0032263	1.000	2.388×10^{-2}	1.000
Abnormal gallbladder morphology	HP:0012437	2.613×10^{-2}	1.000	1.000
Cholelithiasis	HP:0001081	3.205×10^{-2}	1.000	1.000
Paralysis	HP:0003470	3.628×10^{-2}	1.000	1.000
Hypochromia	HP:0032231	4.863×10^{-2}	1.000	1.000

Table 4-S 5. Over-representation analysis (ORA) of up- and down-regulated differentially expressed genes (DEGs) identified using clusterProfiler. Gene Ontology (GO) Molecular Function terms significantly enriched (Padj < 0.05) among up- and down-regulated DEGs in the gill, intestine, and genotype × tissue interaction contrasts (Benjamini-Hochberg method for multiple testing correction).

Tissue	Direction	ID	Description	Gene Ratio	Fold Enrichment	p.adjust	Count
Gill	Down	GO:0140678	molecular function inhibitor activity	29/654	3.155	2.63E-05	29
Gill	Down	GO:0004857	enzyme inhibitor activity	25/654	3.104	1.51E-04	25
Gill	Down	GO:0030414	peptidase inhibitor activity	18/654	3.730	2.51E-04	18
Gill	Down	GO:0004866	endopeptidase inhibitor activity	17/654	3.863	2.51E-04	17
Gill	Down	GO:0061135	endopeptidase regulator activity	17/654	3.657	3.93E-04	17
Gill	Down	GO:0140662	ATP-dependent protein folding chaperone	9/654	6.855	3.93E-04	9
Gill	Down	GO:0044183	protein folding chaperone	10/654	5.419	9.49E-04	10

Tissue	Direction	ID	Description	Gene Ratio	Fold Enrichment	p.adjust	Count
Gill	Down	GO:0061134	peptidase regulator activity	18/654	3.019	0.002	18
Gill	Down	GO:0120015	sterol transfer activity	6/654	8.052	0.004	6
Gill	Down	GO:0120020	cholesterol transfer activity	6/654	8.052	0.004	6
Gill	Down	GO:0008199	ferric iron binding	5/654	10.064	0.004	5
Gill	Down	GO:0030215	semaphorin receptor binding	7/654	5.802	0.007	7
Gill	Down	GO:0052689	carboxylic ester hydrolase activity	15/654	2.659	0.023	15
Gill	Down	GO:0120013	lipid transfer activity	7/654	4.697	0.025	7
Gill	Down	GO:0004252	serine-type endopeptidase activity	16/654	2.477	0.029	16
Gill	Down	GO:0000774	adenyl-nucleotide exchange factor activity	4/654	8.671	0.030	4
Gill	Up	GO:0003779	actin binding	44/1052	1.947	0.013	44
Gill	Up	GO:0070003	threonine-type peptidase activity	7/1052	6.132	0.021	7
Gill	Up	GO:0033549	MAP kinase phosphatase activity	7/1052	5.574	0.021	7

Tissue	Direction	ID	Description	Gene Ratio	Fold Enrichment	p.adjust	Count
Gill	Up	GO:0017017	MAP kinase tyrosine/serine/threonine phosphatase activity	6/1052	6.570	0.021	6
Gill	Up	GO:0008330	protein tyrosine/threonine phosphatase activity	5/1052	7.963	0.021	5
Gill	Up	GO:0033550	MAP kinase tyrosine phosphatase activity	5/1052	7.963	0.021	5
Gill	Up	GO:0004029	aldehyde dehydrogenase (NAD^+) activity	6/1052	6.183	0.021	6
Gill	Up	GO:0004030	aldehyde dehydrogenase [$NAD(P)^+$] activity	6/1052	6.183	0.021	6
Gill	Up	GO:0008138	protein tyrosine/serine/threonine phosphatase activity	7/1052	4.542	0.045	7
Gill	Up	GO:0008242	omega peptidase activity	6/1052	5.256	0.045	6
Interaction	Interaction	GO:0030695	GTPase regulator activity	18/252	3.012	0.006	18

Tissue	Direction	ID	Description	Gene Ratio	Fold Enrichment	p.adjust	Count
Interaction	Interaction	GO:0060589	nucleoside-triphosphatase regulator activity	18/252	3.012	0.006	18
Interaction	Interaction	GO:0140662	ATP-dependent protein folding chaperone	5/252	9.883	0.017	5
Interaction	Interaction	GO:0005085	guanyl-nucleotide exchange factor activity	11/252	3.673	0.020	11
Interaction	Interaction	GO:0005496	steroid binding	6/252	6.180	0.031	6
Interaction	Interaction	GO:0044183	protein folding chaperone	5/252	7.032	0.043	5
Intestine	Down	GO:0019199	transmembrane receptor protein kinase activity	15/737	3.990	0.003	15
Intestine	Down	GO:0046332	SMAD binding	9/737	5.627	0.007	9
Intestine	Down	GO:0052689	carboxylic ester hydrolase activity	18/737	2.831	0.014	18
Intestine	Down	GO:0070411	I-SMAD binding	5/737	9.618	0.015	5
Intestine	Down	GO:0017134	fibroblast growth factor binding	5/737	8.931	0.016	5

Tissue	Direction	ID	Description	Gene Ratio	Fold Enrichment	p.adjust	Count
Intestine	Down	GO:0004714	transmembrane receptor protein tyrosine kinase activity	11/737	3.717	0.016	11
Intestine	Down	GO:0015103	inorganic anion transmembrane transporter activity	17/737	2.624	0.021	17
Intestine	Down	GO:0051020	GTPase binding	15/737	2.799	0.021	15
Intestine	Down	GO:0008509	monoatomic anion transmembrane transporter activity	16/737	2.685	0.021	16
Intestine	Down	GO:0030695	GTPase regulator activity	33/737	1.888	0.021	33
Intestine	Down	GO:0060589	nucleoside-triphosphatase regulator activity	33/737	1.888	0.021	33
Intestine	Down	GO:0004713	protein tyrosine kinase activity	15/737	2.718	0.021	15
Intestine	Down	GO:0019838	growth factor binding	10/737	3.572	0.021	10
Intestine	Down	GO:0031267	small GTPase binding	14/737	2.714	0.028	14

Tissue	Direction	ID	Description	Gene Ratio	Fold Enrichment	p.adjust	Count
Intestine	Down	GO:0035091	phosphatidylinositol binding	16/737	2.440	0.037	16
Intestine	Down	GO:0015108	chloride transmembrane transporter activity	13/737	2.687	0.042	13
Intestine	Down	GO:0005543	phospholipid binding	24/737	1.981	0.042	24
Intestine	Up	GO:0015020	glucuronosyltransferase activity	20/948	9.042	2.93E-12	20
Intestine	Up	GO:0097153	cysteine-type endopeptidase activity involved in apoptotic process	6/948	9.720	0.003	6
Intestine	Up	GO:0008194	UDP-glycosyltransferase activity	24/948	2.607	0.003	24
Intestine	Up	GO:0016757	glycosyltransferase activity	38/948	2.069	0.003	38
Intestine	Up	GO:0030170	pyridoxal phosphate binding	11/948	4.193	0.005	11
Intestine	Up	GO:0070279	vitamin B6 binding	11/948	4.193	0.005	11

Tissue	Direction	ID	Description	Gene Ratio	Fold Enrichment	p.adjust	Count
Intestine	Up	GO:0016758	hexosyltransferase activity	28/948	2.213	0.007	28
Intestine	Up	GO:0020037	heme binding	21/948	2.474	0.009	21
Intestine	Up	GO:0004029	aldehyde dehydrogenase (NAD^+) activity	6/948	6.862	0.009	6
Intestine	Up	GO:0004030	aldehyde dehydrogenase [$NAD(P)^+$] activity	6/948	6.862	0.009	6
Intestine	Up	GO:0046906	tetrapyrrole binding	21/948	2.374	0.013	21
Intestine	Up	GO:0004197	cysteine-type endopeptidase activity	14/948	2.895	0.017	14
Intestine	Up	GO:0070003	threonine-type peptidase activity	6/948	5.832	0.020	6
Intestine	Up	GO:0050660	flavin adenine dinucleotide binding	13/948	2.939	0.021	13
Intestine	Up	GO:0017116	single-stranded DNA helicase activity	5/948	6.943	0.022	5
Intestine	Up	GO:0005506	iron ion binding	21/948	2.183	0.028	21
Intestine	Up	GO:0008131	primary methylamine oxidase activity	4/948	7.776	0.043	4

Tissue	Direction	ID	Description	Gene Ratio	Fold Enrichment	p.adjust	Count
Intestine	Up	GO:0008519	ammonium channel activity	4/948	7.776	0.043	4

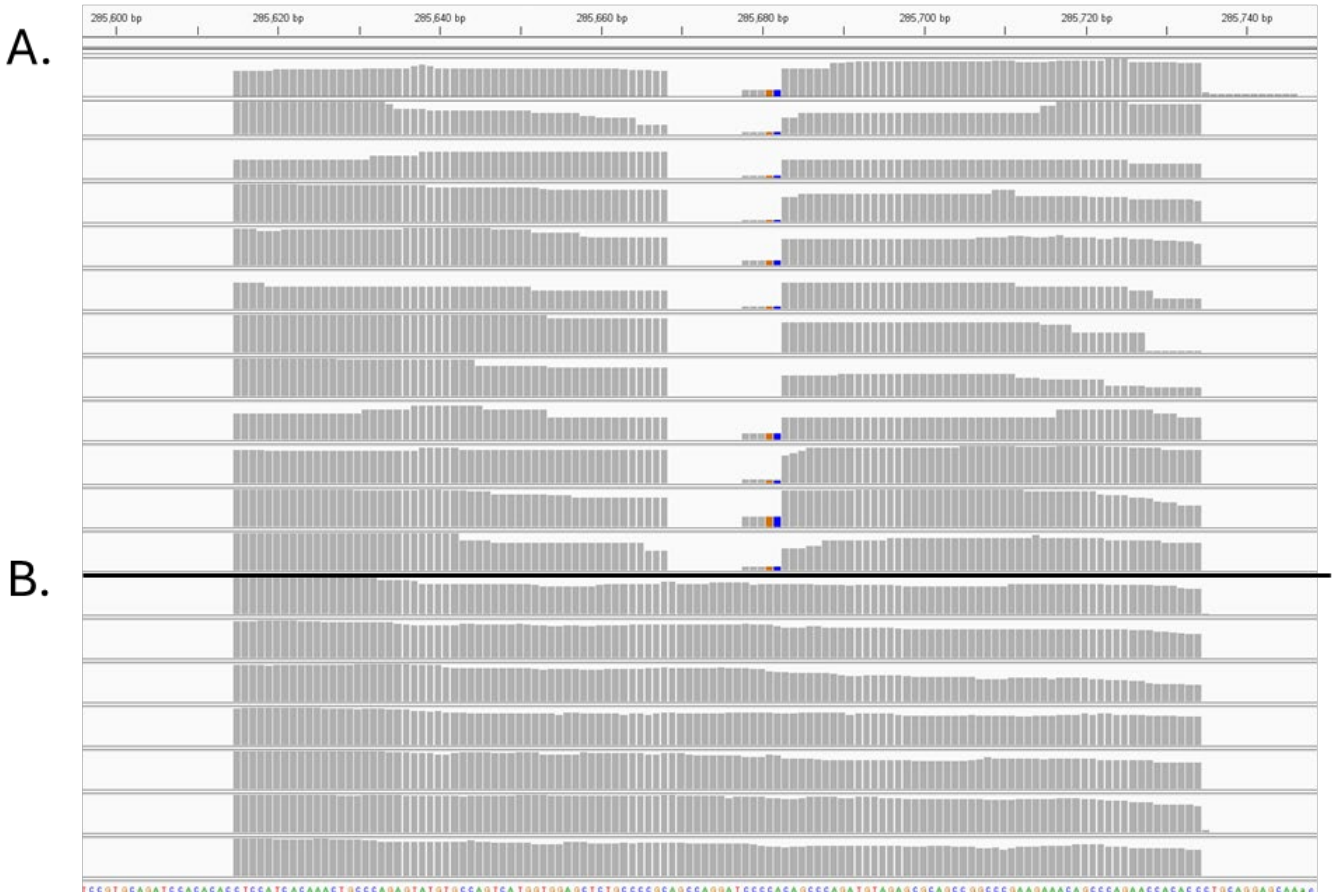

Figure 4-S 1. Read alignment of *dmt1* exon 5 in DMT1 knockout and wildtype (WT) zebrafish. Sequencing reads are aligned to the reference genome using STAR (spliced transcripts alignment to a reference) and visualized in IGV (integrative genomics viewer) to show **(A)** the presence of a 14 base pair deletion in *dmt1* (NC_007122.7) exon 5 in mutants and **(B)** an intact sequence in the WT. The deletion is located within the iron-binding motif (285,669 - 285,682 bp) and results in a frameshift mutation.

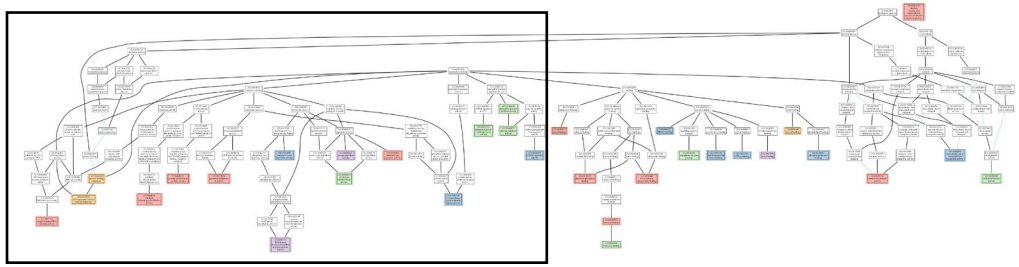

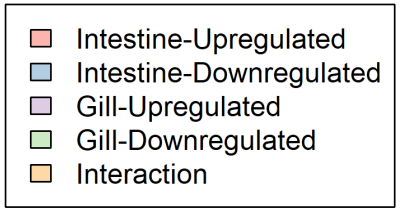
Intestine-Upregulated
Intestine-Downregulated
Gill-Upregulated
Gill-Downregulated
Interaction

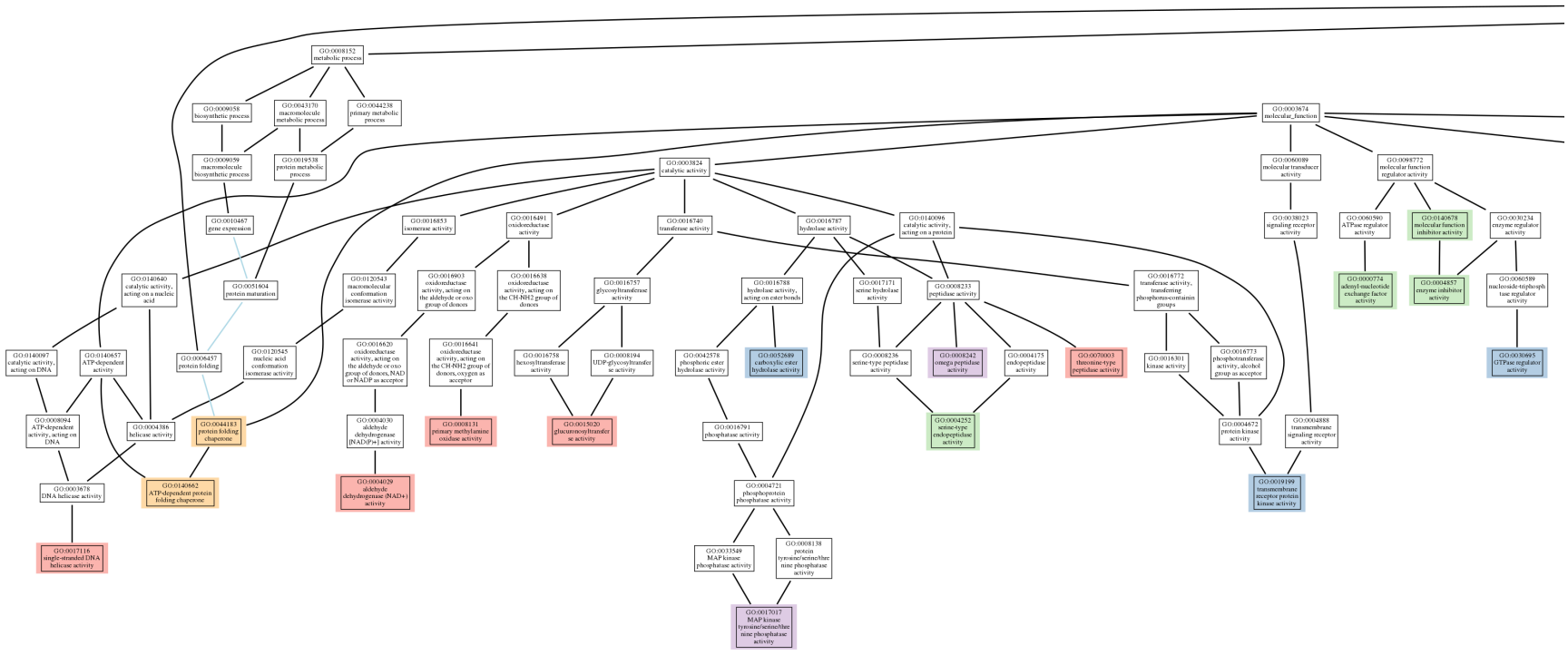
GO:0008152 metabolic process
GO:0009058 biosynthetic process
GO:0043170 macromolecule metabolic process
GO:0044238 primary metabolic process
GO:0009059 macromolecule biosynthetic process
GO:0019538 protein metabolic process
GO:0010467 gene expression
GO:0140640 catalytic activity, acting on a nucleic acid
GO:0051604 protein maturation
GO:0140097 catalytic activity, acting on DNA
GO:0140657 ATP-dependent activity
GO:0006457 protein folding
GO:0120545 nucleic acid conformation isomerase activity
GO:0008094 ATP-dependent activity, acting on DNA
GO:0004386 helicase activity
GO:0044183 protein folding chaperone
GO:0003678 DNA helicase activity
GO:0140662 ATP-dependent protein folding chaperone
GO:0017116 single-stranded DNA helicase activity
GO:0003824 catalytic activity
GO:0016853 isomerase activity
GO:0016491 oxidoreductase activity
GO:0016740 transferase activity
GO:0016787 hydrolase activity
GO:0140096 catalytic activity, acting on a protein
GO:0120543 macromolecular conformation isomerase activity
GO:0016903 oxidoreductase activity, acting on the aldehyde or oxo group of donors
GO:0016638 oxidoreductase activity, acting on the CH-NH2 group of donors
GO:0016757 glycosyltransferase activity
GO:0016788 hydrolase activity, acting on ester bonds
GO:0017171 serine hydrolase activity
GO:0008233 peptidase activity
GO:0016772 transferase activity, transferring phosphorus-containing groups
GO:0016620 oxidoreductase activity, acting on the aldehyde or oxo group of donors, NAD or NADP as acceptor
GO:0016641 oxidoreductase activity, acting on the CH-NH2 group of donors, oxygen as acceptor
GO:0016758 hexosyltransferase activity
GO:0008194 UDP-glycosyltransferase activity
GO:0042578 phosphoric ester hydrolase activity
GO:0052689 carboxylic ester hydrolase activity
GO:0008236 serine-type peptidase activity
GO:0008242 omega peptidase activity
GO:0004175 endopeptidase activity
GO:0070003 threonine-type peptidase activity
GO:0016301 kinase activity
GO:0016773 phosphotransferase activity, alcohol group as acceptor
GO:0004030 aldehyde dehydrogenase [NAD(P)+] activity
GO:0008131 primary methylamine oxidase activity
GO:0015020 glucuronosyltransferase activity
GO:0004252 serine-type endopeptidase activity
GO:0004672 protein kinase activity
GO:0004888 transmembrane signaling receptor activity
GO:0004029 aldehyde dehydrogenase (NAD+) activity
GO:0016791 phosphatase activity
GO:0004721 phosphoprotein phosphatase activity
GO:0019199 transmembrane receptor protein kinase activity
GO:0033549 MAP kinase phosphatase activity
GO:0008138 protein tyrosine/serine/threonine phosphatase activity
GO:0017017 MAP kinase tyrosine/serine/threonine phosphatase activity
GO:0003674 molecular_function
GO:0060089 molecular transducer activity
GO:0098772 molecular function regulator activity
GO:0038023 signaling receptor activity
GO:0060590 ATPase regulator activity
GO:0140678 molecular function inhibitor activity
GO:0030234 enzyme regulator activity
GO:0000774 adenyl-nucleotide exchange factor activity
GO:0004857 enzyme inhibitor activity
GO:0060589 nucleoside-triphosphatase regulator activity
GO:0030695 GTPase regulator activity

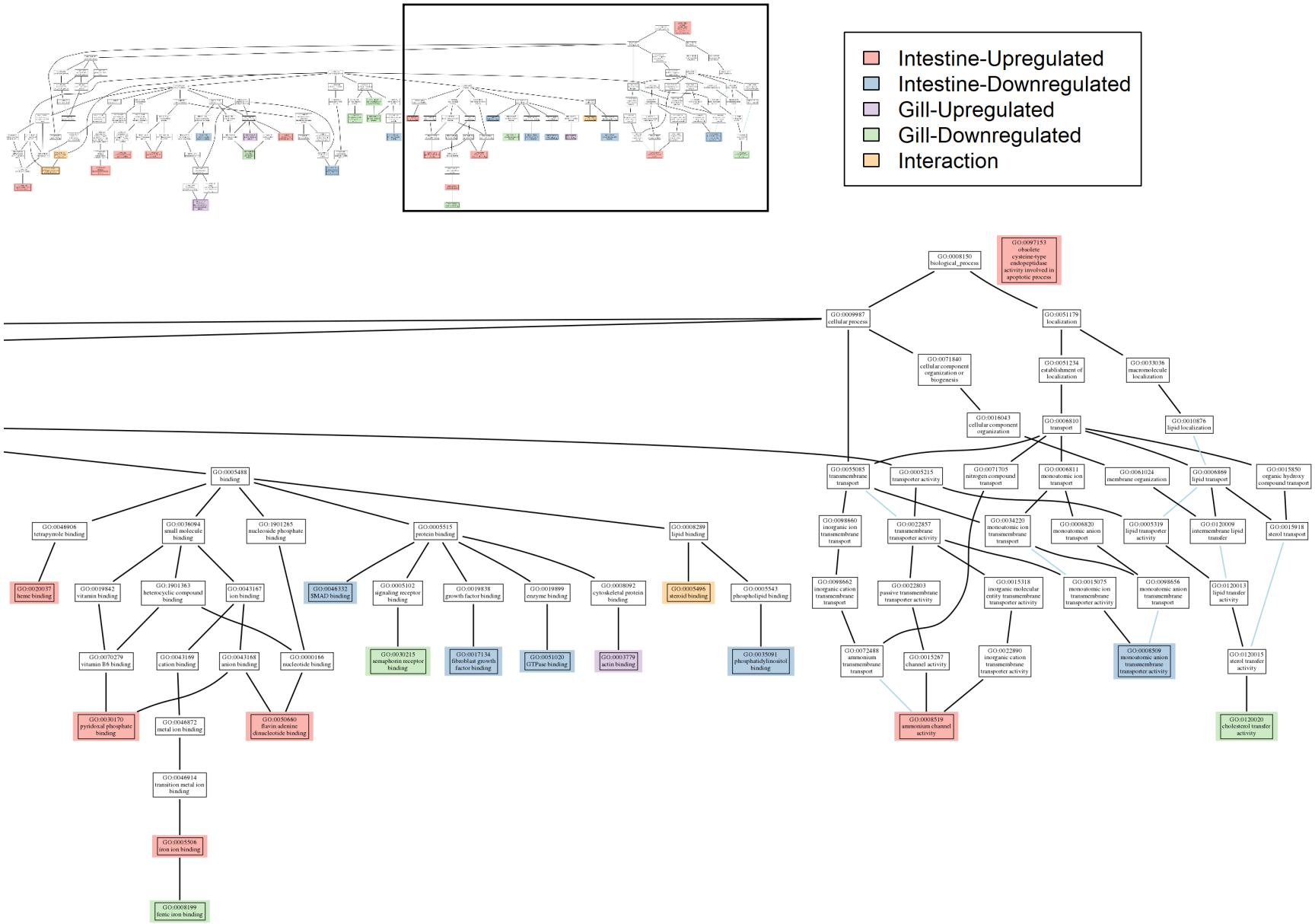
Intestine-Upregulated
Intestine-Downregulated
Gill-Upregulated
Gill-Downregulated
Interaction
GO:0008150 biological_process
GO:0097153 obsolete cysteine-type endopeptidase activity involved in apoptotic process
GO:0009987 cellular process
GO:0051179 localization
GO:0071840 cellular component organization or biogenesis
GO:0051234 establishment of localization
GO:0033036 macromolecule localization
GO:0016043 cellular component organization
GO:0006810 transport
GO:0010876 lipid localization
GO:0005488 binding
GO:0055085 transmembrane transport
GO:0005215 transporter activity
GO:0071705 nitrogen compound transport
GO:0006811 monoatomic ion transport
GO:0061024 membrane organization
GO:0006869 lipid transport
GO:0015850 organic hydroxy compound transport
GO:0046906 tetrapyrrole binding
GO:0036094 small molecule binding
GO:1901265 nucleoside phosphate binding
GO:0005515 protein binding
GO:0008289 lipid binding
GO:0098660 inorganic ion transmembrane transport
GO:0022857 transmembrane transporter activity
GO:0034220 monoatomic ion transmembrane transport
GO:0006820 monoatomic anion transport
GO:0005319 lipid transporter activity
GO:0120009 intermembrane lipid transfer
GO:0015918 sterol transport
GO:0020037 heme binding
GO:0019842 vitamin binding
GO:1901363 heterocyclic compound binding
GO:0043167 ion binding
GO:0046332 SMAD binding
GO:0005102 signaling receptor binding
GO:0019838 growth factor binding
GO:0019899 enzyme binding
GO:0008092 cytoskeletal protein binding
GO:0005496 steroid binding
GO:0005543 phospholipid binding
GO:0098662 inorganic cation transmembrane transport
GO:0022803 passive transmembrane transporter activity
GO:0015318 inorganic molecular entity transmembrane transporter activity
GO:0015075 monoatomic ion transmembrane transporter activity
GO:0098656 monoatomic anion transmembrane transport
GO:0120013 lipid transfer activity
GO:0070279 vitamin B6 binding
GO:0043169 cation binding
GO:0043168 anion binding
GO:0000166 nucleotide binding
GO:0030215 semaphorin receptor binding
GO:0017134 fibroblast growth factor binding
GO:0051020 GTPase binding
GO:0003779 actin binding
GO:0035091 phosphatidylinositol binding
GO:0072488 ammonium transmembrane transport
GO:0015267 channel activity
GO:0022890 inorganic cation transmembrane transporter activity
GO:0008509 monoatomic anion transmembrane transporter activity
GO:0120015 sterol transfer activity
GO:0030170 pyridoxal phosphate binding
GO:0046872 metal ion binding
GO:0050660 flavin adenine dinucleotide binding
GO:0008519 ammonium channel activity
GO:0120020 cholesterol transfer activity
GO:0046914 transition metal ion binding
GO:0005506 iron ion binding
GO:0008199 ferric iron binding

Figure 4-S 2. Hierarchical relationships among GO Biological Process terms from the over-representation analysis of DEGs (clusterProfiler). Enriched terms are coloured by DEG expression pattern (red: upregulated in intestine; blue: downregulated in intestine; purple: upregulated in gill; green: downregulated in gill; yellow: interaction). Uncolored GO terms were automatically added to trace ancestry to the root term. Light blue lines indicate the "part_of" ontology relation; black lines indicate the "regulates" ontology relation. Portions of the figure are magnified for clarity.

Chapter 5

General Discussion and Integration

5.1 **Overview**

Iron is an essential trace element required for numerous biological and physiological processes, but it can also create a unique regulatory challenge because both deficiency and excess iron can be detrimental to health (Chandrapalan & Kwong, 2021). In fish and other vertebrates, iron homeostasis is a highly coordinated process that balances environmental and dietary iron availability to meet systemic demands (Wood et al., 2011). However, many aspects of iron homeostasis including iron absorption, regulation, and excretion are not fully understood in fish, and is further complicated by dual exposure routes (waterborne and dietary), multi-metal interactions (zinc, copper, manganese, cobalt, and calcium), and overlapping metal transport pathways (divalent metal transporter 1, DMT1; Zrt- Irt-like (ZIP) family; epithelial calcium channel, ECaC) (Chandrapalan & Kwong, 2020; Kwong & Niyogi, 2009). While the diet is considered the primary route of iron acquisition in fish, many of the physiological and molecular effects of variable iron availability are not fully resolved, especially from developmental, tissue-specific, and multi-generational perspectives. Moreover, iron concentrations in many lakes and rivers across the world are on the rise due to natural and anthropogenic factors and as such, the ability to maintain metal homeostasis during fluctuating metal availability may be a critical determinant of fish survival (Björnerås et al., 2017; Chandrapalan et al., 2025). Importantly, wild fish populations experience metal stress in parallel with other environmental stressors such as hypoxia, elevated temperatures, and pollution, which can further exacerbate the effects of iron imbalance. Therefore, it is increasingly important to understand the physiological and ecological consequences of dietary iron in shaping individual and population fitness.

In this dissertation, I resolved iron homeostasis at an ecological, individual, and molecular level. My research aimed to:

1. **Identify the physiological consequences of dietary iron availability** on swimming performance, metabolism, and reproduction, including potential intergenerational effects (Chapter 2).
2. **Characterize the developmental and systemic importance of DMT1**, the principal non-heme iron transporter, in regulating iron and other trace metals using *dmt1*$^{-/-}$ fish (Chapter 3).
3. **Elucidate the transcriptional regulation and tissue-specific compensatory mechanisms** underlying iron transport and homeostasis in the gill and intestine during DMT1 loss (Chapter 4).

Collectively, these studies provide a comprehensive understanding of iron regulation in fish from whole-animal physiology to the cellular and molecular mechanisms. In this chapter, the principal findings of this dissertation are outlined.

5.2 Integrated main findings

5.2.1 *Dietary iron can modulate key fitness traits and can exert intergenerational effects*

Chapter 2 established the ecological and physiological significance of this thesis by demonstrating that dietary iron availability can have extensive implications, affecting growth, metabolism, swimming performance, reproduction, and offspring fitness in zebrafish. The results also highlighted a sensitive relationship between nutrition and performance whereby zebrafish exhibited tolerance to both low and high dietary iron levels, but physiological performance was largely dependent on exposure duration.

Sub-acute exposure (20 days) to an iron-enriched diet improved aerobic scope, maximum metabolic rate, and swimming capacity in zebrafish. These changes are consistent with enhanced oxygen transport efficiency, possibly through greater hemoglobin synthesis and ATP production, which can be supported by the increased iron availability. Similarly, reproductive output as measured by embryo survival and early development was also improved by iron supplementation. However, prolonged exposure (40 days) to a high iron diet diminished these benefits to health and was also associated with tissue-specific iron accumulation in the intestine and brain. The contrasting effects of a high iron diet during short and long-term exposures demonstrate the narrow physiological window between iron sufficiency and overload, further highlighting the properties of iron as both essential and potentially toxic. Interestingly, zebrafish were able to tolerate a low-iron diet and performed comparably to controls, suggesting that pre-existing iron reserves and limited iron excretion may be able to buffer short-term deficiency. Together, these findings reveal that zebrafish can sustain metabolic function under varying dietary iron availability, but under chronic imbalance, trade-offs in performance and possibly redox stress appear.

Importantly, dietary iron exposure can also have intergenerational consequences on fish health and performance. Offspring of high-iron-exposed parents displayed superior aerobic capacity and swimming performance compared to offspring of low-iron-exposed parents. These enhancements in performance imply that parental iron status can influence offspring physiology, either through nutritional provisioning or epigenetic mechanisms. Nonetheless, the intergenerational effects of parental iron status on offspring swimming performance can have great implications on shaping ecological fitness. In aquatic environments where iron levels can fluctuate drastically and are confounded by multiple other environmental stressors, the consequences of metal pollution on fish populations may be far greater.

5.2.2 DMT1 is integral for iron and trace-metal homeostasis

Using CRISPR-Cas9 mutagenesis, the *in vivo* significance of DMT1 in iron and trace metal balance in fish was characterised for the first time using *dmt1*$^{-/-}$ zebrafish. The loss of DMT1 was associated with iron deficiency and hypochromic anemia in developing zebrafish. *Dmt1*$^{-/-}$ fish exhibited reduced whole-body iron content and had visibly pale, low-hemoglobin erythrocytes. These phenotypes were similar to mammalian microcytic anemia (*mk*) mice and Belgrade (*b*) rats, demonstrating the strong evolutionary conservation of DMT1 function in vertebrate iron absorption. At the same time, *dmt1*$^{-/-}$ larvae exhibited delayed growth and reduced survival, further emphasizing the importance of DMT1 for optimal health. Notably, DMT1 loss disrupted the homeostasis of multiple other trace elements including zinc, manganese, cobalt, and selenium, which supports the broad specificity of DMT1 and potential interactions between metals and metal transport pathways. These results aligned with the metal-metal interactions also observed in Chapter 2 following dietary iron exposure, reaffirming that the homeostasis of essential metals is highly interconnected through shared transporter networks.

By incorporating assessments at both early development and in adulthood, it was clear that despite early metal dysregulation, adult *dmt1*$^{-/-}$ fish displayed partial phenotypic recovery and near normal physiological indices. Together, the viability of *dmt1*$^{-/-}$ fish as well as their partial recovery in adulthood, suggests the presence of alternate iron uptake routes that compensate for the loss of DMT1. Potential candidates included the heme carrier protein 1 (HCP1), ZIP family of transporters (ZIP4, ZIP8, and ZIP14), and ECaC. ddPCR analyses in developing fish identified dynamic changes in the mRNA expression levels of these transporters, particularly around the onset of exogenous feeding, where dietary iron and heme iron become available. During this window of metal rebalance, *dmt1*$^{-/-}$ fish maintained transporter expression and had elevated *hcp1* and *zip4*

levels, whereas wildtype fish exhibited a developmental decline in most transporters from 5 to 14 dpf. As such, DMT1-independent pathways for iron or heme assimilation and the accumulation of sufficient iron reserves over time enable the survival of *dmt1* mutants.

While zebrafish display remarkable flexibility in mitigating DMT1 loss, these regulatory responses were nonetheless insufficient to fully compensate for DMT1 function. Adult *dmt1*$^{-/-}$ fish had lower iron stores, persistent anemia, and showed tissue-specific metal imbalances (elevated hepatic copper and selenium). These findings highlight the importance of DMT1 in systemic iron homeostasis and its integral role in optimal iron metabolism.

5.2.3 Dmt1$^{-/-}$ *mutants exhibit transcriptional reprogramming involving broad and tissue-specific compensatory mechanisms*

The molecular mechanisms underlying iron homeostasis were elucidated in Chapter 4, which incorporated CRISPR-Cas9 technology with RNA sequencing to study the two major sites of iron acquisition, the gills and intestine, in wildtype and *dmt1*$^{-/-}$ zebrafish. The results of this study identified the broad transcriptional reprogramming that underlies the maintenance of iron homeostasis and physiological performance during metal dysregulation as described in Chapters 2 and 3.

Fundamentally, the transcriptional reprogramming evident in *dmt1*$^{-/-}$ fish centered on rebalance during DMT1 KO-mediated iron-deficiency. The mutants exhibited strong induction of ferric reductase (*cybrd1*), transferrin receptors (*tfr1a* and *tfr1b*), ferritin (*fth1a*), and many genes involved in erythropoiesis (*alas2*, *gata1a*, *tal1*, *hbba1*, and *hbaa1*). Furthermore, *dmt1*$^{-/-}$ fish also displayed suppression of hepcidin and the BMP-Smad signaling pathway in alignment with the increased need for iron uptake. These transcriptional responses reflect a highly coordinated effort

to restore iron uptake, enhance iron mobilization, and protect against redox imbalance, all consistent with the phenotypic anemia and partial compensation observed in Chapter 3.

At the tissue level, there was distinct segregation of function in the gill and intestine for maintaining iron homeostasis. The gills exhibited upregulation of *cybrd1* and *ecac*, along with genes related to tight-junction formation (*cldn3d*), and ion transport. These changes highlight the prioritization of barrier integrity and controlled transcellular ion flux in the gills, which is the critical interface for waterborne metal uptake and ionoregulation. The intestine displayed elevated *tfr1b* expression and enrichment of vesicle-trafficking and receptor-mediated endocytosis pathways, consistent with transferrin-dependent iron uptake and nutrient absorption. It was also characterized by downregulation of genes related to ROS generation and antibacterial defense (*mpx* and *nox1*), possibly suggesting a metabolic trade-off in immune function during iron deficiency. Additional suppression of apical transporters (*slc26a3* and *slc3a1*) and modulation of lipid and xenobiotic metabolism indicated a reprioritization of energy and detoxification processes to mitigate oxidative stress.

Most importantly, upregulation of *zip4* in the intestine and *ecac* in the gills provides two potential major candidates for non-heme iron uptake/homeostasis during DMT1 loss. These compensatory pathways, along with further induction of erythropoietic and membrane trafficking genes, suggest a highly coordinated network underlying systemic iron homeostasis, which aims to increase iron assimilation and oxygen transport, providing a mechanistic explanation for the viability of *dmt1*$^{-/-}$ fish.

5.3 Significance of research

This thesis addresses critical gaps in our understanding of how dietary iron availability and transporter function regulate physiological performance, trace metal balance, and intergenerational outcomes in fish. By examining environmentally relevant dietary iron exposures, this thesis highlights how iron status influences key fitness traits like swimming performance, metabolism, and reproduction. It also demonstrates the potential intergenerational consequences of dietary iron exposure which can have ecological significance in shaping population dynamics.

Furthermore, the establishment of the first CRISPR-Cas9 *dmt1*$^{-/-}$ zebrafish model enables the direct *in vivo* assessment of the physiological and molecular roles of DMT1 in fish. This model can not only validate the integral role of DMT1 in systemic iron and multi-metal balance, but it can also be used for future studies examining the toxicological significance of DMT1 in toxic metal uptake (e.g. lead and cadmium) and its and pathological importance in disorders of iron metabolism (e.g. anemia and Parkinson's disease). Zebrafish show a high degree of conservation in iron metabolism with other vertebrates and provide a valuable model for elucidating the ecophysiological impacts of both dietary and waterborne metal exposure. Beyond advancing our understanding of vertebrate iron biology, these findings also have practical implications for aquaculture nutrition, water quality regulations, and provide insight into population-level responses to metal stress in natural environments.

The incorporation of transcriptomic analyses also provides novel tissue-specific and system-wide resolution of compensatory responses employed by the mutants during DMT1 loss. It provides a comprehensive assessment of potential alternate pathways for iron acquisition and coordinated multi-metal regulatory networks which underly the viability and resilience of *dmt1*$^{-/-}$ mutants.

By integrating physiological, ecological, and molecular approaches this thesis has broad significance: it advances fundamental knowledge of vertebrate iron metabolism, provides mechanistic insight into how fishes adjust to fluctuating metal environments, and can inform environmental monitoring and aquaculture practices. More broadly, this research also contributes to comparative physiology by identifying conserved and compensatory pathways that may be relevant across taxa.

5.4 Conclusion and future directions

Collectively, this dissertation demonstrates that iron is a central regulator of physiological performance and fitness in fish, influencing both individual and intergenerational outcomes. Zebrafish exhibit remarkable plasticity in adjusting to fluctuating dietary iron availability and deficiency, but they are constrained by chronic imbalance. It is also evident that DMT1 is indispensable for maintaining optimal iron metabolism and gene disruption to *dmt1* triggers broad remodeling of transport and regulatory networks. These findings highlight the existence of a highly interconnected system for coordinating multi-metal homeostasis, with iron also linked to several metabolic, developmental, and performance-related outcomes.

Future research can expand on these findings through functionally validating the transcriptomic results and proposed compensatory pathways using protein quantification, transporter localization, and ion-flux assays. Assessing oxidative stress and ferroptosis markers provides a mechanistic link between iron overload and diminished physiological performance during chronic iron exposures. Finally, integrating epigenetic and multi-omics approaches would be valuable to reveal how parental metal status can reprogram offspring physiology, thereby providing crucial insight into the mechanisms that sustain physiological resilience and shape population dynamics in aquatic ecosystems.

5.5 References

Björnerås, C., Weyhenmeyer, G. A., Evans, C. D., Gessner, M. O., Grossart, H. P., Kangur, K., Kokorite, I., Kortelainen, P., Laudon, H., Lehtoranta, J., Lottig, N., Monteith, D. T., Nõges, P., Nõges, T., Oulehle, F., Riise, G., Rusak, J. A., Räike, A., Sire, J., … Kritzberg, E. S. (2017). Widespread increases in iron concentration in European and North American freshwaters. *Global Biogeochemical Cycles*, *31*(10), 1488–1500. https://doi.org/10.1002/2017GB005749

Chandrapalan, T., & Kwong, R. W. M. (2020). Influence of dietary iron exposure on trace metal homeostasis and expression of metal transporters during development in zebrafish. *Environmental Pollution*, *261*, 114159. https://doi.org/10.1016/j.envpol.2020.114159

Chandrapalan, T., & Kwong, R. W. M. (2021). Functional significance and physiological regulation of essential trace metals in fish. *The Journal of Experimental Biology*, *224*(24), jeb243834. https://doi.org/10.1242/JEB.238790

Chandrapalan, T., Walia, S., & Kwong, R. W. (2025). Intergenerational effects of dietary iron on swimming and metabolic performance in zebrafish. *Frontiers in Physiology*, *16*, 1693900. https://doi.org/10.3389/FPHYS.2025.1693900

Kwong, R. W. M., & Niyogi, S. (2009). The interactions of iron with other divalent metals in the intestinal tract of a freshwater teleost, rainbow trout (*Oncorhynchus mykiss*). *Comparative Biochemistry and Physiology. Toxicology & Pharmacology : CBP.*, *150*(4), 442–449. https://doi.org/10.1016/j.cbpc.2009.06.011

Wood, C. M., Farrell, A. P., & Brauner, C. J. (2011). Homeostasis and toxicology of essential metals. In *Fish Physiology* (Vol. 31A, Issue PA). Academic Press. https://doi.org/10.1016/S1546-5098(11)31010-2